

ENGINEERING SOCIETIES MONOGRAPHS

HARRISON W. CRAVER, *Consulting Editor*

PLASTICITY

ENGINEERING SOCIETIES MONOGRAPHS

FOUR national engineering societies, the American Society of Civil Engineers, American Institute of Mining and Metallurgical Engineers, The American Society of Mechanical Engineers, and American Institute of Electrical Engineers, have made arrangements with the McGraw-Hill Book Company, Inc., for the production of selected books adjudged to possess usefulness for engineers or industry, but not likely to be published commercially because of too limited sale without special introduction. The societies assume no responsibility for any statements made in these books. Each book before publication has, however, been examined by one or more representatives of the societies competent to express an opinion on the merits of the manuscript.

ENGINEERING SOCIETIES MONOGRAPHS COMMITTEE

A. S. C. E.
LYNNE J. BEVAN
GEORGE W. BOOTH

A. I. M. E.
REED W. HYDE
SAMUEL H. DOLBEAR

A. S. M. E.
C. B. PECK
G. B. KARELITZ

A. I. E. E.
F. MALCOLM FARMER
W. I. SLICHTER

HARRISON W. CRAVER,
CHAIRMAN

*Engineering Societies Library,
New York*

PLASTICITY

A Mechanics of the Plastic State of Matter

BY

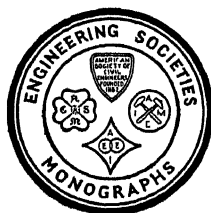
A. NÁDAI

Consulting Engineer, Westinghouse Electric and
Manufacturing Company East Pittsburgh, Pa.;
Research Professor, University of Pittsburgh

ASSISTED BY

A. M. WAHL, Ph.D.

Research Laboratories of the Westinghouse Electric
and Manufacturing Company, East Pittsburgh, Pa.



REVISED AND ENLARGED FROM
THE FIRST GERMAN EDITION

THIRD IMPRESSION

McGRAW-HILL BOOK COMPANY, Inc.
NEW YORK AND LONDON
1931

Copyright, 1931, by the

UNITED ENGINEERING TRUSTEES, INC.
All rights reserved. This book, or parts thereof,
may not be reproduced in any form without per-
mission of the publishers.

Printed in the United States of America

THE MAPLE PRESS COMPANY, YORK, PA.

ENGINEERING SOCIETIES MONOGRAPHS

For many years those who have been interested in the publication of papers, articles, and books devoted to engineering topics have been impressed with the number of important technical manuscripts which have proved too extensive, on the one hand, for publication in the periodicals or proceedings of engineering societies or in other journals, and of too specialized a character, on the other hand, to justify ordinary commercial publication in book form.

No adequate funds or other means of publication have been provided in the engineering field for making these works available. In other branches of science, certain outlets for comparable treatises have been available, and besides, the presses of several universities have been able to take care of a considerable number of scholarly publications in the various branches of pure and applied science.

Experience has demonstrated the value of proper introduction and sponsorship for such books. To this end, four national engineering societies, the American Society of Civil Engineers, American Institute of Mining and Metallurgical Engineers, The American Society of Mechanical Engineers, and American Institute of Electrical Engineers, have made arrangements with the McGraw-Hill Book Company, Inc., for the production of a series of selected books adjudged to possess usefulness for engineers or industry but of limited possibilities of distribution without special introduction.

The series is to be known as "Engineering Societies Monographs." It will be produced under the editorial supervision of a Committee consisting of the Director of the Engineering Societies Library, Chairman, and two representatives appointed by each of the four societies named above.

Engineering Societies Library will share in any profits made from publishing the Monographs; but the main interest of the societies is service to their members and the public. With their aid the publisher is willing to adventure the production and dis-

tribution of selected books that would otherwise be commercially unpractical.

Engineering Societies Monographs will not be a series in the common use of that term. Physically the volumes will have similarity, but there will be no regular interval in publication, nor relation or continuity in subject matter. What books are printed and when will, by the nature of the enterprise, depend upon the manuscripts that are offered and the Committee's estimation of their usefulness. The aim is to make accessible to many users of engineering books information which otherwise would be long delayed in reaching more than a few in the wide domains of engineering.

ENGINEERING SOCIETIES MONOGRAPHS COMMITTEE
Harrison W. Craver, Chairman.

FOREWORD

The translation into English and publication in the United States of Dr. A. Nádai's book on Plasticity were proposed to the Publications Committee of The American Society of Mechanical Engineers by the society's Professional Division on Applied Mechanics as a part of its program of developing the literature of this subject for the benefit of engineers unfamiliar with the German language. In making the proposal the division's executive committee pointed out the dearth of information on plasticity and the unique opportunity that existed by reason of the presence in this country of the distinguished author and his willingness not only to cooperate with the translator but also to bring his work up to date. Favorable consideration was given by the Publications Committee to the proposal, and it was decided to recommend to the Editorial Committee of the Engineering Societies Monographs that Dr. Nádai's work be made the first of the series. Acceptance of this recommendation has resulted in the publication of the present volume under the sponsorship of the Applied Mechanics Division of the A.S.M.E.

The A.S.M.E. Applied Mechanics Division considers it a privilege to endorse the English translation of Dr. Nádai's "Plasticity." Dr. Nádai is an authority on the subject and his work is already well known, especially in Europe. The publication of the English translation renders a valuable service to engineers and designers.

PREFACE

A review of the development of the theory of elasticity will show that during the period of over two hundred years the theory has gradually developed into an exact part of mechanics which today is the solid foundation for the design of engineering structures. During the last few decades much valuable information has been obtained regarding elastically imperfect materials, the mechanical properties of ductile metals, and the conditions of rupture in solids. However, a more satisfactory understanding of the plastic state of engineering materials and of the conditions of rupture has been reached since the constitution and the crystalline structure of metals and alloys, the mechanical and thermal history of metallic bars and sheets from the beginning of the casting of the ingot to the last annealing of the finished product, and the mechanical properties of metallic single crystals as special objects of investigation have been carefully studied from a broader physical standpoint.

Considerations of the plastic state of matter are today of interest to many branches of science and of engineering. The steel and metal worker desires to control more accurately the mechanical processes of forming metals at forging temperatures. Because of the large quantity of energy at the present time consumed in steel mills during the process of rolling, a more economical use of the energy required is needed. On the other hand, in order to choose the right materials for various parts of his machines, the machine designer must carefully consider the mechanical properties of these materials. He is not only interested in a more exact knowledge of the limiting conditions of stress at which, in his machine parts, permanent set begins to develop and danger of yielding or fracture is to be expected or fatigue cracks start to form; but also in several cases he will have to consider the possible change in shape of machine parts exposed to long duration of stressing. He may base his calculations as far as they refer to purely elastic deformation upon the theory of elasticity, but he lacks in the theory of strength of materials a similarly certain basis when considering the transition

from the elastic to plastic deformations or the conditions of rupture.

The physicist and the metallurgist are interested in the laws of plastic flow from several points of view. The experiments carried out in recent years with large metallic single crystals indicate clearly that plasticity is an essential and general property of solid matter in its crystalline state of aggregation. It has also been shown that under certain idealized conditions plastic flow of the polycrystalline metals under low temperatures follows rules or laws which in their simplicity and mathematical applicability to a variety of cases are comparable to the well-established foundations upon which the theory of elastic deformation rests. It may suffice to mention in this connection that since the first attempts of de St. Venant and C. Duguet, who years ago first tried to establish a mathematical theory of plastic deformation of metals, by the efforts of a number of more recent mathematicians and engineers a mechanics of the plastic state of metals has been revived with success and further developed in many new aspects.

In minerals and rocks many evidences of plastic deformations have been found. The changes in the structure of metals produced by plastic deformation are in many respects analogous to certain phenomena observed in minerals and rocks. These evidences show the correspondence which exists between the changes in structure in severely deformed metals and the slow processes occurring during the formation of certain rocks as observed and described in petrography. The conditions encountered in the deeper strata of rock: long duration of small differences in principal stress, elevated temperatures, and high average pressure, are those favorable for producing plastic deformations in solids. To these must be attributed some of the causes of the magnificent effects produced by mountain building and the dislocation of the continental plates which are observed in nature on a large scale. The remarkably regular profiles of some of the German and North American rock-salt domes, in which a layer of a highly plastic material such as rock salt has been pressed out by means of mountain pressure, may be mentioned as an example where evidences of plastic deformations are disclosed.

In the description of the plastic states of stress extensive use was made of the surfaces of slip. The flow or slip lines, which frequently appear as a pattern with an astonishingly regular

symmetry on the surface or in sections of solid bodies stressed above the plastic limit, have proved an extremely interesting object of investigation and a valuable means for analyzing the stress distributions under which they were produced. The strange laws which seem to apply to the surfaces of slip have attracted recently the mathematicians and the engineers and have been discussed with success by R. v. Mises, H. Hencky, L. Prandtl, and others. In the hands of the geologists, who in their faults have observed similar phenomena on a large scale for a long time, these surfaces might serve to decipher the riddles in the formation of high mountain chains, just as their smaller relatives have helped to describe more precisely the plastic states in permanently deformed bodies. They might possibly in the future still serve to study by mechanical means and to reconstruct the history of the crustal movements of the whole continents, which since the work of Alfred Wegener and F. B. Taylor we know are nothing but thin shells drifting slowly over the earth globe and their plastic substratum.

Acknowledgment should be made to the Notgemeinschaft der deutschen Wissenschaft in Berlin, to the Helmholtz Gesellschaft in Düsseldorf, and to the Verein deutscher Ingenieure in Berlin, who have made it possible for the author to carry out experimental work by placing at his disposal equipment for tests in the Institute of Applied Mechanics of the University of Göttingen. Particularly to Dr. F. Schmidt-Ott, of Berlin, former Minister of Education and President of the German Society for Encouragement of Scientific Work, the author wishes to express sincere gratitude for kindness and encouragement in the support of his plans. His further thanks for much valuable help are due to Dr. L. Prandtl, Director of the Laboratory, with whom he worked for nearly eight years at Göttingen.

The author is also much indebted to the Westinghouse Electric and Manufacturing Company for placing at his disposal facilities for continuing this work at the Research Laboratories in East Pittsburgh. He is especially thankful to Dr. S. M. Kintner, Vice President of the company, for his willingness to support everything necessary for this English publication and correlated work; to Mr. J. M. Lessells, former Manager of the Mechanics Division of the Research Laboratories, for help along the same lines, and to Dr. S. Timoshenko, Professor at the University of Michigan, for much good advice.

The author would never have accomplished the task of completing the English edition, had he not possessed the enthusiastic help of Mr. A. M. Wahl, who voluntarily took upon himself the task of revising the manuscript and who has prepared the English translation of the German edition on the subject as far as it has been included. Mr. P. G. McVetty deserves especial mention, particularly for valuable information regarding the plastic behavior of metals at elevated temperatures, subjects in which he has had much experience.

To W. Bader, W. Lode, and G. Mesmer, who have, at the author's suggestion, carried out a large part of the tests at Göttingen the author owes thanks. Dr. Bader has carried out the first series of tests on plastic torsion, Dr. Lode those on combined stress, and Dr. Mesmer those on concentrated pressure. At Pittsburgh, Mr. H. Friedman helped to carry out the recent tests on torsion. Messrs. C. W. MacGregor and W. O. Richmond read the proofs. To all these the author wishes to express his sincere appreciation.

A. NÁDAI.

RESEARCH LABORATORIES,
WESTINGHOUSE ELECTRIC AND MANUFACTURING COMPANY,
EAST PITTSBURGH, PA.,
July, 1931.

NOTE BY THE TRANSLATOR

The translator wishes to express his indebtedness to the Westinghouse Electric and Manufacturing Company, particularly to Dr. S. M. Kintner, Vice President, and Mr. J. M. Lessells, former Manager of Mechanics Division, Research Laboratories, for much encouragement received during the translation of Dr. Nádai's German book on "Plasticity." He is also greatly indebted to Dr. Nádai, not only for encouragement and advice received during the work, but also for his complete review of the original translation and for many additions and revisions at various points, as new knowledge of the subject has become available.

A. M. WAHL.

RESEARCH LABORATORIES,
WESTINGHOUSE ELECTRIC AND MANUFACTURING COMPANY,
EAST PITTSBURGH, PA.,
March, 1931.

CONTENTS

	PAGE
ENGINEERING SOCIETIES MONOGRAPHS	v
FOREWORD.	vii
PREFACE	ix
NOTE BY THE TRANSLATOR.	xiii
NOTATIONS.	xxiii

PART I

THE PLASTIC STATE OF MATTER WITH SPECIAL REFERENCE TO METALS AND MECHANICAL ENGINEERING PROBLEMS

CHAPTER 1

SOLID AND FLUID STATES—PLASTICITY AND VISCOSITY.	3
--	---

CHAPTER 2

BEHAVIOR OF MATTER UNDER HIGH PRESSURE	7
Effects of Pressure on (a) Polymorphism, (b) Viscosity—(c) The Compressibility of Metals, (d) of Glasses, (e) of Liquids—(f) Effect on the Rigidity—(g) The Cohesion of Liquids—(h) Optical and Other Effects.	

CHAPTER 3

THE ORDERED AND UNORDERED STATES OF MATTER.	14
---	----

CHAPTER 4

EFFECT OF GRAIN STRUCTURE AND OF CHANGING TEMPERATURE UPON THE STRENGTH—TIME EFFECTS.	18
Effects of (a) Constitution, (b) Absolute Size of Crystalgrains, (c) Imperfections in Structure, (d) Temperature, (e) Time.	

CHAPTER 5

ELASTIC AND PERMANENT DEFORMATION.	23
(a) Distinction of Different Stress-strain Curves (of Iron-, of Copper Type)—(b) After-flow—(c) Elastic Hysteresis—(d) Elastic After-effect.	

CHAPTER 6

ON THE MECHANISM OF PLASTIC DEFORMATION IN THE GRAIN STRUCTURE	30
(a) Slip; Translations in the Crystal Lattice—(b) Formation of Twins—(c) Changes of Position of Atoms Because of Agitation Due to Heat—(d) Breakdown of Structure—Gradual Loosening of Structure with Increasing Stress—Structure-sensitive and Structure-insensitive Properties of Solids—The Mosaic Crystal.	

CHAPTER 7

STRESS	39
The Analysis of the Homogeneous State of Stress—Normal and Shearing Stress—Principal Stresses.	

CHAPTER 8

MOHR'S REPRESENTATION OF STRESS	43
(a) Mohr's "Stress plane"—(b) Mohr's "Stress Circle" for Plane Stress—(c) The Principal Shearing Stresses.	

CHAPTER 9

STRAIN	48
The Analysis of the Homogeneous State of Strain—Unit Elongation, Unit Shear—Principal Strains—Strain Ellipse—Pure and Simple Shear.	

CHAPTER 10

INFINITESIMAL STRAIN.	53
-------------------------------	----

CHAPTER 11

LIMITING STATES OF STRESS	55
The Limiting Surfaces of Yielding and of Rupture—Brittleness and Ductility—Complexity of Mechanical Conditions for Rupture.	

CHAPTER 12

THEORIES OF STRENGTH AND RELATED TESTS.	59
Theories of (a) Maximum Stress, (b) Maximum Strain, (c) Constant Energy of Deformation, (d) Maximum Shear and (e) Theory of O. Mohr—Advantages of the Latter over Other; Limits of Its Validity—(f) Tests Relative to Conditions of Yielding in Polycrystalline Materials—(g) The Influence of the Mean Principal Stress on the Yielding of Metals—(h) Fracture.	

CHAPTER 13

NEW THEORIES.	70
Representation of Limiting Surface of Yielding According to Various Theories—Condition of Plasticity According to R. von Mises.	

CHAPTER 14

THE STATIONARY FLOW OF A PLASTIC MASS	75
The Three Rules of Yielding—The Stress-strain Relations for Plastic Flow.	

CHAPTER 15

TENSION.	80
(a) The Stress-strain Curve and the Curve of True Stresses for Ductile Metals—(b) Mechanical Similarity—(c) Upper and Lower Yield Stress for Steel.	

CHAPTER 16

STRAIN OR FLOW FIGURES	86
(a) Strain Figures in Mild Steel; Luders' Lines; Method of Etching Them; Observing Them by "Schlierenmethod"—(b) Phenomena Occurring in Flow Layers—(c) The Peak of the Stress-strain Curve of Steel—(d) The Production of Flow Lines by Notches and Holes—(e) Elastic Stress Distribution and the Beginning of Plastic Flow in a Plate with a Circular Hole—(f) How Plastic Flow Starts around a Hole—Appendix: Hole in Region Subjected to Pure Shear.	

CHAPTER 17

COMPRESSION	108
(a) Development of the Flow Layers. Compressed Cylinders—(b) The Plane Problem in Compression—(c) Prisms—(d) Compression Tests with Metals—Comparison of the Stress-strain Diagrams in Tension and Compression—Siebels Compression Test.	

CHAPTER 18

TORSION OF A CYLINDRICAL BAR OF CIRCULAR CROSS-SECTION . . .	126
The Stress-strain Curve for Pure Shear.	

CHAPTER 19

THE PROBLEM OF PLASTIC TORSION. EXPERIMENTAL REPRESENTATION OF STRESS DISTRIBUTION.	129
(a) Elastic Torsion—Prandtl's Soap-film Analogy—The Elastic Stress Function for Torsion. (b) The Plastic Stress Function of Torsion—The Sand-heap Analogy. (c) Apparatus for Experimental Determination of Stress Distribution—Sand Heaps.	

CHAPTER 20

TORSION TESTS. THE SLIP LAYERS IN TWISTED STEEL BARS	144
(a) Study of Structure of Twisted Steel Bars—(b) Structure Due to Cooling and Fluidal Structure.	

CHAPTER 21

EFFECT OF HOLES OR GROOVES IN A REGION SUBJECTED TO PURE SHEAR.	151
(a) Longitudinal Groove with Semicircular Cross-section—Model Tests with Rubber Membrane—Spreading of Plastic Region from Hole or Notch—(b) Bars with Cylindrical Hole—(c) Bars with Longitudinal Grooves—Tests.	

CHAPTER 22

BENDING OF BARS WITH ARBITRARY LAW OF DEFORMATION	160
---	-----

CHAPTER 23

PURE BENDING OF BAR WITH RECTANGULAR CROSS-SECTION	164
(a) To Determine from Known Stress Strain Relation How the Bending Moment Varies with the Deflection—(b) Inverse Problem: To Determine Stress-strain Curve from Bending Test—Examples.	

CHAPTER 24

BAR SUBJECTED TO PLASTIC BENDING	168
(a) Initial Yield or Flow in Steel Bar—(b) Example of the Spread of the Plastic Regions in a Bar Stressed Slightly above the Yield Point.	

CHAPTER 25

PLASTIC BENDING CONSIDERING WORK HARDENING.	173
Examples. Flow Layers Produced by Bending.	

CHAPTER 26

BUCKLING OF BARS AFTER THE YIELD POINT IS EXCEEDED.	178
---	-----

CHAPTER 27

THE PLANE PROBLEM	182
(a) Plane Strain—Condition of Plasticity—(b) Plane Stress—Ellipse of Plasticity.	

CHAPTER 28

THE THICK-WALLED TUBE UNDER INTERNAL PRESSURE	186
(a) Tube under Internal Pressure Yielding without Change of Axial Length—(b) Yielding in Thin Plate with Circular Hole or Flat Rings Radially Stressed—(c) Comparison of Both Cases with That of Perfectly Elastic Tube—(d) Partial Yielding in Thick Walled Tube.	

CHAPTER 29

PLASTIC FLOW IN HOLLOW CYLINDER FOR ARBITRARY LAW OF DEFORMATION CONSIDERING WORK HARDENING.	201
(a) Yielding of a Die-cast Aluminum Tube—(b) Similarity of Three Stress Distributions under General Law of Plastic Flow.	

CHAPTER 30

DISTRIBUTION OF STRESS IN ROTATING CYLINDERS AND DISCS	208
(a) Plastic Flow in Rotating Cylinder under Plane Strain—(b)	
Comparison with Elastic Rotating Cylinder—(c) Rotating Disc	
—(1) Solid Disc; Partial and Complete Yielding—(2) Rotating	
Disc with Hole.	

CHAPTER 31

GENERAL PROBLEM OF PLASTIC FLOW WITH AXIAL SYMMETRY ABOUT AN	
AXIS	215
(a) Hollow Cylinder Subjected to Internal Pressure and Axial	
Load—(b) Combined Torsion and Axial Tension in Solid Cylindrical Bar.	

CHAPTER 32

SYSTEMS OF SLIP LINES IN TWO-DIMENSIONAL PROBLEMS.	218
--	-----

CHAPTER 33

PLASTIC MASS PRESSED BETWEEN TWO ROUGH PARALLEL PLATES . .	221
Active and Passive States—Slip Lines—Tests Showing Distorsion of	
Soft Mass after Compression.	

CHAPTER 34

OTHER CASES OF PLANE PLASTIC FLOW	227
(a) Radial Yielding—(b) Circles as Envelopes of Slip Lines—(c)	
Vortical Flow in a Plastic Mass—(d) Radial Distribution in a	
Wedge-shaped Space.	

CHAPTER 35

HARDNESS.	233
Brinell's Ball—Ludwik's Cone—Shore's, Rockwell's, Herbert's	
Hardness Tests—Penetration of Cylindrical Punches in Zinc,	
Copper, Mild Steel, and Paraffin.	

CHAPTER 36

THE PROBLEM OF CONTACT OF ELASTIC BODIES.	241
(a) General Remarks—(b) Contact of Two Elastic Spheres—(c)	
Contact of Two Elastic Cylinders.	

CHAPTER 37

PHOTO-ELASTIC CONTACT TESTS AND OBSERVATION OF SLIP LINES UNDER	
PLASTIC IMPRESSIONS	243
(a) Shearing Stress Lines (Isochromatics) and Shearing Stress	
Trajectories (Slip Lines)—(b) Single Force Acting on an Infinite	
Plane—(1) Michell's Radial Stress Distribution—(2) Uniform	
Pressure along Half Plane—(3) Uniform Pressure along a Parallel	
Strip—(4) Rigid Punch—(5) Slip Lines—(c) Two Concentrated	
Loads—Plastic Flow in the Rolling Process—Tests.	

CHAPTER 38

INHERENT AND RESIDUAL STRESSES	258
(a) First Method of Calculating Residual Stresses—Examples:	
(1) Twisted Bar, (2) Hollow Cylinder Stressed by Internal Pressure	
—(b) Experimental Demonstration of Residual Stresses—(c) Second	
Method of Finding Residual Stresses.	

CHAPTER 39

ELASTICITY AND PLASTICITY AT ELEVATED TEMPERATURES. CREEP OF METALS	270
(a) Isotropic Elasticity—(b) Perfect Plasticity—(c) Work Harden-	
ing—(d) Recovery—(e) Influence of Velocity of Deformation—	
(f) the Stress-strain-velocity Diagram—(g) Homologous Tempera-	
tures—(h) the Effect of Temperature on Elasticity—(i) The	
Effect of Temperature on Plasticity—(j) Viscosity—(k) Change of	
Viscosity of Liquids with Temperature—(l) Creep of Metals.	

PART II

SOME APPLICATIONS OF THE MECHANICS OF THE PLASTIC STATE OF MATTER TO GEOLOGY AND GEOPHYSICS

CHAPTER 40

FINITE HOMOGENEOUS STRAIN	291
(a) Distortion without Change of Volume—(b) Plane Strain	
—(c) Simple Shear—(d) Determination of Principal Axes of Plane	
Strain—(e) Simple Shear of Rock Layers—(f) Pure Shear—(g) The	
Phenomenon of Slip in Rocks—Surfaces of Slip for (1) Finite	
Simple Shear and (2) for Pure Shear—(h) Plastic Deformation	
with Volumetric Extension.	

CHAPTER 41

THE PRESSURE IN THE EARTH'S INTERIOR	308
(a) The Elastic Compressibility of the Rocks—(b) The Change in	
Gravitational Acceleration and Pressure with Depth—(1) Homo-	
geneous Sphere—(2) Parabolic Distribution of Density—(3) The	
Metal Core and the Silicate Shell.	

CHAPTER 42

MOUNTAIN BUILDING	315
-----------------------------	-----

CHAPTER 43

PLASTIC LAYER BETWEEN BRITTLE LAYERS. THE ORIGIN OF THE ROCK- SALT DOMES	319
The observations of E. Seidl.	

CONTENTS

xxi

PAGE

CHAPTER 44

THE WEIGHT OF THE CONTINENTS	324
Isostasy. Compression and Extension of Parts of the Earth's Crust in a Horizontal Direction.	

CHAPTER 45

TRACES OF MOTION IN THE STRUCTURE OF ROCKS	328
(a) The Streaks and Joints in Granite—The Observations of H. Cloos on Granite Stocks—(b) Tension Cracks—Shearing Surfaces— (c) Ordered Arrangement of the Rock Inclusions—(1) The Trachyte Cone of the "Drachenfels," (2) The Bulging Out of Molten Volcanic Masses—Oriented Structure of Rocks Developed in the Solid State.	
BIBLIOGRAPHY FOR CHAPTERS 40 TO 45	340
INDEX.	341

NOTATIONS

x, y, z	rectangular coordinates.
r, φ or r, ϕ	polar coordinates.
t (or z)	time.
s	stress.
s_{xx}	normal stress.
$s_{xy} = s_{yx}$	shearing stress.
s_x	sometimes used also for normal stress s_{xx} .
s_1, s_2, s_3	the principal stresses.
p	pressure (compression stress).
p_{xx}	compression stress parallel to the x axis.
s_0	yield stress in pure tension.
k	yield stress in pure shear
ϵ	unit elongation, strain.
ϵ_{xx}	unit elongation in a direction parallel to the x axis.
ϵ_{xy}	unit shear in the x, y plane (change of angle between two straight lines which were originally parallel to the x and y axis respectively).
ϵ_x	sometimes used for unit elongation ϵ_{xx} .
$\epsilon_1, \epsilon_2, \epsilon_3$	the principal strains.
γ	sometimes also used for unit shear, for example, in twisted bars.
γ	used also as the weight per unit of volume.
E	modulus of elasticity (Young's modulus).
G	modulus of rigidity.
ν	Poisson's ratio.
K	bulk modulus.
A, a	area of cross section.
u, v, w	components of displacement of a point parallel to the x, y, z axes, respectively.
a_x, a_y, a_z	direction cosines.
M	bending moment, or torque.
θ	angle of twist per unit of length.
F	stress function.
$\Delta = \frac{\partial^2}{\partial x^2} + \frac{\partial^2}{\partial y^2}$	Laplacian operator for two dimensions.
b	width (breadth) of bent bar.
h	height of cross-section of bar.
I	moment of inertia of cross-section.
η	viscosity coefficient.
ρ	density.
g	gravitational acceleration.

PART I

**THE PLASTIC STATE OF MATTER WITH SPECIAL
REFERENCE TO METALS AND MECHANICAL
ENGINEERING PROBLEMS**

PLASTICITY

CHAPTER 1

SOLID AND FLUID STATES—PLASTICITY AND VISCOSITY

In the study of mechanics it is useful to ascribe to materials certain ideal properties. For example both the motion of material bodies and the states of equilibrium existing in these bodies may be studied from a common standpoint, if we attribute to the material certain definite, simple properties. Thus, we are led to such definitions as those of rigid bodies, uniformly distributed masses, isotropic elastic bodies, perfect and viscous fluids, etc.

In the science of physics, the usual classification of matter into the solid, liquid, and gaseous states cannot be dispensed with, since experience has proven such a classification to be of great help to physicists. In order to avoid difficulties and contradictions, however, it should be noted that this classification of materials in many cases is fundamentally unnecessary and in others entirely unsatisfactory.

As an example of a case where such a classification is unnecessary, consider the flow of gases (aerodynamics). As long as the velocity of flow is much smaller than the velocity of sound in the gas, the flow may be considered from the same standpoint as the flow of liquids (hydrodynamics). Here is then a case where the division into liquid and gaseous states is unnecessary. The form of the Andrew isothermals of carbon dioxide shows that this gas may be liquefied by sufficiently increasing the pressure and subsequently decreasing the temperature, it being unnecessary to specify a definite temperature and a definite pressure at which liquefaction occurs. Liquefaction may thus be brought about by choosing a curve in the p, v plane (p = pressure, v = volume) to connect the initial and final states of the gas in such a way that the curve runs above the "critical point."

It is known that certain amorphous materials may be brought from the solid into the fluid states without sudden change in

volume while a definite melting point may not be noticed. For example, glass gradually softens if heated and hardens if cooled. It has no definite melting point since no definite temperature exists at which the state of aggregation of the glass changes abruptly from the fluid to the solid state.

A mechanical characteristic of a perfect fluid is the easy mobility of the small elementary parts thereof. A condition expressing this property, in the case of a fluid at rest, is that the pressure at any internal section is always directed perpendicularly to this section. On the contrary, the elements of a solid may carry, in addition to tensile and compressive stresses acting perpendicularly to the cross-section, certain forces, called "shearing stresses," which act in the plane of the cross-section in a tangential direction and which may often be of considerable magnitude.

The viscous fluids occupy a position, with respect to behavior, midway between solids and liquids. At rest they behave similar to perfect fluids. During motion, however, tangential forces are produced by the action of layers of the fluid as they slide over one another. These tangential or shearing forces increase as the fluid velocity changes along a line perpendicular to the direction of motion. The simplest example of a laminar (non-turbulent) flow of a viscous fluid is the flow between two parallel plates placed closely together, one plate being stationary and the other moving with a uniform velocity in its plane. It will be found that a force is necessary to cause motion of the movable plate. The faster this plate is moved and the smaller its distance from the stationary plate, the greater the force necessary. If we take the ratio between the force acting in the direction of motion between two neighboring layers of the fluid and the surface on which this force acts, it is found that this ratio approaches a limiting value, if the surface is indefinitely decreased. This limiting value is called the "internal friction" of the fluid. The simplest expression for this property of a viscous fluid is that the internal friction or the shearing stress s acting between moving parallel layers is equal to:

$$s = \eta \cdot \frac{\partial u}{\partial y}, \quad (1)$$

where u is the velocity and y a direction perpendicular to the surface of the layer or the direction of the motion. The

factor η is called *the coefficient of viscosity*, or more simply, *the viscosity*.

The above-mentioned properties of fluids and solid bodies do not suffice entirely to classify materials with regard to their mechanical behavior, as a few examples will indicate. For instance, certain bituminous solids possess, besides the above mentioned characteristics, such as no definite melting point, the property of gradual, permanent change in shape at a relatively low temperature, at which they usually are considered as solids. This change in shape is continuous under the action of small forces, such as, for example, the weight of the body. It is only necessary to allow sufficient time for the action to take place. Thus, hard asphalt may flow out of a small crack in a leaky barrel. If a steel ball be placed on the surface of a barrel filled with asphalt it will in time sink below the surface and fall gradually to the bottom. A bar of sealing wax, supported at both ends, may bend under its weight after a time. Moreover, certain crystalline materials may under certain conditions deform permanently. For instance, ductile metals may be bent, drawn, and compressed by rolling or hammering, even though cold. A knowledge of the properties of solids, relative to permanent change in shape, is of great practical value to our present-day industries, in solving questions involved in the fabrication of metals.

On the basis of these random observations, to which countless others may be added, it may be concluded that the above discussed properties, relative to continuous, permanent change in shape, are very generally characteristic of all solid materials. It is an established fact that even the strongest metals, such as steel and iron, and materials with a crystalline structure, such as minerals and rocks, under certain definite mechanical conditions may be brought into a new state—the *plastic state*—in which permanent deformation may occur without fracture. We say that solid bodies in this condition “flow” or “yield” if the permanent deformation is sufficiently great so as to be perceptible to the unaided eye.

Examples of deformation of considerable amount without fracture are well known to the geologist. The study of the exceedingly slow movements of the deeper layers of rock in the earth's crust has made it evident that many rocks, especially those encountered beneath the great mountain chains of the earth, have been deformed permanently to considerable amounts since

their formation in the early geological periods. The circumstances existing in the deep rock strata, namely high pressure, elevated temperature and long duration of the action of the forces, are conditions which are particularly favorable for the occurrence of plastic deformation.

CHAPTER 2

BEHAVIOR OF MATTER UNDER HIGH PRESSURE

It may be shown that the terms "solid" and "fluid" which serve to differentiate the states of aggregation of matter are in many cases entirely insufficient. This is especially true if we consider the behavior of materials under high pressure. A knowledge of how matter behaves in the solid or liquid states when exposed to high hydrostatic pressures is in many respects of great interest. It can easily be shown that in the smaller and comparatively colder cosmic bodies like the earth, the pressure due to the weight of the outer layers increases with depth, up to several million atmospheres at the center ($1 \text{ atm.} = 1 \text{ kg./cm.}^2 = 14.2 \text{ lb./in.}^2$). In certain gaseous stars with enormous densities, of the type of the dark companion of Sirius, pressures of thousands of millions and possibly of thousands of billions of atmospheres probably exist.¹ The questions relating to the equilibrium in the colder cosmic bodies with an aggregation of matter like that in the earth in which not only the pressure but also the temperature increases considerably with depth, are of great interest for both the astronomer and the geophysicist, as well as for the geologist. In contrast with these enormous pressures it has so far been possible to obtain maximum hydraulic pressures of the order of 20,000 atm. in the laboratory. However, it is noteworthy that even within this range of pressure very remarkable changes in the properties of solids and liquids may be observed, and these

¹ According to JAMES H. JEANS, ("Astronomy and Cosmogony," p. 73, University Press, Cambridge, Eng., 1929, cf. also "The Universe around Us," by the same author, p. 250, The Macmillan Company, New York, 1929) the faint companion to Sirius is one of the most remarkable stars in the sky. The average density in this comparatively small cosmic body has been estimated to be fifty to sixty thousand times that of water. In this faint star, which belongs to a group of stars called the "white dwarfs," matter is condensed to the utmost limit. Due to the high temperatures therein the atoms are thought to be almost completely broken up into their constituent nuclei and electrons, both of which move about like the molecules of a gas.

observations throw light on many questions of interest to engineers and scientists.

The most reliable and comprehensive tests on which the present knowledge of the behavior of matter under high hydrostatic pressure is based, are those of Prof. P. W. Bridgman¹ to which reference will be made in the following.

a. Polymorphism.—To illustrate the point mentioned in the introductory remarks to this and the first chapter, we may say that many materials composed of one fundamental substance only, such as chemical elements and compounds, have not one, but several solid states. Among the elements, exhibiting such modifications of the solid state the following examples may be mentioned: sulphur, below about 20,000 lb. per square inch, is monoclinic, while above this pressure the rhombic sulphur is in thermal equilibrium with the fluid.² If we plot the temperatures t at which the changes from one state to the other occur, with varying pressures p , three equilibrium curves in the pressure-temperature diagram will result, which (in the p, t plane, having p as abscissæ and t as ordinates) separate the three regions: monoclinic, rhombic, and fluid sulphur. The three curves meet at a "triple point" at 20,000 lb. per square inch and 152°C. Other well-known examples are: iron (formerly thought to have four modifications known as α , β , γ , and δ iron; these modifications, however, have probably but two kinds of crystals having different structures or arrangements of the atoms in the space lattice³), phosphorus, carbon (graphite, diamond).

In 1900, G. Tammann discovered two varieties of ice denser than the usual kind. These he designated as ice I and ice II. Since the fundamental investigations of P. W. Bridgman,⁴ which covered a wider range of pressures, it has been shown that

¹ The author is much indebted to Prof. P. W. Bridgman of Harvard University, Cambridge, Mass., for his kindness in furnishing complete reports of his extensive experimental work on high pressure and related questions.

² TAMMANN, G., "Aggregatzustände, die Zustandsänderungen der Materie in Abhängigkeit von Druck und Temperatur," Leopold Voss, Leipzig, 1922.

³ WEYER, F., *Stähleisen*, vol. 45, p. 1208, 1925; *Mitt. aus dem Eisenforschungsinstitut*, Düsseldorf, vol. 7, 1925; also F. KOERBER, *Schmelzen, Erstarren, Sublimieren*, "Handbuch der Physik," vol. 10, p. 192, Julius Springer, Berlin.

⁴ BRIDGMAN, P. W., Thermodynamic Properties of Liquid Water up to 80°C and 12,000 kg./cm.², *Proc. Amer. Acad. Arts. Sci.*, vol. 48, no. 9, 1912.

water in the solid state occurs under high pressure in five different modifications. In changing from one kind of ice to another the specific volume changes abruptly. The kinds of ice occurring under higher pressures are the denser. On the basis of careful investigations relative to the behavior of water, it may be mentioned that the well-known lowering of the freezing point of water by pressure is observed only in the case of ice I up to a pressure of 2,200 atm. and a temperature of -22°C . At higher pressures than this the melting temperature of ice increases with the pressure. Bridgman has investigated the melting curve (the bounding curve between the fluid and the solid state in a diagram with the pressure as abscissæ and with the temperature as ordinates) of ice VI to above 20,000 atm. and to a temperature of $+76^{\circ}\text{C}$. The melting temperatures of ices III to VI increase with the pressure in a similar way as do the melting temperatures of most materials when the pressure is increased. Ice VI melts at $+26^{\circ}\text{C}$. under 10,000 atm. pressure and at $+76^{\circ}\text{C}$. under 20,000 atm.

b. Viscosity.—The behavior of fluids with respect to viscosity under high pressure is of very considerable interest from a practical as well as a scientific standpoint. As already mentioned, the viscosity of fluids manifests itself as a kind of inner resistance or internal friction, which opposes each change of shape by the relative sliding of the small particles or layers of fluid. If a solid sphere is allowed to fall through a liquid having considerable viscosity, after a certain time it will attain a constant speed. The higher the viscosity of the liquid, the smaller will be the velocity of the falling sphere through the viscous liquid under the force of gravity. The coefficient of viscosity, as introduced by Eq. (1), page 4, can readily be determined by measuring the time of fall of bodies in liquids. It is by this method that Bridgman¹ has determined the viscosity of liquids exposed to increasing pressures, relative to their viscosity at atmospheric pressure. He found that the coefficient of viscosity increased rapidly with the pressure. In general, the effect of pressure on viscosity is greater than on any other physical property. The effect of pressure on viscosity also varies greatly with the liquid. It must be expected that liquids exposed to suffi-

¹ *Proc. Amer. Acad. Arts Sci.*, vol. 61, p. 86, 1925; vol. 62, p. 187, 1927; compare also tests by Faust and Tammann, referred to in the book by the latter, mentioned above.

ciently high hydrostatic pressures will congeal so that they become solids.

The relation between pressure and viscosity appears to be an exponential function, *i.e.*, if the pressure is increased by equal amounts the viscosity increases as the terms of a geometric series. The more complicated the structure of the chemical molecule of the fluid, the more the viscosity increases with pressure. For example, according to the investigations of Bridgman at 12,000 atm. the viscosity increases by 30 per cent for mercury, over its value at zero pressure, and 2.7-fold for water, both at 30°C. and from 10 times to 1,000,000 times its original value for very viscous mineral oils. Kiesskalt¹ recently has shown that at 1,000 atm. the viscosity of mineral oils is six to twenty-two times as great as under atmospheric pressure. Under high pressures such as exist in the journals and bearings of high-speed rotating machinery, as for example, steam turbines, the change in the viscosity of the oil may become sufficient to affect its lubricating qualities considerably.

As in other respects, water shows in this an exceptional behavior. At low temperatures viscosity decreases at first with increasing pressure, but this is an abnormal phenomenon and the curves soon tend again to rise for greater pressures or higher temperatures.

c. The Compressibility of Metals.—The volume of solids and fluids decreases slightly under pressure. This decrease in volume is usually, at small pressures, so small that it may be detected only by the aid of sensitive measuring instruments. It is also a perfectly reversible or an elastic change, since, if the pressure is removed, most solid and liquid materials take on their initial volume. An exception to this is the case of porous materials (wood, cast iron, for example) which can be permanently compressed by high hydrostatic pressure.

In order to give an idea of the compressibility of metals a few numerical data will now be given. The investigations of Bridgman² show that for *iron* the ratio of the decrease in volume Δv to the initial volume v_0 (the initial volume taken at 1 atm. pressure and some standard temperature, which was 30°C. in Bridgman's tests) is equal to:

¹ *Mitt. u. Forschungsarb. V.D.I.*, vol. 291, 1927.

² The Compressibility of Thirty Metals, *Proc. Amer. Acad. Arts Sci.*, vol. 58, no. 5, p. 166, 1923.

For iron

$$\frac{\Delta v}{v_0} = 10^{-7} \cdot (5.87 - 2.10 \cdot 10^{-5} p)p,$$

where p is the pressure in kilograms per square centimeter. A more exact definition of the compressibility k is the ratio of the decrease in volume produced by a pressure increase of 1 atm. or $\partial v / \partial p$ to the volume v existing at the time considered:

$$k = \frac{1}{v} \cdot \frac{\partial v}{\partial p}.$$

For most materials the compressibility k decreases gradually with pressure; in other words, compressed metals, for the same increase in pressure, change in volume a smaller amount, the higher the compression. The measurements of Bridgman give (pressures p are in kilograms per square centimeter):

For copper

$$\frac{\Delta v}{v_0} = 10^{-7} p (7.32 - 2.7 \times 10^{-5} p)$$

For aluminum

$$\frac{\Delta v}{v_0} = 10^{-7} p (13.34 - 3.5 \times 10^{-5} p)$$

For lead

$$\frac{\Delta v}{v_0} = 10^{-7} p (23.73 - 17.25 \times 10^{-5} p).$$

The greatest compressibilities are exhibited by the alkali metals. Of all elements, caesium is the most compressible, the volume of caesium decreasing by one-third at 15,000 atm. pressure.

As one may see from the foregoing the volume of steel or iron decreases only about 0.0006 of its initial volume at a pressure of 1,000 atm. Consequently, as a rule we may neglect such changes in volume due to pressure, when considering the deformation due to plastic flow which may occur in ductile metals.

On the other hand, compressibility plays an important part if the state of equilibrium of the rocks at great depths in the earth is investigated. Because of the effect of pressure the density of these rocks must be considerably increased when compared with their density at the surface of the earth. In connection with possible applications of these facts to geophysical questions some

results of tests of Bridgman on non-metallic materials will here be mentioned.¹

d. The Compressibility of Artificial and Natural Glasses.²

Silica	$a = 27.74 \times 10^{-7}$	$b = 7.17 \times 10^{-12}$
Pyrex glass	$a = 30.08 \times 10^{-7}$	$b = 4.86 \times 10^{-12}$
Tachylite Kilauea (Hawaii) . . .	$a = 13.74 \times 10^{-7}$	$b = -9.1 \times 10^{-12}$

The compressibility is here given at 75°C. as $\Delta v/v_0 = ap + bp^2$; the constants a and b are given for p in kg./cm.². It is remarkable that with exception of the last example the coefficient b is positive and hence these glassy substances are the more compressible the higher the pressure. This abnormal behavior, found only in glassy substances, seems apparently to be connected with the silica content.

e. The compressibility of liquids is in general much greater than that of solids and amounts at 12,000 atm. to about 20 per cent for water and about 30 per cent for ether, one of the most compressible liquids. For

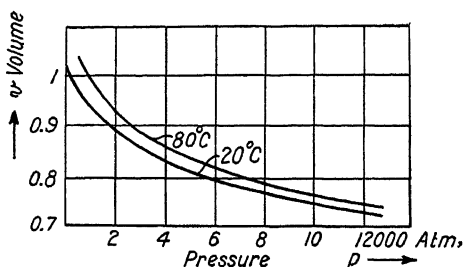


FIG. 1 —Compressibility of ether. (According to P. W. Bridgman.)

most liquids the compressibility decreases much more rapidly at the lower pressures than at the higher. A curve typical of most liquids is shown in Fig. 1. This curve is for ether and is reproduced from the tests of Bridgman.

f. The Effect of Pressure on the Rigidity of Metals.—By measuring the relative movement of two helical springs one consisting of steel and the other of the metal to be tested, which were immersed in a liquid in a pressure vessel, P. W. Bridgman³ was able to determine the relation of the moduli of rigidity. The two springs were attached to each other and the effect of pressure on the modulus of rigidity of the steel spring had previously been determined by absolute measurements. The modulus of rigidity under a pressure of 10,000 kg./cm.² was increased above its value at zero pressure by the following amounts:

¹ The compressibility of minerals and rocks with special reference to problems of geophysics has been investigated particularly by L. H. Adams and his collaborators in the Geophysical Laboratory at Washington, D. C. These tests will be referred to in Part II, Chap. 41, where further experimental data on the elastic compressibility of rocks are given.

² BRIDGMAN, P. W., *Amer. Jour. Sci.*, vol. 10, p. 359, 1925.

³ *Proc. Amer. Acad. Arts Sci.*, vol. 64, no. 3, p. 39, 1929.

	Per cent
Tantalum	+ 0.3
Platinum.	+ 2.4
Nickel.	+ 1.8
Spring steel.	+ 2.2

These results may be of importance, if the influence of the tremendous pressures in the central core of the earth on the velocity of propagation of the earthquake waves passing through it is to be considered. The velocity of the distortional waves depends on the modulus of rigidity and as the pressures in the central part of the earth reach millions of atmospheres or so, the effect of pressure on rigidity at these great depths may therefore be appreciable.

g. Cohesion in Liquids.—A few remarks at this point may be in order, although their relation to the behavior of matter under high pressure is not immediately obvious. A. A. Griffith¹ has shown that very thin filaments of silica glass were much stronger above their softening temperature than in the cold condition. At first glance this is the opposite of what would usually be expected. From capillarity phenomena it is known, however, that very thin films of liquids may sustain extremely high tensile stresses. From these and numerous other considerations it must be concluded that in fluids under suitable conditions a considerable resistance against tearing apart (the effect of the cohesive forces acting between the atoms or of the "cohesion") is observed, a property which usually is ascribed only to materials in the solid state.

h. Optical and Other Effects.—By means of a very skillfully designed arrangement which consisted of a special steel pressure cylinder of an inverted T-shape containing a movable piston and two glass windows, Thomas C. Poulter² succeeded in observing various additional effects, due to high hydraulic pressures up to about 20,000 atm., on material properties, as for example upon the index of refraction (of glass and of paraffin) and upon the rotation of the plane of polarization of optically active compounds in solution (sugar). Other physical properties, such as the electric or thermal conductivity, etc., under high pressure, were investigated by P. W. Bridgman.

¹ *Phil. Trans. Roy. Soc., London, ser. A, vol. 221, p. 163, 1921.*

² Typewritten reports on these tests were made available to the author through the kindness of Prof. T. C. Poulter, Physics Department, Iowa Wesleyan College, Mount Pleasant, Iowa.

CHAPTER 3

THE ORDERED AND UNORDERED STATES OF MATTER

So far we have classified materials according to their state of aggregation, *i.e.*, "solid" or "fluid," depending on their behavior under various states of stress. We now consider a different mode of classification, namely, that given by their internal structure. According to G. Tammann,¹ the *anisotropic* state of matter should be distinguished from the *isotropic*. The elementary particles of matter (atoms, ions, molecules) out of which all materials, according to the modern views of physics are composed, are, in the first (the anisotropic) state arranged in a definite geometrical and regular way; while in the second (the isotropic) state, they are unordered. To the first state belong the crystals and the crystalline materials; to the second state belong the gases, liquids, and vitreous (solid or fluid) materials.

The view of an ordered arrangement of the elements of crystals is supported by many and varied observations, so that we may take it as almost a certainty. These views were originally suggested from the geometrically regular shape of natural crystals, those precipitated from solutions, or those formed by fusion. The best proof of the correctness of these views is, however, given by the interference observations on *x*-rays² passing through crystals. Other observations in support of this view are the extraordinarily regular markings which one may produce upon the polished surface of crystals by etching (etching figures), by slow plastic strains (slip lines), or by impact strains (impact figures).³

¹ "Aggregatzustände, etc.," Leopold Voss, Leipzig, 1922.

² EWALD, P. P., *Der Aufbau der festen Materie und seine Erforschung durch Röntgenstrahlen*, "Handbuch der Physik," vol. 24, chap. 4, p. 191; M. BORN and O. F. BORNOW, in *Theoretische Grundlagen*, *ibid.*, chap. 5, p. 370; W. H. AND W. L. BRAGG, "X-rays and Crystal Structure," London, B. Bell, 1924; R. WYCKOFF, "The Structure of Crystals," Chemical Catalogue Company, New York, 1924; R. GLOCKER, "Materialprüfung mit Röntgenstrahlen," J. Springer, Berlin, 1927.

³ ANTON MÜLLER in the Tammann Institut ("Metallographische Studien," Dissertation, Göttingen, 1926) has shown that extraordinarily

In vitreous solids, on the contrary, no orderly arrangement of the atomic elements can be detected by *x*-ray methods. This is regular figures may be produced by pressing a needle on the crystals of metals.

The space lattice of copper, aluminum, silver, gold, and γ -iron is a face-centered cubic, that of α -, β -, and δ -iron is a body-centered cubic, while that of zinc is a hexagonal lattice. The elementary cubes of the former contain an atom in each corner and the middle of each side. In the body-centered cubic lattice there is also an atom in the middle of the cube, besides that in the corners. In zinc crystals, the atoms have approximately the same arrangement as the middle points of balls when piled in a large heap in the densest manner possible.

In a copper crystal certain definite crystallographic planes are the planes of a cube, an octahedron, and a rhombic dodecahedron. The octahedron results if we join the atoms of the middle of each side of a cube while the planes of the rhombic dodecahedron lie oblique to the 12 edges of the cube



FIG. 2.



FIG. 3.

FIGS. 2 and 3.—Slipbands produced by impression of a needle on a copper crystallite. Fig. 2, impression on a cubic plane; Fig. 3, on an octahedral plane. (*A. Muller.*)

According to Muller, if a needle is pressed upon a crystal of copper there is produced in the neighborhood of the impression the system of lines shown schematically in Figs. 2 and 3. If the needle is pressed upon a plane of the cube the slip lines of Fig. 2 result while if pressed upon an octahedron plane the lines of Fig. 3 are produced. Under plastic deformation the octahedron planes of the copper crystals slide the most easily; hence their traces on

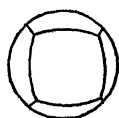


FIG. 4.

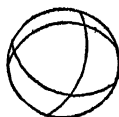


FIG. 5.

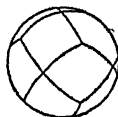


FIG. 6.



FIG. 7.

FIGS. 4 to 7.—Etching figures on spheres cut from copper single crystals. These figures were obtained by using different solutions and are reproduced schematically. On the surface of the etched copper balls a figure appears, which shows the contour lines of a cube in Fig. 4, of an octahedron in Fig. 5, of a rhombic dodecahedron in Fig. 6, and the combination of a cube with an octahedron in Fig. 7. (*According to K. W. Haussner and P. Scholz.*)

the polished surface appear under the microscope as the system of lines of Figs. 2 and 3. Other observations on figures produced by pressure and etching are given in "Moderne Metallkunde" by Czochralski.

On large balls, about the size of a billiard ball, cut out of single crystals of copper, HAUSSNER AND SCHOLZ (*Wiss. Veröffentlichungen aus dem Siemens-*

also the case with fluids.¹ With the exception of monomolecular films, we may therefore regard vitreous solids as under-cooled fluids.² Whether or not the elementary particles of liquids and vitreous substances are completely unordered, is by no means established with certainty. What we know is, that ordinary liquids certainly are not united in an orderly arrangement as are the elements of a crystal lattice. In fluids or vitreous substances these elementary particles may, however, form long chains or layers fastened together in such a way that at higher temperatures they may, more or less easily, bend or slide over one another in all directions. On the basis of certain observations, A. A. Griffith³ was led to this view.⁴ Such a theory is also supported on the basis of capillarity phenomena by the enormous value of cohesion forces, observed in very thin films of liquids, in very viscous quartz filaments, and in the surface layers of fluids. For example, Griffith took a hardened steel ball, such as is used in ball bearings, and fitted it to a very carefully made hole in a plate, such that there was only an extremely small amount of clearance between the ball and the plate. The ball would easily fall through the hole, if it were dry; however, when a drop of water was placed in the annular space between the ball and plate, the ball stuck in the hole and could only be forced through by applying a large force. According to Griffith, the molecules of water fasten themselves in chains to the surface of the ball and the hole. These

Konzern, vol. 5, pt. 3, 1927) have made very remarkable observations. They obtained, by an etching process, the system of lines on the surface of the balls shown schematically in Figs. 4 to 7. The lines in these figures indicate curves where the mode of reflection changes on the polished and etched surface of the balls. Hausser and Scholz were able to produce, on the surface of balls consisting of single crystals of copper (or silver), a system of lines with a cubic, a pure octahedron, or a pure rhombic dodecahedron symmetry, depending on the particular etching agent or etching procedure.

¹ In "Die Lehre von den flüssigen Kristallen" (Bergmann, Wiesbaden, 1918) Lehmann describes "flowing" and "fluid crystals," using certain substances having a complicated molecular structure but which we may regard as fluid. However, although they may be shown optically to be anisotropic like crystals, x-ray analysis showed that they have no lattice structure (see E. HÜCKEL, Dissertation, Gottingen, 1921).

² TAMMANN, G., "Aggregatzustände, etc." Leopold Voss, Leipzig, 1922.

³ *Loc. cit*

⁴ A spontaneous parallel arrangement of the molecules of a fluid is explained by the electric or magnetic moments produced by these molecules (see E. HÜCKEL, Dissertation, 1921; and BORN: *Ber. d. Berl. Akad.*, 1916.)

chains reach across the circular space between the ball and the hole and by virtue of their great tensile strength hold the ball fast.

It is also apparent that under certain conditions the arrangement of the elements in the structure of a given material may undergo changes caused by the atomic motions set up by heat agitation or also by other possible disturbances in the equilibrium positions of the atoms. For example single atoms or groups of atoms may interchange their location with respect to the boundary surfaces of crystal grains or the two sides of inner surfaces (minute cracks), which may exist in the interior of solid or semi-solid masses. After a sufficiently long time the effects of these small movements become noticeable as plastic flow or they may, for example, be observed by the aid of a microscope in the form of what the metallurgist calls a "re-crystallized grain structure."

CHAPTER 4

EFFECT OF GRAIN STRUCTURE AND OF CHANGING TEMPERATURE UPON THE STRENGTH—TIME EFFECTS

In most solids having a crystalline structure, such as minerals, the commonly used metals and rocks employed as materials of construction, the smallest parts having uniform properties—namely the crystal grains—are at most, of very small dimensions as compared with the dimensions of most material bodies. The mean diameter of these grains is, at most, of the order of a few millimeters; usually it is only $\frac{1}{10}$ to $\frac{1}{100}$ mm. In contrast to this the distance between the elements of a crystal lattice is of the order of 10^{-8} cm. The fine crystalline structure of materials of construction can be observed only with the aid of a microscope. Such study has shown that, for the most important materials, such as pure metals or the alloys of metals the substance with the finest grain in general is the strongest. A metal with a very fine grain has in general a greater strength than a metal with a coarse granular structure. It is more easily worked by rolling, pressing, etc., and its tensile properties are made relatively better by hot working. The structure may, however, be changed by suitable handling.

In order to determine the resistance of solids with respect to permanent change of shape a great many factors must be taken into account. Certain of these factors do not lend themselves to an exact analysis by means of principles of mechanics and they will therefore not be considered here. Reference regarding these important factors must be made to treatises on metallography and the technical production of metals.¹ From the

¹ For the sake of convenience a few books in which these subjects are treated in detail might be quoted here: ALBERT SAUVEUR, "The Metallography and Heat Treatment of Iron and Steel," 3d ed., 535 pp., McGraw-Hill Book Company, Inc., New York, 1926; HENRY MARION HOWE, "The Metallography of Steel and Cast Iron," 641 pp., McGraw-Hill Book Company, Inc., New York, 1916; W. C. ROBERTS-AUSTEN, "Metallurgy," 478 pp., Charles Griffin & Co., London, 1910; S. L. LLOYD, "Metallography," pt. I, Principles, 256 pp., 1920; pt. II, 462 pp., McGraw-Hill Book Company,

following considerations will also be excluded the phenomena of plasticity observed on all those semi-solid substances which contain a more or less fluid constituent at ordinary temperature (wet clay, plastic earthy masses, paints, etc.) or which are mixtures (suspensions, colloidal solutions, etc.) containing solid particles suspended in a liquid.¹

Of the various factors which have an influence on the magnitude of the forces under which a material will yield plastically, the following should briefly be mentioned here:

a. The structure of the material as dependent on the constitution of the substance, especially of alloys.

b. The absolute size of the crystal grains constituting a polycrystalline material.

c. The imperfections and disturbances in the crystal lattice, whether they exist in the union of the atoms inside the crystal lattices or on the surfaces of the grains or finally in the intercrystalline boundary substance separating the grains.

d. The effect of temperature.

e. The effect of time.

A few remarks may explain what is meant by these terms. For example, by dissolving a foreign substance in a metal, the resistance to plastic deformation may be greatly changed. Thus, the mechanical properties of steel in the iron-carbon system are determined by very small amounts of carbon. Pure iron with

Inc., New York, 1921; F. W. HARBOLD and I. W. HALL, "The Metallurgy of Steel," vols. I, II, Charles Griffin & Co., London, 1923; ZAY JEFFRIES and ROBERT S. ARCHER, "The Science of Metals," 460 pp., McGraw-Hill Book Company, Inc., New York, 1924; L. GUILLET and A. PORTEVIN, "Introduction to the Study of Metallography and Macrography," 289 pp., G. Bell & Sons, London, 1922; German books: G. TAMMANN, "Lehrbuch der Metallographie," 2d ed., Leopold Voss, Leipzig, 1921; P. OBERHOFFER, "Das technische Eisen. Konstitution und Eigenschaften," 2d ed., J. Springer, Berlin, 1925; CZOCHRAŁSKI "Moderne Metallkunde in Theorie und Praxis," J. Springer, Berlin, 1924; P. GOERENS, "Lehrbuch der Metallographie," Halle, 1925; F. KOERBER, Schmelzen, Erstarren, Sublimieren, "Handbuch der Physik," vol. 10, Thermische Eigenschaften der Stoffe, J. Springer, Berlin; GUERTLER, "Handbuch der Metallographie," Gebr. Bornträger, Berlin, 1913; G. SACHS, "Grundbegriffe der mechanischen Technologie der Metalle," Akad. Verlag, Leipzig, 1925; A. REJTO, "Einige Prinzipien der theoretischen mechanischen Technologie der Metalle," V.D.I. Verlag, Berlin, 1927.

¹ Cf. BINGHAM, EUGENE C., "Fluidity and Plasticity," 440 pp., McGraw-Hill Book Company, Inc., New York, 1922, regarding the laws of plasticity of these substances.

only small traces of carbon, manganese, etc., is a soft and plastic metal, easily deformed and worked, while a quenched steel having 0.6 to 1.1 per cent of carbon, has a high yield point and is worked only with difficulty. Small impurities influence the yield point of metals, as well as the tensile properties, in a most complicated manner. For example, the minute quantities of gases such as hydrogen, nitrogen, or oxygen, which may be dissolved in a steel have an influence on the yield point and also on the shape of the function which determines the relation between stress and amount of plastic deformation.

The effect of these impurities depends on whether the atoms are dispersed throughout the crystal lattice or form compounds with the metal. These compounds may occur in the shape of inclusions or small crystals, or are distributed along the grain boundaries. Certain foreign substances, which may accumulate along the grain boundaries produce a strengthening effect, as for example, the cementite in the pearlite in steel; in other cases, however, the effect is very injurious. This is the case, for example, with iron sulphide in steel¹ or copper oxide in copper. In these cases the strength is decreased. Although by including small amounts of additional substances consisting of suitable materials, a metal or an alloy may be made considerably stronger with respect to plastic deformation than the pure metal, in other cases, the disturbances or imperfections produced in the lattice of the crystal grains (infinitesimal holes, cracks, and fissures) have the opposite effect and these imperfections tend to diminish the strength of the crystal-grain aggregation considerably.

With regard to the influence of temperature upon the magnitude of the stress at which the material becomes plastic and begins to flow, it may be said that in general the magnitude of the stress necessarily decreases with increasing temperature. Use is made of this important property of matter in the hot working of metallic materials. At forging temperatures, steel and iron are much more easily worked, *i.e.*, plastically deformed, than under ordinary temperatures. At forging heats the forces necessary to produce a given deformation are perhaps one-tenth to one-twentieth those necessary at ordinary temperatures. Amorphous solids also behave similar to crystalline materials with respect to the effect of temperature on the stress necessary

¹ GOERENS, P.: Über Stahlqualitäten und ihre Beziehungen zu den Herstellverfahren, *Kruppsche Monatshefte*, 1927.

to cause plastic flow, although their plasticity must be attributed to a different atomic mechanism than in the case of crystalline matter. They soften gradually under heat.¹

Finally the effect of time on plastic deformation may be briefly mentioned. It is known that the shape of a material body may be greatly changed under small stresses, if only an extremely long time is allowed for the change to take place. The deformation, without fracture, of the rocks in the earth's crust is one of the most striking and best-known examples of this effect. Also in ductile metals, large permanent deformations may be produced by long-time loading, at sufficiently high temperatures.

If we consider only such lengths of time as are necessary for carrying out the usual tensile test, we will come to the conclusion that the stresses at which yielding at normal temperatures begins, depend but slightly on the speed of deformation. An increase in the speed, with which, for example, a test piece of wrought iron is deformed plastically at ordinary temperatures in testing machines, will produce only a relatively small increase in the force corresponding to a given extension. Even if this speed is doubled or increased 10 times, an increase of only a few thousandths or at most a few hundredths in the tensile strength is produced. If, however, we compare the influence of the speed of plastic deformation at the extremely small velocities of deformation occurring in the so-called "long-time tensile tests" at high temperature, it will be seen that a doubling of a load will produce perhaps a doubling of the velocity of extension. Hence, at very small velocities of deformation, we must therefore conclude that the speed has a large influence on the stresses occurring during plastic deformation. In other words, the stress is a function of the velocity of deformation $v = d\epsilon/dt$. Mathematically the stress $s = f(v)$, and this function will probably be a linear function where v approaches 0. Thus at very small velocities of flow $s = \eta v$, where the constant η is very large and largely dependent on the temperature. On the other hand, at values of v and s occurring in the usual tensile test, the stress s in so far as it depends on the rate of flow v , has probably the character of a function:

$$s = s_1 + s_2 \log_e \frac{v}{v_0}$$

¹ Cf. chap. 39 below, regarding the effect of temperature.

where v_0 , s_1 , and s_2 are constants.¹ This question will be treated in more detail later (see chap. 39).

¹ The last relation is confirmed by the beautiful tests of P. LUDWIK, "Elemente der technologischen Mechanik," p. 47, 1909, with tin wires; and the tensile tests of CASSEBAUM, *Ann. d. Phys.*, 4th ser., vol. 34, p. 106, 1911, with soft iron. Regarding long-time tests made in Germany, those of POMP AND DAHMEN, "Die Dauerstandfestigkeit von Eisen und Stahl bei erhöhten Temperaturen," *Werkstoffausschussbericht des V.D.E.*, No. 98, Dusseldorf; and those made by WELTER, *Z. f. Metallkunde*, are of especial interest.

CHAPTER 5

ELASTIC AND PERMANENT DEFORMATION

a. If a bar of ductile metal with a constant cross-section is loaded in a tensile testing machine, it will lengthen uniformly under the action of an applied load. If we mark two lines on this bar and designate the length between these marks as l , under the tension load P , this length will lengthen by an amount Δl . If the extension Δl be plotted against the corresponding load P in a right-angled coordinate system (Fig. 8), these points, in general, will lie on a continuous curve OIA . If the bar, after being unloaded exactly assumes its original length, the extensions under the given loading are called "elastic." The tensile force per unit area of cross-section P/A , where A is the cross-sectional area is called the "unit stress."

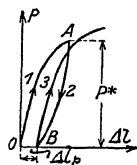


FIG. 8.—Tensile test. P , load; Δl , elongation.

In the following this will be designated by the letter s .

If we unload the bar, after being loaded by a force P^* , the curve on unloading will be as shown in the figure by $A2B$ which is different from the loading curve OIA . If after unloading the point B does not coincide with the initial point O , the length of the bar l has extended permanently by the amount $\Delta l_p = OB$. If the bar is again loaded, we obtain in general a new branch 3, which is different from the unloading curve 2 and which makes a loop with the second branch. There are materials, however, for which the three branches, 1, 2, 3 practically coincide, if the force is below a certain limiting value, with a common straight line.

Such materials are called perfectly elastic materials. The deformations of the crystalline minerals (quartz) and also the initial deformations of certain metals composed of crystal aggregates, below certain limiting loads, approximate the ideal of a perfectly elastic body. For example, the small elastic deformations of a wrought-iron bar in tension are elastic and proportional to the stress as long as the stress $s = P/A$ (the load P divided by the cross-sectional area A) remains below a certain

limiting stress s_0 . In contrast to this, in certain other metals, for example soft annealed copper, the smallest loading produces permanent deformation.

If a wrought-iron bar is loaded in tension by a load P starting from zero, we usually obtain an initial stress-strain curve $P = f(\Delta l)$ such as is represented in the two examples of Figs. 9 and 10. The force P at first increases in exact proportion to the increase in length Δl . At a certain stress $s_0 = P_0/A$ which has a value, for

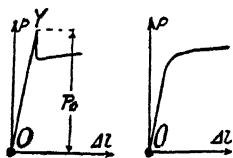


FIG. 9. FIG. 10.

FIGS. 9 and 10.—Load elongation curves showing transition from elastic to plastic stage for mild steel.

soft annealed wrought iron, of between 25,000 to 50,000 lb. per square inch, permanent deformation suddenly begins to appear. This tensile stress s_0 is called the *yield stress* of the iron. At this time a sharp break occurs in the stress-strain diagram (point Y, Fig. 9), and the strains increase greatly after this point is reached. The transition to the horizontal branch of the curve can either begin with a sharp peak and subsequent decrease in the load,

as shown in Fig. 9; or it may be gradual, as shown in Fig. 10. Along the steep straight part of the curve as the load increases, the extension is practically elastic, while after the yield point is reached, large permanent deformations appear.

Besides the curves shown in Figs. 8 to 10, which represent various modes of transition from the elastic to the plastic stage, there occurs frequently in the case of ductile metals a curve such as is represented in Fig. 11. If a bar of soft annealed copper or

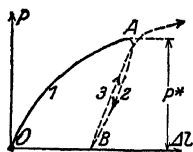


FIG. 11.

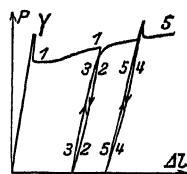


FIG. 12.

FIGS. 11 and 12.—Tensile tests. Figure 11 shows "copper," Fig. 12 "iron" type of load-elongation diagram.

aluminum be loaded in tension, the initial deformation curve $P = f(\Delta l)$ contains no straight portion and no definite yield point exists. The permanent deformations begin gradually to develop at the smallest load and are initially of the same order of magnitude as the elastic deformations. That the yield stress,

however, also has a certain physical meaning in the case of these metals, will be recognized, if, after the bar has been stretched for some time, it be unloaded and again reloaded. We will now consider what happens under such conditions.

It is important to note, that the character of the curve may change after unloading. If the bar is loaded with a force P^* and then unloaded again, the curve drops steeply along the dotted line 2 from A to B in Fig. 11 and often approaches an approximately straight line. If the bar is loaded again, the force increases at first along the line 3, which is almost a straight line. This line bends over, however, at a load which differs but little from the load P^* , with a more or less sharp change in direction, so that the curve again approximates a continuation of the initial curve.

While in the first part of the initial curve $P = f(\Delta l)$ a yield point does not occur, however, after unloading it does appear and is more pronounced the more the metal is strained. The transition between a second loading curve 3-3 (Fig. 12) and a continuation of the initial curve 1-1 may in the case of iron be of various shapes. If the test is only interrupted for a short time by the unloading and the bar is quickly loaded again the curve bends over according to the line 3-3 in Fig. 12. If, however, a long time (several hours or days) occurs between the unloading and subsequent reloading, the yield point is raised, as Bauschinger has established, and the new curve bends over according to the line 5-5. This transition often is such that the sharp peak with subsequent decrease in load which occurred at the yield point Y as shown in Fig. 12 is repeated.¹

If an iron or copper bar be unloaded, after permanent deformation under a tensile load P^* has occurred, and if it be loaded again in the same direction to a load below the load P^* and again unloaded it behaves elastically, similar to a bar in the elastic

¹ This phenomenon is known as "ageing." Regarding these characteristics of load-deformation curves, P. Ludwik came recently to very remarkable conclusions (see "Streckgrenze, Kalt- und Warmspredigtheit," *Z. V. d. I.*, p. 379, 1926). A 1-per cent stretched electrolytic iron, after lying a half hour had its yield point increased over 13 per cent; after 24 hours a 25 per cent increase was noticed and after three months a 33 per cent increase. A very great increase was produced by heating at 100°C., whereupon the yield stress was increased 50 per cent. See also P. LUDWIK and R. SCHEU, *Über die Streckgrenze von Elektrolyt- und Fluss-eisen*, *Werkstoffausschussbericht* 70, 1925.

part OY of the load-deformation curve in Fig. 12. If, however, a test piece of ductile metal, whose stress-strain curve is similar to that shown in Fig. 11 is first loaded in tension to a load P^* , is unloaded, and then subjected to a compression, one obtains the branch of the curve QP^{**} (Fig. 13). This branch is sharply

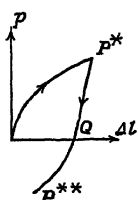


FIG. 13.—
Shape of load-
deformation
curve after re-
versal of load.

curved in contrast to the straighter unloading curve. There has been produced, in effect, a lowering of the yield point for the opposite direction of loading.

The above observations regarding elastic and permanent deformation may be summarized as follows:

1. When a metal is loaded above the yield point in tension or compression, the yield point, for stresses in the same direction, is raised.

2. A soft metal, after plastic deformation in tension, acquires elastic properties, so to say, in a purer form, if it is stressed again in tension. The ability of a metal to behave elastically reappears after a certain plastic deformation.

3. After plastic flow and a reversal of direction of loading (from tension to compression or *vice versa* or from twisting in one sense to twisting in the opposite sense) comparatively large plastic deformations are produced by very small loads.¹ In other words the yield point for the opposite kind of stress is lowered.

b. After-flow.—In the foregoing description of the process of deformation, as a first approximation the question was considered as one under equilibrium conditions. This idea involves the tacit assumption that, in the region of plastic deformation after the interruption of the flow process, all elastic changes in shape depend only on the actual value of the stresses, and are not affected by values of the stresses previously acting. This assumption is the

¹ Certain of these observations were first pointed out by Bauschinger (The behavior of metals mentioned under 3 is sometimes named after him "The Bauschinger Effect.") Recent investigations (W. BADER, W. LÖBE, Dissertations, Göttingen, 1927) have shown that, for example, soft iron exhibits, under certain conditions of stress application, a curved transition from the elastic to the plastic branch of the stress-strain curve. Among the causes for such changes in particular the following may be mentioned: a reversal of the direction of stress, but also a rotation of the directions of the principal stresses in the body, and finally a change in the three principal stresses. Also G. Masing and W. Mauksch have carefully determined the stress-strain curve for brass under alternate tension and compression.

one usually made for elastic deformation. However, more exact observations of the deformation, occurring after a sudden change in the load or after a slow interruption of the flow process, show that the deformation depends on the previous plastic deformation, on the velocity with which the applied forces change, and upon the time which elapses between observations. When a bar flows under an almost constant load, if we consider the processes occurring in the microstructure of the material where the flow has its origin, we are led to believe that we do not have here a state of equilibrium. Furthermore, as has already been mentioned, the stresses occurring during plastic flow at normal temperature depend to some extent on the velocity of flow. A definite time is necessary to bring about the interruption of flow; during this time the material yields to some extent. These phenomena are comprised under the heading "After-flow."

c. Elastic Hysteresis.—Besides the plastic deformation of ductile metals, brittle metals or other materials also show permanent deformations, which probably to some extent are caused by the imperfections of the microstructure. For example, cast iron when stressed in tension or compression behaves to a considerable degree almost inelastically. In tests with such metals the loading and unloading curves contain no straight lines but rather curved ones¹ (Fig. 14), and both curves enclose loops of considerable width, whose area is a measure of the work lost during each reversal of loading. This work is dissipated as heat. This loss, in the case of materials which have a very soft component in their composition, probably is brought about by friction. The best-known example is cast iron with its embedded particles of soft graphite. The phenomenon represented by a stress-strain curve for increasing load differing from that for decreasing load, both curves forming a loop, is called "elastic hysteresis."

Gray cast iron contains from 2 to 3 per cent of graphite. If we assume, according to Bardenheuer, the specific weight of graphite as 2.1 and that of cast iron as 7.3, it will be found that the 3 per cent by weight of graphite corresponds to 10.4 per cent by



FIG. 14.—
Elastic-hysteresis loops.
 P , tensile load; ΔL , elongation.

¹ See BACH, C., and BAUMANN, R., "Elastizität und Festigkeit," 9th ed., Julius Springer, Berlin, 1914. The elastic properties of such materials have been exhaustively investigated by C. Bach especially.

volume, *i.e.*, about a tenth part by volume of cast iron is filled by the soft graphite particles.¹ Under stress the cast iron yields mainly in the soft graphite flakes or temper-carbon particles. The harder constituents of the structure are displaced like rigid bodies along the leaves of graphite; if these minute surfaces, along which sliding occurs, are under pressure, the internal friction tends to prevent this sliding and after the reversal of stress causes a vertical shifting of the stress-strain curve, thus producing what has been described as the phenomenon of "elastic hysteresis."

It is well known, that brittle materials with a comparatively loose grain structure, such as sandstone, concrete, cast iron, etc., under pressure show the phenomenon of the formation of loops in the stress-strain diagram. This indicates, that one main reason for the formation of loops may be attributed to the sliding of the crystal grains on each other under pressure or of aggregates of grains along inner surfaces of imperfections. Such inner surfaces of weakness may be caused by soft inclusions (for example the graphite particles in cast iron) or by minute cracks or also by a weak boundary substance separating the crystal grains.²

¹ BARDENHEUER, *Der Graphit im grauen Gusseisen*, *Stahl und Eisen*, vol. 47, p. 857, 1927.

² It is true, that this explanation in the case of pure tension involves certain difficulties. In the case of pure tension one may expect that the inner surfaces of weakness if situated at an angle to the direction of the tensile stress will open up and thus friction will not act. But it must be noted, that in the vicinity of a small spherical or cylindrical hole subjected to pure tension in some points compressive stresses also act and these secondary compressions may produce friction.

Elastic hysteresis shows in many respects an analogy to the phenomenon of magnetic hysteresis which has been much studied by physicists. A first attempt to work out this analogy and to study the shape of cyclic stress-strain curves, by means of analytic expressions, seems to have been made by Berliner (Dissertation, Gottingen, 1906). Certain inelastic properties of solids were discovered long ago, but it seems that they have been correlated more to what is called "elastic after-effect" (*cf.* below) than to elastic hysteresis. On the other hand, looping in stress-strain curves may easily be produced by plastic flow and what was called above "after-flow." It is therefore first necessary to treat these *three* more or less independent causes of the same or similar effects in stress-strain cycles separately until more complicated cases are considered, in which for example after-flow as well as elastic hysteresis may be combined. Regarding these phenomena *cf.* tests of Ewing, E. Warburg, F. Koerber and W. Rohland (1924), Timoshenko and Lessells, "Applied Elasticity," p. 406, 1925, and many others.—

d. **The Elastic After-effect.**—Besides hysteresis and after-flow the elastic after-effect should be mentioned, a phenomenon, which was first discovered and known long before the others.¹ This effect can be observed for example in materials which are known for their perfect elastic properties, such as glass at low temperatures. It includes phenomena observed for example in elastic springs (the tubes of Bourdon manometers), wires of silica in delicate instruments (galvanometers), also in glass thermometers in the form of recovery, or such as the change in length with time after a load has been removed, or as the slight change of length (drift) of a bar after a load has been applied and held constant for a time. These phenomena have been discussed mathematically by Maxwell and L. Boltzmann. The latter drew interesting conclusions with respect to the action of previous cycles of stress upon the deformations produced by the acting load. If, for example, a cylindrical rod is twisted in one sense, then untwisted, and again twisted in the other sense, in the elastic after-effect both previous cycles of stress may be recognized by a change of sign of the after-effect. The material exhibits a behavior, which might be compared with memory, the material, so to say, recalling the previous types of stress to which it has been subjected.²

L. Prandtl devised a mechanical model for demonstrating hysteresis and suggested a new theory which took into account the effect of the thermal agitation of the molecules on the elastic hysteresis, *Z. fur. ang. Math. u. Mech.*, 1928.—Comparative calculations of the energy loss per cycle and unit volume for a given shape of loop can be found in the valuable paper by G. H. KEULEGAN, Statical Hysteresis in the Flexure of Bars, *Bur. of Stand. Technol. Paper 332*, vol. 21, p. 145, 1926; also 365, vol. 22, 1928.

¹ The elastic after-effect seems to have been discovered by the physicist Wilhelm Weber in 1835.

² G. H. Keulegan calls the hysteresis caused by the elastic after-effect "hereditary hysteresis" in contrast to "static hysteresis," which is what we call "elastic hysteresis."

CHAPTER 6

ON THE MECHANISM OF PLASTIC DEFORMATION IN THE GRAIN STRUCTURE

The elastic deformation of crystalline materials under the action of external forces is the result of distortion of the crystal lattice in which the atoms, ions, or molecules are arranged. Likewise, the volume change and elasticity, with respect to change in shape of vitreous solids and the volume changes of liquids due to pressure, are the consequences of the changes in the distances between the molecules. If we disregard the elastic deformation, which at usual pressures up to several hundred or thousand atmospheres is small in comparison with the possible permanent (plastic) changes in shape, there remain for the explanation of plastic flow in solid materials only the permanent displacements in the relative positions of the elements or atoms in the crystal lattices.¹

Although the mechanism of plastic deformation in the crystal lattice of solid materials is not yet fully known, some typical phenomena likely to occur in combination with plastic flow may be mentioned. The most important of these elementary phenomena are the following:

a. Slip. Parallel displacements ("translations") of the elements of the crystal lattice.

b. Formation of twins. Shifting as a whole, or a part of a crystal, to a second position, symmetrical with respect to certain planes in the lattice of the remaining part of the crystal.

¹ The phenomena occurring during the plastic flow of the crystalline solids are best studied by means of test pieces consisting of single crystals of the size used as specimens for testing of materials. Regarding the mechanical properties and the plastic deformations of metal single crystals which have been the subject of numerous valuable researches in recent years, reference is made to "Handbuch der Physik," vol. 6, chapter on Plasticity, section on Single Crystals. The mechanical laws governing plastic flow in metal single crystals have been particularly elucidated by G. I. Taylor and his collaborators in Cambridge (*cf.* "The Distortion of an Aluminum Crystal during a Tensile Test," Bakerian Lecture, *Proc. Roy. Soc.*, London, Vol. 102, p. 643, 1923, and many others of his papers), by Miss C. J. Elam, by M. Polanyi, by E. Schmid in Berlin, and others.



FIG. 15.—Copper. Initially polished surface of specimen showing numerous slip bands in the crystal grains, after plastic deformation. (Magnification about 100.)

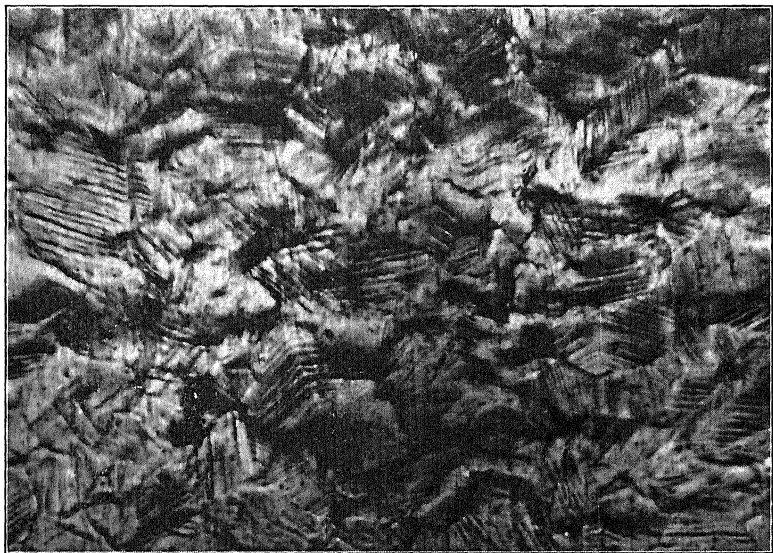


FIG. 16.—Copper. The deformed surface of a highly polished copper piece showing numerous slip bands in the crystal grains. The deformation was produced by the impression of a punch. (Magnification about 100.)

c. Change of position of atoms occurring because of agitation of atoms due to heat.

d. Breakdown of structure, occurring often quite gradually under an increasing load. Displacements of crystal grains accompanied by a partial destruction of the cohesion. This results in a gradual loosening or tearing apart of the structure under increasing stress.

The phenomenon of slip or translation consists of a parallel sliding of parts of a crystal along planes, relative to one other, for distances which are perhaps many thousand times the

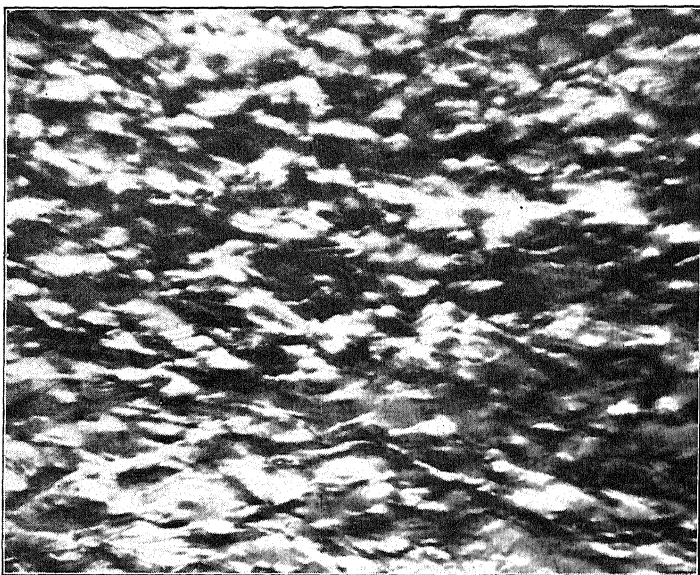


FIG. 17.—Distorted surface of an initially highly polished copper specimen which has been severely deformed. The slip bands can hardly be detected. (Magnification about 100.)

distance between the atoms in the lattice. These displacements usually occur along one or more crystallographically definite planes in the crystal; moreover the directions of sliding coincide with certain crystallographically definite straight lines in the space lattice. Sliding in the grains often occurs in numerous parallel planes, the number of planes increasing with the increasing stress. This type of deformation often is evidenced by numerous parallel strips or markings well observable under the microscope on the surface of a metal crystal, or in the crystal grains of a deformed metal which has been polished before it is subjected to a plastic distortion.

The second kind of phenomena occurring during plastic deformation of a crystal, known as crystal twinning, is a shifting of the position of the lattice in a part of a crystal into a second position, so that the second part is in a symmetrical position relative to the first part and some plane of symmetry. An example is exhibited by the deformation of crystals of calcite. These crystals split if loaded in a suitable way,¹ in the manner shown in Fig. 19. This kind of deformation, also designated by Mügge² as "pure shear," has been observed in the crystal grains of naturally or artificially deformed marble³ and in certain metals.

As has already been mentioned the shear stress, necessary to produce the plastic state, is a definite function of the temperature. Hence in the mechanism of plastic deformation of solid materials under high temperature, the thermal vibrations of the atoms must play an important part. The capacity for forming slip planes in the crystals is considerably increased by heating. Thus, near the melting temperature the formation of slip planes may be brought about by very small shear stresses.

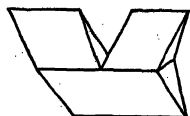


FIG. 19.—Formation of twins in a calcite crystal. (According to Niggli.)

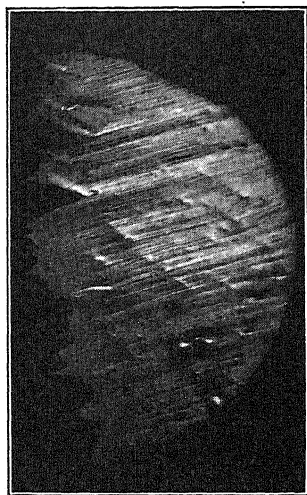


FIG. 18.—Slip bands in a crystal grain of deformed brass.

Noteworthy contributions to our knowledge of the properties of ideal crystals, in line with earlier conceptions of Tammann, were made by R. Becker and A. Smekal.⁴ A visual picture of

¹ Niggli, "Lehrbuch der Mineralogie," p. 176, Gebrüder Bornträger, Berlin, 1920.

² "Kristallphysik, Handbuch der Naturwissenschaften," vol. 5, p. 1135, 1914.

³ See the tests under combined axial and lateral pressure, made with marble test pieces of cylindrical shape by T. v. KÁRMÁN, *Mitt. u. Forschungsarb. V. D. I.*, No. 118, Berlin, 1913.

⁴ BECKER, R., Über Plastizität, Verfestigung und Rekristallisation, *Z. techn. Phys.*, No. 7, p. 547, 1926; SMEKAL, A., Zur Molekulartheorie der Festigkeit und der Verfestigung, *loc. cit.*, No. 11, 1926, and *Akad. d. Wiss. Wien, Anzeiger*, Dec. 2, 1926, Jan. 27, March 17, 1927.

the mechanism of slipping in a metallic crystal, as given by R. Becker, is as follows. We may first conceive of certain layers in the crystal whose boundary planes coincide with definite planes of the crystal lattice. These layers are bounded by rough surfaces. The roughnesses stand out like teeth or bumps and fit in corresponding depressions in the bounding layers. These correspond to the force fields of the atoms. For example, in single crystals of copper, whose atoms form a face-centered cubic lattice, in which the octahedron planes act as slip planes, and the edges of the octahedron represent the direction of slip, the middle points of these bumps must lie upon a net composed of a mesh of equilateral triangles. The forces emanating from the atoms hold the layers together. As soon as the laws obeyed by the inter-atomic forces, are known, it is possible to calculate the shearing force S necessary to cause a displacement of these layers sufficient to bring these bumps opposite each other. This force S would then produce failure by slipping. This theory of action within crystals was extended by R. Becker to include the effects of the thermal agitation of the atoms. In general terms this may be explained as follows: If we assume that the shearing force in the crystal has a value but little smaller than the force S necessary to produce permanent slip, it follows that there will only be elastic deformations in a lattice with the atoms at rest. However, if we consider the thermal vibrations of the atoms due to heat, the picture changes. Since a variable shearing force s is exerted by the vibrating atoms it follows under these conditions that it varies periodically about a mean value S_m . It is thus possible that in certain planes the force s may for an instant become greater than S . When this occurs, as mentioned above, slip in the layers of the crystal follows, where $s > S$. The plasticity of the crystal, according to this theory, is affected by the temperature; the higher the temperature the more frequently will the slip layers occur. The velocity of plastic deformation would depend on the number of planes in which sliding occurs.¹

¹ In a seminar in 1921, L. Prandtl, in considering questions of elastic hysteresis and after-effects, utilized the instability of the quasi-elastic equilibrium of the atoms in solids for the construction of a model to illustrate the process of hysteresis and considered the thermal motion in a similar way to the method used by Becker. See L. PRANDTL, *Z. f. ang. Math. u. Mech.*, vol. 8, p. 85, 1928.

In connection with the above-mentioned conception of Griffith,¹ A. Smekal assumed that crystals (even the most perfect specimens), as well as amorphous solids, are weakened by countless small flaws. By means of ingenious experiments on small bars of rock salt, plastically bent (by coloring them by means of exposure to radium radiation), he was able to show that in the plastically deformed part of rock-salt crystals the loosening up in the lattice was greater than in the unstrained portion. Such changes of the microstructure of ductile metals by means of severe cold working are well known to engineers. The metal becomes "more brittle" after severe cold working.

The plasticity of amorphous materials is, according to R. Becker, determined by the shifting in position of single atoms or molecules from their equilibrium positions. We may conceive that in the inside of solid materials countless minute cracks occur. Under increasing temperature the energy of motion of the atoms at the surface of these cracks, when vibrating about their equilibrium positions, becomes greater and greater. Therefore, certain atoms along the surfaces of these minute cracks will finally attain such large amplitudes of vibration that they approach the force fields of the atoms on the opposite surface of the crack. There they will, therefore, be caught and held by the fields of the atoms on the other side of the crack. In this way the crack will gradually change its shape. Where the cohesion of the material is weakened most by means of these spontaneous opening cracks, both parts of the body will shift with respect to each other by a small amount. The totality of these infinitesimal displacements may be observed as a plastic flow or permanent change in shape of amorphous masses.

On the other hand Polanyi and E. Schmid have shown,² that in metal single crystals plasticity due to ordinary slip can be observed at the lowest possible temperatures (liquid helium). Hence one main part of plasticity due to ordinary slip must be attributed to a mechanism which is not affected by the thermal agitation of the atoms.

F. Zwicky³ has raised doubts against the assumption that the presence of imperfections (minute cracks or flaws) in crystals

¹ *Loc. cit.*

² *Naturwissenschaften*, vol. 17, p. 301, 1929; *cf.* also several papers by E. Schmid in *Z. f. Physik*, 1929 and 1930.

³ The Imperfections of Crystals, *Proc. Nat. Acad. Sci.*, vol. 15, p. 253, 1929. On Mosaic Crystals, *ibid.*, vol. 15, p. 816, 1929; also *ibid.*, vol. 16, p. 211, 1930. See also *Helvetica Physica Acta*, vol. 3, p. 269, Zürich, 1930.

should exert the large effect on certain mechanical properties of the crystals (such as strength, the plastic limit) as had been supposed heretofore.

In the solid state of matter, according to Smekal and Zwicky, two kinds of properties have to be distinguished. Certain physical properties of the crystals are known to be *structure insensitive*, while others are *structure sensitive*. To the first group of physical properties of the crystal lattices belong density, specific heat, elasticity (compressibility), thermal expansion, and others; to the second belong mechanical strength, the limit of plasticity, dielectric strength, certain optical properties, and others. The first kind of properties seem to have about the same values for single crystals as for the polycrystalline material of the same chemical constitution. The latter group seem to be affected more than the former by impurities, by a previous deformation, and by temperature (annealing, tempering).¹

According to Zwicky, there are two reasons against the validity of the assumption that minute cracks and flaws are the main cause of the lowering of the mechanical "molecular" strength as deduced from atomic theory to its actually observed low "technical" values.²

On the basis of these views, one would be led to expect that the behavior of the real crystals would become more similar to that of the ideal crystals, depending on the degree the accidental disturbances during the growing of the crystals are avoided. Observations, however, show that the contrary is true. The second reason is that if the lowering of the strength is caused by a random distribution of minute cracks, the values of the properties observed in actual tests would have to be distributed accord-

¹ Zwicky himself states that there does not exist a sharp limit between these two groups of properties. The elasticity constants or the thermal expansion coefficients of metals, for example, are known to change with increasing temperature to a considerable amount. The variation in these properties is perhaps of the order of 25 to 50 per cent if the metal is heated from room to melting temperature. Possibly some of the structure-insensitive properties change with rising temperature and become at elevated temperatures structure sensitive.

² According to Polanyi and Zwicky and to the atomic theory, the molecular tensile strength of, for example, a rocksalt crystal should be about a tenth of the mean value of the elastic moduli of this substance $s = E/10$ or about 2 to $4 \cdot 10^4$ kg./cm.², while actually rocksalt becomes plastic even at a stress of 20 kg./cm.² or so and breaks at a stress of perhaps 50 kg./cm.².

ing to rules of probability, while as a matter of fact they can be reproduced within comparatively narrow limits.

To avoid these and other difficulties not mentioned here (which arise from the above assumptions, according to Zwicky) small but finite periodic changes consisting of slight variations in the distances within the lattice must be assumed in the crystals. Upon the primary lattice of the ideal crystal, as determined by *x*-ray analysis, secondary disturbances are superimposed, these consisting of small periodic variations of the density or of the distances between the elements of the lattice. The structure-insensitive properties are caused by the primary lattice, the structure-sensitive properties by the secondary disturbances.

These investigations show that the ideal lattice is thermodynamically less stable than the *mosaic crystal*, *i.e.*, a crystal having slight periodic variations (contractions) in the lattice. This secondary structure within the primary lattice would cause effects such as lowering of strength, plastic deformation, and others. To give an idea of the order of magnitude of the blocks caused by the secondary structure, it may be said that the distance between two contracted parts within the lattice of a rocksalt crystal are thought perhaps of the order of twenty times the distances between the elements in the undisturbed lattice, so that the cubic block of the mosaic crystal of rocksalt would contain about 8,000 to 10,000 atoms. This checks with Smekal's previous estimates of the size of the secondary blocks limited by the imperfections.

The phenomenon of a gradual breakdown of the structure with increasing stress consisting in countless relative movements of parts of crystal grains to each other may be also observed on a larger scale. In materials with a relative loose microstructure, a kind of plasticity seems to appear under increasing stress. Permanent deformations result, since the cohesion under the increasing load is gradually destroyed. An extreme case of this kind is illustrated by a conical-shaped body made of paraffin and loaded

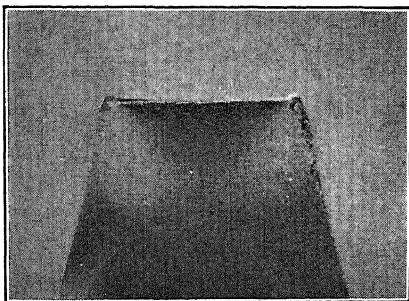


FIG. 20.—Longitudinal section of a paraffin test piece after compression test showing destruction of structure.

under compression (Fig. 20). A longitudinal section of this body shows that the structure is broken down or severely deformed, much worse at certain points than at others. The parts having the destroyed structure are recognized by the discoloration or bright color. Another sample is shown in Fig. 21 exhibiting a remarkably regular system of shear lines. Many brittle materials may behave probably in a similar manner

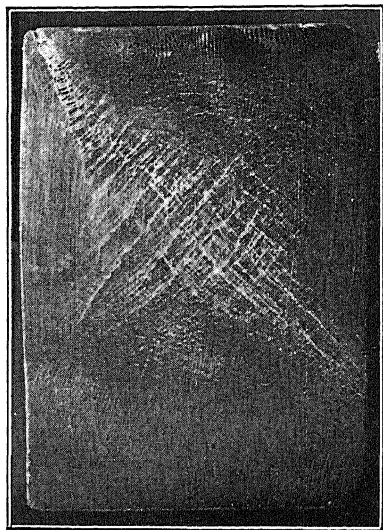


FIG. 21.—Regular markings on face of compressed prism of paraffin.

when stressed by axial compression or tension. The small crystal grains loosen or break prematurely before any motion of translation may occur. For example, in a compression test with a cast-zinc test bar we may observe, simultaneously with the occurrence of slip surfaces in the crystal grains, the appearance of countless fine hair cracks which prematurely destroy the cohesion of the material.

The various phenomena, above considered, characteristic of plastic deformation, often occur in combination with each other. Hence it may not be possible to separate them from one another. This explains the great variations in the mechanical behavior of solids encountered when they are brought into the plastic state.

CHAPTER 7

STRESS

Let us consider a body in equilibrium under the action of external forces. Taking a cross-section of this body and investigating the equilibrium of the forces acting on each part thereof we see that, in general, forces from one part of the body will be transmitted across the cross-section to the other part. The ratio of the force acting on a small portion of the cross-section to the surface area of this portion approaches a limiting value, if this small area is taken smaller and smaller. This limit is called the "unit stress" at the point considered. This stress may be divided into two components, one perpendicular to the cross-section and the other in the cross-section. The former is called a normal stress; the latter a shearing stress. Stresses are designated by the letter s ; normal and shearing stresses in general will be distinguished by subscripts attached to the letter s . Normal stresses are taken positive or negative depending on whether they are tension or compression while the sign of the shearing-stress component may be arbitrarily fixed for each case. In the bodies it will in general be necessary also to consider in addition to these stresses, or forces acting on the surface, the continuously distributed forces due to inertia or weight of the mass.

The stress distribution at any given point in the inside of a stressed body is known, if the normal-stress component s_n and the shearing-stress component s_s at this point are known for each arbitrary position of the cross-section. We may locate the point by means of its coordinates taken with respect to a right-handed rectangular system of axes x, y, z . The position of the cross-section under consideration is determined by the angle which the external normal to this section makes with the positive direction of the axes.

Consider a small element of a stressed body cut out by planes parallel to the planes of the coordinate axes, and having the edges dx, dy, dz . On a cross-section of this element parallel, for

example, to the yz plane, a normal stress s_x will act. The shearing stress acting on this section may be divided into two components s_{xy} and s_{xz} , parallel respectively to the axes y and z . In this method of designation of the stress components, it will be noted that the single subscript of a normal stress such as s_x and the first subscript of a shearing stress such as s_{xy} correspond with the direction of the normal to the section, while the second subscript of s_{xy} indicates the direction in which the component is to be

taken. We thus have the following nine stress components parallel to the various coordinate axes:

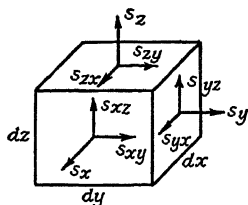


FIG. 22.—Components of stress.

$$\begin{array}{lll} s_x, & s_{xy}, & s_{xz}, \\ s_y, & s_{yx}, & s_{yz}, \\ s_z, & s_{zx}, & s_{zy}. \end{array}$$

These have the meaning and positive directions shown in Fig. 22. From the condition of equilibrium with respect to moments or rotation of the small element (Fig. 22), the shear stress components must satisfy the following equations:

$$s_{xy} = s_{yx}, \quad s_{yz} = s_{zy}, \quad s_{zx} = s_{xz}.$$

Let us now consider a small tetrahedron cut out from the body (Fig. 23) by three planes parallel to the planes xy , yz , and zx and a fourth plane oblique to the coordinate planes. From the condition of equilibrium of the forces acting on the four faces of this tetrahedron the relations between the stresses in the various sections may be determined. If we choose the area of the oblique cross-section equal to unity, the areas of the sides of the tetrahedron parallel to the planes yz , zx , and xy are equal to the direction cosines a_x , a_y , and a_z respectively of the normal n to this oblique cross-section. If we denote by S_x , S_y , and S_z the components of the stress S acting in the oblique cross-section, the equilibrium of the forces acting on the tetrahedron may be expressed by the following three equations:

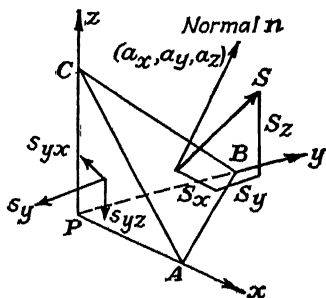


FIG. 23.—Stress components acting in faces of a small tetrahedron.

$$\left. \begin{aligned} S_x &= s_x a_x + s_{xy} a_y + s_{xz} a_z, \\ S_y &= s_{yx} a_x + s_y a_y + s_{yz} a_z, \\ S_z &= s_{zx} a_x + s_{zy} a_y + s_z a_z. \end{aligned} \right\} \quad (1)$$

We now divide the stress S acting on the oblique cross-section into its normal and tangential components s_n and s_s . Since the normal stress s_n is equal to the sum of the projections of the stresses S_x , S_y , and S_z on the normal to the cross-section, we have:

$$s_n = S_x a_x + S_y a_y + S_z a_z \quad (2)$$

and the shearing stress s_s is given by

$$s_s^2 = S^2 - s_n^2 = S_x^2 + S_y^2 + S_z^2 - s_n^2 \quad (3)$$

Substituting in the first of these equations the expressions for S_x , S_y , S_z , given by (1), we obtain the following equation for the normal stress s_n :

$$s_n = s_x a_x^2 + s_y a_y^2 + s_z a_z^2 + 2s_{xy} a_x a_y + 2s_{yz} a_y a_z + 2s_{zx} a_z a_x \quad (4)$$

If from a fixed point O , we lay off a segment $OQ = r$ parallel to the normal (a_x, a_y, a_z) and choose the length of this segment such that its square is inversely proportional to the normal stress s_n , we have:

$$\overline{OQ}^2 = r^2 = x^2 + y^2 + z^2 = \frac{c}{s_n}.$$

Considering that,

$$a_x = \frac{x}{r}, \quad a_y = \frac{y}{r}, \quad a_z = \frac{z}{r},$$

Eq. (4) becomes:

$$c = s_x x^2 + s_y y^2 + s_z z^2 + 2s_{xy} xy + 2s_{yz} yz + 2s_{zx} zx \quad (5)$$

This is the equation of a surface of the second degree. From it we may see how the components of a stress distribution are changed if the direction of the axes xyz is changed into $x'y'z'$. Thus in case of a rotation of the coordinate axes the six stress components are changed in the same way as the constants in the equation of a surface of the second degree. In particular, we may, by rotation of the axes, transform them to coincide with the principal axes of the surface; *i.e.*, we may bring Eq. (5) into a form in which the terms containing xy , yz , and zx do not occur. Therefore, we see that for each state of arbitrary homogeneous stress, there are three mutually perpendicular axes—the principal axes of stress—corresponding to which Eq. (4), for the normal stress s_n takes the simple form:

$$s_n = a_x^2 s_1 + a_y^2 s_2 + a_z^2 s_3 \quad (6)$$

In the cross-sections perpendicular to the principal axes, the normal stress reaches its extreme values s_1, s_2, s_3 . These are called principal stresses; in these cross-sections the shearing stresses must vanish (since the mixed terms do not appear in Eq. [4]).

If we choose the principal axes of the state of stress as coordinate axes x, y, z , Eqs. (1) simplify to the following form:

$$S_x = a_x s_1, \quad S_y = a_y s_2, \quad S_z = a_z s_3 \quad (7)$$

Using Eq. (3) we obtain an expression for the shearing stress s_s ,

$$s_s^2 = a_x^2 s_1^2 + a_y^2 s_2^2 + a_z^2 s_3^2 - (a_x^2 s_1 + a_y^2 s_2 + a_z^2 s_3)^2 \quad (8)$$

CHAPTER 8

MOHR'S REPRESENTATION OF STRESS¹

a. **Mohr's "Stress Plane."**—If s_1, s_2, s_3 represent the principal stresses, a_x, a_y, a_z , the direction cosines of the normal to a given cross-section, and s_n and s_s , the normal and shearing stresses in this cross-section, according to Eqs. (6) and (8), with respect to a system with coordinates x, y, z , coinciding with the directions of principal stress we may express the normal and shearing stresses as follows:

$$s_n = a_x^2 s_1 + a_y^2 s_2 + a_z^2 s_3, \quad (9)$$

$$s_s^2 = a_x^2 s_1^2 + a_y^2 s_2^2 + a_z^2 s_3^2 - (a_x^2 s_1 + a_y^2 s_2 + a_z^2 s_3)^2. \quad (10)$$

To these equations may be added a third:

$$a_x^2 + a_y^2 + a_z^2 = 1. \quad (11)$$

These equations show how the normal and shearing stresses s_n, s_s acting on any cross-section depend on the direction cosines a_x, a_y, a_z of this cross-section, and thus permit a visual represen-

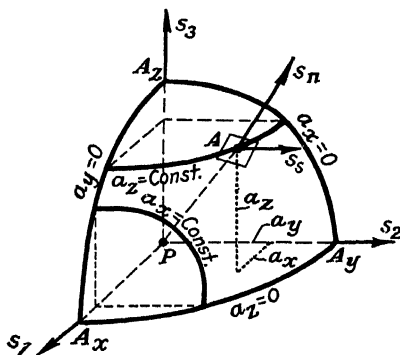


FIG. 24.—Mohr's sphere.

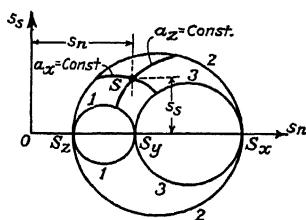


FIG. 25.—Mohr's stress plane.

tation of the stress distribution. By means of Eqs. (9) and (10) a point A (Fig. 24) having the rectangular coordinates a_x, a_y, a_z corresponds to a definite value of s_n and s_s or a definite point S in a "stress plane" (Fig. 25). In this plane the abscissæ are

¹ MOHR, OTTO, "Abhandlungen," 2d ed., W. Ernst u. Sohn, Berlin, 1914.

chosen equal to the normal stress s_n and the ordinates equal to the shearing stress s_s , which act in the section considered. The points A lie upon a sphere (Fig. 24), whose radius is equal to unity, for the coordinates a_x, a_y, a_z of A satisfy Eq. (11).

Solving the three Eqs. (9), (10), (11), for a_x^2, a_y^2, a_z^2 , we obtain:

$$\begin{aligned} a_x^2 &= \frac{(s_2 - s_n)(s_3 - s_n) + s_s^2}{(s_2 - s_1)(s_3 - s_1)}, & a_y^2 &= \frac{(s_3 - s_n)(s_1 - s_n) + s_s^2}{(s_3 - s_2)(s_1 - s_2)}, \\ a_z^2 &= \frac{(s_1 - s_n)(s_2 - s_n) + s_s^2}{(s_1 - s_3)(s_2 - s_3)}. \end{aligned} \quad (12)$$

If, for example, we hold a_x equal to a constant, the points A (Fig. 24) on the sphere $a_x^2 + a_y^2 + a_z^2 = 1$, lie upon a circle which is perpendicular to the a_x -axis. In the "stress plane" s_n, s_s to this circle corresponds a curve, whose equation is obtained from (12) if we hold a_x constant in the first expression. We then obtain:

$$\begin{aligned} &\left(s_n - \frac{s_2 + s_3}{2}\right)^2 + s_s^2 \\ &= (s_2 - s_1)(s_3 - s_1)a_x^2 - s_2s_3 + \frac{(s_2 + s_3)^2}{4} = \text{const.} \end{aligned} \quad (13)$$

With s_n and s_s as variables, this is the equation of a circle with the middle point lying on the s_n axis (Fig. 25) at a distance $(s_2 + s_3)/2$ from the origin and passing through the point S . In Fig. 25 only a small arc of this circle is shown. If $a_x = 0$, the radius of this circle is $(s_2 - s_3)/2$. The three largest circles $a_x = 0, a_y = 0, a_z = 0$ on the sphere (Fig. 24) (see Eq. [11]) correspond, in Mohr's "stress plane" to the three principal circles 1, 2, 3, (Fig. 25). The radii and the distances of the middle points of these circles from the origin are as follows:

$$\frac{(s_2 - s_3)}{2}, \frac{(s_1 - s_3)}{2}, \frac{(s_1 - s_2)}{2}, \quad (14)$$

$$\frac{(s_2 + s_3)}{2}, \frac{(s_1 + s_3)}{2}, \frac{(s_1 + s_2)}{2}. \quad (15)$$

The three principal circles cut off, on the s_n -axis (Fig. 25), the three principal stresses s_1, s_2, s_3 . An octant of the sphere $A_x A_y A_z$ (Fig. 24) with unit radius (Eq. [11]) is represented by the spherical triangle $S_x S_y S_z$ bounded by the three principal circles in Fig. 25.

b. Mohr's Stress Circle for Plane Stress.—We obtain such a stress distribution in the xy plane if we take the normal stress $s_x = 0$ as well as both shearing stresses $s_{xz} = 0$ and $s_{zy} = 0$. Consider a small prismatical element (Fig. 26) formed by two planes parallel to the xy plane, one parallel to the xz plane, and one

parallel to the zy plane together with an oblique plane parallel to the z axis. The equilibrium of the forces is expressed by the following equations:

$$\left. \begin{aligned} s_n \cos \alpha - s_s \sin \alpha &= s_x \cos \alpha + s_{xy} \sin \alpha \\ s_n \sin \alpha + s_s \cos \alpha &= s_y \sin \alpha + s_{xy} \cos \alpha \end{aligned} \right\} \quad (16)$$

In these equations s_n represents the normal stress and s_s the shearing stress in the oblique section, α the angle between the normal to the oblique cross-section and the x axis, and s_x , s_y , s_{xy}

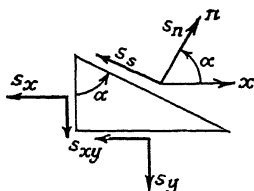


FIG. 26.—Plane stress.

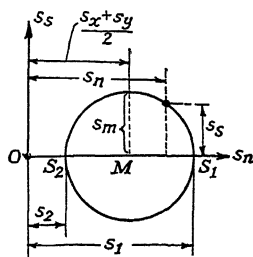


FIG. 27.—Mohr's stress circle for plane stress.

the stress components in the other sections. Solving these equations for s_n and s_s , we obtain:

$$\left. \begin{aligned} s_n &= \frac{s_x + s_y}{2} + \frac{s_x - s_y}{2} \cos 2\alpha + s_{xy} \sin 2\alpha \\ s_s &= -\frac{s_x - s_y}{2} \sin 2\alpha + s_{xy} \cos 2\alpha \end{aligned} \right\} \quad (17)$$

By transposing the term $(s_x + s_y)/2$ in the first equation to the left side, squaring and adding there results an equation of a circle in the variables s_n and s_s :

$$\left(s_n - \frac{s_x + s_y}{2} \right)^2 + s_s^2 = s_m^2; \text{ where } s_m^2 = \left(\frac{s_x - s_y}{2} \right)^2 + s_{xy}^2. \quad (18)$$

The normal stress s_n reaches its extreme value at the points S_1 and S_2 of the stress circle (Fig. 27), if:

$$\frac{ds_n}{d\alpha} = 0, \quad \tan 2\alpha' = \frac{2s_{xy}}{s_x - s_y}, \quad (19)$$

while the shearing stress s_s reaches its extreme values at the points where:

$$\frac{ds_s}{d\alpha} = 0, \quad \tan 2\alpha'' = -\frac{s_x - s_y}{2s_{xy}}.$$

Since

$$\tan 2\alpha' \cdot \tan 2\alpha'' = -1, \quad (20)$$

the shearing stresses reach their extreme values in sections which make angles of 45° to the axes of principal stress. From Eq. (18) of the stress circle, by putting $s_s = 0$, we obtain the following values of principal stresses:

$$s_1 = \frac{s_x + s_y}{2} + s_m, \quad s_2 = \frac{s_x + s_y}{2} - s_m. \quad (21)$$

The absolute value of the largest shearing stress is:

$$s_{\max} = s_m = +\sqrt{\frac{(s_x - s_y)^2}{4} + s_{xy}^2}. \quad (22)$$

This is also equal to the radius of the stress circle:

$$s_m = \frac{|s_1 - s_2|}{2}.$$

Conversely if both principal stresses s_1 and s_2 of a state of plane stress and the angle α which the algebraically larger principal stress s_1 makes with the x axis, are given, the three components s_x , s_y , s_{xy} may be computed using the equations:

$$\begin{aligned} s_x &= \frac{s_1 + s_2}{2} + \frac{s_1 - s_2}{2} \cos 2\alpha, \\ s_y &= \frac{s_1 + s_2}{2} - \frac{s_1 - s_2}{2} \cos 2\alpha, \\ s_{xy} &= \frac{s_1 - s_2}{2} \sin 2\alpha. \end{aligned} \quad (23)$$

We may write these equations as the conditions of equilibrium of a small prismatical element bounded by the sections across which the principal stresses s_1 , s_2 act and by an oblique section chosen parallel either to the x or to the y axis.

c. The Principal Shearing Stresses.—The values of principal shearing stresses are defined as the radii of Mohr's three principal circles (Fig. 25),

$$t_1 = \frac{s_2 - s_3}{2}, \quad t_2 = \frac{s_3 - s_1}{2}, \quad t_3 = \frac{s_1 - s_2}{2}. \quad (24)$$

From these we see that

$$t_1 + t_2 + t_3 = 0. \quad (25)$$

Since we may resolve the general case in three states of plane stress, for the general state of stress, according to Mohr's circle, the maximum shearing stress occurs at sections making angles of 45° with the sections across which the principal stresses act.

If we place a cube (Fig. 28) in such a way that its sides coincide with the planes of principal stress, the sections of principal shearing stress, if $s_1 \neq s_2 \neq s_3$, form a rhombic dodecahedron surround-

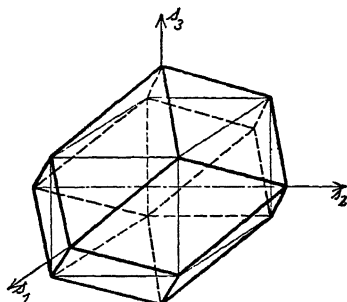


FIG. 28.—The cube is oriented with its faces perpendicular to the principal stress directions. The faces of the rhombic dodecahedron are parallel to the planes of principal shearing stress.

ing the cube. The directions of the principal shearing stresses form a regular octahedron whose corners lie upon the principal axes. Using t_1 , t_2 , t_3 the shearing stress s_s at any given cross-section may be expressed according to Eq. (10) as follows:

$$s_s^2 = 4(a_x^2 a_y^2 t_3^2 + a_y^2 a_z^2 t_1^2 + a_x^2 a_z^2 t_2^2). \quad (26)$$

CHAPTER 9

STRAIN

If we wish to determine the change in shape of a body under stress, we have to compare the position of its material points in the unstrained state with their position in the strained state.

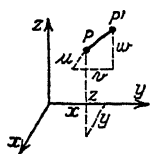


FIG. 29.

Thus, when a body distorts under stress, a point P (Fig. 29) is displaced from its initial position with the coordinates x, y, z to some point P' having the coordinates x', y', z' . The components of the segment PP' (Fig. 29) parallel to the coordinate axes are:

$$u = x' - x, \quad v = y' - y, \quad w = z' - z.$$

These three components of displacement u, v, w of the point P are in general functions of the coordinates x, y, z and the time.

The simplest cases of strained bodies are those in which the displacements u, v, w are linear functions of the coordinates x, y, z . In this kind of deformation, all points, which initially lie in a plane, after distortion lie again upon a plane; moreover, parallel planes after stressing remain parallel. For example, if all points are displaced parallel to the x axes, the displacements u being proportional to x , and $v = w = 0$ we have:

$$u = cx, \quad v = 0, \quad w = 0.$$

This first type of homogeneous deformation is called pure extension in the x direction. If, however, all points are displaced in a direction parallel to the x axis through distances proportional to y , we have:

$$u = cy, \quad v = 0, \quad w = 0.$$

This second type of homogeneous deformation is called simple shear. The measure of the extension of the body parallel to the x axis, in the first case, is the extension per unit length or the *unit extension*. In the above case of shear all planes originally parallel to some definite plane, for example the xz plane, slide in a definite direction without changing their distances from each

other. These displacements are proportional to their distances from the given plane. The measure of shear is the *unit shear*, or the distance, by which two of these planes, of unit distance apart, are displaced with respect to each other.

In the case of two pure extensions in two given directions, the length of all straight lines which are perpendicular to the plane containing the axes of the two extensions is not changed. From this it follows that the most general case of linear strain is produced by three pure extensions, which are, however, not parallel to any single plane. Hence this case is represented by the three linear homogeneous functions:

$$\left. \begin{aligned} x' &= \alpha_x x + \beta_x y + \gamma_x z, \\ y' &= \alpha_y x + \beta_y y + \gamma_y z, \\ z' &= \alpha_z x + \beta_z y + \gamma_z z. \end{aligned} \right\} \quad (1)$$

In this case it is assumed that the initial point O , having the coordinates $(0, 0, 0)$, does not change its position. The deformation given by these Eqs. (1) may be visually described as follows: Consider the sphere whose coordinates satisfy the equation:

$$x^2 + y^2 + z^2 = r^2 \quad (2)$$

We may think of this sphere as described inside the body, its center being at the origin O and ask to find the distortion it will undergo under stress. If we introduce in Eq. (2) the values of x, y, z obtained by solving (1) there results a function of the second degree in x', y', z' . Since according to (1) x', y', z' are everywhere finite, the surface can only be an ellipsoid. Its middle point is the point O . Consider a cube circumscribed about the sphere in the undistorted condition. Under strain this cube becomes an oblique-angled parallelepiped circumscribing the ellipsoid while three mutually perpendicular diameters of the sphere result in three conjugate diameters of the ellipsoid. Since this must also hold for those three mutually perpendicular diameters of the sphere, which after distortion become the principal axes of the ellipsoid, *i.e.*, which before distortion were perpendicular and which after distortion again are mutually perpendicular, it may be recognized that each case of linear distortion may be divided into: (1) three pure extensions of the body along three mutually perpendicular directions and combined with (2) a rotation of the body such as to bring these three directions into coincidence with three other mutually perpen-

dicular straight lines, namely, the principal axes of the ellipsoid. Since a rotation of a rigid body about a fixed point is described by three parameters, while Eq. (1) contains nine constants, we see that the case of pure strain may be described by six quantities.¹

¹ Examples of various kinds of deformation are the following:

1. Volumetric extension without change in shape:

$$u = cx, \quad v = cy, \quad w = cz.$$

The angles remain constant.

2. Longitudinal extension with constant volume:

$$u = cx, \quad v = -c'y, \quad w = -c'z, \\ c' = 1 - \frac{1}{\sqrt{1+c}}.$$

3. Pure shear:

$$u = cx, \quad v = -\frac{c}{1+c}y, \quad w = 0.$$

In this case a certain rhombus $ABCD$ (Fig. 30) is changed under strain into

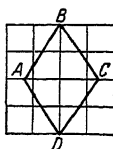


FIG. 30.

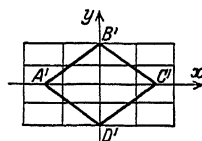


FIG. 31.

FIGS. 30 and 31.—Pure shear. Left initial, right final state of strain.

a congruent rhombus $A'B'C'D'$ (Fig. 31), in which the acute angles and the obtuse have been interchanged.

4. Simple shear:

$$u = cy, \quad v = 0, \quad w = 0.$$

Two groups of straight lines under this state of strain remain of constant length, namely, the straight line $y = \text{constant}$ and the straight lines $y =$



FIG. 32.

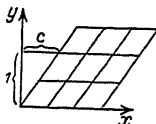


FIG. 33.

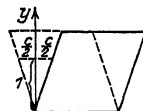


FIG. 34.

FIGS. 32 to 34.—Simple shear. Left initial, right final state of strain.

$-\frac{2x}{c} + \text{constant}$. Under strain the last group of straight lines becomes the lines $y = \frac{2x}{c} + \text{constant}$, as shown in Figs. 33 and 34. This type of deformation is well known in the case of plastic deformation of crystals. For the case of calcite see Fig. 19 (p. 33).

The most general expression for the components of the displacement u, v, w in the case of pure strain without rotation is given by the three symmetrical functions:

$$\left. \begin{aligned} u &= \epsilon_{xx}x + \frac{\epsilon_{xy}}{2}y + \frac{\epsilon_{xz}}{2}z, \\ v &= \frac{\epsilon_{yx}}{2}x + \epsilon_{yy}y + \frac{\epsilon_{yz}}{2}z, \\ w &= \frac{\epsilon_{zx}}{2}x + \frac{\epsilon_{zy}}{2}y + \epsilon_{zz}z, \end{aligned} \right\} \quad (3)$$

provided that in this expression $\epsilon_{xy} = \epsilon_{yx}$, . . . Since the three extensions

$$u = \epsilon_{xx}x, \quad v = \epsilon_{yy}y, \quad w = \epsilon_{zz}z$$

produce no rotation of the principal axes and this is also true of shearing displacements having the form (see Fig. 35):

$$u = \frac{\epsilon_{xy}}{2}y, \quad v = \frac{\epsilon_{yx}}{2}x, \quad w = 0$$

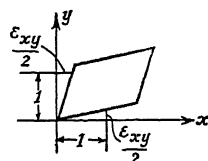


FIG 35.

Eq. (3) is a case of pure strain without rotation.

The unit extension ϵ_r of a radius $r = OP$ of the sphere given by Eq. (2) is:

$$\epsilon_r = \frac{\overline{OP'} - \overline{OP}}{\overline{OP}} = \frac{r'}{r} - 1. \quad (4)$$

The extension ϵ_r takes on its extreme values $\epsilon_1, \epsilon_2, \epsilon_3$ along the principal axes of the ellipsoid. The values $\epsilon_1, \epsilon_2, \epsilon_3$ are called "principal extensions." If, under strain, the directions of principal extensions remain fixed, the strain, taken with respect to these axes as coordinate axes, is given by the three equations:

$$u = \epsilon_1 x, \quad v = \epsilon_2 y, \quad w = \epsilon_3 z. \quad (5)$$

The coordinates x, y , and z are transformed to the new coordinates x', y', z' , by the following equation:

$$x' = (1 + \epsilon_1)x, \quad y' = (1 + \epsilon_2)y, \quad z' = (1 + \epsilon_3)z \quad (6)$$

The radius vector r' becomes:

$$r'^2 = x'^2 + y'^2 + z'^2 = (1 + \epsilon_1)^2 x^2 + (1 + \epsilon_2)^2 y^2 + (1 + \epsilon_3)^2 z^2 \quad (7)$$

If we take:

$$a_x = x:r, \quad a_y = y:r, \quad a_z = z:r. \quad (8)$$

as the direction cosines of the radius vector r in the unstrained body, the unit extension ϵ_r of the radius r' after strain is given, using (4), (7), and (8), by the following equation:

$$(1 + \epsilon_r)^2 = (1 + \epsilon_1)^2 a_x^2 + (1 + \epsilon_2)^2 a_y^2 + (1 + \epsilon_3)^2 a_z^2. \quad (9)$$

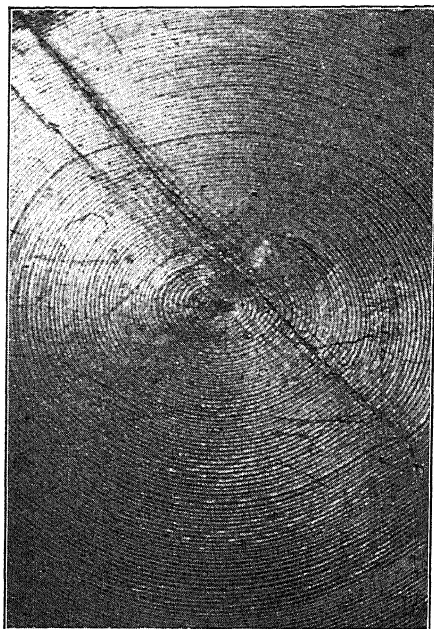


FIG. 36.—Strain ellipses on compression test piece of paraffin.

On one side of the specimen circular scratches were cut by turning the face in a lathe. The ellipses shown in the photograph were formed by the compression from the circular scratches. By this method the axes of principal strain in a state of plane stress and the magnitude of the principal strains can be determined experimentally.

CHAPTER 10

INFINITESIMAL STRAIN

The equations for a pure strain (not containing a rotation) have, as we have seen, the form:

$$\left. \begin{aligned} u &= \epsilon_x x + \frac{\epsilon_{xy}}{2} y + \frac{\epsilon_{xz}}{2} z, \\ v &= \frac{\epsilon_{yx}}{2} x + \epsilon_y y + \frac{\epsilon_{yz}}{2} z, \\ w &= \frac{\epsilon_{zx}}{2} x + \frac{\epsilon_{zy}}{2} y + \epsilon_z z. \end{aligned} \right\} \quad (10)$$

In order that u, v, w , remain small in comparison to the coordinates x, y, z , the constants ϵ_x, \dots must be small relative to unity. The constants $\epsilon_x, \epsilon_y, \epsilon_z$ are the unit extensions in the direction of the axes x, y, z , and $\epsilon_{xy} = \epsilon_{yx}, \epsilon_{yz} = \epsilon_{zy}, \epsilon_{zx} = \epsilon_{xz}$ are the unit shears. By means of these equations the components of the displacement u, v, w may be represented as linear functions of the three components x, y, z , of a second vector r , in a way similar to that in which the three components S_x, S_y, S_z of the stress vector S in Eq. (1), page 41, were given as depending on the three direction cosines a_x, a_y, a_z . We obtain, therefore, the expressions for the strain from the corresponding laws for the case of stress if we replace in all equations referring to the state of stress the six components of stress:

$$s_x, \quad s_y, \quad s_z, \quad s_{xy}, \quad s_{yz}, \quad s_{zx},$$

by the six components of strain:

$$\epsilon_x, \quad \epsilon_y, \quad \epsilon_z, \quad \frac{\epsilon_{xy}}{2}, \quad \frac{\epsilon_{yz}}{2}, \quad \frac{\epsilon_{zx}}{2}$$

If Eqs. (10) are referred to the principal axes of the strain, they become, taking $\epsilon_1, \epsilon_2, \epsilon_3$ as principal extensions:

$$u = \epsilon_1 x, \quad v = \epsilon_2 y, \quad w = \epsilon_3 z. \quad (11)$$

In any given direction the extension is equal to:

$$\epsilon = a_x^2 \epsilon_1 + a_y^2 \epsilon_2 + a_z^2 \epsilon_3. \quad (11a)$$

In this a_x, a_y, a_z are the direction cosines of the given arbitrary direction. We obtain this equation if the squares of ϵ_1, \dots

are neglected in Eq. (9). On account of the complete analogy between stress and strain a further enumeration of the expressions for the strain corresponding to Mohr's expressions for stress (page 43) will not be given here.

If the unit extensions and shearing strains change from place to place and are functions of the coordinates, we proceed as follows. Consider the change in length and change in angles of a small element $dx dy dz$. Since a length dx parallel to the x axis changes under strain by a value $\frac{\partial u}{\partial x} dx$, the unit extension in the x direction is $\epsilon_x = \partial u / \partial x$. Corresponding to this $\epsilon_y = \partial v / \partial y$ and $\epsilon_z = \partial w / \partial z$. The three unit extensions in the direction of the x, y, z axes are therefore:

$$\epsilon_x = \frac{\partial u}{\partial x}, \quad \epsilon_y = \frac{\partial v}{\partial y}, \quad \epsilon_z = \frac{\partial w}{\partial z}. \quad (12)$$

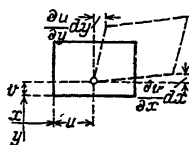


FIG. 37.

Furthermore, during deformation the right angle between the edges dx and dy (Fig. 37) of an infinitely small parallelepiped changes by a small value $\epsilon_{xy} = \frac{\partial u}{\partial y} + \frac{\partial v}{\partial x}$. The unit shearing strains in the material are therefore:

$$\epsilon_{xy} = \frac{\partial u}{\partial y} + \frac{\partial v}{\partial x}, \quad \epsilon_{yz} = \frac{\partial v}{\partial z} + \frac{\partial w}{\partial y}, \quad \epsilon_{zx} = \frac{\partial w}{\partial x} + \frac{\partial u}{\partial z}. \quad (13)$$

The volume of this right-angled parallelepiped $dx dy dz$ in the distorted condition is $(1 + \epsilon_x)(1 + \epsilon_y)(1 + \epsilon_z)dx dy dz$. If the strains are small the increase in volume is:

$$e = \epsilon_x + \epsilon_y + \epsilon_z = \frac{\partial u}{\partial x} + \frac{\partial v}{\partial y} + \frac{\partial w}{\partial z}. \quad (14)$$

Here e is called the cubical dilatation.

CHAPTER 11

LIMITING STATES OF STRESS

One of the most important problems in strength of materials is to determine the mechanical conditions which cause materials to become plastic or which cause fracture in engineering structures. Ordinarily it is assumed that there are a variety of states of stress in which a stressed body may either greatly change its shape plastically or else fail by fracture. In the determination of the danger of plastic deformation only the mechanical conditions depending on stress and strain will be considered here. It has already been pointed out that, besides the circumstances mentioned above, the causes of plastic deformation must be formulated in a more general way. There are for example materials that have no definite yield point in their initial stress-strain curves; in these the transition from elastic to plastic deformation occurs gradually (see Fig. 11, page 24). The plastic deformation depends also on the previous stressing of the material. Relatively small forces may at high temperature produce large permanent deformations, if they are of sufficient duration. All these considerations which may under certain conditions not be neglected, will at first be disregarded in the following treatment, the mechanical conditions producing failure alone being considered.

Since the state of stress in any material body is determined by six quantities, for example by the three principal stresses and the directions of the principal axes, the state of stress which is just necessary to produce failure by plastic yielding or by fracture may be represented by three quantities, for example, the three principal stresses s_1, s_2, s_3 . These values may be visually represented by the rectangular coordinates of a point P . The totality of the points P representing different states of stress just necessary to produce yielding or plastic deformation forms a surface:

$$f_1(s_1, s_2, s_3) = 0 \quad (1)$$

which we will call the *limiting surface of yielding*.

According to previous knowledge it may be assumed that most solid materials will withstand very high pressures without fracture if the pressure acts uniformly from all sides. Hydrostatic pressures, such as may be produced in liquids or which must exist at great depths in the ocean, will produce, in general, in solid bodies not only elastic but also permanent deformation. Materials with a loose or porous structure, such as wood, will undergo, under high hydrostatic pressure, large permanent deformation. Crystalline solids (metals, impervious rocks) under these conditions are, however, compressed chiefly in an elastic way. With respect to their compressibility the impervious polycrystalline solid materials behave similar to liquids. The general behavior of matter under high hydrostatic pressure has been already noted (see page 10). Suffice it to say here that compact solid materials, when subjected to high hydrostatic pressure, behave like elastic bodies and will withstand such pressures to almost any possible value. In less compact solid materials, subjected to fluid pressure, however, marked evidences of failure have repeatedly been observed, for example, in marble (Kármán) and in wood (A. Föppl). These evidences of failure have revealed a secondary effect. If special precautions were not taken, the liquid, used to transmit pressure, penetrates the material. This results in opening up countless fine fissures and cracks in the inside of the material. The flow of the liquid in these cracks involves a pressure gradient, with the result that the edges of the canals or cracks are not under a pure hydrostatic state of stress. The liquid penetrating the pores tends to burst or explode the material. This crumbling may be prevented if the body is surrounded by a thin metal sheet such as a brass sheet, which prevents the entrance of the liquid into the pores of the material.¹

In contrast to this behavior of materials under high pressure, it is quite certain that solids under a uniform tension acting in all

¹ Further noteworthy observations on this bursting action of a liquid used to transmit pressure were made by Bridgman, who found that cylinders of hardened chrome-nickel steel were less able to withstand an internal pressure if the liquid transmitting the pressure was mercury instead of viscous oil. It appears that the hardening cracks in this material aid in the premature destruction of the pressure vessel, if the small atoms of the mercury are able to penetrate these cracks. On the other hand, the large molecules of the oil are not able to penetrate the cracks so easily. The presence of stresses set up by quenching may have a further deleterious effect upon the strength of vessels exposed to high hydrostatic pressures.

directions ($s_1 = s_2 = s_3$) are only able to resist certain definite stresses. Under these conditions no plastic deformation has been observed. In many materials a simple tension (only one of the three principal stresses being positive and different from 0) alone suffices to rupture the body, without appreciable plastic deformation. For such materials, in the region of tensile stresses, there corresponds to the totality of limiting states of stress s_1, s_2, s_3 just sufficient to rupture the body, a second surface:

$$f_2(s_1, s_2, s_3) = 0 \quad (2)$$

We will call this the *limiting surface of rupture*.

From physical conceptions it must be assumed that a definite time is necessary for slip to take place along the slip planes of a crystal. Plastic deformation occurs in a finite time and with a definite velocity. Tensile tests have shown that the stress at which flow takes place increases with increasing velocity of extension; under ordinary conditions, however, the influence of the speed of testing on the stresses, occurring during plastic flow, is relatively insignificant. If, on the other hand, the increase in force occurs so suddenly that plastic deformation has, so to say, no time to occur, failure will obviously occur by fracture. For example, a piece of pitch, if loaded slowly, will deform permanently, while under impact it breaks like brittle glass. All hard materials behave in a similar way if they are only loaded sufficiently fast. If we think of a bar submerged in a liquid exposed to high pressure to which a tensile load is suddenly applied, it may be expected that it will fracture without appreciable plastic deformation. The limiting *surface of rupture* must therefore, under such conditions, have a meaning even in the domain of compressive stresses.

Although test results, relative to the limiting stress distributions at which materials begin to flow or break, are available in large number,¹ the more exact form of both surfaces:

$$f_1(s_1, s_2, s_3) = 0, \quad f_2(s_1, s_2, s_3) = 0 \quad (3)$$

¹ A summary of these investigations is given in several textbooks on strength of materials. Compare especially an article by VON KÁRMÁN, Festigkeitsprobleme im Maschinenbau, in "Encyclopädie der math. Wissenschaften," vol. IV, art. 27; and of P. ROTH, Die Festigkeitstheorien und die von ihnen abhängigen Formeln des Maschinenbaues, *Z. f. Math. u. Phys.*, 1902. See also VON KÁRMÁN, Festigkeitsversuche unter allseitigem Druck, *Mitt. u. Forschungsarb. d. V. D. I.*, Heft 118, and on recent tests W. LODÉ: Versuche über den Einfluss der mittleren Hauptspannung auf das

is for the most important materials, not known with the certainty that could be desired.

By means of these two limiting surfaces, a general mechanical property of all solid materials is described in a very inclusive way, which has found its expression in daily usage. The engineer describes his materials of construction as *ductile* or as *brittle*, depending on whether or not they undergo much permanent deformation before fracture.

Tests of materials carried out under high pressure show however, that the so-called "brittle" materials, without exception, may, under suitable mechanical conditions, be brought into the plastic state. It is therefore more correct to speak, not of brittle or ductile materials, but rather of the brittle or the plastic state of these materials.

In solid materials a fracture by tearing apart of the material following plastic deformation may occur under increasing stress in various ways. The occurrence of these fractures sets a definite limit to the strength of materials. On account of the fairly complicated conditions existing in the mechanism of plastic deformation of crystal-grain aggregations, of which most solid materials are composed, it can scarcely be expected that conditions causing fracture of materials may be predicted by means of simple rules. The behavior of a material under similar mechanical conditions, for example, under tension, under compression, or under torsion may vary considerably. There are materials, for example, wrought iron, soft-annealed copper or aluminum, or pure metals, which behave plastically in the ordinary tensile tests. Other materials, such as cast metals with impurities, cast iron, granite, glass, do not behave as plastic materials when tested in tension or compression in the usual manner. In still other materials, such as impure cast zinc, plastic behavior occurs to some extent under compression, but not under tension. The mechanical conditions necessary to produce a fracture are in such cases not easily predetermined, the more so because such a failure is often the result of a gradual loosening of the texture of the material. In other cases, failures result from sudden disturbances of equilibrium, or because of the instability of the equilibrium of the forces acting on the stressed body.

Fließen der Metalle Eisen, Kupfer, und Nickel, *Z. f. Phys.*, vol. 36, p. 913, 1926; and Dissertation, Göttingen, published in *Mitt. u. Forschungsarb. V.D.I.*, No. 303, Berlin, 1928.

CHAPTER 12

THEORIES OF STRENGTH AND RELATED TESTS

Because of their historic value a few of the earlier theories relative to the conditions causing failure of material by fracture or plastic yielding may here be briefly mentioned.¹ In describing these theories it should be noted that they were referred originally to very different modes of failure, for example, some referred to failure by yielding, while others to such completely different phenomena as failure by fracture.

a. Maximum Stress Theory.—According to this theory the maximum principal stress in the material determines failure regardless of what the other principal stresses may be. According to this theory, material will fail when the maximum principal stress is equal to the ultimate strength determined by a tensile test, regardless of the values of the other principal stresses. That this theory is not correct for determining the condition under which materials become plastic will be realized if one remembers that according to this hypothesis all materials should yield plastically when subjected to sufficiently high hydrostatic pressure. This as we found above is not the case.

b. Maximum Strain Theory (Theory of the so-called “equivalent stress,” *St. Venant*).—According to this theory the maximum positive elastic extension of the material in a stressed body determines failure by fracture or by plastic flow. Since the maximum positive elastic extension for pure compression is $\epsilon = \nu s$, where ν is Poisson’s ratio and s the compression stress, the yield stress for compression, according to this theory, must be three or four times that for tension (the number ν lies between $\frac{1}{3}$ and $\frac{1}{4}$ for most metals). This is not the case for ductile metals. In the improved form of this theory, in which, for negative extensions, also a definite limiting value but different from that for tension should exist, the theory likewise cannot hold. For, under sufficiently high hydrostatic pressure, the maximum limiting strain must certainly be reached and therefore, according to this theory, the material should fail. However, as we have seen, most metals are able to withstand any arbitrary amount of hydrostatic pressure without failure or without starting to yield plastically.

c. Theory of Constant Energy of Deformation. (*Beltrami*).—The total energy stored in a material as elastic energy before reaching the plastic state can have no significance as a limiting condition, since tests under high

¹ MOHR, OTTO, “Abhandlungen aus dem Gebiete der technischen Mechanik,” 2d ed., p. 192, W. Ernst u. Sohn, Berlin, 1914.

hydrostatic pressure show that very large amounts of elastic energy may be stored without the occurrence of fracture or permanent deformation.

d. Maximum Shear Theory.—Extrusion tests on the flow of metals through orifices led Tresca to the assumption that the criterion for the occurrence of the plastic state was not a limiting value of one of the principal stresses characteristic of a given material but rather their greatest difference. Long before, however, it had been assumed, in a theory by Coulomb, that permanent deformation in a compression test, because of yielding of the material, resulted in definite layers at an angle to the direction of the compression. In these layers certain relations between the stresses were fulfilled. According to the views of Tresca and others, permanent deformation should occur in the planes of the maximum shear t_{\max} . These planes are at an angle of 45° to the direction of the largest and smallest principal stress s_1, s_3 . The condition for yielding is according to this theory (see Eq. (24) page 46)

$$t_{\max} = \frac{s_1 - s_3}{2} = \text{const.} \quad (1)$$

The behavior of materials under high pressure and also under other conditions is predicted by this theory in a satisfactory manner. Likewise certain

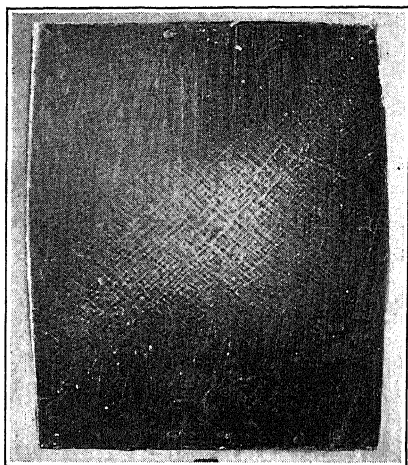


FIG. 38.—Pattern of strain or flow figures appearing on face of a paraffin prism after compression.

observations with respect to flow figures (Lüders' lines) tend to confirm it. These strain or flow figures are regular markings which one may produce on the surface of strained bodies under favorable conditions. Essentially they consist of the traces of layers along which a part of the material has slid with respect to the remainder.¹ According to the maximum shear

¹ The strain or flow figures which accompany the transition from the elastic to the plastic state in mild steel will be described later in more detail (*cf.* Chaps. 16, 17).

theory, the planes of this sliding should coincide with the planes of maximum shear. This we find to be approximately true in mild steel in which the slip layers practically coincide with the planes of maximum shear. On the other hand, for brittle materials which do not behave plastically under the usual tensile or compressive loading, the angle of the slip planes differs considerably from the direction of the surfaces of maximum shear. Likewise in these materials the observed values of the tensile and the compressive strength are not equal. This latter fact is obviously in contradiction to

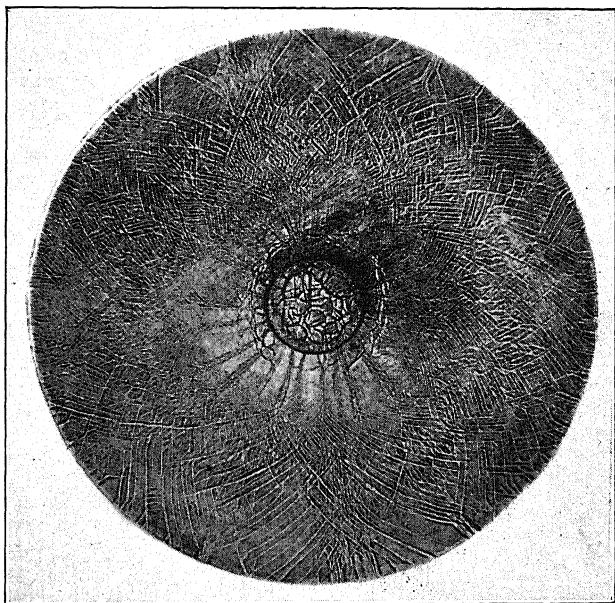


FIG. 39.—Strain figures on a circular steel plate deformed by a load at center.
(According to L. Hartmann.)

the maximum shear theory, which would demand that the tensile and the compressive limit of plasticity should be equal for a given material.

e. **Mohr's Theory.**—Since the occurrence of the plastic state in ductile metals apparently depends upon the value of the shearing stress in the surface along which slip occurs, Mohr¹ gave this condition a more general meaning when he assumed that, besides the shearing stress, the normal stress in the slip planes has also an influence on the occurrence of the plastic state. According to Mohr: "the elastic limit and ultimate strength of a material are determined by the stresses in the planes of slip and of fracture," and "the shearing stress s_s in the planes of slip reaches at the limit a maximum value dependent on the normal stress s_n acting in the same planes and on the properties of the material."¹ These limiting conditions may, in a

¹ *Loc. cit.*, p. 59.

convenient way, be described by means of Mohr's representation of stress (see page 43). Any point P in the "stress plane" with the coordinates s_n and s_s corresponds to a definite value of normal stress s_n and shearing stress s_s acting in a given cross-section.

As shown above the state of stress is given by the three principal stress circles. The condition that the limiting shearing stress s_s in the slip surface

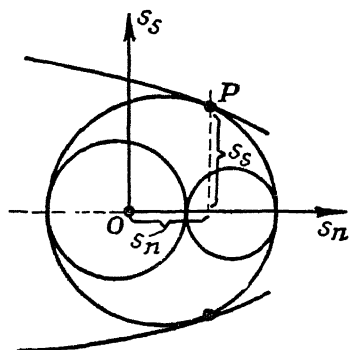


FIG. 40.—Mohr's enveloping (limiting) curve of the largest principal stress circles. The abscissæ s_n and the ordinates s_s of the points P on the enveloping curve indicate the value of the normal and the shearing stress acting in the planes of slip, along which the material will yield.

is a function of the normal stress s_n acting on this surface is expressed by a curve $s_s = f(s_n)$ in the s_n, s_s plane. This limiting curve may not be cut at any place by a stress circle. For, if it would be cut by the largest principal stress circle, there would exist shearing stresses which would be greater than their values along the limiting curve. This latter must, therefore, be the envelope of all the largest principal circles. The largest principal circles representing the states of stress at the limits of plasticity or at the limits of fracture have an enveloping curve which is represented in Fig. 40 by the two heavy lines. The analytical expression for this condition is that if $s_1 > s_2 > s_3$, at the limit $(s_1 - s_3)$ must be a function of $(s_1 + s_3)$. To each limiting condition correspond two slip planes whose intersection lies in the

direction of the mean principal stress s_2 and which make equal angles with the direction of the largest and smallest principal stresses s_1 and s_3 . The mean principal stress s_2 is, according to this assumption, without influence on the shape of the envelope of all the largest principal circles and, hence, upon the occurrence of the plastic state.

The correctness of the assumptions made by Mohr seems to be verified by numerous observations which have been made on the occurrence of slip lines or figures. These figures appear on the surface of stressed bodies after the limit of plasticity has been reached (*cf.* Chaps. 16, 17) and can be explained as the intersections of two thin layers of material with the surface, the plastic deformations in these layers, for a short time, being larger than in the vicinity. These two surfaces of slip always intersect in the direction of the mean principal stress s_2 and make an angle greater than 45° with the algebraically greatest principal stress s_1 . Mohr's theory explains and accounts for an interesting fact, namely that the angle of these surfaces of slip (with the principal stress s_1) may change from material to material and also under work hardening. The more brittle a material becomes because of work hardening, the more the angles seem to differ from 45° , while they tend to approach 45° for very ductile metals, such as soft steel or annealed copper. The different values of the tensile and compressive strengths at the yield point, observed in some materials and test results, taking note of the position and shape of the fractured surfaces in tensile and compression

tests, appear to confirm some of the fundamental assumptions on which Mohr's strength theory is based.

There are, however, two facts which seem to establish difficulties regarding certain predictions of this theory of strength. One is that fracture of brittle materials in tension, or under states of stress with two or all three principal stresses positive (tensile), does not follow the laws as expressed by an enveloping curve of the greatest stress circles. The other is the observed effect of the mean principal stress s_2 on the condition of yielding. According to Mohr's assumptions the shape of the characteristic enveloping curve of all the principal stress circles for all limiting stress distributions, producing yielding, should not depend on the mean principal stress. If, for example, a material would yield in tension under the same stress as in compression, so that the largest principal stress circle for both cases (pure tension, pure compression) would have the same diameter, the yield stress in pure shear should be equal to one-half the value of the yield stress either in tension or in compression. This has not been verified, as recent tests made with such materials show a ratio considerably higher than one-half. Some remarks regarding these points will be made in the following.

f. Tests Relative to Conditions of Yielding in Polycrystalline Materials.—Among the recent experimental investigations on this subject those of J. Guest¹ with ductile metals; of A. Föppl² with rock materials; of T. v. Kármán³ with marble and sandstone under combined stress; of R. Böker⁴ with the same substances and zinc; of F. B. Seely and W. I. Putnam⁵ with steel; of F. E. Richart, A. Brandtzaeg, and R. L. Brown⁶ with concrete under combined stress; of the author and W. Lode⁷ with iron, copper and nickel; of P. Ludwik⁸ with steel and other metals; and of M. Ros and A. Eichinger⁹ with metals and rock materials might be mentioned here.¹⁰ J. Guest carried on his tests with thin

¹ *Phil. Magazine*, 1900.

² *Mitt. a. d. Mech. Tech. Laboratorium*, München, 1900.

³ *Forschungsheft* 118 and *Z. d. V. D. I.*, 1911.

⁴ *Dissertation*, Techn. Hochschule, Aachen, 1914.

⁵ *University of Illinois Bull.* 115, vol. 17, Eng. Exp. Sta., 1919.

⁶ *University of Illinois Bull.* 185, vol. 26, Eng. Exp. Sta., 1928.

⁷ *Berichte des Werkstoffausschuss, V.D.E.*, Düsseldorf, 1925; also *Proc., 2d Intern. Congress of Applied Mechanics* in Zürich, 1926; and W. Lode, *Mitt. u. Forschungsarb.*, Heft 303, 1928.

⁸ *Bruchgefahr und Materialprüfung, Ber. 13. Schweiz. Verband f. Materialprüfungen*, Zürich, November, 1928; cf. also his "Elemente der technologischen Mechanik," Julius Springer, Berlin, 1909; and many other reports in the *Z. d. V. D. I.* and in *Stahl und Eisen*, in recent years.

⁹ *Proc. 2d Intern. Congress of Applied Mechanics*, in Zürich, 1926, also *Ber. 28, Eidgen. Materialprüfungsanstalt*, Zürich.

¹⁰ A more detailed discussion of these tests is contained in W. Lode's paper quoted above.

tubes of steel, iron, and copper. These were subjected either to pure axial tension, to axial tension simultaneously with internal hydraulic pressure, or to a twisting moment and a tensile force. The diameters of the largest principal (Mohr's) circles representing the state of stress at the yield points were found for these ductile metals to be equal, except for small differences which were especially noticeable for the case of pure torsion ($s_1 = c$, $s_2 = 0$, $s_3 = -c$). These tests indicated therefore an approximately constant value of the maximum shearing stress at the yield point. The mean principal stress did not appear to have a marked influence.

In the tests of A. Föppl cubes of rock were loaded in a special apparatus upon two or four sides and tested in compression to failure. The result was that the mean principal stress appeared to be without influence on the breaking strength. Only tests to fracture were made.

Relative to the plasticity of materials, which under an ordinary tensile or compression test behave in a brittle manner, the tests under axial and simultaneous lateral pressure by T. v. Kármán and R. Böker may be mentioned. Both loaded cylindrical test pieces of marble and sandstone either in axial compression or in a steel vessel under axial compression combined with lateral hydraulic pressure. The results of their tests may be summarized as follows: With increasing hydraulic pressure the diameter of the largest principal Mohr's circle increased and approached a limit for the highest hydraulic pressures. The determination of this maximum diameter proved difficult in these tests under the higher pressures, since the marble possessed, under these circumstances and the high pressures, a steep stress-strain curve having no definite yield point. With respect to the influence of the mean principal stress no conclusion could be drawn from these tests. However, the acute angles which the slip planes made with the direction of the principal compression were measured in the test pieces and were also determined from the Mohr limiting curve. In the enveloping curve of the principal stress circles the angle which the normal of the limiting curve makes with the s_n axis is the angle of the slip planes (Figs. 41 and 42). On account of the large plastic deformation, the angle observed at the end of a test had to be corrected to allow for the change in shape of the test piece. In this way a satisfactory agreement between the measured and calculated angles of slip was obtained.

These angles increased in plastic marble from 53° with no hydraulic pressure to 73° with a hydraulic pressure of 685 atm. The tests showed that a low pressure corresponds to behavior as a "brittle" material with a small angle of slip, while the large pressure corresponds to behavior as a "plastic" material with an angle of slip which approaches 90° .

If we plot the maximum difference in principal stresses $s_1 - s_2$, under constant external pressure, as ordinates, against axial compression as abscissæ, we obtain "deformation curves" under various external pressures. These are represented in Fig. 43 for the Kármán tests on marble.

In this figure we see the various well-known types of stress-strain curves of brittle, of partially brittle, and of ductile materials to appear

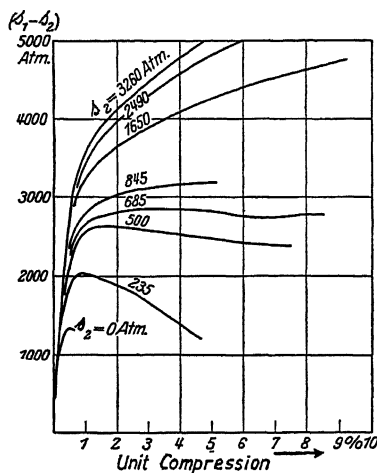


FIG. 43.—Kármán's compression tests with marble cylinders tested under combined axial and lateral hydraulic pressures. s_1 axial compressive stress, s_2 lateral hydraulic pressure. The principal stress difference $s_1 - s_2$ is plotted against the axial unit compression, while in each test the lateral pressure s_2 was kept constant.

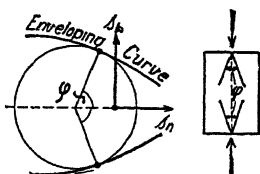


FIG. 41. FIG. 42.

FIGS. 41 and 42.—The normal to Mohr's enveloping (limiting) curve determines the angle ϕ between slip planes.

in one and the same material. If the stress-strain curve of the marble had a sharp break corresponding to a very definite yield point with subsequent decrease in stress (see curve for 235 atm. pressure in Fig. 43), very pronounced flow or slip lines were noted on the material. Under the higher external pressures, the test pieces under compression exhibited a comparatively more uniform bulging, than under the lower external pressures, when they bulged out only in the middle. After an ordinary compression test, the microstructure of the material showed countless fine cracks and fissures and the crystals appeared to have loosened along their boundaries. On the other hand, if the marble was deformed *plastically*, "twin

markings" in the grains were especially numerous. The lateral hydrostatic compression had prevented the breaking

up of the marble crystals. Although marble is brittle under ordinary conditions of loading, these tests clearly show that under high mean pressures it became considerably plastic. Consequently the calcite crystals composing marble deformed by twinning as mentioned before on page 33.

g. The Influence of the Mean Principal Stress on the Yielding of Metals.—Regarding this question W. Lode,¹ at the suggestion of the author, has carried out a great number of tests at the Institute for Applied Mechanics at the University of Göttingen

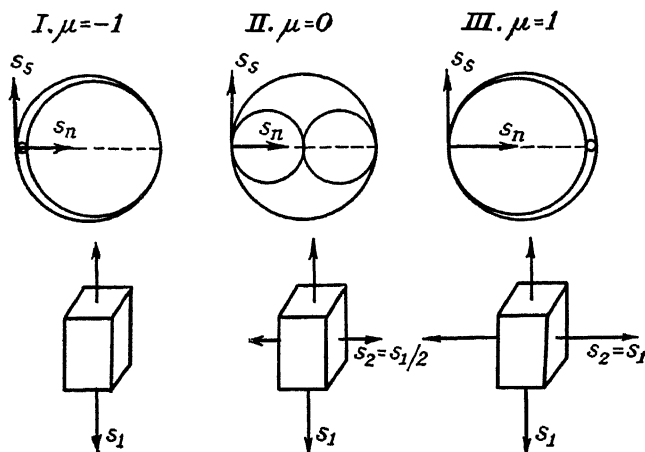


FIG. 44.—Principal stress circles for Lode's three states of stress, I, II, III, produced in thin-walled tubes subjected to combined axial tension and internal hydraulic pressure. I. For tube under axial tension alone, II. for tube under internal pressure alone; and III. for tube under combined action of both.

(Germany). In thin-walled tubes of iron, copper, and nickel subject to axial tension combined with an internal hydraulic pressure, it was found possible to produce three states of stress in the region of tensile stresses, which for the sake of brevity will be designated by I, II, and III and which in a certain sense could be considered to correspond to the simple cases of pure tension, pure compression, and of pure shear. Mohr's principal stress circles of these three states of stress are shown in Fig. 44. Since the mean principal stress s_2 in the stress distribution I was equal to the smallest principal stress, in the stress distribution III it was equal to the largest principal stress, and in the stress distribution II equal to half the largest principal

¹ Cf. footnote on p. 63.

stress (in all three cases the smallest principal stress being approximately or exactly equal to zero), the influence of the *mean* principal stress on the value of the diameter of the largest principal circle should in these tests be quite marked. Moreover, the simultaneous small change of the mean tension $(s_1 + s_2 + s_3)/3$

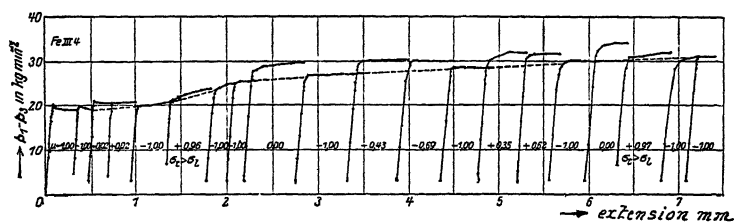


FIG. 45.—Lode's tests with steel tube under various combined tensile stresses. Abscissa: axial extension of 100 mm. gage length in millimeters. Ordinates: greatest principal stress difference in kilograms per square millimeter.

could be neglected since its influence on the characteristics of ductile materials is small. With one test piece a number of stress-strain curves were taken. In plotting stress-strain diagrams one of the three principal extensions (for example, the extension of the specimen along the axes) was taken as strain and difference of the largest and smallest principal stress, as stress. Curves plotted in this manner are shown in Fig. 45. The dis-

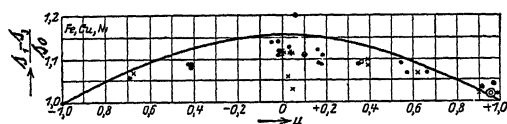


FIG. 46.—Variation of the greatest principal stress difference with intermediate principal stress according to Lode's tests.

turbing influence of the gradual strengthening of the metal, due to progressive plastic deformation (work hardening), was in this way eliminated. The results of various tests are represented in Fig. 46. In this figure the abscissa μ represents a quantity dependent upon the mean principal stress s_2 :

$$\mu = \frac{s_2 - \frac{s_1 + s_3}{2}}{\frac{s_1 - s_3}{2}} \quad (2)$$

This quantity may have values between -1 and $+1$.¹ As

¹ See Fig. 49 and p. 77.

ordinates in this figure the ratios of the stress difference $s_1 - s_3$ to the yield stress for pure tension s_0 were plotted.

I. We see that to "pure tension" correspond the values of $\mu = -1$, $s_2 = s_3 = 0$. (Axial tension acting on the tube.)

II. To "pure shear" correspond $\mu = 0$, $s_2 = s_1/2$, $s_3 = 0$. (The tube is subjected to internal hydraulic pressure.)

III. To "pure compression" correspond $\mu = 1$, $s_2 = s_1$, $s_3 = 0$. (Internal pressure and axial tension [see Fig. 44, case III].)

The observed points in Fig. 46 may be represented by means of a parabolic curve passing through the points $\mu = -1$ and $\mu = +1$, $(s_1 - s_3):s_0 = 1$, and having its vertex in the middle of the interval at $\mu = 0$ and $(s_1 - s_3):s_0 = \sim 1.12$. Instead of this curve another of similar shape has been traced in Fig. 46 having its vertex at $\mu = 0$ and $(s_1 - s_3):s_0 = 1.155$, the significance of which will be explained in the next chapter.

Summing up the results of Lode's tests we see that the mean principal stress s_2 , contrary to what should be the case corresponding to the Mohr theory, shows a marked influence on the diameter of the largest principal stress circle. For such ductile materials as mild steel or copper, which have the same yield stress in pure tension or in pure compression $= \pm s_0$ according to the theory of maximum shear and Mohr's generalized theory the yield stress in pure shear ($\mu = 0$) should be equal to $s_0:2 = 0.500s_0$, whereas the tests of Lode clearly indicated that this latter was considerably greater, about $= 0.56s_0$.

The tests of Seely and Putnam and of Ros and Eichinger, referred to above, indicated a similar conclusion. Seely and Putnam found, that the correct value of the elastic shearing strength of steel as measured by the proportional limit (or a useful limit point) is from $55/100$ to $65/100$ of the elastic tensile strength.

h. Fracture.—A few remarks relative to certain differences exhibited by the appearance of the surfaces of rupture may now be opportune. If a piece of brittle material, of glass or cast iron, for example, is dropped on the floor and broken, the surface of rupture has in general a smooth appearance. A closer investigation shows that the surface of rupture through a tensile test specimen always runs in a direction perpendicular to the tensile stress. On the contrary, if a cast-iron cylinder or prism is broken in an ordinary compression test, the surface of rupture is always inclined to the direction of compression

Furthermore, this surface has quite a different appearance and often contains many fragments. The Mohr theory cannot account for these observations, which seem to indicate that there is apparently a fundamental difference in the two types of rupture, namely by tensile and by compression stresses. As the questions regarding the conditions of rupture seem to be of a much more complex nature than those determining the conditions of plasticity in solids, these questions cannot be discussed further here. Reference in connection with this matter will only be made to the beautiful tests of A. A. Griffith,¹ which have thrown new light on the general conditions under which rupture in amorphous solids occurs, by introducing into the discussion and treatment of this phenomenon a new element, namely, the condition of instability and the energy of surface tension.

¹ The Theory of Rupture, *Proc. 1st Intern. Congress for Applied Mechanics*, p. 55, Delft, 1924.

CHAPTER 13

NEW THEORIES

In reviewing the facts mentioned in the preceding chapter and in attempting to develop those available for the formulation of a mathematical theory in order to explain the experimental results, we may find it convenient to summarize the results of the tests mentioned above as follows:

1. By means of the Mohr theory the behavior of materials, such as brittle rocks, under compression and under conditions which produce plastic deformation is satisfactorily explained. This is not the case with the maximum shear theory.

2. Since recent tests on ductile materials have shown that the mean principal stress has an influence on the radius of the largest principal stress circle, the Mohr envelope of the maximum stress circles loses its meaning as a general limiting curve of all possible largest stress circles.

3. Failure by tensile fracture does not follow the conditions specified by the Mohr theory.

4. The Mohr assumption of an envelope of the maximum principal stress circles involves considerable difficulties with respect to a mathematical formulation of the conditions of plasticity. These are also found if the simplest special case of the Mohr theory, namely, the maximum shear theory is considered and an attempt is made to formulate mathematically the conditions of plasticity. H. Hencky¹ and R. von Mises² have shown that the mathematical difficulties may be avoided if the conditions for the occurrence of plasticity are formulated in a slightly different way.

The relations between these theories may be more easily visualized if we represent the shape of the *limiting surface of*

¹ Zur Theorie plastischer Deformationen, etc., *Z. ang. Math. u. Mech.*, vol. 4, p. 323, 1924; and Über das Wesen der plastischen Verformung, *Z. V. D. I.*, vol. 69, p. 695, 1925.

² Mechanik der festen Körper im plastisch-deformablen Zustand, *Nachr. d. Gesellsch. d. Wissensch. zu Göttingen, Math.-phys. Klasse*, 1913.

yielding $f_1(s_1, s_2, s_3) = 0$, according to the suggestions of Haigh¹ and H. M. Westergaard² by means of a right-angled coordinate system with the coordinates s_1, s_2, s_3 . By means of this system the various theories described in Chap. 12, a, b, c, etc., may be visually represented.

In this way the maximum stress theory is represented by a cube with the boundary surfaces $s_1 = \pm k$, $s_2 = \pm k$, $s_3 = \pm k$, since according to this theory each of these stresses acts as a limiting stress independently of the others.

The maximum strain theory is represented by an oblique parallelepiped. The condition that the principal extension, for example $\pm \epsilon_1 = \frac{1}{E}[s_1 - \nu(s_2 + s_3)]$, has a constant value, corresponds in the stress space to two parallel planes oblique to the axes. A diagonal of the parallelepiped must coincide with the space diagonal of the first octant.

If we consider the plane $s_1 + s_2 + s_3 = 0$, i.e., all stress distributions having the mean value of principal stresses equal to 0 and determine the points for which according to the maximum shear theory, the maximum shear stress has a constant value $s_{s\max} = k$, we find that they lie along a regular hexagon in this plane. If,

for example, $s_1 > s_2 > s_3$, $s_{s\max} = \frac{s_1 - s_3}{2} = k$. In the stress space the equations $s_1 + s_2 + s_3 = 0$ and $s_1 - s_3 = 2k$ represent a straight line which passes through both points $s_1 = 4k/3$, $s_2 = s_3 = -2k/3$ and $s_1 = s_2 = 2k/3$, $s_3 = -4k/3$. In a similar way are obtained the other sides of the hexagon. All states of stress having zero mean tension, in which the limits of plasticity have not been reached must therefore lie within a regular hexagon having the corners:

$$s_1 = \pm \frac{4k}{3}, \quad s_2 = s_3 = \mp \frac{2k}{3},$$

$$s_2 = \pm \frac{4k}{3}, \quad s_3 = s_1 = \mp \frac{2k}{3},$$

$$s_3 = \pm \frac{4k}{3}, \quad s_1 = s_2 = \mp \frac{2k}{3}.$$

¹ The Strain Energy Function and the Elastic Limit, *Engineering*, vol. 109, p. 158, 1920; and *Repts. Brit. Association*, 1919, 1921, 1923.

² On the Resistance of Ductile Materials to Combined Stresses, *Jour. Franklin Inst.*, May, 1920.

The sides of this hexagon have the length $2\sqrt{\frac{2}{3}}k$. From this it follows that the yield-point surface corresponding to the maximum shear theory is a hexagonal prism having the above determined regular hexagon as a base. The axis of this prism makes equal angles with the coordinate axes. When superimposing tension or compression acting equally in all directions on the above stress distributions, the hexagon is only displaced parallel to itself in the direction of the space diagonal of the first octant of the axes s_1, s_2, s_3 .

The discontinuities inherent in the maximum shear theory (the limiting surface of yielding consists of six different planes in the stress space) were eliminated by von Mises by the use of an expression which corresponds to a continuous surface. He assumed for the limiting surface of yielding the equation:

$$(s_1 - s_2)^2 + (s_2 - s_3)^2 + (s_3 - s_1)^2 = 8k^2 = \text{const.} \quad (1)$$

This equation apparently represents a circular cylinder circumscribed about the six-sided prism representing the maximum shear theory. Its axis makes equal angles with the three coordinate axes and has the direction cosines $1/\sqrt{3}$. Its radius is $2\sqrt{\frac{2}{3}}k$. That this surface is a circular cylinder may be determined by finding the intersections of the surface with the coordinate planes (which are obviously ellipses).

It was shown later,¹ that the expression on the left side of the equation has a definite physical meaning. It represents, except for a constant factor, the potential energy of distortion stored in the material under pure elastic strains. If we take, for example, $\epsilon_1, \epsilon_2, \epsilon_3$, as principal extensions, E the modulus of elasticity, $G = \frac{E}{2(1 + \nu)}$, the modulus of rigidity, and ν Poisson's ratio, the total energy stored in the material per unit volume by elastic distortion is:

$$\frac{(s_1 \epsilon_1 + s_2 \epsilon_2 + s_3 \epsilon_3)}{2} \quad (2)$$

¹ Cf. HENCKY, H., Zur Theorie plastischer Deformation, *Z. f. ang. Math. u. Mech.*, vol. 4, p. 323, 1924. In the discussion of this condition of plasticity at the First International Congress for Applied Mechanics in Delft (1924) it developed that M. I. Huber (Lemberg) had also independently suggested Eq. (1) as the condition of yielding.

If we replace here the principal unit extensions $\epsilon_1, \epsilon_2, \epsilon_3$ by the principal stresses s_1, s_2, s_3 using Hooke's law for elastic deformation:

$$\left. \begin{aligned} E\epsilon_1 &= s_1 - \nu(s_2 + s_3), \\ E\epsilon_2 &= s_2 - \nu(s_3 + s_1), \\ E\epsilon_3 &= s_3 - \nu(s_1 + s_2), \end{aligned} \right\} \quad (3)$$

we obtain:

$$\frac{1}{2E}[s_1^2 + s_2^2 + s_3^2 - 2\nu(s_1s_2 + s_2s_3 + s_3s_1)]. \quad (4)$$

If we subtract from this energy of deformation the work:

$$\frac{(s_1 + s_2 + s_3)(\epsilon_1 + \epsilon_2 + \epsilon_3)}{6} = \frac{(1 - 2\nu)(s_1 + s_2 + s_3)^2}{6E}, \quad (5)$$

which is used in changing the volume, we obtain, for the stored elastic energy used in changing the shape per unit volume, the expression:

$$A = \frac{1}{6G}\{s_1^2 + s_2^2 + s_3^2 - (s_1s_2 + s_2s_3 + s_3s_1)\},$$

or

$$A = \frac{1}{12G}[(s_1 - s_2)^2 + (s_2 - s_3)^2 + (s_3 - s_1)^2]. \quad (6)$$

The principal stress differences appearing in this expression are according to Chap. 8, c page 46, equal to:

$$s_1 - s_2 = 2t_3, \quad s_2 - s_3 = 2t_1, \quad s_3 - s_1 = 2t_2,$$

if t_1, t_2, t_3 represent principal shear stresses. The energy due to change in shape may then be written as follows:

$$A = \frac{1}{3G}(t_1^2 + t_2^2 + t_3^2).$$

For simple tension where the principal stresses s_2 and s_3 are zero this energy at the yield point of the material $s_1 = 2k$ is according to Eq. (6) equal to:

$$A = \frac{s_1^2}{6G} = \frac{2k^2}{3G}. \quad (7)$$

Comparing Eqs. (1) and (6), it is seen that the condition of plasticity of von Mises and Hencky is identical with the requirement that the energy due to change in shape should have the constant value given in Eq. (7). The equation representing the condition of yielding:

$$\frac{(s_1 - s_2)^2 + (s_2 - s_3)^2 + (s_3 - s_1)^2}{6} = 8k^2 = 2s_0^2 \quad (8)$$

may also be written in the form:

$$\underline{t_1^2 + t_2^2 + t_3^2 = 2k^2} \quad (9)$$

In this $s_0 = 2k$ is the yield stress in simple tension.

The stresses t_1, t_2, t_3 in a coordinate system with the coordinates t_1, t_2, t_3 , correspond to the intersection of a sphere having the equation given by Eq. (9) with the plane $t_1 + t_2 + t_3 = 0$. We see therefore that the principal shearing stresses t_1, t_2, t_3 at the plastic limit have a limiting curve which is obviously a circle with the radius $\sqrt{2} \cdot k = s_0/\sqrt{2}$. According to this condition a material stressed in pure shear $t_2 = t_3 = t_1/2$ will begin to flow under a maximum shear stress of:

$$t_1 = \frac{2}{\sqrt{3}}k.$$

This means that yielding begins at a shear stress $t_1 = s_0/\sqrt{3} = 0.577s_0$, where s_0 is the yield stress in tension.

In Fig. 46, page 67, the parabolic curve represents the position of the limits of yielding according to this condition of plasticity. As will be recognized from this figure the test points obtained by W. Lode come quite near to this curve.¹

¹ As mentioned in their paper: *Versuche zur Klärung der Frage der Bruchgefahr*, *Erdgen. Material Prüfungsamt*, Zürich, 1926, M. Ros and A. Eichinger were led to similar results. According to tests of American engineers (see the work of W. Lode and H. Hencky, *loc. cit.*), it appears that the yield point for soft metals in pure shear possesses a value 0.6 of the yield point in tension.

A further generalization of the condition of plasticity Eq. (8) may be referred to here. This generalization was suggested by F. Schleicher, *Z. f. ang. Math. u. Mech.*, vol. 6, p. 199, 1926, to explain the behavior of materials in which the shearing stresses in the slip planes depend on the pressure or on the normal stresses acting across these planes.

CHAPTER 14

THE STATIONARY FLOW OF A PLASTIC MASS

We now consider the simplest case of the slow flow of a plastic mass in which the change in shape of the mass is relatively small. At the same time the plastic part of the extension may be regarded sufficiently large so that the elastic part is negligible compared to it. We also assume that at each position in the slowly flowing mass both the value and the direction of the principal stresses are known, and that the directions of the principal stresses at a given point do not change during the flow. In line with these assumptions we may postulate that the principal stresses s_1 , s_2 , s_3 will change but slightly in magnitude and direction during the motion. In order to define the deformation of the mass we may consider a small cube at an arbitrary point in the body in its initial condition. We will take the sides of this cube in the planes of the principal stresses. The question, as to what deformation of the plastic mass under the given stress distribution is to be expected, may be formulated as follows: In which way will a small cube the edges of which are parallel to the directions of principal stress distort? Does the material yield in the direction of mean principal stress s_2 and if so, what increase in extension occurs along the corresponding edges of the small cube? The answers to these questions may be stated in the form of three rules as follows:

First Rule: The directions of the principal extensions coincide with those of the principal stresses at all times.

Second Rule: The density or the volume of the mass does not change appreciably.

Third Rule (the Law of Yielding): The figure consisting of Mohr's three principal strain circles remains continuously similar geometrically to that consisting of the group of three principal stress circles (see Figs. 47 and 48).

In what follows, ϵ , γ are the coordinates in Mohr's representation of strain and s , t the coordinates in Mohr's representation of stress (cf. Chaps. 8, 9 and 10). ϵ is the unit elongation corre-

sponding to some given direction, γ the unit shear of the planes perpendicular to this direction, s is the normal stress, and t the shearing stress in these planes. In the figure of the principal strain circles (Fig. 47) the origin O of the axes ϵ , γ must be chosen so that Eq. (10) below is satisfied. (Figure 47 shows a simple construction by means of which the location of O may be determined.)

We will now consider these statements in order. The first rule is only another expression of the experimental truth that the directions of the largest shearing displacements coincide with the directions of the maximum shear stresses. We must conceive of

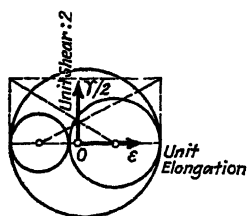


FIG. 47.

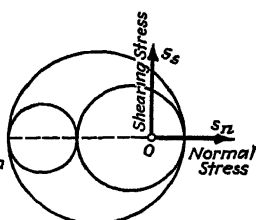


FIG. 48.

FIGS. 47 and 48.—For stationary plastic flow, the figure composed of the principal strain circles (at left) remains geometrically similar to that composed of the principal stress circles (at right).

the plastic state of engineering materials to be such that parts of the mass slide with respect to one another simultaneously along countless "slip planes" which may be recognized in the form of flow figures or Lüders' lines.

The second rule records the usual behavior of materials. To be sure, while very exact measurements of the extension during large plastic deformations have shown a small change in the volume (since the microstructure usually breaks up, the volume increases a little), these changes are, in the case of metals plastically deformed, of the order of the elastic deformations so that they may be neglected. The second rule is expressed by the condition:

$$\epsilon_1 + \epsilon_2 + \epsilon_3 = 0, \quad (10)$$

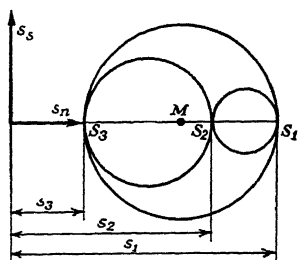
in which ϵ_1 , ϵ_2 , ϵ_3 are the principal strains, if, as assumed, the change in shape of the mass is relatively small.

The third rule is corroborated by the tests of Lode. Its meaning may be illustrated as follows: We know the way in which a plastic mass deforms under a homogeneous state of pure ten-

sion, under pure shear, and under pure compression. For example, we know that:

under pure tension	$s_1 = s, s_2 = s_3 = 0$
the deformation is given by.....	$\epsilon_2 = \epsilon_3 = -\epsilon_1/2;$
under pure shear	$s_1 = s, s_2 = 0, s_3 = -s$
the deformation is given by.....	$\epsilon_1 = -\epsilon_3, \epsilon_2 = 0;$
under pure compression.....	$s_1 = s_2 = 0, s_3 = -s$
the deformation is given by.....	$\epsilon_1 = \epsilon_2 = -\epsilon_3/2.$

Since these three principal conditions in stress and strain correspond to geometrically similar groups of Mohr circles, it appears reasonable to assume Rule III to be true for all stress conditions. In order to fix the position of the mean principal stress s_2 , with respect to s_1 and s_3 we use the ratio μ (Fig. 49) as introduced by the relation:



$$\mu = \frac{MS_2}{MS_1} = -\frac{s_2 - \frac{s_1 + s_3}{2}}{\frac{s_1 - s_3}{2}}. \quad (11)$$

FIG. 49.—The quantity μ defined in the text is the ratio $\mu = \overline{MS_2} : \overline{MS_1}$.

In a corresponding way we define the ratio

$$\nu = \frac{\epsilon_2 - \frac{\epsilon_1 + \epsilon_3}{2}}{\frac{\epsilon_1 - \epsilon_3}{2}} \quad (12)$$

We thus have

for pure tension.....	$\mu = \nu = -1,$
for pure shear.....	$\mu = \nu = 0,$
for pure compression...	$\mu = \nu = 1,$

and we observe thus, that in these three cases $\nu = \mu$.

The third rule states that this condition holds for all possible stress distributions:

$$\mu = \nu \quad (13)$$

or

$$\frac{s_2 - s_1 + s_2 - s_3}{s_1 - s_3} = \frac{\epsilon_2 - \epsilon_1 + \epsilon_2 - \epsilon_3}{\epsilon_1 - \epsilon_3}. \quad (14)$$

The first rule contains three conditions, i.e., the three conditions which determine the position of three perpendicular straight lines in space; the second and third rule each contain one condition, thus, in the three laws

of yielding, five conditions are involved with respect to the stress-strain relations, which must hold.

The third rule may be formulated in two additional ways. We have

the principal stresses s_1, s_2, s_3 the principal shearing stresses t_1, t_2, t_3		the principal strains $\epsilon_1, \epsilon_2, \epsilon_3$ the principal shearing strains $\gamma_1, \gamma_2, \gamma_3$
$t_1 = \frac{s_2 - s_3}{2}$		$\gamma_1 = \epsilon_2 - \epsilon_3$
$t_2 = \frac{s_3 - s_1}{2}$		$\gamma_2 = \epsilon_3 - \epsilon_1$
$t_3 = \frac{s_1 - s_2}{2}$		$\gamma_3 = \epsilon_1 - \epsilon_2$

For the principal shearing stresses the following identity holds:

$$t_1 + t_2 + t_3 = 0 \quad (15a)$$

For the principal shearing strains we have the identity:

$$\gamma_1 + \gamma_2 + \gamma_3 = 0 \quad (15b)$$

The rule governing the change in shape $\mu = \nu$ corresponding to Eq. (14) may be written in a different form, namely:

$$t_1:t_2:t_3 = \gamma_1:\gamma_2:\gamma_3. \quad (16)^1$$

This may be shown as follows. If we express t and γ in terms of s and ϵ we obtain:

$$\frac{s_2 - s_1}{s_1 - s_3} = \frac{\epsilon_2 - \epsilon_1}{\epsilon_1 - \epsilon_3} \text{ and } \frac{s_2 - s_3}{s_1 - s_3} = \frac{\epsilon_2 - \epsilon_3}{\epsilon_1 - \epsilon_3} \quad (17)$$

or after adding

$$\frac{s_2 - s_1 + s_2 - s_3}{s_1 - s_3} = \frac{\epsilon_2 - \epsilon_1 + \epsilon_2 - \epsilon_3}{\epsilon_1 - \epsilon_3}, \text{ i.e., } \mu = \nu.$$

A third form of the third rule containing also rule II: $\epsilon_1 + \epsilon_2 + \epsilon_3 = 0$ is finally:

$$\left. \begin{aligned} \epsilon_1 &= c[s_1 - \frac{1}{2}(s_2 + s_3)] \\ \epsilon_2 &= c[s_2 - \frac{1}{2}(s_3 + s_1)] \\ \epsilon_3 &= c[s_3 - \frac{1}{2}(s_1 + s_2)] \end{aligned} \right\} \quad (18)$$

This holds since if we substitute these expressions in the right side of Eq. (17) we obtain the left side; and if we take the sum of the three principal

¹ These are not two independent equations, for if we assume the validity of the equation $t_1:t_2 = \gamma_1:\gamma_2$, it follows immediately, because of the identities $t_1 + t_2 + t_3 = 0$ and $\gamma_1 + \gamma_2 + \gamma_3 = 0$ (see Eq. [15a] and [15b]) that the second equation $t_3:t_2 = \gamma_3:\gamma_2$ holds.

strains as given by (18) we obtain 0. Since Hooke's law for elastic bodies is given by:

$$\left. \begin{aligned} \epsilon_1 &= \frac{1}{E}[s_1 - \nu(s_2 + s_3)] \\ \epsilon_2 &= \frac{1}{E}[s_2 - \nu(s_3 + s_1)] \\ \epsilon_3 &= \frac{1}{E}[s_3 - \nu(s_1 + s_2)] \end{aligned} \right\} \quad (19)$$

we may say that in the case of flow of plastic masses (for small strains and under the above-mentioned limitations), a similar system of equations holds as for the case of elastic deformations. The difference between the two sets of Eqs. (18) and (19) is only that for the case of plastic flow Poisson's ratio is $\nu = \frac{1}{2}$ and that instead of a constant "modulus of elasticity" E an arbitrary constant $1/c$ appears.

CHAPTER 15

TENSION

a. The Stress-strain Curve.—If a prismatical or cylindrical test piece of ductile material be loaded in a testing machine in tension, and if we plot the increase in length Δl of a length l_0 chosen in the unstrained condition as abscissæ and the tensile loading P as ordinates we obtain curves of the kind shown in Figs. 52 to 54. They represent tests on soft annealed wrought iron, copper, and aluminum. In order to make these curves independent of the dimensions of the test pieces we take the abscissæ to be, instead of the change in length Δl , the unit extension along the length l_0 :

$$\epsilon = \frac{l - l_0}{l_0} = \frac{\Delta l}{l_0}. \quad (1)$$

We also take the ordinates equal to the unit stress s_0 by dividing the load P by the original cross-section A_0 :

$$s_0 = \frac{P}{A_0}. \quad (2)$$

We thus obtain a stress-strain curve $s_0 = f(\epsilon)$ as shown in the

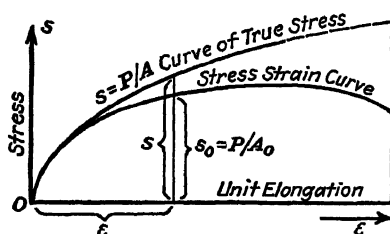


FIG. 50.—Stress-strain curve and curve of true stresses for a tensile test.

the lower curve of Fig. 50. The tensile load reaches its maximum value at the instant the uniform extension of the test piece stops. At this point the test piece begins to neck and consequently the load on the test piece begins to decrease as indicated by the last part of the stress-strain curve. Finally, the test piece fractures at the narrowest point of the neck.

Instead of plotting the stress $s_0 = f(\epsilon)$ in dividing the load P by the *original* cross-sectional area A_0 we may compute the *true*

tensile stresses s at the time the load acts according to a method suggested by P. Ludwik.¹ These latter stresses are equal to:

$$s = \frac{P}{A},$$

where A is the actual cross-section at the time the load acts. Neglecting the elastic deformation and the very small permanent change in volume during a tensile test we may consider the volume of the bar as constant and we have therefore,

$$Al = A_0 l_0, \quad \frac{l}{l_0} = 1 + \epsilon, \quad (3)$$

from which we obtain:

$$A = \frac{A_0 l_0}{l} = \frac{A_0}{1 + \epsilon}. \quad (4)$$

The true stress s then becomes²

$$s = \frac{(1 + \epsilon) P}{A_0} = (1 + \epsilon) s_0. \quad (5)$$

By means of these formulæ we may either determine the curve of the true stresses $s = F(\epsilon)$ in the case of a known stress-strain curve $s_0 = P/A_0$, by means of:

$$s = F(\epsilon) = (1 + \epsilon) s_0, \quad (6)$$

or, in the case of a known curve of the true stresses $s = F(\epsilon)$, we may determine the load P as a function of the extension ϵ :

$$P = \frac{A_0 s}{1 + \epsilon} = \frac{A_0 F(\epsilon)}{1 + \epsilon}. \quad (7)$$

From the last formula it follows that, at the maximum load P_{\max} :

$$\frac{dP}{d\epsilon} = \frac{A_0}{(1 + \epsilon)^2} \left[(1 + \epsilon) \frac{ds}{d\epsilon} - s \right] = 0,$$

from which

$$\frac{ds}{d\epsilon} = \frac{s}{1 + \epsilon}. \quad (8)$$

¹ "Elemente der technologischen Mechanik," Julius Springer, Berlin, 1909.

² If we refer the extensions to the actual length l instead of the initial length l_0 and define it by $\epsilon = \int_{l_0}^l dl/l$, this may sometimes be also of advantage (see Ludwik, *loc. cit.*).

If we plot the stress s_0 taken with respect to the original cross-section A_0 and the true stress s as functions of the unit extension ϵ we usually obtain curves such as shown by the lower and upper curves of Fig. 50. The

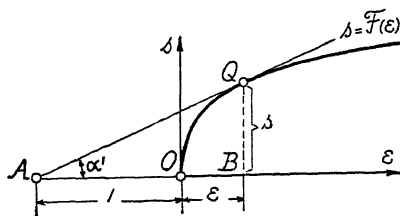


FIG. 51.—Curve of true stresses.

From the point A at the end of this length a line is drawn, tangent to the curve $s = F(\epsilon)$. The point of tangency Q gives the corresponding value of the true stress $s = \overline{QB}$, since at this point

$$\tan \alpha' = \frac{\overline{QB}}{\overline{AB}} = \frac{s}{1 + \epsilon} = \frac{ds}{d\epsilon} \quad (9)$$

In Figs. 52 to 54 the stress s_0 referred to the initial cross-section and the true stress s referred to the actual cross-section are plotted

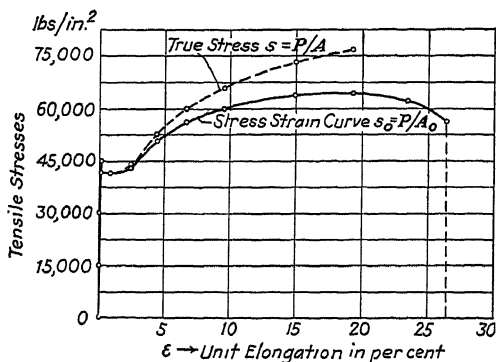


FIG. 52.—Tensile test of wrought iron. (Annealed during 1 hr. at 1000°C.)

against the unit extension ϵ for three tensile tests. Figure 52 represents a tensile test with a flat test piece of wrought iron, Fig. 53 one of copper, and Fig. 54 one of aluminum; these test pieces were annealed before the tests for one hour at a 1000°, at 800°, and at 350° C., respectively.

¹ This construction is mentioned in "Einige Prinzipien der theoretischen mech. Technologie der Metalle," by A. REYER, p. 268, V.D.I., Verlag, Berlin, 1927.

The maximum ordinate of the ordinary stress-strain diagram, commonly known in the technical literature as the "ultimate strength," has merely, as Ludwik¹ emphasized a long time ago,

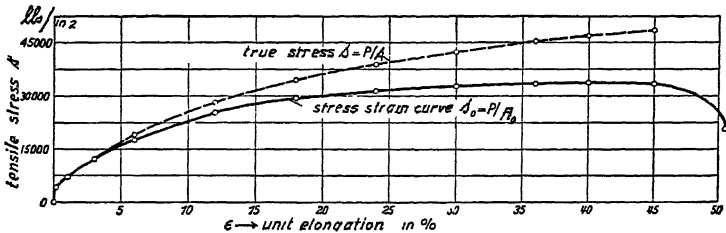


FIG. 53.—Tensile test of copper. (Annealed during 1 hr. at 800°C.)

the meaning that at this point the uniform extension of test piece ceases. In the curve of the true stresses $s = F(\epsilon)$, this stress $s = QB$ (Fig. 51) does not have a physical meaning different from that of any of the other stresses.

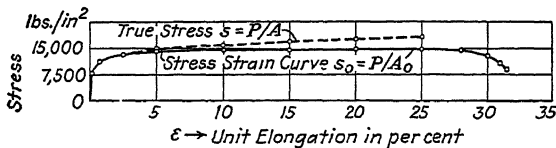


FIG. 54.—Tensile test of aluminum. (Annealed during 1 hr. at 350°C.)

In the stress-strain diagram the curve of the true stresses may occasionally be approximated by a power function:

$$s = s_1 \epsilon^n.$$

To this corresponds the ordinary stress-strain diagram:

$$P = \frac{A_0 s_1 \epsilon^n}{1 + \epsilon}.$$

If, for example, the extension at the point of maximum load P_{\max} is 25 per cent, $\epsilon = \frac{1}{4}$ and the formula $dP/d\epsilon = 0$ gives:

$$n = \frac{\epsilon}{1 + \epsilon} = \frac{\frac{1}{4}}{\frac{5}{4}} = \frac{1}{5} \text{ and } s = s_1 \sqrt[5]{\epsilon}.$$

If, however, the deformation curve is a horizontal line $s = s_1 = \text{constant}$, i.e., the strength of the material does not increase under plastic flow, the load

$$P = \frac{A_0 s_1}{1 + \epsilon}$$

¹ "Elemente der technologischen Mechanik," Julius Springer, Berlin, 1909.

decreases, when plotted in the ordinary stress-strain diagram, along an equilateral hyperbola with the unit extension ϵ .

If, instead of taking the unit extension,

$$\epsilon = \frac{l - l_0}{l_0}, \quad (10)$$

we take the relative decrease in cross-section¹

$$q = \frac{A_0 - A}{A_0} \quad (11)$$

as the independent variable, since,

$$\frac{A}{A_0} = 1 - q = \frac{1}{1 + \epsilon}, \quad q = \frac{\epsilon}{1 + \epsilon} \quad (12)$$

we obtain the true stress²

$$s = \frac{s_0}{(1 - q)} \quad (13)$$

The condition for the maximum load is then:

$$\frac{ds}{dq} = \frac{s}{1 - q} \quad (14)$$

When the test piece begins to neck after the maximum load is reached, there results in the neck a complicated stress distribution, so that the determination of the "true tensile strength" or cohesion, *i.e.*, the stress at which the material fractures, is made considerably more difficult. A useful approximate calculation of the stress distribution in the neck of a test piece was given by E. Siebel.³

b. Mechanical Similarity.—In the case of two cylindrical test pieces, one of which has a diameter n times as great as that of the other, *i.e.*,

$$d' = nd'',$$

the forces P' and P'' , which produce the same stress and therefore the same unit elongation vary as:

$$P':P'' = d'^2:d''^2 = n^2$$

If, in the case of short test pieces, we wish to obtain the same degree of necking (two geometrical similar cones produced by necking), the length of the cylindrical part of the test piece must vary as the diameter.

A cylindrical test piece and a flat test piece can only behave mechanically similar in the region of uniform extensions; after the occurrence of necking, the stress distribution in the constricted parts of both test pieces will be entirely different.

In the German standards (D.I.N. 1605) a rule for the determination of the gage length l of a flat bar having a cross-section A is

$$l = 11.3\sqrt{A}$$

¹ Cf. KOERBER, F., *Mitt. aus d. Kaiser Wilhelm Institut für Eisenforsch.*, vol. 3, pt. 2, Düsseldorf, 1924.

² Werkstoffausschussbericht No. 71 des V.D.E., Düsseldorf, *Stahl und Eisen*, 1925.

This length is obtained by prescribing that the ratio of l^2 to the length l'^2 of the standard cylindrical bar should be as A to $\pi d^2/4$. Taking as length of the cylindrical bar $l' = 10d$ the above formula results. As stated above beyond the beginning of necking no rigid mechanical similarity between a round bar and a flat bar can exist.

In general to insure mechanical similarity in the process of plastic deformation in two geometrically similar bodies which are loaded only by forces acting on their surfaces (no forces due to weight or inertia acting) the forces must vary as the square of the ratio of the linear dimensions. True mechanical similarity is insured if the trajectories of principal stress in the bodies are geometrically similar.

c. Upper and Lower Yield Stress for Steel.—As has already been mentioned, the transition in the stress-strain curve, from the domain of elastic deformation into that of the plastic state, has in the case of metallic crystal aggregations many different forms. In the case of a metal which has not been previously subjected to plastic deformation, we obtain after suitable heat treatment an "initial curve." In the case of most soft annealed metals no definite yield point may be noticed, plastic deformation beginning at very low loads. In contrast to this, mild steel shows the usual phenomenon of the upper and lower yield point which C. Bach first observed.¹ While the load gradually increases, at a certain point the pointer of the testing machine suddenly reverses and the load drops, often very suddenly, about 5 to 20 per cent, while the test piece begins to stretch plastically. The corresponding unit stresses:

$$s_1 = \frac{P_1}{A_1} \text{ and } s_2 = \frac{P_2}{A_2}$$

were called by Bach *the upper and lower yield stresses*, respectively.²

In the case of test pieces which have been previously strained and which are composed of metals which show in their initial stress-strain curve no definite yield point, it is usually found that if the test pieces are again subjected to the same stress (tension) a definite yield point is noted (*cf.* Chap. 5, p. 24).

¹ Zum Begriff der Streckgrenze *Z. d. V. D. I.*, p. 1040, 1904; and Zur Kenntnis der Streckgrenze, *Z. d. V. D. I.*, p. 615, 1905.

² With reference to the upper and lower yield stress for steel, *cf.* also Chap. 16c, p. 93.

CHAPTER 16

STRAIN OR FLOW FIGURES

a. **Strain Figures in Mild Steel.**—If a tensile test piece of mild steel, especially a flat bar, is given a mirror-like polish and then tested in tension in a testing machine, at the instant of the drop in the load at the yield point often fine dull lines appear on the polished surface of the bar at an angle to the axis of tension. These lines, known to engineers as *flow or strain figures* or as "*Lüders' lines*," quickly spread over the length of the bar while at the same time their thickness increases. The observation of the occurrence and spread of these fine markings on the surface of steel test pieces gives valuable information on the phenomena taking place in the structure of the material at the instant it yields.¹

On account of the regular occurrence of these flow figures on stressed specimens of mild steel and of the remarkably regular orientation of these layers of slip with respect to the directions of the principal stresses it is of a greater interest to study how they originate, because of the close relation which seems to exist between the orientation of these thin layers of slip and the state of stress in a steel piece stressed to the plastic limit. On bars of mild steel covered with a coating of rust or mill scale, the flow or strain figures may also be observed. If such bars have been deformed beyond the yield stress the scale begins to flake off and thus regular markings on the surface of bars may be seen,

¹ The flow figures seen in soft steel were first described by LUDERS, *Dingler's Polytechn. Jour.*, 1854. Cf. also MARTENS-HEYN "Materialienkunde," Berlin. The French artillery officer, L. HARTMANN, appears to have been the first to study these lines thoroughly in his book: "Distribution des Déformations dans les Métaux Soumis à des Efforts," Berger-Levrault, Paris, 1896. The importance of these lines for the mechanics of the plastic state of metals was recognized by OTTO MOHR, *Z. d. V. D. I.*, 1900. The formation of the flow figures has been recently studied by several investigators among whom T. H. TURNER and I. D. JEVONS, *Jour. Iron and Steel Inst.*, vol. 111, No. 1, p. 169, 1925, and E. W. FELL, *ibid.*, 1927, may be mentioned here.

which are identical with these flow figures. Some examples of flow figures on polished specimens are shown in Figs. 55, 56 and 57.

In a tensile test the first flow lines generally appear suddenly, usually at or near points on the piece where it begins to enlarge near the heads of the

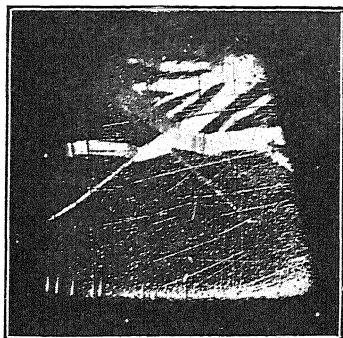


FIG. 55.—Strain or flow figures (Lüders' lines) on compressed steel specimen.

piece. An example of the way these lines appear is shown by the sketches of both flat sides of a test piece in Fig. 58. The first line to occur was that represented by the black line *a*. At the instant that this line became visible, the load on the test piece which was at the "upper" yield point dropped about 5 per cent and, while the load dropped 2 per cent more, a second line *b*

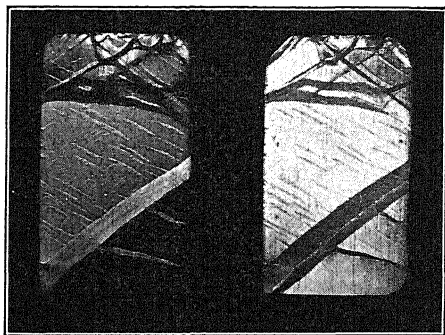


FIG. 56.

FIG. 57.

Figs. 56 and 57.—Strain or flow figures (Lüders' lines) on compressed steel specimen.

formed. From these two lines there gradually spread out, under constant tension, a wide dull band *c* (see Fig. 58). Two such bands are often observed at the yield point in positions as shown in Fig. 59, the middle portion of the test piece having shifted sideways a small amount. In the case of compression tests with mild-steel specimens a similar phenomenon may be observed as shown in Fig. 60.

In the narrow dull strips or lines, which mark the position where the plastic layers intersect the surface of the test piece, the direction of the relative movement of the unchanged bounding portions of the material, with respect to each other or the slip layer, may be recognized. These lines

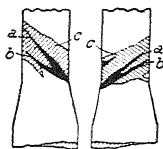


FIG. 58.—
Strain figures on
a flat bar of steel.

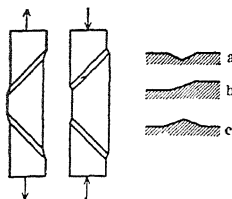


FIG. 59. FIG. 60. FIG. 61.

FIGS. 59, 60, and
61.—Formation of slip
layers by tension or
compression.

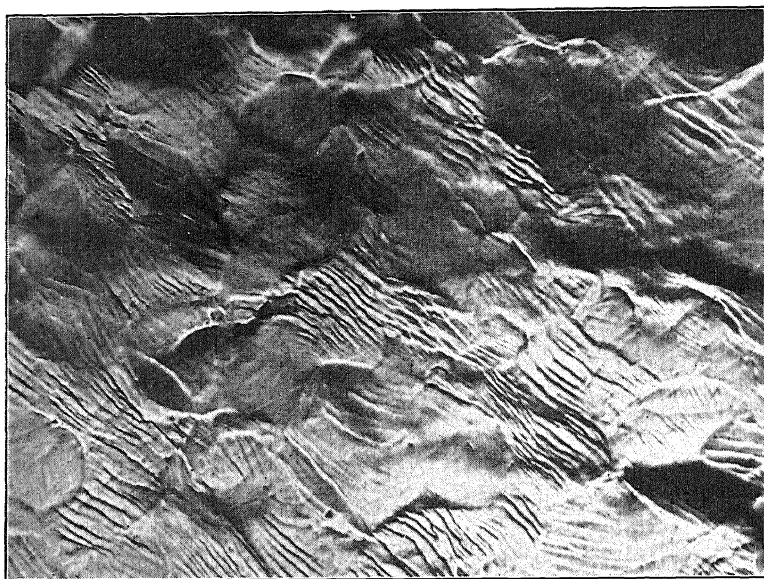


FIG. 62.—Micrograph of the slightly distorted surface of a well-polished specimen of mild steel just after the yield stress has been reached. Note the tendency of the slip bands appearing in the crystal grains to orient themselves parallel to a certain direction. The micrograph was taken along the border line of a strain figure (Lüders' line).

or strips may have either the profile of a shallow groove (Fig. 61a) in case of tension, or of a shallow ridge in case of compression (Fig. 61c), or they may form a flat slope (Fig. 61b), which appears scaly under the microscope. The grooves appear where the dull strips run in a direction about 45° to the axis

of the test piece, while the flat slopes form, where the dull strips are perpendicular to the direction of tension. Where the direction of slip runs parallel to the surface of the test piece, these shallow grooves result. In a steel test piece under compression, there result likewise similar flow lines. In such cases, however, the flow lines have, instead of the profile of shallow grooves, that of a flat ridge (Fig. 61c). Under the microscope the flakes or scales visible in these flow lines often prove to be groups of crystal grains displaced along neighboring layers and deformed plastically. In the grains

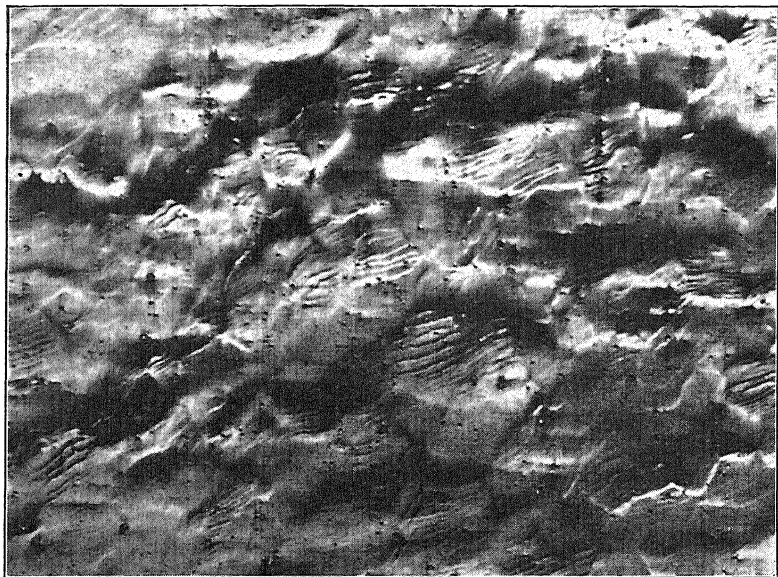


FIG. 63.—Micrograph of the structure of a steel bar, bent permanently to a small degree. The micrograph was taken along the border line of a strain figure (Lüders' line). Observe that the crystallites slipped together in groups and were displaced in parallel layers. In the deformed grains slip bands appear. (*Magnified about 70 times.*)

dark wavy lines may be recognized (see the photographs of Figs. 62 and 63). These markings may be identical with the wavy lines which Taylor and Elam¹ found in plastically deformed single crystals of iron.

The production of the shallow grooves on the surface of a stretched test piece of mild steel and the flat ridges on the surface of a steel prism loaded in compression is apparently the consequence of local yielding. In both cases the length changes only about 2 to 4 per cent and the load after the sudden drop at the yield point remains nearly constant while the test specimen stretches. A permanent extension of 2 to 4 per cent in the axial direction in a tensile test corresponds to a lateral contraction of 1 to 2 per cent. An oblique section of the test piece taken at an angle of 45° to the direction of tension, the trace of this section on the surface being the

¹ *Proc. Roy. Soc., London, Ser. A, vol. 112, p. 337, 1926.*

groove of the flow line, must therefore contract about 1 to 2 per cent while the bounding part of the test piece does not change its dimensions.

One property of the flow or slip layers has an especial bearing on the mechanics of the plastic state. The planes of the thin slip layers in which the iron is apparently more severely deformed than elsewhere coincide approximately with two of the planes

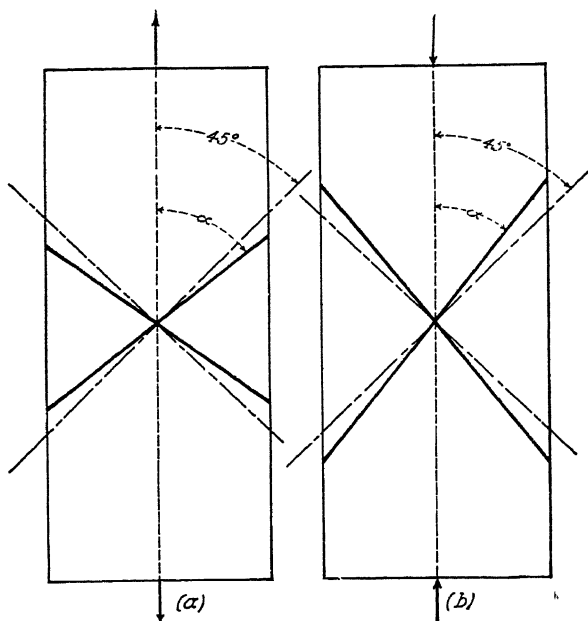


FIG. 64.

FIG. 65.

FIGS. 64 and 65.—Orientation of the slip planes in a tensile and a compression test piece.

of principal shearing stress. The angle α which the slip layers make with the axis of the test piece is in the case of tension usually a little greater (47°) and in the case of compression usually a little less than 45° ¹ (see Figs. 64 and 65). Since these properties of the flow layers also are exhibited in complicated three-dimensional distributions of stress, observations relative to their position form a valuable aid in the investigation of states of stress in plastically deformed solids which will often be used in what follows. The brittle layer of scale, which covers hot-rolled or forged steel bars, flakes off frequently where these bars have subsequently been stressed in the cold state above the plastic

¹ For measurements of this angle cf. SCHOLL, "Versuche über Gleit- und Brucherscheinungen," *Z. d. V.D.I.*, p. 406, 1925.

limit. In the neighborhood of punched rivet holes, markings of considerable regularity are often revealed. These lines are identical with *Lüders' lines*.

For observing the flow figures, two methods are available. In the first method, which was worked out by A. Fry,¹ for steel the test piece after being stressed is heated to 200 to 250°C., after which it is etched by a very strong solution containing hydrochloric acid and copper chloride. The traces of the flow layers on the cross-section appear as dark lines. Fry and Strauss² have been able to obtain, with the help of this etching method, valuable information regarding the fundamental changes which iron undergoes at the plastic limit.

A second method is to make the flow lines visible and to photograph the flat relief shown by the depressions and ridges on a finely polished metal surface by means of the Töpler "Schlieren-methode," which was applied by the author at the suggestion of L. Prandtl.³ The photographs of slightly distorted metal surfaces, given frequently throughout this book, were taken by the use of this method.

¹ Kraftwirkungsfiguren in Flusseisen, dargestellt durch ein neues Ätzverfahren, *Kruppsche Monatshefte*, July, 1921; also *Stahl und Eisen*, 1921.

² *Kruppsche Monatshefte*, July, 1921.

³ *Schweiz. Bauztg.*, vol. 83, nos. 14 and 15, 1924. The author is indebted to Dr. Lihotzky of Wetzlar for optical equipment which has served this purpose very well and which was attached to a metallic microscope manufac-

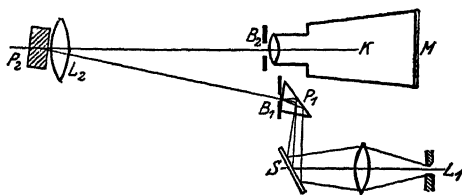


FIG. 66.—"Schlieren"-Method for observing flow or strain figures on polished metal test pieces. L_1 , source of light; S , mirror; P_1 , prism; L_2 , large lens; P_2 , test specimen; K , camera; M , ground glass; B_1 and B_2 , diaphragms.

tured by Ernest Leitz of Wetzlar; this arrangement is represented in the sketch of Fig. 66. In this sketch L_1 is an arc lamp or source of light, S a mirror, P_1 a totally reflecting prism, L_2 a good lens with a large aperture, P_2 the test specimen, K a photographic camera, M a ground glass, B_1 and B_2 two diaphragms. In operation the screen opening B_1 illuminated by the arc lamp is projected by means of the lens L_2 and the reflecting test piece P_2 on the plane of the screen B_2 .

b. Phenomena Occurring in Flow Layers.—In many kinds of steel the flow lines appear as sharp lines on finely polished surfaces. In other kinds, however, a gradual dulling of the surface or a dull area with indefinite limits is often observed at the yield point. Microscopic examinations of the surface show that those kinds of steel which show a sharp drop of the load at the yield point have in most cases a fine granular structure, while those steels in which the surface does not show flow lines but rather a dull appearance have a coarse granular structure. Moreover, such steels do not show any appreciable drop of load at the yield point. Since it is known from tests of metal single crystals that these are extraordinarily ductile and that they start to yield under a very low stress (which depends, however, on their orientation to the stress field),¹ the high yield stress of a very fine-grained wrought iron (a pure iron with only about 0.05 per cent carbon content) may perhaps be attributed to the action of a very rigid intercrystalline substance. The characteristic and varying behavior of mild steel with respect to its initial yield point and with respect to the size of its crystal grains may perhaps be explained if we assume that the intercrystalline substance in the case of soft iron has very great strength. Thus, the cementite distributed in the grain boundaries forms a rigid skeleton which at first prevents plastic deformation of the soft ferrite crystals. At the yield point the skeleton breaks down, allowing the ferrite crystals to deform plastically. In a coarse-grained steel, on the other hand, the intercrystalline substance does not form such hindrance to the plastic deformation of the soft-iron grains. Such a steel behaves more like a single crystal or like soft polycrystalline copper, both of which have in their initial stress-strain curve a very low or no definite yield point.

According to the tests of P. Ludwik and Scheu² the yield point of electrolytic iron may be raised by combined mechanical and thermal preliminary treatment. Ludwik and Scheu have especially emphasized that there may be other fundamental factors, than those mentioned above (carbon content), which may affect the properties of steel and have a considerable influence on the magnitude of the stress causing the first breakdown at the yield

¹ Cf. "Handbuch der Physik," vol. 6, article on Plasticity, Julius Springer, Berlin.

² Über die Streckgrenze von Elektrolyt- und Flusseisen, Werkstoffausschussbericht No. 70, V.D.E., *Stahl und Eisen*, Düsseldorf, 1925.

point. Among these factors recent investigations more definitely call attention to the content of steel on minute quantities of dissolved gases which seem to affect the limit of plasticity and to be the causes of the phenomena of "aging" in steel. W. Köster¹ especially calls attention to the nitrogen content in steel. Small quantities of nitrogen of 0.005 to 0.01 per cent, which can be dissolved in steel or precipitated from it under various conditions, seem not only to cause some of the effects (for example the "aging" of steel with respect to its magnetic properties), but also to affect the developing of the dark lines by *Fry's* etching solution.

Some of the suppositions mentioned above have been confirmed by the observations of A. Fry (*loc. cit.*) on the fundamental changes occurring in the structure of the flow layers of steel. By means of microscopic observations he was able to show *three* kinds of disturbances in the microstructure of plastic iron: disturbances along the grain boundaries (these latter appear much thicker in the etched micrographs within the plastic layers than in the elastically deformed parts of the steel pieces); disintegration of the grains (cracks and slip surfaces are visible within the individual crystal grains); and, finally, certain disturbances in the grains themselves, distributed continuously over the grains without actual disintegration. (The grains appear darker in the etchings within the plastic layers than in the surrounding, only elastically stressed parts of the steel specimen.) According to these observations it must be concluded, that the skeleton of the intercrystalline substance between the ferrite grains of soft iron appears to be greatly disturbed after the yield point has just been reached and that also other disturbances occur within the grains in the thin plastic layers which form the flow or Lüders lines on the surface of the specimen stressed above the yield point.

c. The Peak of the Stress-strain Curve of Steel.—The drop in the load at the yield point in a tensile test of iron is a result of the instability of the elastic-plastic equilibrium of a long bar occurring at the yield point. As F. Koerber and M. Moser have shown, it is possible by special precautions to eliminate this drop in load, if, by means of a sudden change in section at the ends of

¹ Zur Frage des Stickstoffs im technischen Eisen, *Stahl und Eisen*, vol. 50, no. 19, p. 629, May 8, 1930.

the cylindrical portion of the test piece, a local non-uniformity with a concentration of stress is produced.

According to tests by the author¹ it appears that tensile test bars containing a groove (which causes a certain concentration of stress, and consequently earlier yielding) give a small drop in the load at the yield point, while test pieces with a very smooth and highly polished surface and having a gradual increase in diameter at both ends showed a very definite drop at the yield point. Tensile tests, using cylindrical specimens of soft iron, having a cylindrical constricted portion (cf. the shape of the test pieces in Figs. 67 and 68), gave values for the

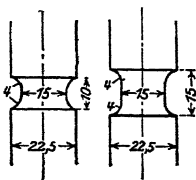


FIG. 67. FIG. 68.

FIGS. 67 and 68.—
Grooved bars for tensile tests.

upper and lower yield stress contained in the following table.

TESTS ON THE DROP OF THE LOAD AT THE YIELD POINT

Kind of test piece	Unannealed bars			Annealed bars		
	Upper yield point, kg./cm. ²	Lower yield point, kg./cm. ²	First yielding, kg./cm. ²	Upper yield point, kg./cm. ²	Lower yield point, kg./cm. ²	First yielding, kg./cm. ²
Cylindrical	3,340	2,990	...	2,970	2,780	
	3,560	3,360	..	3,390	3,250	
	3,400	2,890	..	3,220	2,680	
	3,290	2,750	..	2,970	2,630	
	3,360	2,900	..	2,800	2,700	
	3,390	2,970	..	2,940	2,820	
	3,370	2,920	2,990	2,930	
Mean value.....	3,387	2,969		3,040	2,827	
With long throat, as shown in Fig. 68	3,170	3,050	2,880	2,790	2,150
	3,170	3,010	2,940	3,110	3,050	2,790
	3,080	3,020	2,940	2,800	2,780	2,380
	3,280	3,150	3,000	2,990	2,950	2,490
	3,280	3,190	3,000	3,030	2,930	2,740
	3,100	2,940	3,030	2,730
	3,280	3,190	3,050	3,040	2,990	2,770
Mean value.....	3,194	3,102	2,964	2,970	2,940	2,570
With short throat, as shown in Fig. 67	3,620	3,530	3,280	3,590	3,570	2,760
	3,730	3,690	3,240	3,630	3,590	2,930
	3,700	3,610	2,940	3,520	3,400	2,950
	3,810	3,700	2,880	3,510	3,440	2,590
	3,560	3,550	2,880	3,360	..	2,420
	3,630	2,830	3,480	3,440	2,420
	3,680	3,560	2,830	3,550	3,420	2,690
Mean value..	3,676	3,612	2,982	3,520	3,465	2,680

In all, 21 tensile test pieces of the same soft wrought iron were tested. Of these, seven pieces were cylindrical with a uniform diameter for a con-

¹ Dissertation, Technische Hochschule, Berlin, 1911.

siderable length, seven had a "long neck" as shown in Fig. 68, while the remaining seven had a "short neck" as shown in Fig. 67. The cylindrical test pieces had a diameter of 15 mm., a cylindrical length of 190 mm., and a total length of 370 mm.; the form was the usual one with a gradual conical transition to the enlarged ends of the test piece. The other test bars had a diameter of 22.5 mm. in the thickest portions and 15 mm. in the necks, the total length being at the same time 370 mm. The dimensions of the neck are shown in Figs. 67 and 68, the cylindrical length in the case of Fig. 68 being 7 mm., in the case of Fig. 67 only 2 mm. All specimens were tested in the unannealed condition, then annealed in a gas oven, measured again, and tested again. In both tests the load was only increased above the yield point sufficiently for its determination. All values of the unit stress were determined by taking into account the change in cross-section due to the permanent deformation in the first tests; in other words, by taking the actual cross-sections of the annealed test pieces. In the case of the bars with grooves this was obviously the smallest cross-section in the throat; for the cylindrical test pieces of 190 mm. length the cross-section at which flow occurred was determined with sufficient accuracy by comparison of the diameters, both before and after the tests as found with a micrometer. The beginning of plastic deformation was determined either by the Martens extensometer or by thermo-electric measurements of the temperature of the test piece.

From the table it would, at first glance, appear that a short constriction apparently tends to increase the yield stress. In truth the contrary is the case. The reason for this is that by a short constriction, the lateral contraction of the constricted portion of the test piece is prevented.¹ On the other hand, in the cases of test bars having grooves, there is very little difference between the upper and lower yield stresses. This is explained by the local concentration of stress in the constricted portion, which tends to prevent any unstable stress condition. In the third column of the table, stresses are recorded at which "first yielding" in the test pieces occurred, i.e., the stresses at which proportionality between stress and strain as observed by the readings of the Martens extensometers ceased. Comparison of the figures of the third column with those of the upper yield stresses for the cylindrical bars shows clearly that, in truth, by a short constriction the load under which the bar *begins* to yield, is diminished. It is known from the theory of elasticity, that because of a sudden change of the cross-section

¹ At this point, it should be noted that the ultimate strength of a test bar having a cylindrical constriction is in many cases considerably higher than that of an ordinary test bar without a constriction. This was shown by the tests of KIRKALDY, BARBA, of BACH and BAUMANN, "Elastizität und Festigkeit," 8th ed., 1924; by MARTENS, *Mitt. u. Forschungsarb. d. V.D.I.*, vol. 3; by RUDELOFF, *Baumaterialienkunde*, vol. 4, p. 85, 1899; and by TETMAYER, "Festigkeitlehre," 2d ed., p. 184, 1904. In this connection see also the test reports of LUDWIK and SCHEU, *Über Kerbwirkungen bei Flusseisen*, *Stahleisen*, vol. 43, p. 999, 1923; and by KÖRBER and MÜLLER, *Die Verfestigung metallischer Werkstoffe beim Zug- und Druckversuch*, *Mitt. aus. d. K.-W.-Institut f. Eisenforsch.*, vol. 8, p. 181, Düsseldorf, 1926.

"stress concentration" is introduced, which lowers the load at which the first yield occurs.

On the basis of careful investigations, instituted by the German Society of Iron and Steel Engineers, the influence of various factors on the shape of the transition curve from the elastic to the plastic stage in the stress-strain diagram has been studied.¹ From these tests it may be concluded that for technical applications more importance is to be attached to the *lower yield stress* than to the upper yield stress, which latter seems to be affected by the conditions discussed above.

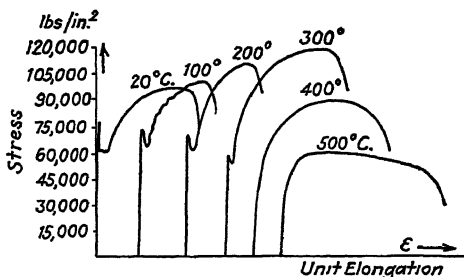


FIG. 69.—Short-time tensile tests with steel at elevated temperatures. (According to C. Bach and R. Baumann.)

Another effect on the upper yield stress may be noted here, namely the influence of temperature. According to tests by Bach and Baumann² and others the phenomenon of an upper and lower yield stress so characteristic for mild steel at normal temperatures disappears gradually with a rising temperature. The various forms of stress-strain diagrams taken at various temperatures on steel are shown in Fig. 69. The phenomenon of the drop in load at the yield point vanishes at the higher temperatures.

d. The Production of Flow Lines by Notches and Holes.—As is known from the theory of elasticity, the stresses in elastic bodies are increased or concentrated at concave boundary surfaces, for example, at the edges of a

¹ Cf. the exhaustive report by M. Moser, Über die Elastizitätsgrenze und Streckgrenze, *Werkstoffausschussbericht* 96 des Vereins Deutscher Eisenhüttenleute, Düsseldorf. Of special interest is the enumeration of certain secondary conditions which have an influence on the shape of the stress-strain curve. Cf. also: M. Moser, Grundsätzliches zur Streckgrenze, (C. Bach Festschrift), *Mitt u. Forschungsarb. d. V.D.I.* No. 295, p. 74, 1927, Berlin.

² "Festigkeitseigenschaften und Gefügebilder der Konstruktionsmaterialien," 2d ed., p. 11, Julius Springer, Berlin, 1921.

cylindrical hole or a spherical cavity in a member subjected to pure tension, compression, or shear. At a sharp reentrant edge the stresses are theoretically infinite. Even if the stresses in the neighborhood of a reentrant edge

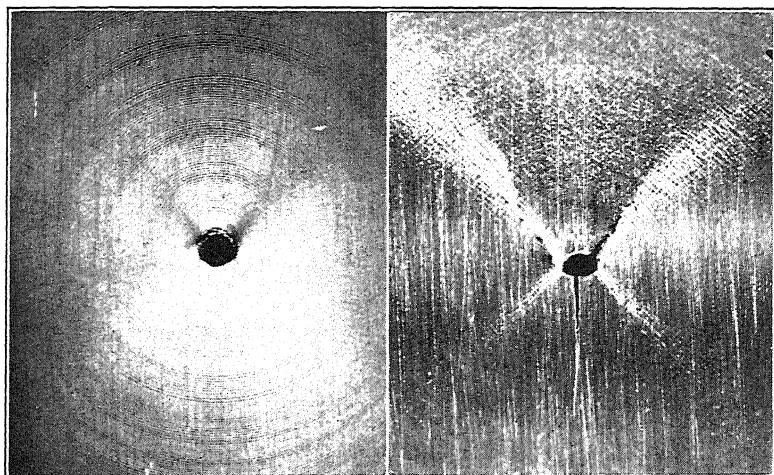


FIG. 70.

FIG. 71.

FIGS. 70 and 71.—Compression tests with paraffin prisms containing a cylindrical hole at right angle to direction of compression. *Left*: Beginning of distortion near hole. *Right*: Formation of two distinct slip layers starting from hole.

have only small values, nevertheless, these may be sufficient to produce plastic deformation or even fracture at the corners.

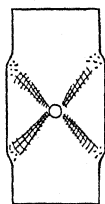


FIG. 72.



FIG. 73.

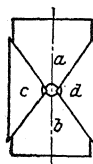


FIG. 74.

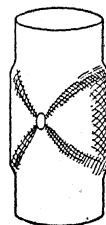


FIG. 75.—Slip layers in cylinder with hole.

FIGS. 72, 73, and 74.—Slip lines on the sides of a paraffin prism having a hole, and stressed in compression.

In compressed test pieces of brittle material, such as cast iron or hard steel, which contain small notches, failure by fracture begins at these notches.¹ By means of small cylindrical holes in an area subjected to pure

¹ LEBLOND, *La Technique Moderne*, vol. 15, p. 7, 1923.

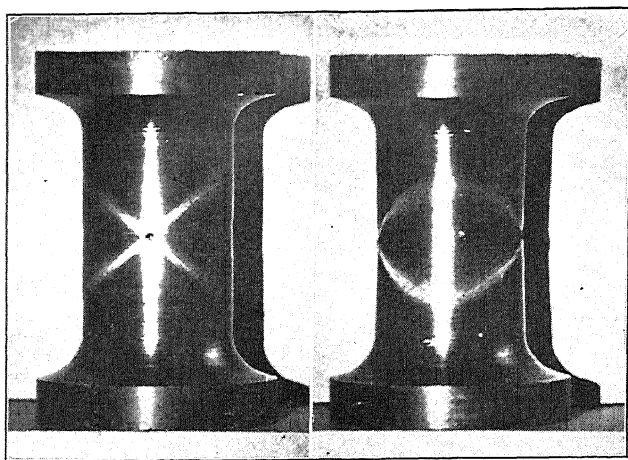


FIG. 76.—Two views of the same paraffin cylinder having a small hole. The cylinder has been subjected to compression in axial direction. The slip layers in the left view form a white cross and appear as ellipses in the second view. (The bright central line parallel to the axis of the cylinder is caused by a reflex of light and not by deformation.)

axial tension or compression, certain disturbances may be produced in plastic materials, as shown in Figs. 70 to 82.



FIG. 77.—Distortion of side of a flat steel bar having two very small grooves on edge. Tensile test.

The local yielding in the neighborhood of a hole or a notch may be studied by means of a test piece made of a soft material.¹ For this purpose test pieces made of soft paraffin and having holes were stressed in compression, the compression being perpendicular to the axis of the hole. Long before the first slip lines were visible the slight deformation of the surface of the test piece showed that the plastic deformation was not uniform but occurred mainly in two planes. These two planes intersected along the axis of the hole and formed equal angles with the direction of the compression. The first distortion of the surfaces of a compressed prism of paraffin is shown in the photograph of Fig. 70. After an increase in loading there resulted the flow lines shown in the photograph of Fig. 71 and indicated in the sketches of Figs. 72 to 74. The test piece split, so to say, into four rigid pieces, separated by two soft plastic layers, as indicated in Fig. 74; the wedges

¹ Recently S. Timoshenko utilized Lüders' lines to indicate the instant at which a definite maximum stress at a dangerous point in a stressed body is exceeded; cf. *Proc. 2d Internat. Congress for Applied Mechanics*, Zürich, 1926.

a and b moved in a vertical direction, thus forcing the wedges c and d to separate in a horizontal direction. Similar phenomena in a paraffin cylinder, having a hole perpendicular to the direction of compression, are illus-

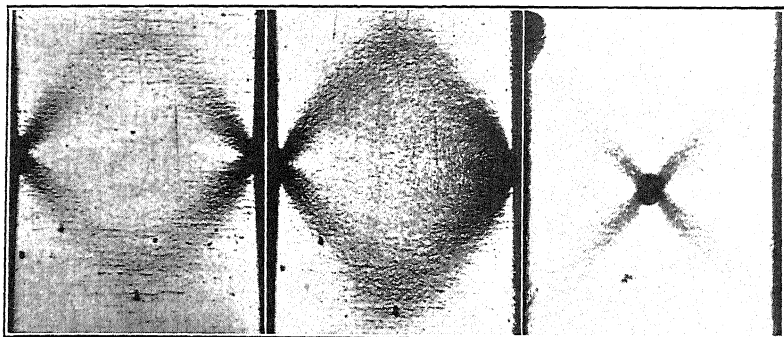


FIG. 78.

FIG. 79.

FIG. 80.

FIGS. 78, 79, and 80.—Slip layers produced by two small grooves (Figs. 78 and 79) or by central hole (Fig. 80) in hard copper prisms loaded parallel to edge in compression.

trated in both views of Fig. 76 and the sketch of Fig. 75. The slip planes appear as white strips in the photographs and are likewise grouped about two planes as indicated. The effects of a small notch or a small hole in



FIG. 81.

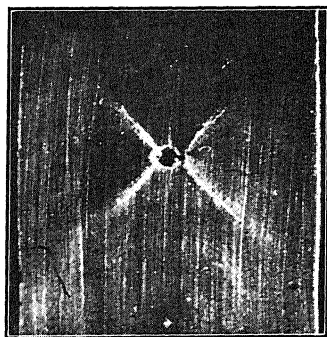


FIG. 82.

FIGS. 81 and 82.—Paraffin. Formation of slip layers crossing at approximately right angles. Produced by an accidental bubble (*left*); by a small hole (*right*).

producing local yielding in two thin layers in metal specimens under compression or tension are shown in the photographs Fig. 77 (steel), Figs. 78, 79 and 80 (copper), and for paraffin in Figs. 81 and 82.

e. Elastic Stress Distribution and the Beginning of Plastic Flow in a Plate with a Circular Hole.¹—In machine construction,

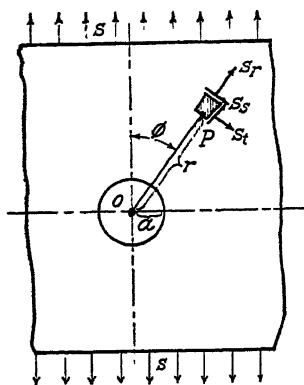


FIG. 83.—Plate with hole in tension.

tension or compression members having holes are very frequently used. It is important to note that the effect of a small cylindrical hole in such members is quite different, according to whether the material around the hole is stressed only elastically or whether it is partially yielding, plastic deformation occurring under a sharply determined yield stress.

The stress distribution in a tension or compression member in the form of a wide plate containing a small cylindrical hole is well known in case of an elastic material.² Referring to Fig. 83 consider a point P , located in the thin plate having a hole of radius a . The polar coordinates of this point are r and ϕ . If the plate is subjected to a uniform tensile stress s in the direction of the polar axis $\phi = 0$, the three components of stress which determine the state of stress in the plate are given by the following expressions:

$$\begin{aligned} \text{Radial stress:} \quad s_r &= \frac{s}{2} \left[1 - \frac{a^2}{r^2} + \left(1 - \frac{4a^2}{r^2} + \frac{3a^4}{r^4} \right) \cos 2\phi \right], \\ \text{Tangential stress:} \quad s_t &= \frac{s}{2} \left[1 + \frac{a^2}{r^2} - \left(1 + \frac{3a^4}{r^4} \right) \cos 2\phi \right], \\ \text{Shearing stress:} \quad s_s &= -\frac{s}{2} \left[1 + \frac{2a^2}{r^2} - \frac{3a^4}{r^4} \right] \sin 2\phi. \end{aligned} \quad (1)$$

On the circumference of the hole the coordinate r is $r = a$ and hence the stresses become equal to:

$$s_r = 0, \quad s_t = s(1 - 2 \cos 2\phi), \quad s_s = 0. \quad (2)$$

The radial and shearing stresses s_r and s_s vanish. The tangential normal stress s_t is a maximum at the points $\phi = \pi/2$ and $= 3\pi/2$, located on the circumference of the hole and on an axis of the plate perpendicular to the direction of the tension. At these points the tangential normal stress is:

$$s_{t\max} = 3s. \quad (3)$$

¹ See BAUD, R. V., WAHL, A. M., and author's paper in *Mech. Eng.*, p. 187, March, 1930.

² This problem was first solved by B. KIRSCH, *Z. d. V. D. I.*, p. 797, July 16, 1898. Further applications of the theory of elasticity to the case of an elliptical hole were made by Inglis and Wolff.

For $r = a$ and $\phi = 0$ or $\phi = \pi$, however, s_t becomes negative (*i.e.*, a compression) and

$$s_t = -s. \quad (4)$$

These formulæ indicate that the presence of a small hole in an infinite plate of an elastic material subjected to a pure tension stress in a given direction causes a considerable increase in the stresses in the vicinity of the hole, the maximum normal stress on the boundary of the hole being three times as large as the stress in an undisturbed portion of the plate.

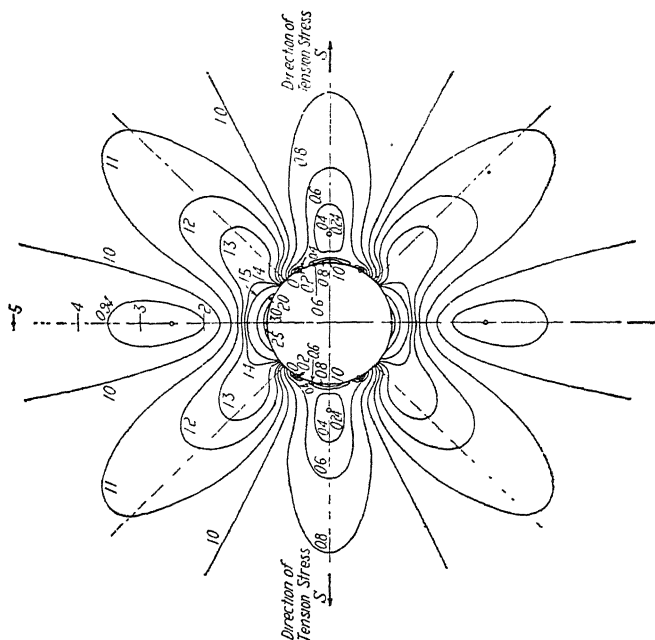


FIG. 84.—Elastic plate with hole in tension. Contour lines indicate curves as computed according to Eqs. (1) and (5) along which maximum shearing stress s_{\max} is constant. These curves correspond in a photo-elastic test to the "isochromatic lines."

To confirm by test these analytical results and to describe the distribution of stress the curves can be calculated along which the maximum shearing stress s_{\max} has a certain constant value.¹ The equation of these curves is given by

$$s_s^2 \max = \frac{(s_t - s_r)^2}{4} + s_s^2 = k^2 \frac{s^2}{4} = \text{const.} \quad (5)$$

where k is a constant. Using here the expressions (1) the contour lines of the distribution of the maximum shearing stress s_{\max} as a function of the

polar coordinates r and ϕ can be determined. These lines are plotted in Fig. 84. For example the contour line marked $k = 1.1$ is the locus of the points where the ratio of s_{\max} to $s/2$ is 1.1. The surface representing the maximum shearing stress s_{\max} above the plane of the plate has two sharp peaks at the points marked $k = 3$ in the figure and situated on the boundary of the hole at $r = a$, $\phi = \pi/2$ and $3\pi/2$.

Figure 84 reveals several remarkable facts: (1) that *the true stress-concentration effect in an elastic material extends only over a comparatively small area*. High values of the maximum shearing stress are encountered only in the vicinity of the peaks of the surface representing $s_{\max} = f(r, \phi)$. (2) The contour lines for the value $k = 1$, i.e., the lines along which the maximum shearing stress is the same as that in the undisturbed parts of the plate, extend to infinity. (3) The effect of stress concentration is furthermore not uniformly distributed around the hole but starts at the two points $k = 3$ (at the "peaks" of the surface $s_{\max} = f[r, \phi]$) on the boundary of the hole and tends then to progress along a cross-shaped area as indicated by Fig. 85.²

f. How Plastic Flow Starts around a Hole.—According to this we must expect that in an elastic material with a well-defined yield stress the first yielding must start at the two points situated on the boundary of the hole on a diameter perpendicular to the direction of the tension and at a tensile stress in the plate which is equal to one-third of the yield stress s_0 in pure tension. But this local yielding is very hard to observe because at first it is practically restricted to two points. As the tensile stress s gradually increases, yielding spreads and very soon tends to progress along two comparatively narrow strips symmetrically situated with respect to the axis of tension and at an angle of about 45° with the direction of tension.

The shape of the contour lines of the surface of maximum elastic shearing stress was checked by photo-elastic tests. A transparent model of bakelite 2 in. wide having a hole of 0.32 in. diameter was tested in tension and projected on a white screen using polarized light. The colored fringes of the loaded

¹ These curves have been calculated by A. M. Wahl and checked by tests by R. V. Baud at the Research Laboratories of the Westinghouse Electric and Manufacturing Company in East Pittsburgh, (*loc. cit.*), to whom the author expresses his indebtedness.

² In brittle materials the presence of a hole or notch with sharp corners is always accompanied by great danger of fracture especially under impact. The effect of a hole or of a concentration of stress on the fatigue limit seems however not to be as pronounced as one would expect. The hole does not lower the endurance limit so much as one would expect from the conclusions drawn from the theory of elasticity mentioned above.

model, which could be observed on the screen, correspond in the photo-elastic test to those points in the plate, where the difference of the two principal stresses is equal to a certain constant. Thus the picture of the colored lines on the screen reveals the lines of constant maximum shearing stress. A photograph of these colored lines is shown in Fig. 86. The agreement between the observed dark bands corresponding to lines of the same color in the photograph, Fig. 86, and the calculated contour lines in Fig. 84 was very satisfactory.

The results of some compression tests with mild-steel test pieces, having drilled

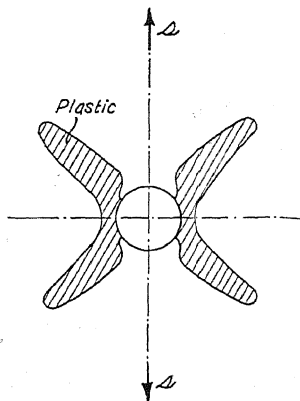


FIG. 85.

FIG. 85.—Spreading of plastic region from hole in a tension member.

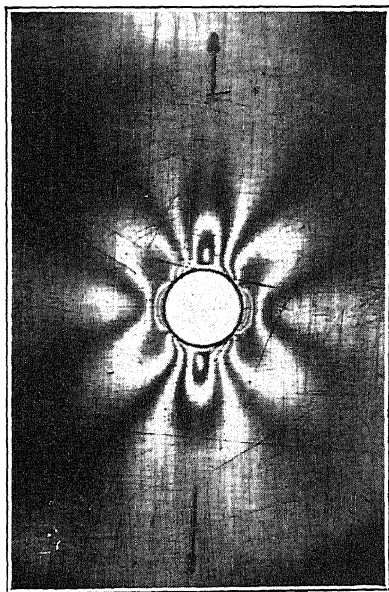


FIG. 86.

FIG. 86.—Photo-elastic test of transparent plate subjected to pure tension in the direction indicated by arrows and having a hole. The dark bands are the pictures of the isochromatic lines (of the lines having certain definite colors) as they appeared on the screen.

holes, are shown in Figs. 87 to 89. The test pieces were approximately prismatic in shape and had, in the middle, a rectangular cross-section of 18 by 24 mm. The surfaces of the specimen containing the holes were photographed using the method described above (page 91). In the test piece of Fig. 87, the hole was perpendicular to the direction of compression, in that of Figs. 88 and 89 the hole was at an angle of 77° and 47° , respectively. A schematic representation of the production of the layers visible on the surface for the case of a hole

perpendicular and for the case of a hole at an angle of 45° to the direction of compression is shown in Figs. 90 and 91. With

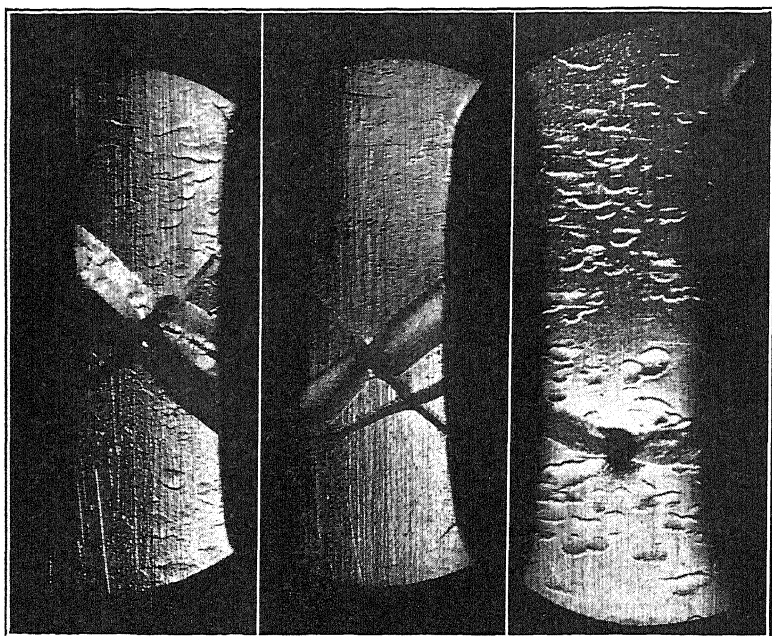


FIG. 87.
 $\alpha = 90^\circ$.

FIG. 88.
 $\alpha = 77^\circ$.

FIG. 89.
 $\alpha = 47^\circ$.

FIGS. 87, 88, and 89.—Flow figures on prisms of mild steel containing holes. Compression tests. α is the angle of axis of hole with axis of prism.

decreasing angles it must be expected that both slip planes tend to come together and at an angle of 45° with the axis of the prism they coincide. This expectation was confirmed by the tests shown in the Figs. 87 to 89. In Figs. 87 and 89, besides the heavy flow lines, a grained appearance of the surface may be noted. These fine relief markings appeared during the progress of the test and were probably caused by an additional bending stress produced by

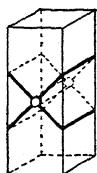


FIG. 90.

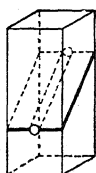
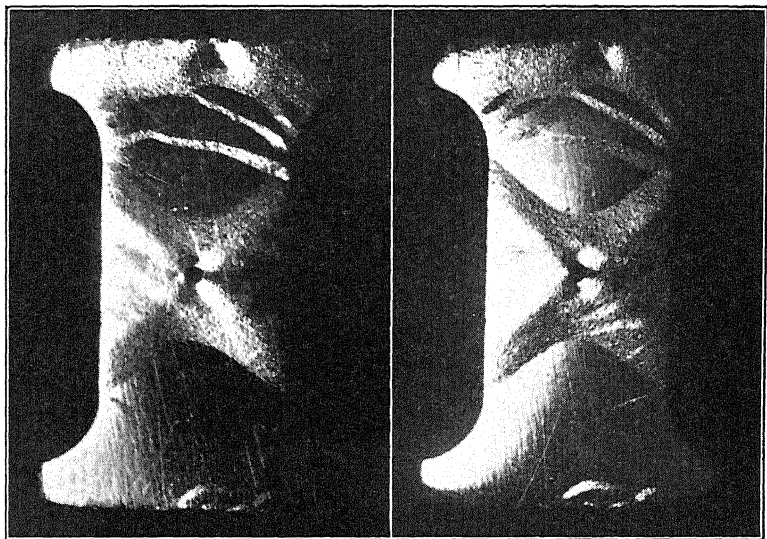


FIG. 91.

an unavoidable eccentricity of loading. The "wave crests" of this fine relief marking, running perpendicular to the direction of compression, are the traces of the flow layers caused by the

superimposed bending stresses due to buckling. Moreover, on the highly polished surface of the rectangle (Fig. 98) may be seen similar markings representing fine flow layers. These slight irregularities of a well-polished surface which are barely visible to the naked eye are shown up well by the special method of illumination described on page 91.

Figures 92, 93 and 94 show the development of slip layers as they progress from a hole under increasing stress, the test pieces



FIGS. 92 and 93.—Flow figures on compression test pieces of steel having hole.

being subjected to compression. The test pieces of low-carbon steel were, after machining, annealed at $930^{\circ}\text{C}.$, polished, and tested.

These and other tests showed that the softer a polycrystalline metal is (*i.e.*, the more gradual the transition of the elastic portion of the stress-strain curve to the plastic portion), the less sharply are the slip layers marked. Test pieces of mild steel having a sharp peak or sharp break in the tensile stress-strain curve with a well-defined yield point show up the two slip layers the best. On the contrary, a soft material like an annealed copper will not show sharp slip layers.

If this point of view is correct, it should be expected that the phenomenon of the formation of Lüders' lines, so characteristic of low-carbon steel and for example not known in tests with copper, should be also produced in materials other than low-carbon steel. This was confirmed. The test piece shown in Fig. 95 was machined from a copper bar which was first subjected to severe cold working by com-



FIG. 94.—Flow figures on mild steel.

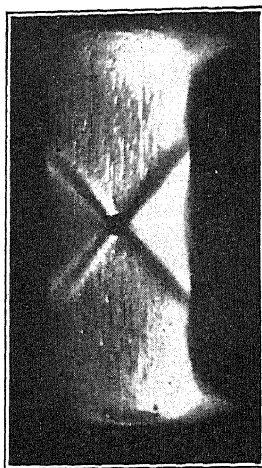


FIG. 95.—Cross of slip layers produced by hole in compression test piece of work-hardened copper.

pressing the bar about 33 per cent. This initial deformation had the effect of cold working the copper and bringing it artificially into a condition mechanically similar to the annealed steel, *i.e.*, both metals showing a well-defined yield point. The specimen of hard copper with a hole showed the cross of slip layers quite in the same way as the steel test pieces described before.

We must therefore conclude that the formation of Lüders' lines in steel, or of similar bands and plastic layers in other metals, must be expected if the material has a well-defined yield point, a slight concentration of stress helping to start or develop these single plastic layers.

APPENDIX

It is of interest to determine the distribution of the lines of constant maximum shear in a plate with a hole, the plate being subjected to pure shear, *i.e.*, a uniform tension combined with an equal compression acting at right angles (see Fig. 96). In such a case, the distribution of the lines of constant maximum shear have the form shown in Fig. 97. These may easily be obtained by superimposing a distribution of stresses represented by Fig. 84 upon another set of stresses similar to those represented by Fig. 84 but displaced through an angle of 90° . The superimposed stresses are to be taken as negative; the result is the series of contour lines shown in Fig. 97. These represent the locus of points having constant values of $k = 2s_{\max}/s$ as before.

It is perhaps worth mentioning here that such a stress distribution around a hole might be obtained in the web of an I-beam, subjected to a severe transverse shearing load. The central part of the web can then be considered as stressed in pure shear, and if the amount of shear is

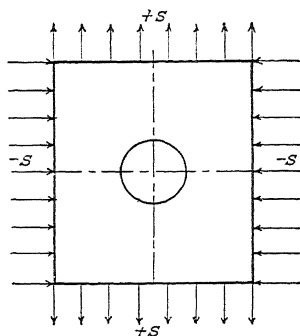


FIG. 96.—Hole in region subjected to pure shear.

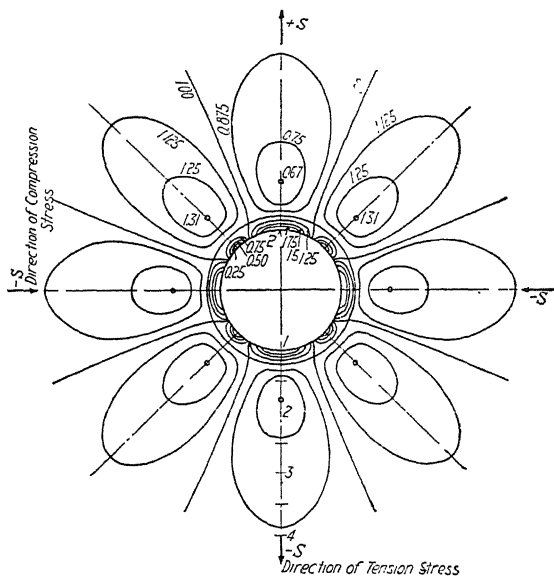


FIG. 97.—Elastic distribution of stress around hole in region subjected to pure shear. The contour lines indicate the curves of constant maximum shear.

large enough, the material should yield in the vicinity of a hole in the web along two perpendicular planes.

CHAPTER 17

COMPRESSION

Although no difficulties are encountered in obtaining a uniform stress distribution in a bar of ductile material under tension until necking begins, special precautions are necessary in order

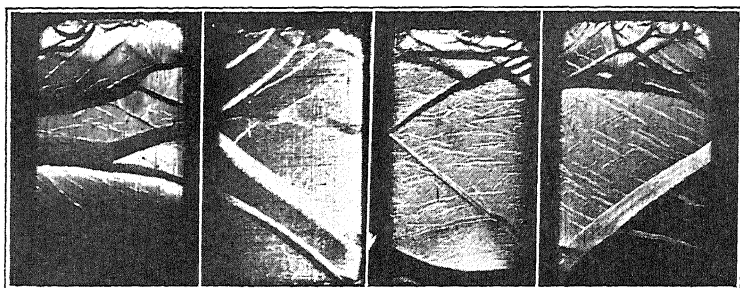


FIG. 98.—Compression test. Flow figures (Lüders' lines) on the four faces of a prism of mild steel.

to load a cylindrical or prismatical bar under axial compression between two hard plates in such a manner that the lateral exten-



FIG. 99a.



FIG. 99b.

FIGS. 99a and 99b.—Flow figures on mild steel. Compression tests.

sion of all cross-sections is the same. Since that part of the test piece which touches the plates producing the compression is hindered from expanding laterally because of the friction, a

bulging in the middle part occurs and there results, especially in the neighborhood of the ends of the test piece, a non-uniform distribution of compressive stress.

The development of the flow layers in the case of compressed mild-steel specimens, shortly after the yield point has been passed, is illustrated in Figs. 98 to 99; *cf.* also Figs. 87 to 94.

a. Cylinders.—If a compression test be made in a testing machine with a cylindrical specimen of a brittle material, such as sandstone, marble, or concrete; or of a ductile metal, certain

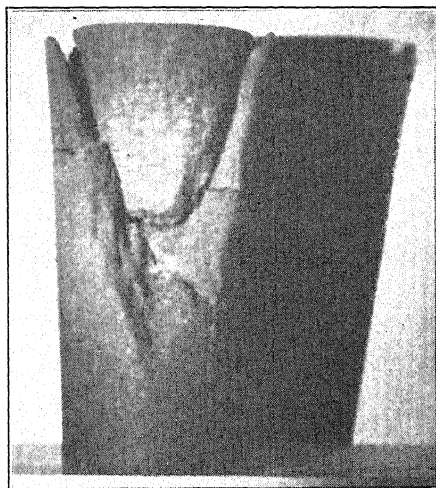


FIG. 100.—Sandstone cylinder broken in compression test exhibiting cone of fracture. (*According to tests of T. v. Kármán.*)

more or less regular markings will be noticed on the specimen before failure. The main thing which will be observed is that the greatest distortion of the material in the specimen usually begins at the edges of the compression surfaces and is generally more or less concentrated along two conical surfaces starting from the ends of the cylinder. In this way two pieces of conical shape split off from the rest of the specimen before failure in the case of brittle materials, and under a larger load these pieces become wedged into the middle part of the specimen and cause this to crack (*cf.* the compressed sandstone cylinder, Fig. 100).

On well-polished cylinders of white marble during a compression test two very regular systems of helical lines may be seen on the surface. Both of these systems of lines make the same

angle with the direction of compression. They are the traces on the surface of the cylinder of two series of helicoidal surfaces in which the marble is more severely distorted than in the neighboring parts. It is possible to make these severely distorted layers visible to the eye if the surface be colored or rubbed by means of a colored pencil. In this way, the markings on the surface of an axially compressed cylinder of Carrara marble (Fig. 101) were obtained. (This cylinder was part of a series of tests on various kinds of rock by Prandtl and Rinne.) A second example of the markings on the surface of a compressed-rock

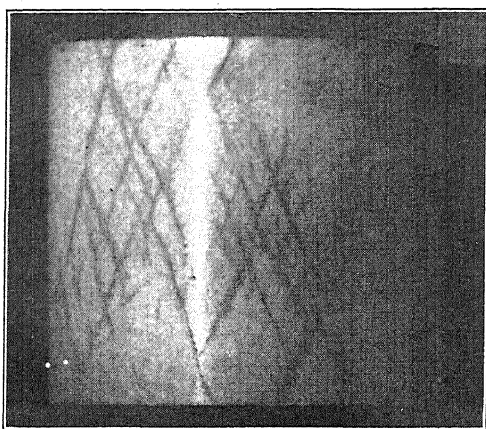


FIG. 101.—Helical slip lines on polished marble cylinder after compression.
(Test by Prandtl-Rinne.)

cylinder is shown by the photograph of Fig. 102. These regular markings indicate that in these tests a distribution of stress with axial symmetry under compression existed.

In order to investigate these phenomena in plastic materials the author made a series of compression tests using very soft materials.¹ These tests will be briefly reviewed in the following:

A dark-colored paraffin having the property of becoming light wherever excessive distortion of the material occurred, was used. By means of the resulting bright lines and markings obtained on the surfaces and cross-sections of these stressed paraffin specimens, the regions in which a severe distortion of the material existed were made plainly visible.

After the maximum load on these compressed paraffin cylinders is reached, markings consisting of fine lines arranged in a more or less regular way

¹ Cf. *Z. f. techn. Phys.*, vol. 5, no. 9, p. 369, 1924; and *Proc. Internat. Congress of Applied Mechanics*, p. 318, Delft, 1924.

develop. These lines which are similar to those in the marble specimens consist of two systems of helical lines crossing each other. These lines make angles of about 45° (usually a little less than 45°) with the generatrices of the cylinder. During the course of the test, single lines or groups of lines become more pronounced until fracture occurs with a resulting drop in the



FIG. 102.—Helical slip lines on stone cylinder after compression test.

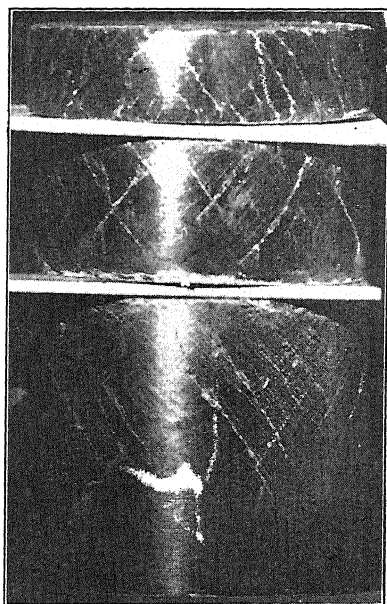


FIG. 103.—Helical systems of slip lines on surface of paraffin cylinders tested in compression.

load. In Figs. 103 to 105, the markings obtained in a series of cylindrical test specimens of five various heights are shown.¹

In Figs. 106, 109, and 111 a few longitudinal cross-sections of compressed paraffin specimens are represented. These sections were taken through the axes of the specimens. Figure 110 represents a schematic sketch of the structural changes observed in the cross-sections of the three cylinders shown in Fig. 103. An external view and a longitudinal cross-section of a truncated

¹ At this point may be mentioned a remarkable phenomenon which was brought out by a series of slowly made compression tests and a second series of rapidly made tests. In the last case, the loading was brought upon the test piece very suddenly, such as would occur if the heavy pendulum of an Amsler testing machine were lifted high and then suddenly released, while the test piece was under a small compressive load. During the rapidly made tests the surface of the cylinder was covered with a much finer and denser network of helical lines than was the case with the slowly made tests.

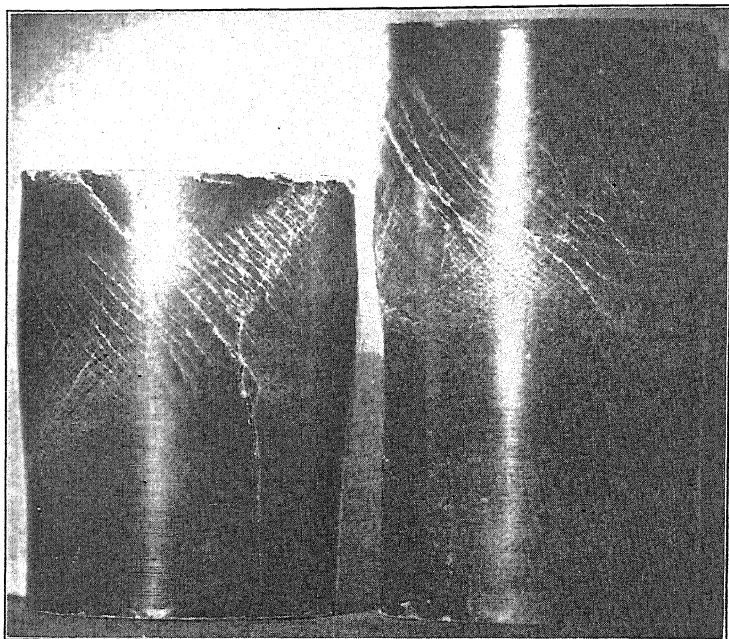


FIG. 104.

FIG. 105.

FIGS. 104 and 105.—Helical systems of slip lines on surface of paraffin cylinders tested in compression.

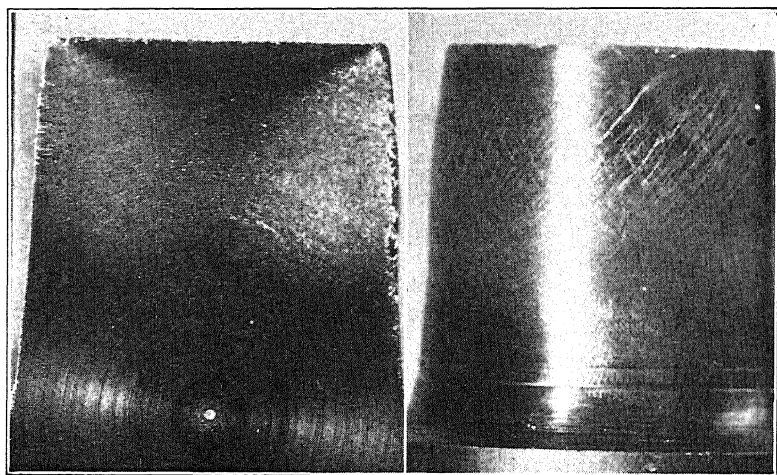


FIG. 106.

FIG. 107.

FIGS. 106 and 107.—Structural changes in longitudinal cross-section (left) and on surface (right) of a paraffin cylinder tested in compression.

cone, having a small angle of cone and tested rapidly in compression, is shown in Figs. 106 and 107.

It will be recognized from the longitudinal cross-section (Figs. 106) that the curves of constant degree of destruction of the material (and of constant intensity of color) have approximately the shape shown by the lines of the sketch of Fig. 108. A more careful consideration of such cross-sections shows that the amount of distortion of the material inside the specimens (the more the material has been deformed the brighter it appears in the photographs) changes throughout the inside of the specimen in a regular manner. Two truncated cones of material at each end of the specimen seemed to adhere to the plates of the testing machine used to transmit the compressive load. (In order to produce a strong adhesion the paraffin specimens were compressed between steel discs having the same radius and intentionally rough-machined surfaces.) These two cones can for example be seen in the dark part of the longitudinal cross-section of a specimen shown in Fig. 109. In the cross-sections the compressed regions *a* (Fig. 110) have a black and white¹ mottled appearance with a fibrous

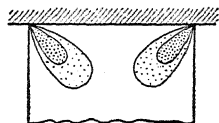


FIG. 108.—Section through axis of a cylinder of soft material near compression plate, showing areas of equal degree of destruction.

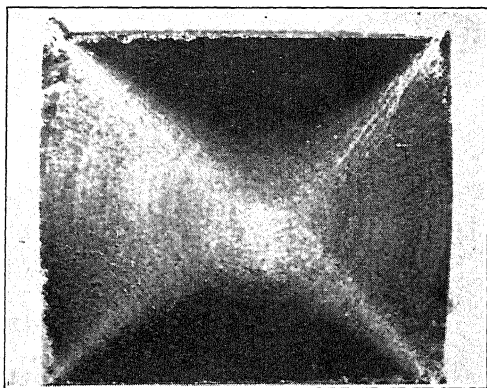


FIG. 109.—Section through axis of a paraffin cylinder after severe compression. If the cylinder had been stressed higher, the cones of fracture would have developed from the four narrow bright sectors originating in the corners.

structure whose direction was perpendicular to the direction of compression. If the two cones extended uniformly into the test piece this mottled surface extended quite deeply towards the middle of the test specimen. This, however, was usually the case only for the shorter specimens. Areas of distortion *c* (Fig. 110) extended like rays from the edges of the cylinders,

¹ The plain white surfaces (not cross-hatched) in the sketches (with exception of the cones *b*) represent likewise regions of changed and distorted texture, in which, however, no definite fibrous structure was recognizable (see Fig. 109).

both systems of slip lines being often very noticeable in these areas. (For example, compare the section through a severely distorted cylinder, Fig. 109.) No slip lines were visible along the axis of the cylinder, a fact which is required from conditions of symmetry.

The angle which the ray-shaped areas of distortion make with the axis of the specimen depends, for the same material, on the friction existing in the compressed surfaces of the specimen and on the ratio of length of cylinder to diameter. Using similar compression plates, three cylinders, having different values of the ratio h/d of length of cylinder to diameter, gave the following values of the angle α between the generatrices of the cone of rupture and the base:

Value of h/d	Value of α
1.00	36°
0.50	25°
0.33	21°

A few of the shorter cylinders occasionally showed on their surface, besides the helical slip lines, countless fissures, running parallel to the

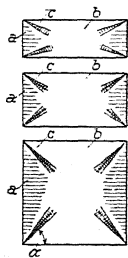


FIG. 110.

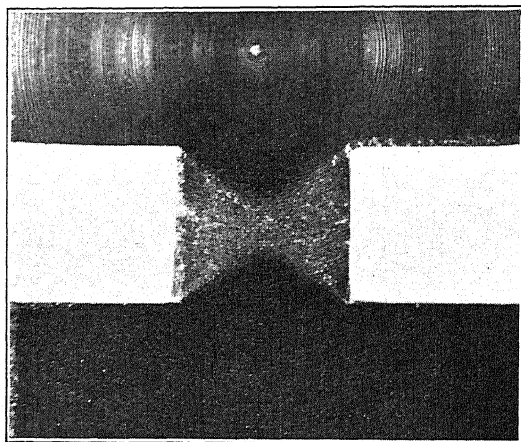


FIG. 111.

FIG. 110.—Longitudinal section through three cylinders of different heights from a soft material, showing structural changes due to compression test.

FIG. 111.—Section through a cylinder of paraffin with constricted portion exhibiting two cones along which fracture would have developed under further loading.

direction of compression. These tended to open up under further loading, and frequently, under close examination, showed a tendency to form jagged lines because of crossing the helical slip lines.

The deformation of a few rings, loaded axially in compression between smooth hard plates, will now be considered. The deformation of two rings is represented in an easily understandable way by the slip lines in Figs. 112 and 113. In the case of a thin ring (Figs. 112 and 114) the deformation was quite different from that in the case of a thick ring (Figs. 113 and

115). Since the conical slip surfaces in a thick ring come to an intersection at the inner surface of the rings near the middle of the height, the displacements were such as to form a ring-shaped swelling on the inside surface of the ring. This bulged-out portion is easily recognizable in the photograph of the longitudinal section. No such deformation could be observed with the thin rings.

The distortion was axially symmetrical only for the case of the shorter cylin-

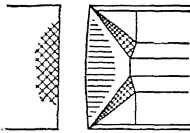


FIG. 112.

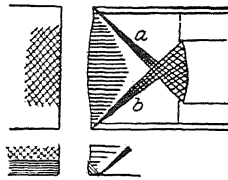


FIG. 113.

FIGS. 112 and 113.—Slip lines in section of rings loaded in axial direction by compression.

ders; as soon as the height of the cylinder exceeded a certain value, the distortion often became unsymmetrical and was, moreover, limited to a short portion of the length (*cf.* Figs. 104 and 105). Cylindrical specimens of brittle material often fracture so that the final surface is composed of portions of both a right- and a left-handed helicoidal slip surface together with a part of the

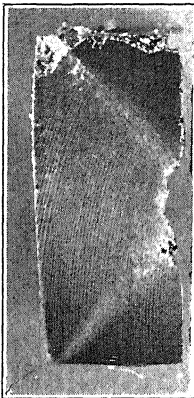


FIG. 114.

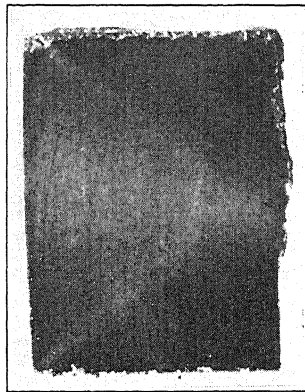


FIG. 115.

FIGS. 114 and 115.—Section of two paraffin rings through axis exhibiting structural changes due to compression.

cone of slip extending from the compression plates. These three surfaces unite to a common surface of fracture, which sometimes may not differ much from an oblique plane.

b. Plane Compression Tests.—Prisms having narrow rectangular cross-sections in planes perpendicular to the direction of compression, were tested between two compression plates.

These gave slip lines such as shown in the photographs of Figs. 116 and 117. Before the tests, the prisms were cut through along a middle plane coinciding with the direction of compression and during the tests both pieces were held together by light pressure. The mode of deformation of the prism is rendered visible by noting the distortion of the grooves left by the cutting tool of a lathe. The test specimens, whose middle cross-sections

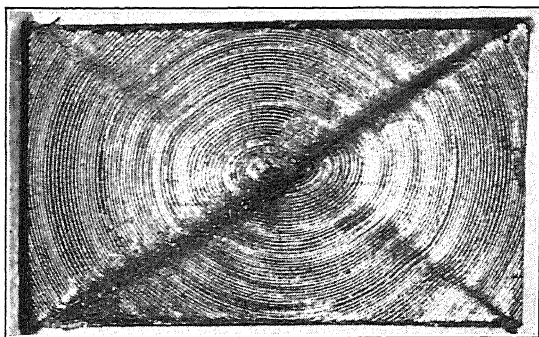


FIG. 116.

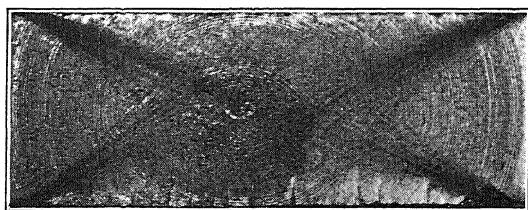


FIG. 117.

FIGS. 116 and 117.—Plane compression tests. Sections through the middle plane of two flat prisms of paraffin subjected to compression in a direction parallel to small edge of rectangle. The distortion of the section can be recognized by the regular markings which were formerly circular.

are shown in Figs. 116 and 117 had approximately equal widths (33 to 35 mm.) and lengths (125 mm.) but a different ratio of height to width.

When the deformation has proceeded sufficiently and has occurred symmetrically, certain regular systems of slip lines extended from the corners of the test piece under compression. These crossed each other in the middle portion of the test specimen in a manner described by L. Prandtl.¹ It will be noted

¹ *Z. f. ang. Math. u. Mech.*, 1923.

that the originally concentric, circular tool marks become ellipses only in the central portion of the cross-section. In the four outer areas of triangular shape (see Fig. 116) the circles remain almost concentric, while the material in four narrow sectors emanating from the corners must have been subjected to extraordinarily high shearing displacements. As a consequence of this non-uniform deformation the material is distorted mainly in these narrow sectors so that finally the test specimen breaks into four pieces. This is indicated by the schematic sketch in Fig. 118.

c. Prisms.—A series of prisms with square cross-sections of 36 mm. length and having heights of 60, 48, 36, and 24 mm., when tested gave the slip figures shown in Figs. 119 to 125. The prisms were compressed between wood plates having rough-grooved surfaces. The relationship between these slip figures with those of the plane problem is unmistakable. However, in this case, the converging systems of slip lines make a greater angle with the direction of compression, corresponding to the different (radially directed) direction of the friction stresses in the compression planes. In the case of the shorter prisms, four portions of the specimen along the four edges parallel to the direction of compression remained undeformed, while the middle portion of the faces of the prism showed a network of slip lines of marked regularity. A bulging out of the middle portions of the sides was also noticeable. If we think of a cylinder inscribed in the prism, its axis coinciding with that of the prism, and the portions of the material near the corners cut away in the manner shown in Fig. 126, we will recognize the network of slip lines of the prisms as a part of the network of helical lines already described for the case of cylinders under compression. They appear on the surface of the prisms, where the inscribed cylinder touches it.

Similar slip lines are exhibited on the surface of compressed marble specimens, as, for example, on the photograph of Fig. 127, showing one of a group of specimens of Carrara marble, tested by Prandtl. Moreover, in this case, the remarkably steep angle of the marble slip lines is exhibited.

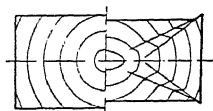


FIG. 118.—Sketch indicating cross-section of a flat prism before (left half of figure) and after (right half) a plane compression test. Direction of compression stress parallel to short edge.

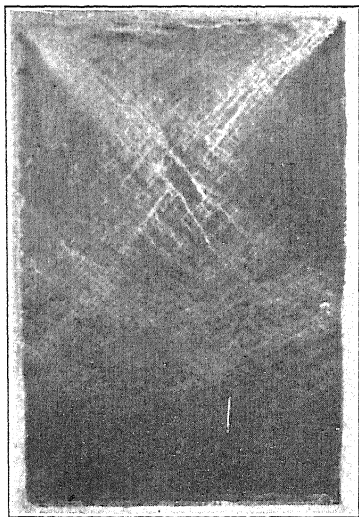


FIG. 119.

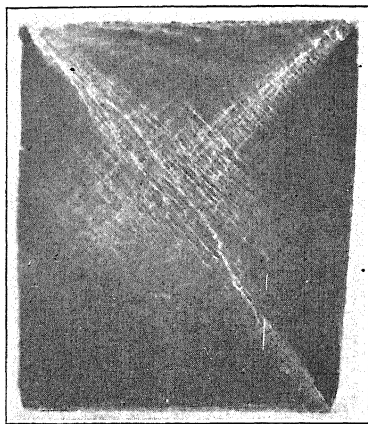


FIG. 120.

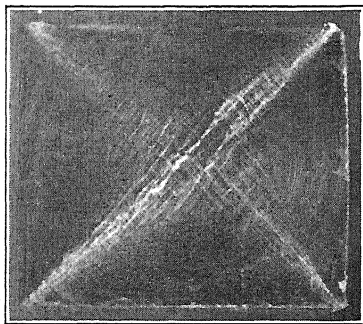


FIG. 121.

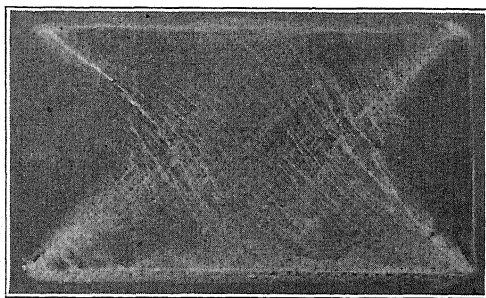


FIG. 122.

Figures 119 to 122.—Compression tests with paraffin prisms of same square cross-section and of different heights.

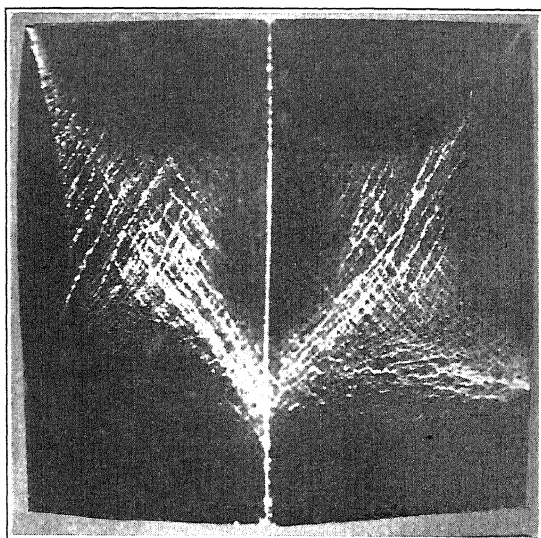


FIG. 123.

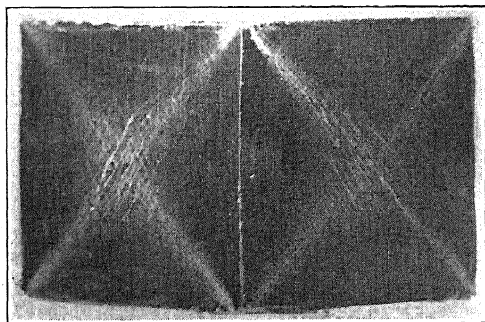


FIG. 124.

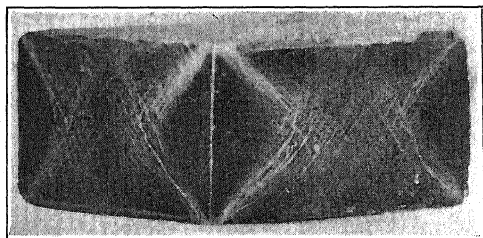


FIG. 125.

FIGS. 123 to 125.—Systems of slip lines appearing on sides of paraffin prisms of square cross-section tested in compression. The effect of the height of the prisms on the shape of the slip lines is noticeable.

d. **Compression Tests on Cylinders of Ductile Metals.**—Although the above described compression tests were carried out only with a material having a very loose texture or on brittle



FIG. 126.

rocks, the phenomena observed will apply at least qualitatively also to compression tests of ductile metals. This has been established by countless observations¹ and tests. The action of the friction between the compressed plates is exhibited by the well-known barrel-shaped form which the shorter metal cylinders assume under compression. Where the cylinders have lengths

from one and one-half to three times the diameter and where ductile metal is used, the deformation is usually such that two symmetrical enlargements or a bulging out of the cylinder in two sections is observed. For longer cylinders, sidewise buckling may occur.

Regions of large shearing deformations diverging from the edges of the cylinders may also be shown to exist in longitudinal sections of cylinders of mild



FIG. 127.

FIG. 127.—Slip lines and surfaces of fracture of a marble prism after compression test. One of the "pyramids of fracture" can be seen in the upper part of the test piece.

FIG. 128.—Section through a steel cylinder after it was pressed between hard plates, showing the distortion of the parallel sets of streaks due to the impurities of the steel. (According to H. Meyer and F. Nehl.)



FIG. 128.

steel. The lines or markings which result in the etched longitudinal section of the test specimen, because of the presence of the inclusions and segregated zones in the ingot, permit one to determine how a mild-steel cylinder deforms when compressed

¹ Cf. the compression tests of Riedel, Hübers, Meyer and Nehl, Siebel, etc., mentioned below.

between two hard-steel plates. In order to decrease the friction between the compressed surfaces, Hübers¹ lubricated the compression plates with a mixture of oil and graphite. He thus

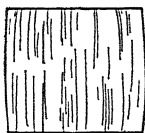


FIG. 129.

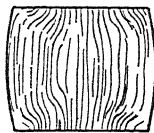


FIG. 130.

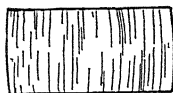


FIG. 131.



FIG. 132.

FIGS. 129 TO 132.—Longitudinal sections of steel cylinders after compression tests. Left figures: lubricated with graphite in compression plane. Right figures: without lubricant. (According to K. Hübers.)

obtained a series of markings as shown in Figs. 128 to 133, which are copied from his photographs. While the cylinders lubricated with graphite expanded laterally in a uniform manner, the unlubricated test specimens showed a barrel-shaped form with a considerable distortion of the system of longitudinal lines or fibers produced by rolling. (Comparing the markings of Figs. 110, 128 and 132, it should be noted that the conical surfaces exhibiting large shearing deformations in the highly compressed steel cylinders are continually forming anew, and their position changes relative to the test specimen. The cylindrical surface near the ends of the cylinder tends to invert, and gradually moves so that it becomes part of the outermost ring-shaped part *x* of the circular area under compression. This is shown by a section of a specimen in Fig. 133.) Meyer and Nehl² have further investigated the phenomena in compressed

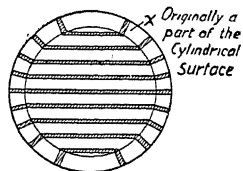


FIG. 133.—Base of a test cylinder after severe compression. Distortion of the formerly parallel streaks due to the impurities, the orientation of which was here perpendicular to axis of cylinder.

¹Das Verhalten einiger technischer Eisenarten beim Druckversuch, *Walzwerkauausschussbericht des V.D.E.*, No. 32, Düsseldorf. This paper gives considerable data relative to compression tests.

²Die grundlegenden Vorgänge der bildsamen Verformung, *Stahl und Eisen*, vol. 45, p. 1961, 1925 (Mitt. aus der Prüfungsanstalt der August Thyssen-Hütte, Hamborn).

iron cylinders by means of etching the longitudinal sections, using Fry's method. They have also investigated the change in load under compression. In the schematic reproduction of an etched longitudinal cross-section of a compressed iron cylinder (Fig. 134) the conical areas in which the friction of the compression plates hinders the lateral expansion may be clearly recognized. In a test specimen with very accurately machined ends Meyer and Nehl were able to demonstrate clearly the presence of the conical surfaces of slip (appearing as black lines in Fig. 135). They obtained the following values for the angle ϕ which this conical surface made with the direction of compression,

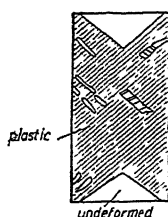


FIG. 134.



FIG. 135.

FIGS. 134 and 135.—Region plastically deformed (left) and conical surfaces of slip (right) in sections of compressed steel cylinders. (According to Meyer and Nehl.)

various ratios of cylinder diameter d to length of cylinder h being considered:

$d/h =$	0.4	0.6	0.8	1.0	1.2
$\phi =$	32°	40°	47°	55°	62°

The conditions of the ordinary compression test have been substantially improved by Siebel and Pomp,¹ who suggested that if it be desired to obtain a uniform distribution of stress, the cylindrical test specimens should be compressed, not between two plane plates, but between two cones (Fig. 136). If the generatrices of these cones make an angle with the plane of compression, equal to the angle of friction, the resultant stress in the compression surfaces of the two cones is parallel to the direction of compression. This produces everywhere in the test specimen a pure axial compressive stress.

¹ Die Ermittlung der Formänderungsfestigkeit von Metallen durch den Stauchversuch, *Mitt. aus d. K.-W. Inst. f. Eisenforsch.*, vol. 9, p. 157, Düsseldorf, 1927. Cf. also E. SIEBEL, "Grundlagen zur Berechnung des Kraft- und Arbeitsbedarfs beim Schmieden und Walzen," Dr.-Ing. Dissertation, Berlin, 1923.

For an ideal compression test with uniform and unrestricted lateral expansion, we have, as in tensile tests, since the volume of the compressed cylinder is practically constant

$$\pi r^2 h = \pi r_0^2 h_0, \quad (1)$$

where r and h are the radius and height respectively of the cylinder at any given time, and r_0 and h_0 are initial values of r and h . The trajectory, which an arbitrary point r, h describes during an ideal compression test, is given by the equation:

$$h = \frac{r_0^2 h_0}{r^2} \quad (2)$$

Putting

$$\epsilon = \frac{h_0 - h}{h_0} \quad (3)$$

and

$$\epsilon_r = \frac{r - r_0}{r_0} \quad (4)$$

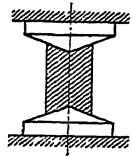


FIG. 136.—
Cylinder
compressed be-
tween conical
end plates.
(According to
E. Siebel.)

as the unit compression and unit lateral expansion, respectively, taken with respect to the initial dimensions, there results from the last equation

(since $r = [1 + \epsilon_r]r_0$ and $h = \frac{h_0}{1 + \epsilon}$) an expression for the unit axial compression:

$$\epsilon = (1 + \epsilon_r)^2 - 1 = (2 + \epsilon_r)\epsilon_r. \quad (5)$$

The compressive stress s taken with respect to the actual cross-section is a function of the unit compression ϵ

$$s = f(\epsilon). \quad (6)$$

This function can be determined experimentally using the conical compression test as described by Siebel and Pomp in the paper mentioned above.

In uniformly compressing a cylinder from a height h_0 to a height h the following work is done:

$$W = \pi \int_h^{h_0} r^2 s dh = \pi r_0^2 h_0 \int_h^{h_0} s \frac{dh}{h} \quad (7)$$

If, in this expression, we substitute, for h , the unit compression ϵ , we obtain (since $h = \frac{h_0}{1 + \epsilon}$, $\frac{dh}{h} = -\frac{d\epsilon}{1 + \epsilon}$) the work of deforma-

tion equal to:

$$W = \pi r_0^2 h_0 \int_0^\epsilon \frac{f(\epsilon) d\epsilon}{1 + \epsilon} \quad (8)$$

If we take the stress s in terms, not of ϵ , but of a new variable z , such that

$$z = \ln \frac{h_0}{h} = \ln(1 + \epsilon) \quad (9)$$

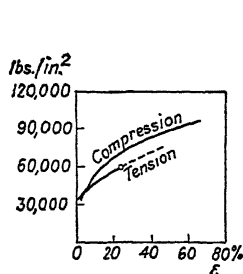


FIG. 137.—Wrought iron,
0.06 C., 0.15 Mn

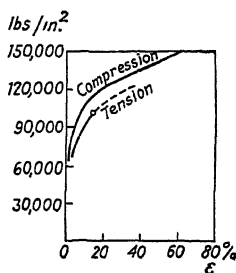


FIG. 138.—Carbon steel,
0.21 C., 0.17 Si., 0.62 Mn.

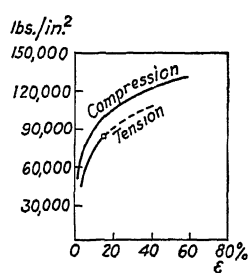


FIG. 139.—Carbon steel,
0.39 C., 0.72 Mn.

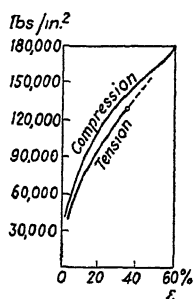


FIG. 140.—Nickel steel,
0.23 C., 0.65 Mn, 24.6 Ni.

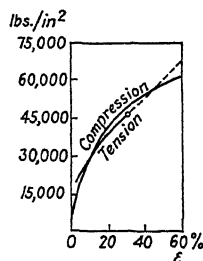


FIG. 141.—Copper.

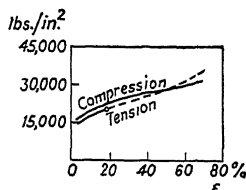


FIG. 142.—Aluminum.

FIGS. 137 to 142.—Deformation curves $s = f(\epsilon)$ for tension and compression. (According to Siebel and Pomp.) (Abscissae: unit elongation or compression ϵ , ordinates: true tensile or compressive stresses s referred to actual cross-sectional area.)

we obtain the work of deformation per unit volume in the simple form given by Siebel and Pomp:

$$W = \int_0^z s \, dz \quad (10)$$

This is the area under the curve $s = f(z)$.

In Figs. 137 to 142, the deformation curves $s = f(\epsilon)$ in tension and compression for soft iron, two carbon steels, a nickel steel,

copper, and aluminum, as determined by Siebel and Pomp, are given. In all cases the curves of stresses in the plastic stage of iron and steel for compression are higher than the corresponding ones for tension. For copper and aluminum the s curves for compression differ but little from those for tension, in agreement with earlier tests of Ludwik and Scheu.¹

¹ Vergleichende Zug-, Druck-, Dreh-, und Walzversuche, *Stahl und Eisen*, vol. 45, p. 373, 1925.

CHAPTER 18

TORSION OF A CYLINDRICAL BAR OF CIRCULAR CROSS-SECTION

THE STRESS-STRAIN CURVE IN PURE SHEAR

In a cylindrical bar of circular cross-section twisted by two couples acting about its longitudinal axis, the distribution of shearing stresses over a cross-section, after the yield point is exceeded, may be described for an arbitrary law of deformation.¹ Let s equal the shearing stress at a distance r from the center of the circular cross-section and a the radius of the bar (Fig. 143). Under torsion two cross-sections, a distance l apart, will rotate with respect to each other through an angle ϕ , which is proportional to the length l

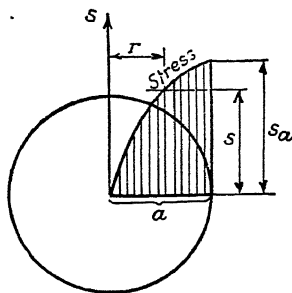


FIG. 143.—Shearing stresses in twisted bar.

$$\phi = \theta \cdot l. \quad (1)$$

In this equation θ is the unit angular twist of the bar, i.e., the angle, through which two cross-sections which are of unit distance apart rotate with respect to each other. Considering two neighboring cross-sections, a point P (Fig. 144), at a distance r from the axis of the bar, is displaced, when twist occurs, along a small circular arc PP' . Under this displacement an element QP , which was initially parallel to the axis of the bar, is displaced through an angle γ' . In its final position the element QP' forms a part of a cylindrical helix. Therefore we have:

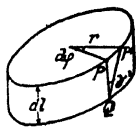


FIG. 144.

$$PP' = r d\phi = r\theta \cdot dl = \tan \gamma' \cdot dl, \quad (2)$$

¹ This apparently was first suggested by CH. DUGUET, "Limite d'élasticité et résistance à la rupture," vol. 1, p. 157, Paris, 1882; then, independently, by P. LUDWIG, "Elemente der technologischen Mechanik," Julius Springer, Berlin, 1909; and by L. PRANDTL, in his university lectures, cf. HERBERT, *Mitt. u. Forschungsarb. d. V.D.I.*, No. 89, 1910.

from which

$$\tan \gamma' = r\theta. \quad (3)$$

In this $\tan \gamma' = \gamma$ is the measure of the unit shear or of the plastic deformation at the distance r . The shearing stress s is a function $s = f(\gamma)$ of the unit shearing strain γ . The function:

$$s = f(\gamma) \quad (4)$$

will be called the stress-strain curve for pure shear.

a. If the stress-strain curve $s = f(\gamma)$ of the material in shear is known, it is possible to determine the twisting moment acting on a bar in terms of the unit angular twist. This curve $M = F(\theta)$, which we will call moment-twist curve, may actually be determined from a torsion test. The twisting moment M is given by the integral:

$$M = 2\pi \int_0^a sr^2 dr. \quad (5)$$

Since the unit shearing displacement γ at a distance r is given by the equation

$$r\theta = \gamma, \quad (6)$$

we may substitute γ instead of r in the integral and since

$$\theta dr = d\gamma \quad (6a)$$

$$M = \frac{2\pi}{\theta^3} \int_0^{\gamma_a} f(\gamma) \gamma^2 d\gamma. \quad (7)$$

The upper limit of the integral is $\gamma_a = a\theta$.

This means that for a given unit angular twist θ , the corresponding twisting moment M acting on the bar is equal to the moment of inertia of the shaded area included under the stress-strain curve $s = f(\gamma)$ (Fig. 145) taken about the s axis, this is to be multiplied by $2\pi/\theta^3$. The shaded portion, whose moment of inertia is to be taken, extends to a unit shear $\gamma_a = a\theta$.

In the case of shearing deformations not much larger than $\gamma = 0.15$ (in the case of a tension or compression test the extension or compression corresponding to this shear is equal to $\epsilon = .2\gamma/3$ or 10 per cent, which is a considerable amount of deformation) it is possible to use the angle γ' under the integral sign instead of the angle γ .¹

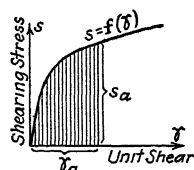


FIG. 145.—Stress-strain curve $s = f(\gamma)$ for pure shear.

¹ If we take instead of γ the angle γ' which the generatrix of the cylinder makes with the helix, we have in the integral instead of $\gamma^2 d\gamma$ the quantity

b. Conversely if the moment-twist curve $M = F(\theta)$ be known from a torsion test, it is possible to use Eq. (7) to determine the unknown stress-strain curve of the material for pure shear $s = f(\gamma)$. The right side of the equation:

$$M\theta^3 = 2\pi \int_0^{\gamma_a} f(\gamma) \gamma^2 d\gamma \quad (8)$$

is a function of the upper limit γ_a and since $\gamma_a = a\theta$, it is also a function of θ . Therefore we have:

$$\frac{d}{d\theta}(M\theta^3) = 2\pi f(a\theta) \cdot a^3 \theta^2 = 2\pi a^3 \theta^2 s_a. \quad (9)$$

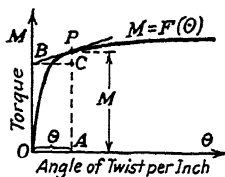


FIG. 146.—Torque-twist curve $M = F(\theta)$.

Since $s_a = f(a\theta)$, the shearing stress at the edge $r = a$ of the circular cross-section is determined. From the last equation the shearing stress s_a at the edge is given by:

$$s_a = \frac{1}{2\pi a^3 \theta^2} \cdot \frac{d}{d\theta}(M\theta^3) = \frac{1}{2\pi a^3} \left(\theta \frac{dM}{d\theta} + 3M \right). \quad (10)$$

Expressed in words this last equation means that the shearing stress s_a corresponding to a unit shear $\gamma_a = a\theta$ in a twisted bar can be constructed from the torque-twist diagram $M = F(\theta)$ of the bar by adding the lengths of two straight lines in this diagram: $\overline{CP} + 3\overline{AP}$ (Fig. 146). The shearing stress s_a corresponding to a unit shear $\gamma_a = a\theta$ is equal to the projection $CP = \theta \cdot dM/d\theta$, of the tangent \overline{PB} to the moment-twist curve, increased by three times the moment $M = \overline{AP}$, this sum $\overline{CP} + 3\overline{AP}$ to be divided by $2\pi a^3$.

The shape of the stress-strain curve for pure shear has been exhaustively studied by P. Ludwik and determined for the various ductile metals.¹

$\left[\frac{\sin \gamma'}{\cos^2 \gamma'} \right]^2 d\gamma'$. If $\gamma \leq 0.15$ this quantity may be replaced by $\gamma'^2 d\gamma'$. We have:

γ' in degrees =	0	10°	20°	30°	40°
γ' in radians =	0	0.175	0.349	0.524	0.698

while

$$\sin \gamma' : \cos^2 \gamma' = 0 \quad 0.178 \quad 0.387 \quad 0.667 \quad 1.096$$

¹ "Elemente der technolog. Mechanik," 1909, and *Stahl und Eisen* 1905; cf. also the torsion tests of W. BADER, Dissertation, Göttingen, 1927.

CHAPTER 19

THE PROBLEM OF PLASTIC TORSION—EXPERIMENTAL REPRESENTATION OF STRESS DISTRIBUTION

It is possible to consider mathematically the stress distribution in a prismatical or cylindrical bar having an arbitrary cross-section and subjected to pure torsion up to the stage where plasticity begins to develop, provided the metal has a definite plastic limit. We have seen that the plastic deformations of mild steel under tensile or compressive stress begin to develop without a large increase in stress if the permanent extension or compression is only of the order of a few per cent. If the permanent strains do not exceed this order of magnitude, it is therefore permissible to introduce an important simplification for metals having a well-defined yield point such as low-carbon steel. This simplification consists in assuming an idealized stress-strain diagram for the beginning of plastic flow consisting of two straight lines as shown in Fig. 147. Since all the elements of a bar subjected to pure torsion are stressed in the same manner and the kind of stress in all the elements of such a bar is a pure shear, the simplest assumption may be made, namely, that stress and strain in each element are related as shown by an idealized diagram such as given in Fig. 147, for pure shear.

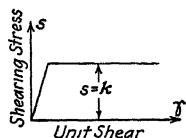


FIG. 147.—Idealized stress-strain diagram.

The following treatment assumes, as does the mathematical theory of elastic torsion of a bar to which it is closely related, that the direct and shearing strains are small, relative to unity. With this assumption the increase in stress under plastic strain or what is commonly called “the effect of work hardening” will be neglected. It will be further assumed, that the elastic constants of the material, when yielding ceases, remain the same as they were initially and that where the material in the bar was not stressed beyond the limit of plasticity, the same relations hold as those which are valid in a perfectly elastic bar under torsion.

In order to analyze the distribution of stress in a twisted bar after the yield point has been reached, it is first necessary to recapitulate how this distribution is determined in an elastic bar.

a. Elastic torsion. Prandtl's Soap-film Analogy. The Elastic Stress Function for Torsion.—The distribution of shearing stresses in an elastically twisted bar may best be visualized by using Prandtl's membrane or soap-film analogy. In order to find the resulting shearing stress s , which exists at a given point P of the cross-section of an elastically twisted bar, a right-angled coordinate system will be used (Fig. 148) with the z axis along the axis of the bar. The resulting shearing stress s will be divided into two components s_x and s_y in the direction of the x and y axes respectively.¹

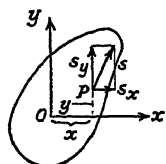


FIG. 148.—Section through twisted bar.

The equilibrium of stresses acting on an element dx, dy, dz is expressed by the equation

$$\frac{\partial s_x}{\partial x} + \frac{\partial s_y}{\partial y} = 0. \quad (1)$$

Let ξ, η, ζ be the small displacements of the point x, y, z relative to its initial position and parallel to the axes x, y, z . Under twist the cross-section of the bar z -constant rotates about the z axis. This is expressed by the equations

$$\xi = -\theta yz, \quad \eta = \theta xz, \quad \zeta = c\phi(x, y) \quad (2)$$

These displacements show that the projection of the point x, y, z , on the x, y plane describes a small arc of length cr (where $r^2 = x^2 + y^2$) with respect to the z axis and that the originally plane cross-sections of the bar are, in general, distorted into surfaces given by the function $\phi(x, y)$. The constant θ in Eq. (2) is the angular twist of the bar per unit of length.

We now express the unit shears γ_{xz} and γ_{yz} by using the Equations (13) page 54 as follows:

$$\left. \begin{aligned} \gamma_{xz} &= \frac{\partial \xi}{\partial z} + \frac{\partial \zeta}{\partial x} = \theta \left(\frac{\partial \phi}{\partial x} - y \right) \\ \gamma_{yz} &= \frac{\partial \eta}{\partial z} + \frac{\partial \zeta}{\partial y} = \theta \left(\frac{\partial \phi}{\partial y} + x \right) \end{aligned} \right\} \quad (3)$$

¹ Shearing stresses will be designated by s_x and s_y as well as by the letter s throughout this chapter. As both components s_x, s_y of the shearing stress s are the only stress components acting on the lateral planes of an element dx, dy, dz in the twisted bar, no danger of ambiguity is introduced by this notation (in contradistinction to the general rules explained on page 40 and used in other parts of this book).—Regarding the theory of elastic torsion cf. A. E. H. LOVE, "Mathematical Theory of Elasticity," 4th ed., chap. 14, The Cambridge University Press.

The shearing stresses s_x and s_y are given by Hooke's law

$$\left. \begin{aligned} s_x &= G\gamma_{xz} = G\theta\left(\frac{\partial\phi}{\partial x} - y\right) \\ s_y &= G\gamma_{yz} = G\theta\left(\frac{\partial\phi}{\partial y} + x\right) \end{aligned} \right\} \quad (4)$$

In this G represents the modulus of rigidity.

From these equations it follows that at each point x, y of the cross-section, the following equation must hold:

$$\frac{\partial s_x}{\partial y} - \frac{\partial s_y}{\partial x} = -2G\theta = \text{const} \quad (5)$$

In order to satisfy Eq. (1) the shearing stresses are taken equal to the derivatives of a certain function $F(x, y)$:

$$s_x = \frac{\partial F}{\partial y}, \quad s_y = -\frac{\partial F}{\partial x}. \quad (6)$$

The function $F(x, y)$ is called the *elastic stress function of the cross-section*.

From this, using Eq. (5) and (6), the following partial differential equation, defining the function F , is obtained:

$$\frac{\partial^2 F}{\partial x^2} + \frac{\partial^2 F}{\partial y^2} = \Delta F = -2G\theta = \text{const.} \quad (7)$$

In order to obtain the boundary conditions, *i.e.*, the conditions which the function F must satisfy at the edges of the cross-section, it should be considered that the resulting shearing stress s at each point of the boundary of the cross-section shall have no components perpendicular to the edge. Let $y = f(x)$ be the boundary curve of the cross-section. Therefore, along the boundary curve $y = f(x)$ the following equation must hold:

$$\frac{s_y}{s_x} = \frac{dy}{dx}, \quad (8)$$

by which the fact that the shearing stress s is tangent to the curve $y = f(x)$ is expressed. Substituting Eq. (6) in Eq. (8), there results

$$-s_y dx + s_x dy = \frac{\partial F}{\partial x} dx + \frac{\partial F}{\partial y} dy = 0. \quad (9)$$

This means that along the boundary curve $y = f(x)$ of the cross-section the ordinates of the function F must be taken as constant.

These equations contain the essentials of the Prandtl membrane or soap-film analogy which is as follows: a thin membrane stressed uniformly in its plane (a soap film) is to be thought of as attached to the boundary curve of the cross-section of a twisted bar. This membrane is loaded by a constant external pressure. It can be easily shown that the deflection of such a membrane would satisfy a differential equation of the form $\Delta u = \text{constant}$, while the deflection u has a constant value along the edge. The curved surface into which the membrane is distorted by the lateral pressure and which may be called the soap-film surface of the cross-section thus satisfies

essentially the same conditions as the function $F(x, y)$ or the elastic stress function of the cross-section. Along the contour lines of this surface is $u = \text{const}$ or $F = \text{const}$. At every point along a contour line according to (9):

$$\frac{dy}{dx} = -\frac{\partial F}{\partial x} : \frac{\partial F}{\partial y} = \frac{s_y}{s_x} \quad (10)$$

This means that the resultant shearing stress s is tangent to the contour lines $F(x, y) = \text{constant}$. Furthermore, we have

$$s^2 = s_x^2 + s_y^2 = \left(\frac{\partial F}{\partial x}\right)^2 + \left(\frac{\partial F}{\partial y}\right)^2. \quad (11)$$

This is the square of the largest slope of the surface (the gradient of the surface) $F(x, y)$. The resultant shearing stress s at any given point x, y of the cross-section is therefore equal to the greatest slope of the stress surface $F(x, y)$ at this point.

Briefly recapitulating, the preceding membrane analogy of elastic torsion may be expressed as follows: A thin membrane is thought of as fastened along the boundary curve of the cross-section and loaded by a uniform surface pressure. The curved surface into which the membrane is distorted is called "the soap-film surface" or "the elastic stress function" $F(x, y)$ of the cross-section. The contour lines of the elastic stress surface $F(x, y)$ represent the stress lines of the cross-section of an elastically twisted bar. At each point the tangent to the contour line gives the direction of the resulting shearing stress s , while this stress itself is proportional to the greatest slope of the stress surface $F(x, y)$. The twisting moment M acting on the bar, is equal to twice the volume enclosed by the stress surface multiplied by a factor depending on the units of length used.

b. The Plastic Stress Function of Torsion. The Sand-heap Analogy.¹—If an iron bar is severely twisted, certain parts of the bar will undergo plastic deformation. At a certain point of the cross-section at which the shearing stress s has reached the yield point, both shear-stress components s_x and s_y must satisfy the condition of plasticity:

$$s_x^2 + s_y^2 = k^2 = \text{const.} \quad (12)$$

The last equation states that of all shearing stresses occurring at various cross-sections of the bar, the largest, which in this case is s , has according to the assumptions made (see Fig. 147) at the

¹*Z. f. ang. Math. u. Mech.*, vol. 3, no. 6, p. 442, 1923. Cf. also: Plastic torsion, an experimental determination of the stress distribution in a bar which has been twisted to the limit of plasticity, *Proc. Am. Soc. Mech. Eng. Mech. Division*, 1931.

yield point a constant value k . These components s_x and s_y must further satisfy the condition of equilibrium:

$$\frac{\partial s_x}{\partial x} + \frac{\partial s_y}{\partial y} = 0. \quad (13)$$

This equation is again satisfied if we put:

$$s_x = \frac{\partial F}{\partial y}, \quad s_y = -\frac{\partial F}{\partial x}. \quad (14)$$

The function $F(x, y)$ determined by these relations may again be represented as a surface over the cross-section. $F(x, y)$ may be called *the plastic stress function of the cross-section*. In those parts of the cross-section in which plastic flow occurs, the plastic stress function F must satisfy, according to (12) and (14), the following equation:

$$\left(\frac{\partial F}{\partial x}\right)^2 + \left(\frac{\partial F}{\partial y}\right)^2 = k^2 \quad (15)$$

The differential expression on the left side of this equation is the square of the absolute value of the gradient "*grad F*" (of the maximum slope of the surface F). Everywhere in the cross-section where flow occurs the following equation must hold true:

$$|\text{grad } F| = k = \text{const.}$$

By means of this property and the further condition:

$$-s_y dx + s_x dy = \frac{\partial F}{\partial x} dx + \frac{\partial F}{\partial y} dy = 0, \quad (16)$$

according to which the shearing stress s at each point along the edge of a plastically distorted part of the cross-section is directed tangential to the edge $y = f(x)$,¹ or the condition that along the edge $F = \text{const.}$, the plastic stress function F of the cross-section is determined. Since an additive constant in F does not affect the value of the stresses (the shearing stresses are the derivatives of F), along the edge, F may be taken equal to zero.

From the above-mentioned properties of F it will be seen that the *plastic stress function is a surface of constant maximum slope* which one may construct over the edge of the cross-section. If the contour of the cross-section be thought of as cut out of a piece of stiff paper and covered with sand while lying horizontally, there results a heap whose natural slope gives a picture of the surface F . Its form is independent of the amount of twist

¹ Cf. Eq. (9), p. 131.

(the angular twist θ). The shape of the plastic stress function $F(x, y)$ is represented by some wooden models in Figs. 149, 150, 151, and 152.

We have now to consider how the plastic areas $A_2, A_3, A_4 \dots$ of the cross-section (Fig. 153) may be differentiated from the

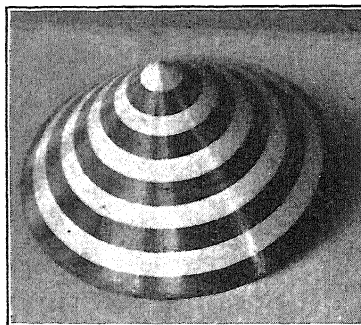


FIG. 149.

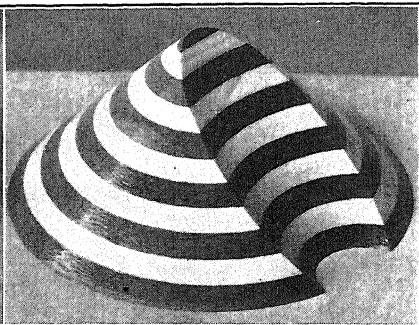


FIG. 150.

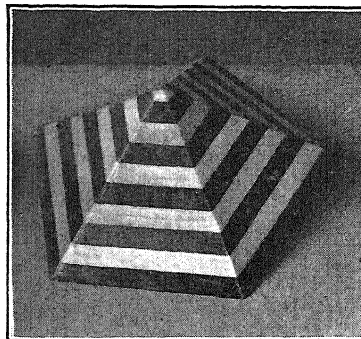


FIG. 151.

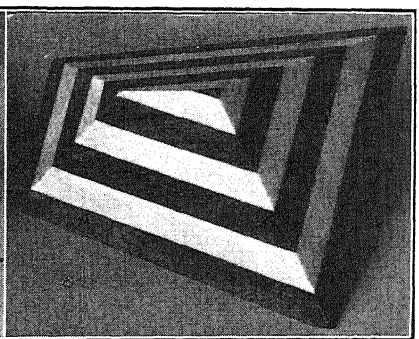


FIG. 152.

FIGS. 149 TO 152.—Examples of plastic stress function for torsion represented by wooden models for various cross-sections.

elastic area A_1 at any given value of twisting moment. We designate with the subscript (1) all values which refer to the elastically distorted parts of the cross-section. With respect to the elastic stress function F_1 , we know that its ordinates taken over the elastic part A_1 of the cross-section satisfy the following differential equation:¹

$$\frac{\partial^2 F_1}{\partial x^2} + \frac{\partial^2 F_1}{\partial y^2} = \Delta F_1 = -2G\theta \quad (17)$$

¹ Cf. Eq. (7), p. 131.

Along the edges of the cross-section the condition $F_1 = 0$ is satisfied. (G represents the modulus of elasticity in shear, θ the unit angular twist of the bar.) We assume for a moment that the values of F_1 are known along the boundary curves of the plastically distorted areas. Then the surface F_1 is determined and it is possible to draw the contour lines $F_1 = \text{constant}$ in the elastically stressed parts of the cross-section. These contour lines at each point x, y give the direction of the resultant elastic shearing stress s . It is clear that the elastic stress lines at their intersections with the boundary curves of the plastic regions must satisfy a further condition: they must suffer no break on passing these points. The shearing stress s must have the same value $= k$, regardless of whether this value be approached from the plastic side or from the elastic side. A break in the stress lines would only be permissible, if the bounding curve of the plastic region bisects the angle of the stress lines, in which case, however, the vector of the resultant shearing stress s at the limiting line must rotate through a finite angle. After the occurrence of an infinitesimal permanent deformation, no reason can be given for such finite rotation. Therefore both branches of a stress line must be tangent to each other at their intersection with the bounding

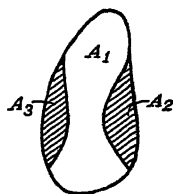


FIG. 153.—Elastic (A_1) and plastic (A_2, A_3) regions in cross-section of a bar twisted above the plastic limit.

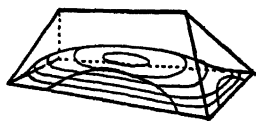


FIG. 154.—Membrane and surface of constant slope.

curve of the plastic region. From this it follows that, if one chooses at a certain point of a limiting curve $F = F_1$, the ordinates F_1 and F , of the elastic and the plastic stress function, must satisfy at all points of the limiting curve the condition $F = F_1$. It will be recognized that for a given angular twist θ of the bar the limiting curves of the plastic area of the cross-section are the projections of those curves on the plane of the cross-section, along which the elastic stress surface F_1 just touches the plastic stress surface F .

From the known properties of the surfaces F and F_1 the following experimental representation of stress distribution in a twisted bar, after the yield point has been reached, may be determined: A horizontally placed piece of cardboard having the geometrical shape of the cross-section is covered with sand so as to form under gravity

a sloping surface or "heap" over the cross-section. From this heap a negative or "hollow" may be made or a roof under a constant slope may be erected according to this surface above the boundary of the section. If the plane base of this roof is closed with a stretched membrane and this membrane is loaded by pressure, parts of the membrane will touch the surface of the roof erected above the section (Fig. 154) when the pressure reaches a certain value. The free parts of the membrane and those resting on the sloping surface, together form the stress surface for the plastically deformed bar in torsion. Under those parts of the membrane touching the sloping surface, the metal yields, while at those corresponding to the free parts of the membrane the metal remains elastic.

The following rules stated for the elastic torsion still hold true after the yield point has been reached: the resulting shearing stress at an arbitrary point x, y of the cross-section is the gradient $[\text{grad } F(x, y)]$ of the stress surface $F(x, y)$, the twisting moment M of the bar is equal to twice the volume $M = 2 \iiint F(x, y) \cdot dx dy$, enclosed by this surface. The contour lines $F(x, y) = \text{constant}$ of the plastic stress surface are the stress lines of the cross-section of the plastically twisted bar.¹

The construction of the contour lines of the plastic stress surface is very much facilitated by some well-known properties of the surfaces of constant maximum slope.² If the edge of the cross-section of a twisted bar is formed

¹ If θ_0 represents the angular twist at an instant at which the yield stress k (the yield stress in pure shear) is reached at one or more points at the edge of the cross-section, this angle is determined from the condition that at this point the maximum value of the gradient of the corresponding elastic stress surface F_1 is equal to:

$$(\text{grad } F_1)_{\max} = k.$$

Then the pressure p_0 at which the membrane first rests on the sloping surface has the same ratio to an arbitrary pressure $p_1 > p_0$ as the corresponding angular twist θ_0 has to θ_1 . The unit angular twist θ_1 of the bar which corresponds to given plastic areas (as indicated by the areas where the membrane touches the "roof") is therefore:

$$\theta_1 = \theta_0 \frac{p_1}{p_0}.$$

² Regarding the properties of surfaces of constant slope cf. F. SCHILLING, in *Z. f. ang. Math. u. Mech.*, vol. 3, no. 3, p. 197. It is sufficient here to make a few remarks: The contour lines of a surface of constant maximum slope are equidistant curves. The contour lines of the plastic stress surface may be obtained if the normals to the boundary curve are constructed and

of straight lines or circular arcs, the plastic stress surface forms a "roof" over the cross-section consisting of planes or portions of circular cones having the same slope.

The mode of penetration of the plastic areas into the inside of a twisted bar with a rectangular cross-section is shown in Figs. 155 and 156. The elastic area shrinks gradually until finally it consists only of thin strips. The middle lines of these strips are represented in the ground plane of the stress surface by the ridge and oblique edges of the "roof" erected on the rectangle. The stress surface for plastically twisted strap iron is a narrow ridge, the peak of the ridge being rounded off by a parabolic cylinder.

On the assumption that deformations are independent of yield stresses, it follows from this schematic representation, that the values of the twisting moment approach asymptotically a certain value given by twice the space enclosed by the plastic stress surface.

The condition in which all parts of a twisted bar yield may be designated as the *completely plastic state*.

For the *completely plastic state* the twisting moment of the bar may be easily calculated. For example, taking a circular bar having a diameter $2a$, the plastic stress surface is a circular cone having the equation:

$$F = k(r - a). \quad (18)$$

In this k is the yield stress for pure shear. For $r = 0$, $F = -ka$, and the cone has a height $h = ka$ and a volume $V = \pi a^2 h / 3$. According to our analogy the twisting moment acting on the bar is equal to twice the volume of the cone, or

$$M = 2V = \frac{2\pi ka^3}{3}. \quad (19)$$

For a bar having a cross-section of the shape of an equilateral triangle, the plastic stress surface is a three-sided pyramid. Each side has a slope equal to $\partial F / \partial n = k$, since the shearing stress is equal to the slope of the stress surface. Therefore, the pyramid has the height $h = ka / 2\sqrt{3}$. The area of the base is $\sqrt{3}a^2 / 4$, its volume $V = a^2 h / 4\sqrt{3}$, and the twisting moment when the bar is completely plastic is equal to twice the volume or

$$M = 2V = \frac{a^2 h}{2\sqrt{3}} = \frac{ka^3}{12}. \quad (20)$$

For a bar with a rectangular cross-section having the sides a and b (a is less than b) the moment in the completely plastic state is:

$$M = \frac{ka^3}{3} + \frac{ka^2(b - a)}{2} \quad (21)$$

points having the same distance from the edge are connected. In order to make a model of a surface of constant slope a vertical cylinder is, according to Schilling, erected on the evolute of the edge curve. A strip of paper cut obliquely so that its angle is equal to the angle of slope, is wound around this cylinder. The oblique straight line describes the sloping surface.

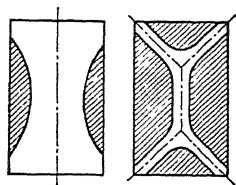


FIG. 155. FIG. 156.

FIGS. 155 and 156.—Shaded areas indicate plastic regions in cross-section of twisted bar.

c. **Apparatus for Experimental Determination of Stress Distribution.**—The foregoing remarks permit the study by means of a special apparatus of the manner in which plastic flow penetrates into a twisted bar of steel. The shape of the stress function on which the stress distribution depends can be experimentally determined with the help of a thin rubber membrane first uniformly stretched in its plane and then loaded by lateral pressure.¹

The apparatus consists of an aluminum disc of 12-in. diameter, upon which a uniformly stretched, thin rubber sheet was fastened by means of an aluminum ring and screws. The rubber membrane was partly supported along the circumference, but a central circular portion of it was completely free. In the empty space closed by the membrane, pressure could be produced by means of a tire pump (see Fig. 157). On the aluminum disc a second aluminum disc could be fastened (*d*) which contained the flat "roof" described in the preceding section. This disc can be seen on the right in Fig. 157. The roofs were one made of glass (in which case it had the advantage of being transparent and thus allowing direct observation of the distorted rubber surface) and the other of brass plates accurately machined. After the disc containing the flat roof was fastened on the base, pressure was applied and the membrane allowed to bulge out, until it partly or nearly completely covered the flat surfaces of the metal roof. To make visible the boundaries of the plastic parts in a cross-section of a twisted bar (*cf.* under **b**, page 134) the rubber sheet was covered with a thin layer of white powder and the roof with a thin film of oil, both put on before the pressure

¹ For the case of elastic torsion the soap-film analogy was first used by Anthes (Doctor's Dissertation, Dresden, 1912), who photographed the picture of a rectangular network of lines, which was reflected by the soap film produced over holes in a metal sheet. Another method also using soap films was proposed by A. A. GRIFFITH and G. I. TAYLOR, *Proc. 1st Internat. Congress for Applied Mechanics*, p. 39, Delft, 1924, who measured the deflections of such films by an electric contact method. An apparatus utilizing a uniformly stretched rubber sheet, over which a pressure difference could be produced by evacuating the air below the membrane, was demonstrated to the author in 1928 by Prof. Enger at the University of Illinois. The principles used in this latter apparatus were adapted in the one described above and constructed at the suggestion of the author by H. Friedman at the Research Laboratories of the Westinghouse Electric & Mfg. Company, East Pittsburgh, Pa., 1929, to whom the author is much indebted for carrying out all the tests referred to above and for photographing the sand heaps.

was applied. After this latter was applied parts of the inflated membrane came in contact with the flat surfaces of the roof and the white powder adhered to the roof, where the rubber sheet rested on it. Thus, white areas of the adhering powder disclosed the shape of the common surfaces of contact or the plastic parts of the cross-section. These parts appear white in the photographs taken of the hollow side of the roof after it had been removed.

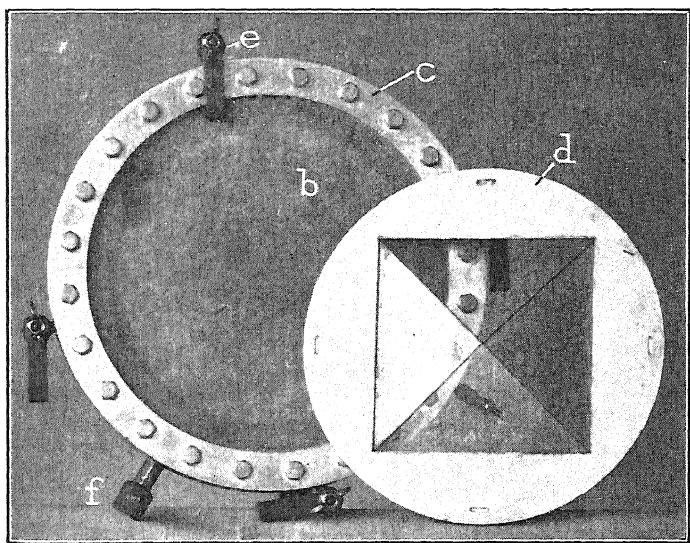


Fig. 157.—Apparatus for experimental demonstration of stress distribution in plastic torsion. An aluminum disc serving as base is covered by rubber membrane *b*; *c*, aluminum ring clamping membrane; *d*, disc containing constant slope surface; *e*, clamps; *f*, connection to pressure measuring device.

A series of tests showing the progress of the plastic regions in a twisted bar with a square cross-section can be seen in the photographs, Figs. 158 to 160. The figures below indicate the pressure; the angle of twist would increase in the same proportion as the pressure. From Figs. 158 to 160 it may be seen, that the white areas are first formed in the middle of the sides of the square, where the shearing stress first reaches the yield point according to the theory of elastic torsion. With increasing twist or moment these white areas, representing the portions which become gradually plastic in the cross-section, grow inward. Finally, under sufficiently large pressure only a narrow dark cross appears

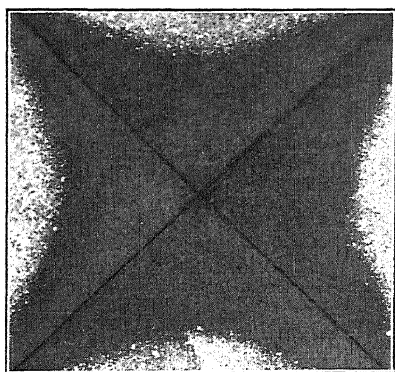


FIG. 158.

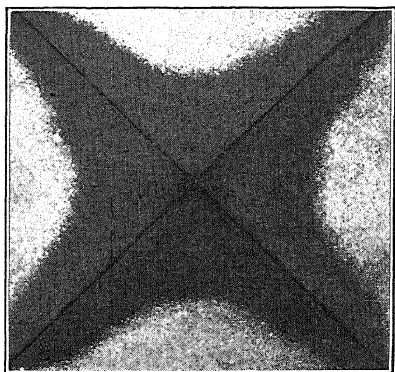


FIG. 159.

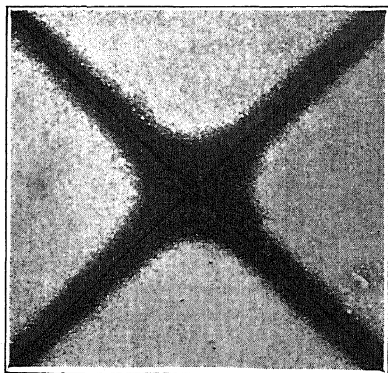


FIG. 160.

FIGS. 158 to 160.—Development of plastic regions in a twisted bar of square cross-section. Elastic areas appear dark, plastic areas bright. (Pressures p acting on rubber membrane were proportional to 1.5:1.75:2.5.)

(Fig. 160), showing that the elastic portion in the cross-section has been reduced practically to two narrow strips, crossing at right angles and following the course of the two diagonals of

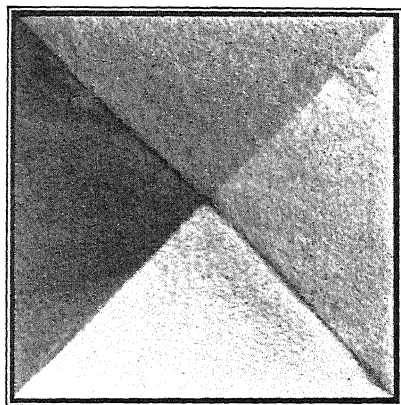


FIG. 161a.

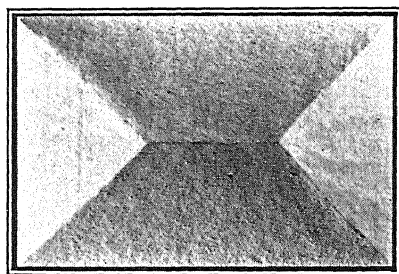


FIG. 161b.

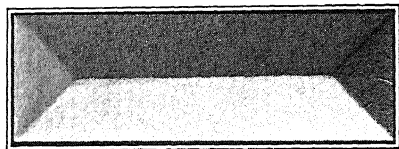


FIG. 161c.

FIGS. 161a, b, and c.—Sand heaps produced over rectangles showing constant slope surfaces.

the square or the projections of the corresponding four edges of the roof.

The shape of the plastic stress function $F(x, y)$ or of the stress surface for the case of complete yielding of the whole bar can be

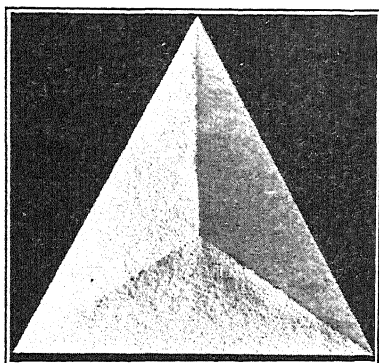


FIG. 162.—Sand heap over equilateral triangle.

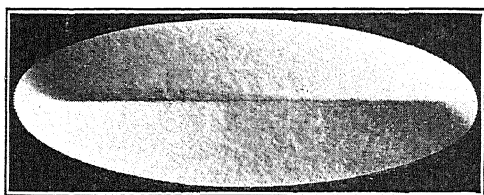


FIG. 163.—Sand heap over an ellipse.

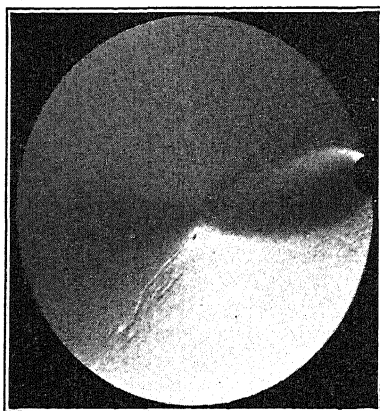


FIG. 164a.

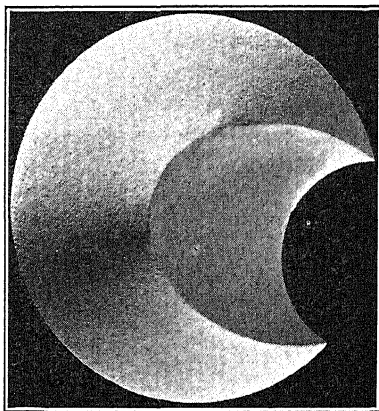


FIG. 164b.

FIGS. 164a and b.—Sand heaps over areas bounded by two circular arcs.

demonstrated by sand heaps covering the figure of the cross-section of the twisted bar. Such sand heaps were produced and can be seen in some photographs (Figs. 161 to 164) taken for the square, rectangular, an equilateral triangular, an elliptical and two circular cross-sections containing grooves of semicircular form. This last case would correspond somewhat to a shaft with a keyway of semicircular cross-section.¹

¹ The case of a twisted shaft with a keyway was also the subject of similar tests as those mentioned above in a paper of E. G. COKER, *Elasticity and Plasticity*, *Proc. Inst. Mech. Eng.*, p. 897, November, 1926, (Thomas Hawksley lecture), to which special reference is made. In this paper Coker has applied the membrane and sandheap analysis for the experimental determination of stress distributions in twisted shafts containing a keyway.

CHAPTER 20

TORSION TESTS. THE SLIP LAYERS IN TWISTED STEEL BARS

a. Flow Layers. Torsion Tests with Steel Bars.—The position of the flow or slip layers in the plastically deformed parts of a twisted bar may be predicted with the help of the sand heap analogy. For a soft metal, such as mild steel, the slip layers coincide approximately with the surfaces of maximum shear or of maximum shearing displacements. These slip layers are, therefore, approximately perpendicular to each other. At an arbitrary point inside of a twisted bar, one surface of maximum shearing stress coincides continuously with the plane of the cross-section. The other surface of maximum shear is parallel to the axis of the bar, *i.e.*, perpendicular to the cross-section. The traces of the second system of slip layers must remain perpendicular to the stress lines of the plastic stress function



FIG. 165.—Orientation of flow layers in a steel bar twisted above the plastic limit.

After the yield stress has been passed in a twisted iron bar, very regular layers or markings may actually be shown to exist.¹ In these, the iron is apparently deformed much more than in the neighboring layers.

These layers may subsequently be made visible in the cross-section of the bar by means of Fry's etching method. In such etched sections the flow layers appear as dark strips and lines. A schematic sketch of their appearance in an oblique cross-section of a bar with square cross-sections is shown in Fig. 165. A series of such etchings on soft-iron bars, using Fry's method, are shown in Figs. 168 to 172 for circular cross-sections, in Figs. 173 to 180 for rectangular cross-sections, and in Figs. 181 to 183 for triangular cross-sections. In the etched

¹ The observations referred to above were published in a paper by W. BADER and the author, *Die Vorgänge nach der Überschreitung der Fließgrenze in verdrehten Eisenstäben*, *Z. d. V.D.I.*, no. 10, p. 317, Berlin, 1927; and in the Doctor's Dissertation by W. BADER, University of Göttingen, 1927.

cross-sections the traces of one of the two systems of slip layers are indicated. Traces of the second system of slip layers could, however, seldom be noted upon the surface parallel to the generatrices of the cylindrical or prismatical bars or in sections inclined to the axis of the bar.

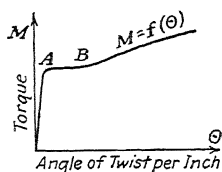


FIG. 166.—Torque-twist diagram of steel showing flow or strain figures.

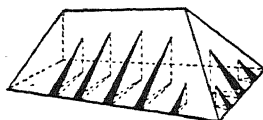
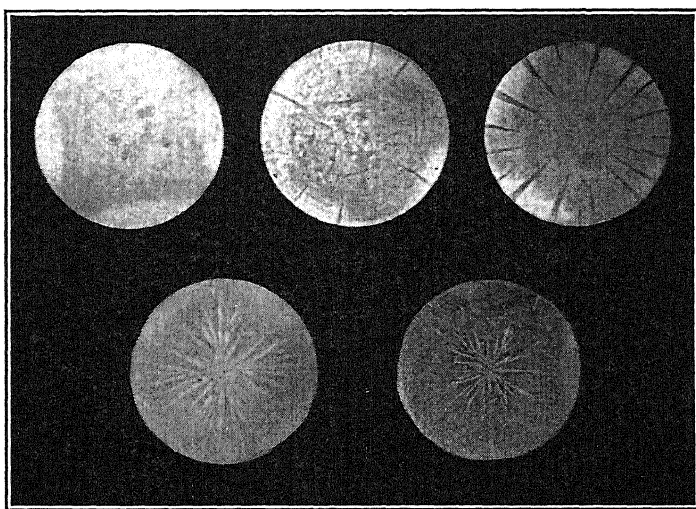


FIG. 167.—Lines of greatest slope on roof.



FIGS. 168 TO 172.—Development of flow layers in twisted steel bars. Diameter of bar 17 mm. Angle of twist per unit of length θ : Fig. 168, $\theta = 0.007^\circ$; Fig. 169, $\theta = 0.04^\circ$; Fig. 170, $\theta = 0.22^\circ$; Fig. 171, $\theta = 1.84^\circ$; Fig. 172, $\theta = 3.02^\circ$.

In a twisted steel bar the flow layers appear uniformly when the twisting moment reaches values corresponding to those along the horizontal portion AB of the moment curve $M = f(\theta)$, Fig. 166. The first flow layers occur at those values of twisting moment at which the outermost part of the cross-section has already been plastically deformed and the moment curve begins

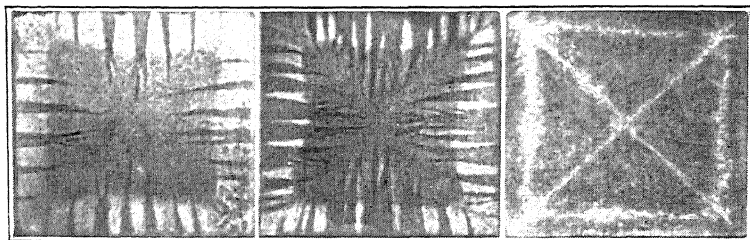


FIG. 173.
 $\theta = 0.38^\circ$.

FIG. 174.
 $\theta = 0.68^\circ$.

FIG. 175.
 $\theta = 0.90^\circ$.

FIGS. 173 to 175.—Fluidal structure in twisted bars with square cross-section. Square 2 by 2 cm. θ , angle of twist per centimeter.

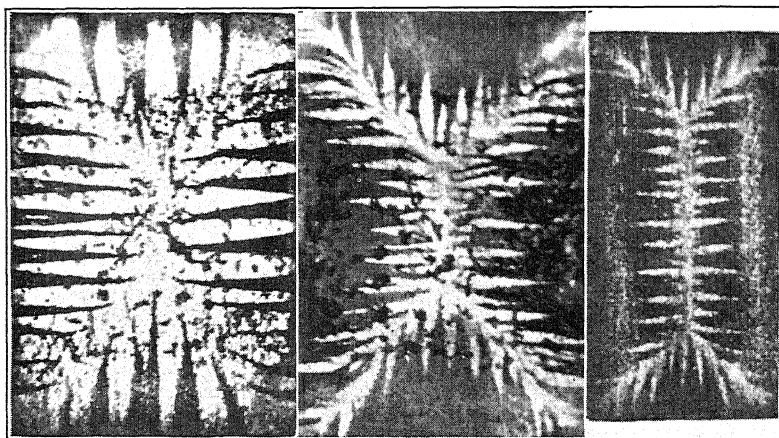
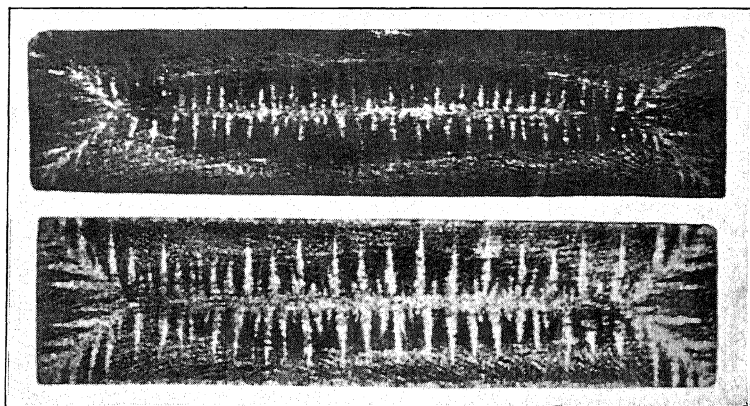


FIG. 176.

FIG. 177.

FIG. 178.



FIGS. 179 and 180.

FIGS. 176 to 180.—Flow layers in twisted steel bars of rectangular cross-section.

to bend over into the horizontal branch. With increasing twist, new layers form beside the old ones, while the latter become longer and thicker. The flow layers appear in the etched cross-sections of the photographs as wedge-shaped areas, the points of the wedges pointing toward the less stressed parts of the cross-section (Fig. 173).

As a rule, it may be concluded that the black flow lines in the cross-sections run mainly perpendicular to the stress lines (the projections of the contour lines of the plastic stress surface). Moreover, these flow lines always remain perpendicular to the edge of the cross-section. Thus, they run in the direction of the

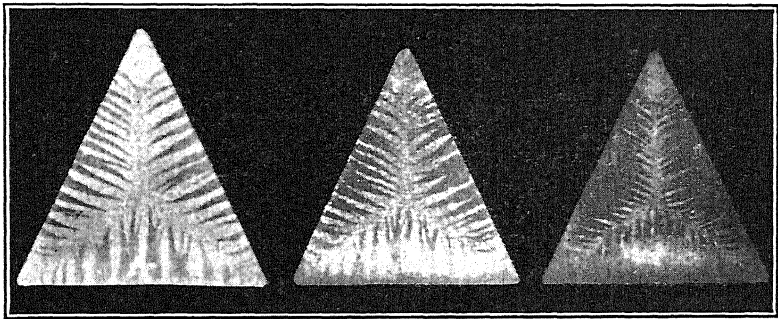


FIG. 181.

FIG. 182.

FIG. 183.

FIGS. 181 to 183.—Flow layers in twisted steel bars of triangular cross-section.

projections of the lines along which water will run off the roof representing the plastic stress surface (Fig. 167). With the more severe deformations the black strips finally cover the whole cross-section. In the etching of the square cross-section of Fig. 175, which corresponds to the most severely twisted bar, the elastic areas may only be recognized as bright areas along the diagonals of the square. In other words, the four ridges of the stress surface F , which is here a four-sided pyramid, are projected on these diagonals.

b. Structure Due to Cooling and Fluidal Structure.—The similarity of the crystalline structure in cast-metal ingots¹ with the photographs here

¹ Remarkable examples are contained in the books by J. CZOCHRALSKI, "Moderne Metallkunde in Theorie und Praxis," pp. 98, 103, 139, Berlin, 1924; and by P. OBERHOFFER, "Das technische Eisen," 2d ed., p. 291, Berlin, 1925; compare also: E. SEIDL and E. SCHIEBOLD, Das Verhalten inhomogener Aluminium-Querblöckchen beim Kaltwalzen, *Z. Metallkunde*, vol. 17, pp. 225ff., 1925.

given of the flow layers in twisted bars, especially for the circular and square cross-section, suggests the necessity for an investigation of whether or not a correspondence exists between the formation of the flow layers in twisted steel bars and the figures which one may observe in the macrostructure of rolled material as the traces of the ingot structure in the cross-sections.

For this purpose a square bar, having the cross-section $EFGH$ (Fig. 184), was cut out from a rolled-iron bar having an initial cross-section $ABCD$.

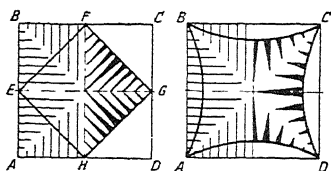


FIG. 184.

FIG. 185.

FIGS. 184 and 185.—Structure of ingot and flow structure in steel bars.

Moreover, a bar with a cross-section made up of four circular arcs (Fig. 185) was machined from a bar $ABCD$ as shown in Fig. 185. The flow structure of these bars, when twisted, was compared with that obtained previously. In Figs. 184 and 185, the structure produced by crystallization in the ingot, which is not changed by rolling, is represented by the thin lines on the left half of the figure, while on the right half of both figures the normal position of the slip or flow layers produced by torsion is given. The flow layers, as found by the etched cross-section of the twisted bars (Figs. 186 to 189), correspond to the actual position of the applied stresses. A marked influence of the structure produced by rolling upon the observed shape of the flow layers does therefore not appear to exist.

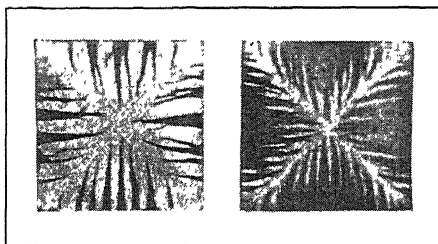


FIG. 186.

FIG. 187.

FIGS. 186 and 187.—Flow layers in twisted steel bars cut from a bar according to Fig. 184.

For comparison the behavior of a brittle cast metal, in this case, a cast-zinc bar (Fig. 190), which has a very definite structure produced by cooling, was investigated. A square bar of zinc was cast in an iron mold and then twisted in a torsion machine. The bar broke in torsion in the manner peculiar to brittle materials and under relatively small stresses by exceeding the tensile strength along a surface inclined at 45° to the axis of the bar. In the fractured surfaces and in the etching of the cross-section the ray-shaped texture of the microstructure produced by cooling of the casting was evident, as shown by Fig. 190.

Further evidence that the fibrous structure produced by rolling has no marked influence on the position of the flow layers, is afforded by the torsion tests of bars with triangular and irregular cross-sections. All these bars were machined from bars with square or rectangular cross-sections; in the etched cross-sections the dark, square shaped zones may often be plainly

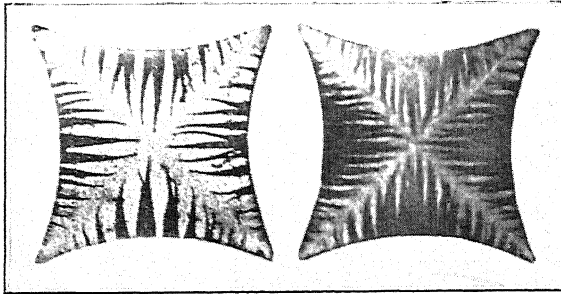


FIG. 188.

FIG. 189.

FIGS. 188 and 189.—Flow layers in twisted steel bars cut from a bar according to Fig. 185.

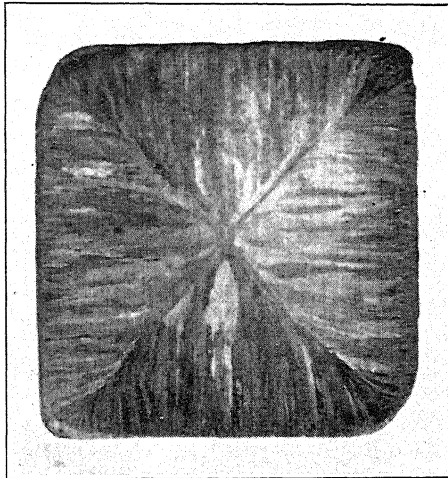


FIG. 190.—Structure of cast zinc showing crystallization due to rapid cooling.

recognized, while the flow layers run in the directions predetermined by the torsion stress field and correspond to the rules laid out above.

A systematic difference in the position of the dark strips in the etched cross-sections from that of the lines of maximum slope of the stress surface must however be noted. The pointed ends of the flow lines appear to bend over and to follow the narrow bright strips in the etchings. It appears as if the lines of maximum slope of the plastic stress surface, after severe

torsional distortion of the test piece, tend to approach again the curves of maximum slope of an *elastic* stress surface. Probably this phenomenon depends on the fact that the strengthening of the steel or cold working begins as a result of preceding plastic deformation, which fact was neglected in the simple theory.¹

¹ Various papers by M. J. Seigle consider the plastic deformation of a twisted bar. Cf. especially: Quelques particularités théoriques et expérimentales de la torsion des barreaux à section non-circulaire, *Rev. de l'industrie minérale*, p. 557, 1925. In the above-mentioned work Seigle used the phenomenon of recrystallization to observe the plastic regions. Relative to further studies see also papers by SEIGLE and CRETIN on torsion and tension in *Génie Civil*.

CHAPTER 21

EFFECT OF HOLES OR GROOVES IN A REGION SUBJECTED TO PURE SHEAR

a. **Longitudinal Groove with Semicircular Cross-section.**—For the case of a bar of circular cross-section in torsion, having a longitudinal groove of semicircular cross-section, qualitative estimates of the positions of the flow layers may easily be made. We will first assume that the radius a of the groove is small in comparison with the diameter d of the bar. It is then permissible to replace the boundary circle of the cross-section by its tangent. The disturbances in the direction of the stress lines may then be determined under the assumption that, at a large distance from the groove, a constant shearing stress acts.

The question is now to determine the stress distribution in a body subjected to pure shear in a direction parallel to one edge and having a small groove with a semicircular cross-section (Fig. 191). For the case of pure elastic shear, the stress lines in the neighborhood of the groove may easily be determined with the help of the membrane analogy.

One only has to think of a thin membrane attached along an edge $ABCDE$ (Fig. 191) of the body, this membrane being stretched in a plane inclined to the plane of the cross-section. The slope of the inclined plane is a measure of the amount of shearing stress in the undisturbed part of the stress field at a large distance from the groove. The contour lines of the stretched membrane near the edge are the stress lines of the region subjected to pure shear (Fig. 192). These lines are closest together in the neighborhood of the point C at the edge of the groove and at a large distance from it they become more and more nearly parallel to the edge. The shearing stress s which exists at a given point P is equal to the slope of the elastic stress surface F .¹

¹ By means of the potential theory the stress function F may easily be determined. Using polar coordinates r and α

$$F = c \left(\frac{a^2}{r} - r \right) \cos \alpha.$$

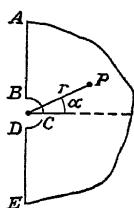


FIG. 191.—
Semicircular
groove on
straight edge.

As the inclination of the plane of the thin membrane is increased, all shearing stresses are increased until the stress at the point C reaches the yield point. Then the membrane must be inclined in a plane $F = kx/2$ with respect to the plane of the cross-section. In order to determine the limits of the plastic area we must think of a sloping surface in form of a cone, erected, as shown in Fig.

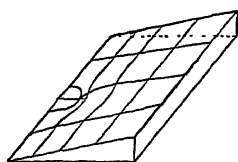


FIG. 192.—Membrane near semicircular notch and straight edge.

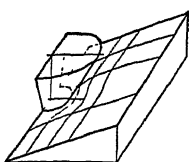


FIG. 193.—Membrane and cone.

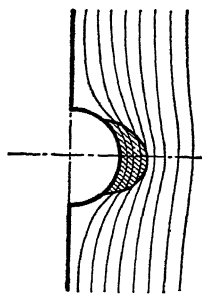


FIG. 194.—Stress lines around semicircular groove in straight edge. Shaded area represents plastic region.

193, above the circle of the radius $r = a$. If the slope of the membrane at C becomes larger than $k/2$, certain neighboring parts of the membrane will lie upon the cone. These parts, which have been shaded in Fig. 194, represent the plastic area of the cross-section. Of especial interest here is the limiting case when the shearing stress $s = c$ approaches the value of the yield stress $s = k$ for pure shear. Calculation¹ showed that when s approaches k and for $x = \infty$ the plastic region becomes bounded

By forming the derivatives of this surface the maximum shearing stress s_{\max} is found to occur at the edge of the groove at the point C , where $r = a$ and $\alpha = 0$ and is $s_{\max} = 2c$, that is twice as large as the shearing stress $s = c = \text{constant}$ at a large distance from the groove. Since when x approaches infinity $F = -cx$ and the shearing stress $s = -\partial F / \partial x = c$. The picture of the contour lines in this case is exactly the same as that of the stream lines of a fluid which circulates around a circular cylinder, the liquid moving perpendicularly to the axis of the cylinder. (Only one-half of the picture of the stream lines around the cylinder has to be considered.)

¹ See *Proc. 2d Internat. Congress for Applied Mechanics*, p. 337, Zürich, 1926. The stress distribution around a hole after the yield point has been reached, has been treated by E. TREFFTZ in *Z. f. ang. Math. u. Mech.*, vol. 5, p. 64, 1925.

by two parallel lines. The plastic region becomes a parallel strip having a *finite width* b which was found equal to:

$$b = \frac{4a}{\pi}.$$

This leads to the interesting conclusion, that in a body stressed by pure shear and having a small semi-cylindrical notch, with the increasing stress only a thin layer of plastic material will be formed. When the shearing stress approaches the yield stress of the material, this plastic layer extends indefinitely and has a width $2/\pi$ times the diameter $d = 2a$ of the notch. It is not difficult

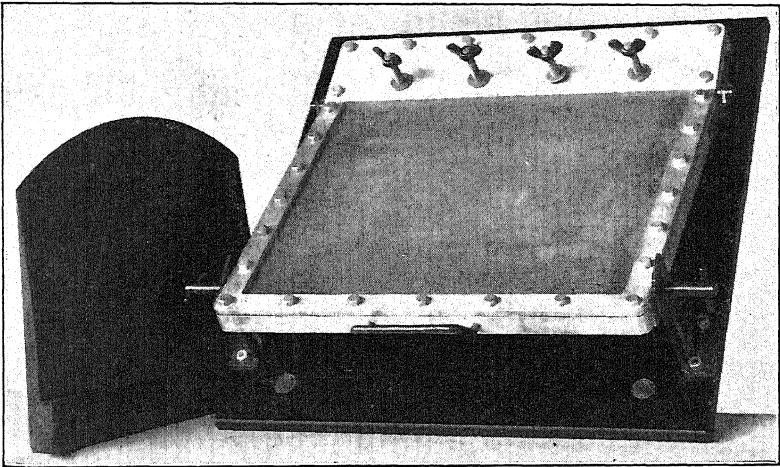


FIG. 195.—Apparatus for experimental demonstration of spreading of plastic region from semicircular notch or cylindrical hole. The dark block at the left is a micarta cone, which can be fastened to the frame by means of the four screws shown.

to obtain the solution of the problem discussed above by means of a mechanical apparatus. Figure 195 shows an apparatus constructed for this purpose, consisting essentially of a sheet of rubber stretched in its plane on a rectangular frame of metal. The plane of this frame could be tilted about one of its sides. The rubber sheet could be brought by this movement in a position, in which it partially touched and covered a cone attached to the frame of the apparatus in the manner indicated in Fig. 193. The contour lines of the plastic region were made visible by the same method as used in the cases of other cross-sections already mentioned. The white areas of an adhering powder on the dark

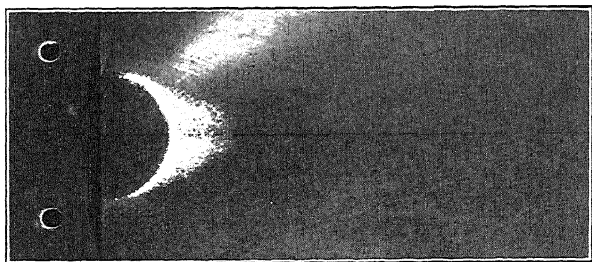


FIG. 196.

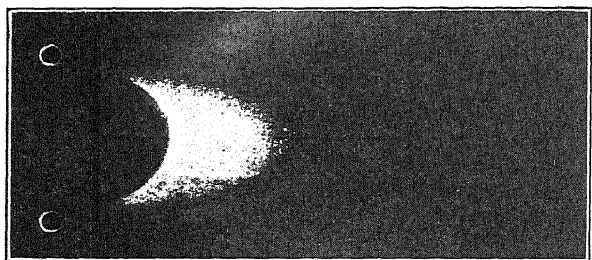


FIG. 197.

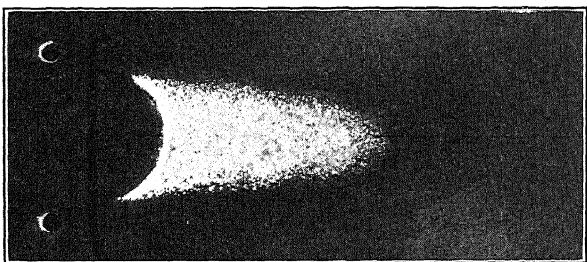


FIG. 198.

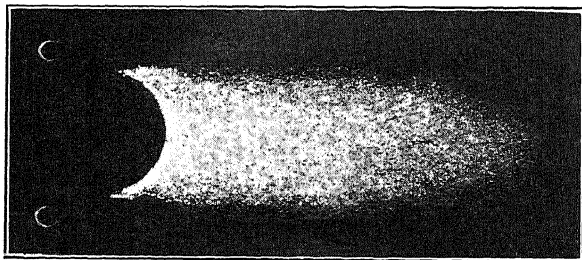


FIG. 199.

Figs. 196 to 199.—Spreading of plastic region (white area) from semi-cylindrical notch or cylindrical hole.

surface of the cone (the latter was machined from a piece of dark micarta) illustrate nicely the shape of the plastic region. The spreading of the plastic region from the edge of a semicircular notch is shown in a series of photographs in Figs. 196 to 199, taken by H. Friedman for various, increasing angles of inclination of the plane of the rubber sheet. The figures indicate that when the shearing stress in the undisturbed parts of the stressed body approaches the yield stress for pure shear, the plastic region tends to take a more and more longitudinal shape.¹

These considerations lead to a somewhat paradoxical conclusion; for according to what has been stated previously, the presence of a small longitudinal groove on the surface of a material strained by pure shear is sufficient to cause the small plastic area at the edge of the groove to extend deeply into the material, if the shearing stress at this edge is increased to the yield point (Fig. 200). Moreover, from this it follows that it is not possible, by increasing the shearing stress, to produce plastic deformation elsewhere than in the narrow flow area. The apparent discrepancy between this conclusion and actual yield tests on bars is easily explained by recalling one of the idealizing assumptions, on which it was based, namely that the yield stress should remain independent of deformation. On the other hand, the above conclusions have been confirmed by numerous observations on the development of the flow layers and flow figures in plastic materials, which begin to flow under a constant or a decreasing stress.

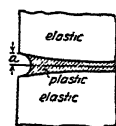


FIG. 200. Plastic area produced by semicircular notch in region subjected to pure shear.

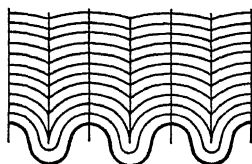


FIG. 200a.—Plastic stress function represented by contour lines for corrugated surface of bar.

¹ Moreover, in the case of a corrugated surface the limits of the plastic areas may be studied easily. If the edge of the cross-section is approximately a wavy line, the plastic stress function forms a roof, having grooves inclined to the edge and being separated by wedge-shaped projecting edges, as shown by the contour lines of Fig. 200a. Since a stretched membrane can never touch these edges, it is seen at once that such unevennesses of the surface of a twisted bar will give rise to oblong flow areas, which under increasing stress, will spread inward from the small grooves in a perpendicular direction to the mean edge of the cross-section.

b. Cylindrical Hole.—In the neighborhood of a small cylindrical hole of diameter d in a region stressed by pure shear, two narrow flow areas of width $2d/\pi$ develop in an analogous way, if the shearing stress is gradually increased to the yield point (Fig. 201). The stress distribution in the neighborhood of a cylindrical hole in an infinite plate corresponds completely with the above-mentioned case of a semi-cylindrical groove; the two cases are mathematically the same. At small holes, notches, or grooves, the axes of which lie in the plane of principal shear, under sufficiently high stresses, narrow flow areas develop. The difference in the action of a small hole, according to whether the strains are purely elastic in the vicinity or whether plastic flow occurs (in the case of a material having a definite yield point) has already



FIG. 201.—Plastic flow layer produced by cylindrical hole in region subjected to pure shear.

been shown by the above-mentioned compression tests of specimens having holes (*cf.* page 100).

If, in the neighborhood of a hole, the strains are purely elastic, the disturbances in stress produced by the presence of the hole rapidly decrease with distance from the hole. In a plastic material which begins to flow under approximately constant stress, there results, however, in the case of axial tension or compression, severe plastic deformation along two planes, the deformation being quite marked even at a large distance from the hole.

In soft-annealed copper test specimens it is usually not possible to observe flow layers after plastic deformation has occurred. If however, the copper is subjected to severe cold working before the test, it acquires a definite plastic limit and it is then possible to produce flow layers.

An essential condition for the production of the narrow flow layers in plastically deformed materials seems to be that the materials possess a definite yield point, *i.e.*, a break in the ordinary stress-strain curve such that the material yields under a constant stress or the load drops suddenly, together with local concentration of plastic deformation because of an increase in stress. A possible origin of such local concentrations of stress is a small flow or a slightly softer inclusion which has a somewhat lower yield point than the neighboring parts.

c. Bars with Longitudinal Grooves.—In Figs. 202 to 219 are shown etchings of twisted cylindrical bars having longitudinal grooves of different shapes and dimensions. In the flow figures found on the cross-sections

of a round bar with a small semicircular groove (Fig. 202), it will be noticed that three wide flow layers extend from the groove. Figure 203 represents a similar round bar whose surface was, however, given a mirror-like polish before the test. Although the twisting moment, applied to this bar, was

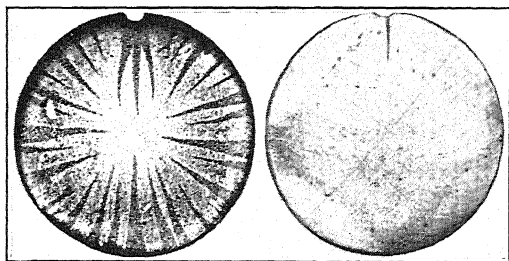


FIG. 202.

FIG. 203.

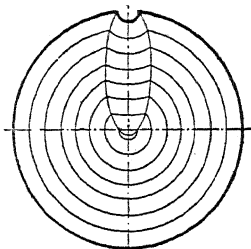


FIG. 204.

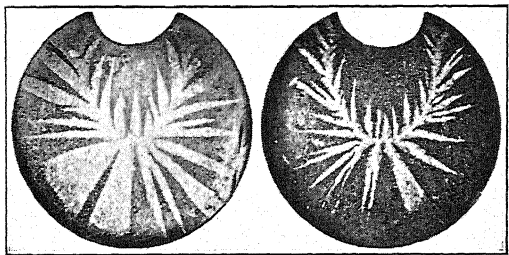


FIG. 205.

FIG. 206.

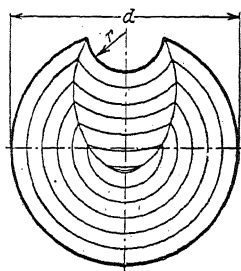


FIG. 207.

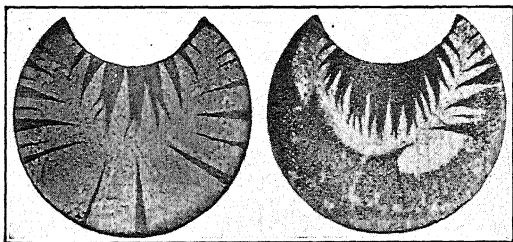


FIG. 208.

FIG. 209.

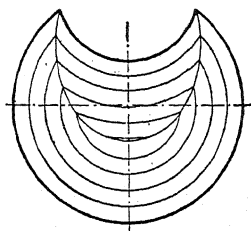


FIG. 210.

FIGS. 202 TO 210.—Fluidal structure in twisted steel bars having notches or grooves. On right the contour lines of plastic stress surface.

about 10 per cent greater than that applied to the bar shown in Fig. 202, only one flow figure was obtained near the groove.

Figures 202, 205, 208, 211, 214, and 217 represent slightly twisted bars; Figs. 203, 206, 209, 212, 215, and 218 represent more severely twisted bars.¹ For each shape of test piece the shape of the plastic stress surface for the

¹ For details regarding dimensions of the bars and applied torque moments cf. *Z. d. V.D.I.*, p. 317, 1927.

completely plastic state is represented in an adjoining figure by contour lines (Figs. 204, 207, 210, 213, 216, and 219). The construction of these contour lines is very much facilitated by the condition that the surfaces in question consist entirely of either planes or straight circular cones (cf.

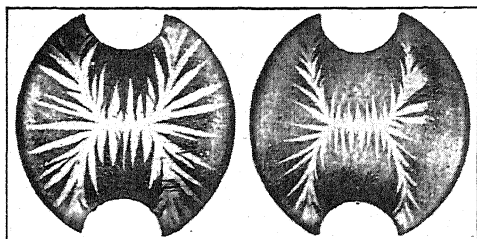


FIG. 211.

FIG. 212.

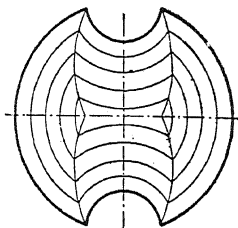


FIG. 213.

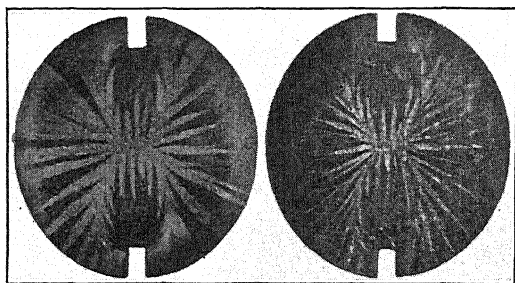


FIG. 214.

FIG. 215.

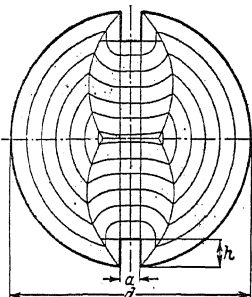


FIG. 216.

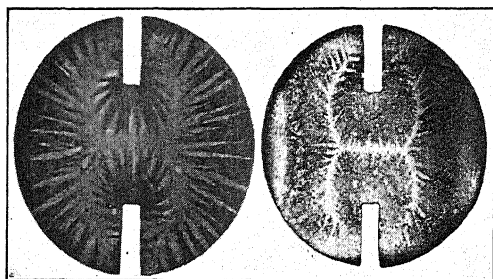


FIG. 217.

FIG. 218.

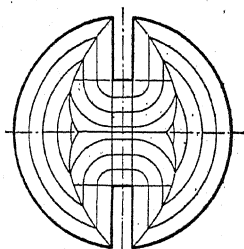


FIG. 219.

FIGS. 211 to 219.—Fluidal structure in twisted steel bars having notches or grooves. On right the contour lines of plastic stress surface.

the wooden models and sand heaps on the previous pages). Therefore, the contour lines consist entirely of straight lines and circular arcs. In the schematic representations the penetration curves of these surfaces are given. According to these assumptions, the elastic area in the cross-section in the completely plastic state must shrink until it coincides with the ridges

(more exactly the projections of the ridges) of the plastic stress surface which may be thought of as erected over the cross-section. It will be recognized by comparison of the etchings with the contour figures that the middle lines of the white jagged-ridge areas in the photographs agree quite well with the curves of the ridges of the plastic stress surface shown in the sketches.¹

¹ At this point the excellent work of E. G. COKER on the experimental determination of stress distribution in transparent models by means of polarized light should be mentioned. For cases of plane elastic stress distribution there exists little difficulty to determine quantitatively the stress distribution by his methods. Relative to his results *cf.* his paper before the First International Congress for Applied Mechanics, Delft, 1924. Since by means of his optical methods the difference in principal stresses at various points of the model may be measured, it would seem advisable to utilize this property of material in its plastic state for experimental determination of the lines of constant principal stress difference. A few tests in this direction with transparent nitrocellulose in its plastic condition are described in a paper of Coker mentioned on page 143. *Cf.* also the work of H. TURNER and J. JEVONS, *The Detection of Strain in Mild Steels*, *Iron and Steel Inst.*, vol. 61, no. 1, 1925. In this, the change in microstructure of soft iron under stress was utilized in the study of plastic deformation.

CHAPTER 22

BENDING OF BARS WITH ARBITRARY LAW OF DEFORMATION

The theory of bending of narrow bars, when the deformations do not obey Hooke's law, may be stated in a relatively simple manner. We assume that the bar has a cylindrical or prismatical shape with constant cross-sectional area and that it is loaded by forces directed perpendicular to its longitudinal axis in one of the principal planes of inertia of the cross-section. The cross-

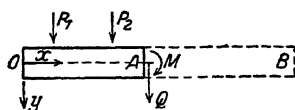


FIG. 220.—Bending of bar.

sectional dimensions of the bar are assumed small, relative to its length, so that the deformation due to shear may be neglected relative to that due to normal stresses. Finally, cross-

sections having profiles, composed at least in part of thin sections, and of unsymmetrical form (angles or channels) will be excluded insofar as in such cases bending may be combined with twisting.

The calculation utilizes certain methods of C. v. Bach and is based on the assumptions made in the usual theory of elastic bending that the cross-sections remain plane during bending. The validity of these assumptions has been shown particularly by C. v. Bach¹ on materials which do not obey Hooke's law and possess no straight-line stress-strain curve for tension or compression. These assumptions were also confirmed by tests by Eugen Meyer² on wrought iron above the yield point.

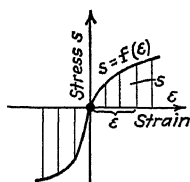


FIG. 221.—Stress-strain curve for bending.

In order to determine the distribution of normal stresses over the cross-section (Fig. 220) at a distance x from the end of the bar, the stress-strain curve of the material for tension or compression

¹ BACH, C., and BAUMANN, R., "Elastizität und Festigkeit," 9th ed., p. 259.

² Z. d. V.D.I., p. 197, 1908.

must be known from tests. We will assume that this stress-strain curve has been determined from a tension and a compression test in the shape of a graphically (Fig. 221) or an analytically given function of the normal stress s :

$$s = f(\epsilon) \quad (1)$$

as dependent on the unit extension ϵ .

It is evident that there is an axis NN (Fig. 222a), the *neutral axis*, along which the stresses and strains produced by bending vanish. If the bar is bent, two neighboring cross-sections x and $x + dx$ are caused to move so as to be slightly inclined to each

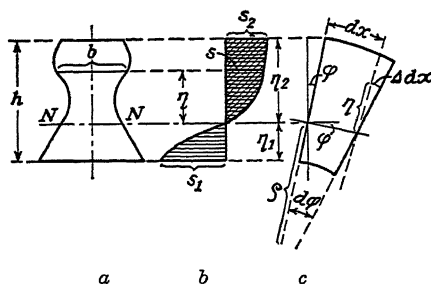


FIG. 222a, b, and c.—Cross-sectional area A and element $A dx$ of a bar with distribution of bending stresses s as depending on distance η from neutral axis NN in section.

other. A length dx (Fig. 222c) at a distance η from the neutral axis undergoes thereby an extension Δdx ; therefore the unit strain at a distance η is:

$$\epsilon = \frac{\Delta dx}{dx}.$$

Since

$$\frac{\Delta dx}{dx} = \frac{\eta}{\rho},$$

we have

$$\epsilon = \frac{\eta}{\rho} \quad (2)$$

In this ρ is the radius of curvature of the elastic line of the bent bar.

The equilibrium of the forces acting on this element dx of the bar is expressed by the two equations:

$$\int s dA = 0 \quad (3)$$

$$\int s \eta dA = M. \quad (4)$$

In these equations dA represents an element of the cross-section at a distance η , and s the normal stress acting on this element. The bending moment which must act to hold these internal stresses in equilibrium is denoted by M .

Instead of the element dA of the area A we may write also $dA = \beta(\eta)d\eta$ if the width of the cross-section at the point η is designated by $b = \beta(\eta)$. Finally, if the variable η be replaced according to Eq. (2) by the unit strain ϵ , Eq. (3) takes the form:

$$\int_{-\eta_1}^{\eta_2} s dA = \rho \int_{-\epsilon_1}^{\epsilon_2} f(\epsilon) \beta(\rho\epsilon) d\epsilon = 0 \quad (5)$$

Here $\epsilon_1 = \eta_1/\rho$, $\epsilon_2 = \eta_2/\rho$ are the absolute values of the unit strains in the points of cross-section farthest from the neutral axis. Since $\eta_1 + \eta_2 = h$ the upper limit ϵ_2 in the integral is equal to $\epsilon_2 = \frac{h}{\rho} - \epsilon_1$ so that the limits are determined by the values of ϵ_1 and ρ . The functions f and β may be taken as given and of the two quantities ϵ_1 and ρ one can be chosen arbitrarily.

Then the integral:

$$\int_{-\epsilon_1}^{\epsilon_2} f(\epsilon) \beta(\rho\epsilon) d\epsilon = 0 \quad (6)$$

becomes an equation for the other unknown quantity. By means of this equation, a function $\epsilon_1 = \Psi(\rho)$, corresponding to a given shape of the cross-section and to a given law of deformation, is determined such that even if no analytical expression exists it may be constructed point by point by trial. (One needs only to choose a ρ for an assumed value of ϵ_1 , calculate the integral (5) and to plot its values as obtained for different values of ρ ; the point where the integral is zero then gives the desired value of ρ .)

If in this way $\epsilon_1 = \Psi(\rho)$ and $\epsilon_2 = \frac{h}{\rho} - \eta_1$ are determined, the maximum stresses are given by $s_1 = f(\epsilon_1)$, $s_2 = f(\epsilon_2)$. For each pair of values ϵ_1 , ϵ_2 (or s_1 , s_2) there corresponds a bending moment M which may be calculated by (4), and a curvature $\frac{1}{\rho} = \frac{\epsilon_1 + \epsilon_2}{h}$. Since the bending moment M is a given function of the variable x , a curvature $1/\rho$ may be found corresponding to the value of M at the point x . Thus a certain curve—the elastic line of the bar—is defined by the differential equation

$$\frac{d^2y}{dx^2} = \frac{1}{\rho} \quad (7)$$

Since $1/\rho$ is a function of M and hence of x , integration of this equation gives the deflection y of the elastic line as a function of x .

In the following chapters a few applications of the above derived relations will be made.

CHAPTER 23

PURE BENDING OF A BAR WITH RECTANGULAR CROSS SECTION

a. To Determine How the Bending Moment Varies with the Deflection.—As in this case, M is independent of x , and $b = \beta(\eta)$ is independent of η , Eq. (5) reduces to:

$$\int_{-\epsilon_1}^{\epsilon_2} f(\epsilon) d\epsilon = 0. \quad (8)$$

If we introduce here the areas under the respective stress-strain curves for compression and for tension (Fig. 223):

$$A_1 = -\int_{-\epsilon_1}^0 f(\epsilon) d\epsilon, \quad A_2 = \int_0^{\epsilon_2} f(\epsilon) d\epsilon, \quad (9)$$

this condition then gives:

$$A_1 = A_2. \quad (10)$$

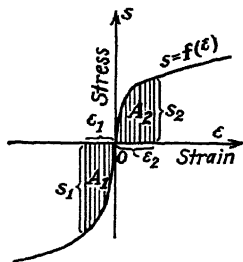


FIG. 223.—Stress-strain curve $s = f(\epsilon)$ for bending.

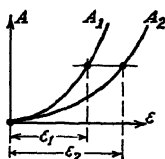


FIG. 224.—Areas A_1 and A_2 as depending on ϵ .

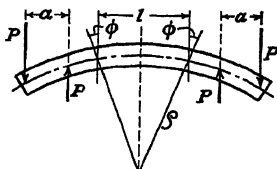


FIG. 225.—Bar in pure bending.

One may then plot A_1 and A_2 as a function of the upper and lower limits respectively of the integral (Fig. 224) and from this determine ϵ_2 as a function of ϵ_1 . The bending moment is then equal to:

$$M = b\rho^2 \int_{-\epsilon_1}^{\epsilon_2} f(\epsilon) \epsilon d\epsilon. \quad (11)$$

The angle which two cross-sections at a distance l apart (Fig. 225) are inclined with respect to one another, is:

$$2\phi = \frac{l}{\rho}. \quad (12)$$

Since

$$\eta_1 = \epsilon_1 \cdot \rho, \quad \eta_2 = \epsilon_2 \cdot \rho, \quad \eta_1 + \eta_2 = h \quad (13)$$

the curvature becomes:

$$\frac{1}{\rho} = \frac{\epsilon_1 + \epsilon_2}{h} \text{ and } \phi = \frac{l(\epsilon_1 + \epsilon_2)}{2h} \quad (14)$$

The results of the calculation may be condensed into the two following formulæ:

Bending moment

$$M = Pa = \frac{h^2 b}{(\epsilon_1 + \epsilon_2)^2} \int_{-\epsilon_1}^{\epsilon_2} f(\epsilon) \epsilon d\epsilon, \quad (15)$$

Slope of the tangent

$$\phi = \frac{(\epsilon_1 + \epsilon_2)l}{2h}. \quad (16)$$

Since M and ϕ may easily be determined by a bending test, these formulæ permit a convenient experimental test of the fundamentals of the calculations. They give the moment M (or the load on the bar $P = M/a$) as a function of the slope ϕ of the elastic line if the law of deformation of the material is known.

b. To Determine the Stress-strain Curve from a Bending Test.—The above equations permit the solution of the inverse problem. It will be assumed that from a bending test with a bar of rectangular cross-section both strains ϵ_1 and ϵ_2 of the outermost fibers have been determined for a series of loads P or what is the same thing, for various values of the bending moment $M = Pa$. One may determine from these observations the shape of the stress-strain curve of the material for tension and compression as follows:

From Eq. (16) the slope of the tangent to the elastic line of the bent bar is given by:

$$\phi = (\epsilon_1 + \epsilon_2) \frac{l}{2h}. \quad (17)$$

The position of the neutral axes is given by (13) and (14):

$$\eta_1 = \rho \epsilon_1 = \frac{\epsilon_1 h}{(\epsilon_1 + \epsilon_2)}. \quad (18)$$

In the integral

$$\int_{-\epsilon_1}^{\epsilon_2} f(\epsilon) d\epsilon = 0, \quad (19)$$

the limits ϵ_1 and ϵ_2 are to be looked on as functions of ϕ . From these it follows therefore:

$$\frac{\partial}{\partial \phi} \int_{-\epsilon_1}^{\epsilon_2} f(\epsilon) d\epsilon = f(\epsilon_2) \cdot \frac{d\epsilon_2}{d\phi} + f(-\epsilon_1) \frac{d\epsilon_1}{d\phi} = 0, * \quad (20)$$

or since,

$$s_1 = -f(-\epsilon_1), \quad s_2 = f(\epsilon_2),$$

we get

$$s_2 d\epsilon_2 = s_1 d\epsilon_1 \quad (21)$$

The apparent meaning of this equation is that the increase of both areas A_1 and A_2 , namely $s_1 d\epsilon_1$ and $s_2 d\epsilon_2$, must remain constantly equal, as the load or moment increases.

The expression for bending moment [Eq. (15)] gives, if the value of ϕ in (16) be substituted, the following equation:

$$M\phi^2 = \frac{bl^2}{4} \int_{-\epsilon_1}^{\epsilon_2} f(\epsilon) \epsilon d\epsilon. \quad (22)$$

From this it follows that:

$$\frac{d}{d\phi} (M\phi^2) = \frac{bl^2}{4} \left[f(\epsilon_2) \epsilon_2 \frac{d\epsilon_2}{d\phi} - f(-\epsilon_1) \epsilon_1 \frac{d\epsilon_1}{d\phi} \right] = \frac{bl^2}{4} \left(s_2 \epsilon_2 \frac{d\epsilon_2}{d\phi} + s_1 \epsilon_1 \frac{d\epsilon_1}{d\phi} \right), \quad (23)$$

or using Eqs. (21) and (16)

$$\begin{aligned} -s_1 d\epsilon_1 + s_2 d\epsilon_2 &= 0, & d\epsilon_1 &= \frac{2h}{l} \cdot \frac{s_2}{s_1 + s_2} \cdot d\phi \\ d\epsilon_1 + d\epsilon_2 &= \frac{2hd\phi}{l}, & d\epsilon_2 &= \frac{2h}{l} \cdot \frac{s_1}{s_1 + s_2} \cdot d\phi, \end{aligned}$$

we finally obtain:

$$\frac{bh^2 \cdot \frac{s_1 s_2}{s_1 + s_2}}{\phi} = \frac{1}{\phi} \frac{d}{d\phi} (M\phi^2). \quad (24)$$

The right side of this equation is known if, from observed test data, the bending moment M is known as a function of the slope ϕ . From the observed strains ϵ_1 and ϵ_2 , the ratio $d\epsilon_1/d\epsilon_2$, and therefore using Eq. (21), s_2/s_1 may be determined for various values of the observed angle ϕ . These expressions permit the calculation of the stresses s_1 and s_2 farthest from the neutral

* In forming the derivatives of the definite integral, we proceed according to the rule:

$$\frac{\partial}{\partial \alpha} \int_a^b f(x, \alpha) dx = \int_a^b \frac{\partial f(x, \alpha)}{\partial \alpha} dx + f(b, \alpha) \frac{db}{d\alpha} - f(a, \alpha) \cdot \frac{da}{d\alpha}$$

In Eq. 19, f does not depend on the parameter ϕ , and for a and b we substitute:

$$a = -\epsilon_1; \quad b = \epsilon_2$$

CHAPTER 24

BAR SUBJECTED TO PLASTIC BENDING

If a bar of ductile metal be loaded in bending under increasing load, at a certain definite load in certain parts of the bar the limit of plasticity will be reached. If the stress-strain curve for the metal in tension and compression is known in both the elastic and plastic stages, the stresses inside a bent bar may easily be calculated by the procedure as set forth in Chap. 23.

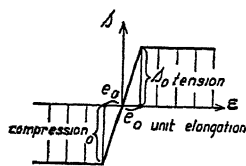


FIG. 227.—Idealized stress-strain curve for pure bending.

a. Initial Yield or Flow in Steel Bar.—For a metal which has a definite yield point as, for example, soft annealed wrought iron, the stress-strain curve may be replaced, for the above purpose of calculation, by three straight lines. It is thus assumed that the strains produced by

plastic bending are not larger than a few per cent. If it be assumed that the yield points for tension and compression are the same and that in the elastic regions $-\epsilon_0 < \epsilon < \epsilon_0$, however the strains may be calculated by taking a constant value of

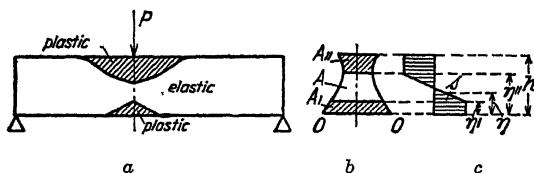


FIG. 228a, b, and c.—Simply supported bar bent by single load beyond plastic limit.

the modulus of elasticity $E = s/\epsilon$, these assumptions correspond to a stress-strain curve which satisfies the following conditions (Fig. 227):

$$\begin{aligned} \text{for } \epsilon < -\epsilon_0, \quad s &= -s_0 = \text{const}, \\ \text{for } -\epsilon_0 < \epsilon < \epsilon_0, \quad s &= E\epsilon, \\ \text{for } \epsilon_0 < \epsilon, \quad s &= s_0 = \text{const}. \end{aligned}$$

In the inside of a bar, subjected to bending, which is stressed above the yield stress, for certain parts of the bar two kinds of regions are to be differentiated according to whether the strains are elastic or plastic (Fig. 228a). Likewise the elastic and plastic areas are to be differentiated in different cross-sections (Fig. 228b). We consider a cross-section of the bar and take η equal to the distance from an arbitrary straight line, perpendicular to the plane of bending (Fig. 228c). In a certain part of the cross-section which we may designate by A' (Fig. 228b), the bending stress s is equal to the yield stress for tension s_0 ; a second part A'' has stresses equal to the yield stress in compression $s = -s_0$. In the middle part A (Fig. 228b), where the bending stresses have not reached the yield point, the stress must satisfy the straight-line law:

$$s = a + b\eta. \quad (27)$$

We set S, S', S'' equal to the static moments relative to the axis OO and J, J', J'' the moments of inertia of the above-mentioned areas A, A', A'' . At the limits of the plastic zones $\eta = \eta'$ and $\eta = \eta''$, the stress $s = \pm s_0$, or

$$\left. \begin{aligned} a + b\eta' &= s_0 \\ a + b\eta'' &= -s_0 \end{aligned} \right\} \quad (28)$$

From this follows that:

$$a = -s_0 \frac{\eta' + \eta''}{\eta' - \eta''}; \quad b = \frac{2s_0}{\eta' - \eta''} \quad (29)$$

The condition of equilibrium:

$$\int s dA = 0, \quad (30)$$

when the above relations are introduced, takes the following form:

$$A \cdot a + S \cdot b = s_0(A'' - A'). \quad (31)$$

If, in this equation, a and b are replaced by the expressions (29), there results a function of η' and η'' . From this function the ordinates η' and η'' , which separate the plastic areas of the bar from the elastic area, may be calculated. If a and b are determined in this way the bending moment may be calculated from:

$$M = \int s \eta dA = Sa + Jb + (S' - S'')s_0. \quad (32)$$

b. An Example of the Spread of the Plastic Regions in a Bar Stressed Slightly above the Yield Point.—As an example we choose a simply supported bar with triangular cross-section of steel, loaded in the middle by a force P . The cross-section of the bar is an isosceles triangle having a

base c and a height h . The length of the bar is l and the abscissa x is measured from the left end. The process of calculation will be briefly outlined.

In the elastic region of deformation the bending stresses are distributed in the cross-sections according to the straight-line law:

$$s = -\frac{12Px}{ch^2}\left(1 - \frac{3\eta}{2h}\right). \quad (33)$$

As the force P increases, the yield point is first reached in the outermost compression fiber ($\eta = 0$) of the middle cross-section where $x = l/2$, at a load:

$$P = P_0 = \frac{ch^2s_0}{6l} \quad (34)$$

Since the stress at a load P_0 is only $s_0/2$ on the tension side ($\eta = h$) of the middle cross-section, the bar begins to yield at first in the neighborhood of the point $\eta = 0$ on the compression side.

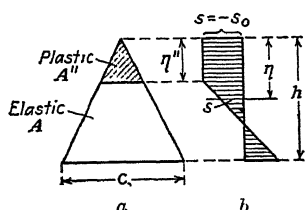


FIG. 229a and b.—Cross-sectional area and distribution of bending stress.

At a load $P > P_0$ there results at first only one plastic region in the bar. This is represented by the cross-hatching in Fig. 229a, its area being designated by A'' .

In the part A not cross-hatched (the elastic part) of the cross-section, the straight-line law gives for the stress:

$$s = a + b\eta. \quad (35)$$

At the limits of A and A' we have for $\eta = \eta''$

$$-s_0 = a + b\eta''. \quad (36)$$

Eq. (31) becomes when $A' = 0$,

$$Aa + Sb = s_0A''. \quad (37)$$

Taking:

$$A = \frac{c(h^2 - \eta''^2)}{2h}, \quad A'' = \frac{c\eta''^2}{2h}, \quad S = \frac{c(h^3 - \eta''^3)}{3h}, \quad (38)$$

and designating:

$$a = s_0\alpha, \quad b = \frac{s_0\beta}{h}, \quad u'' = \frac{\eta''}{h} \quad (39)$$

from the foregoing expressions we obtain:

$$\alpha = -\frac{2 + u''^3}{2 - 3u'' + u''^3}, \quad \beta = \frac{3}{2 - 3u'' + u''^3}. \quad (40)$$

This determines the stress distribution in the cross-section; for example, for

$$u'' < u < 1, \quad s = (\alpha + \beta u)s_0,$$

and for

$$0 < u < u'', \quad s = -s_0,$$

while the bending moment M becomes:

$$M = \frac{ch^2s_0}{12} \cdot \frac{3u''^4 - 4u''^3 + 1}{u''^3 - 3u'' + 2}. \quad (41)$$

The above expressions hold as long as:

$$0 < u'' < \frac{\sqrt{3}-1}{2} = 0.3661. \quad (42)$$

As soon as u'' becomes > 0.3661 , $P > 1.80P_0$ and the bar begins to yield also on its tension side. At a loading $P > 1.80P_0$, there are two different regions inside the bent bar in which the stresses are at the plastic limit.

In order to determine the stress distribution under this loading the following three equations are available:

$$\left. \begin{aligned} a + b\eta' &= s_0, \\ a + b\eta'' &= -s_0, \\ Aa + Sb &= s_0(A' - A'). \end{aligned} \right\} \quad (43)$$

In this

$$\begin{aligned} A' &= \frac{c(h^2 - \eta'^2)}{2h}, \quad A'' = \frac{c\eta''^2}{2h}, \quad A = \frac{c}{2h}(\eta'^2 - \eta''^2), \\ S &= \frac{c(\eta'^3 - \eta''^3)}{3h}. \end{aligned} \quad (44)$$

Using the above symbols as defined in (39) and taking

$$u = \frac{\eta}{h}, \quad u' = \frac{\eta'}{h}, \quad u'' = \frac{\eta''}{h}, \quad (45)$$

we obtain from the first two equations (43):

$$\alpha = -\frac{u' + u''}{u' - u''}, \quad \beta = \frac{2}{u' - u''}. \quad (46)$$

From the third we obtain:

$$u'^2 + u'u'' + u''^2 = 3_2. \quad (47)$$

This is the equation of an ellipse whose minor semi-axis $a = 1$ has the direction of the bisector of the axes $u' = u''$ and whose major semi-axis $b = \sqrt{3}$. We consider only that part of the ellipse where:

$$u' = 1, \quad u'' = \frac{\sqrt{3}-1}{2} \text{ to } u' = u'' = \frac{1}{\sqrt{2}} \quad (48)$$

To the one limiting point corresponds the point in the bar where the second plastic region begins. If, however:

$$u' = u'' = \frac{1}{\sqrt{2}} \quad (49)$$

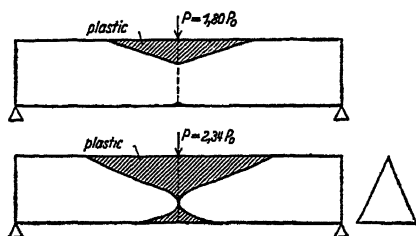
there results a limiting case of bending of the bar. In this case both the above different plastic regions touch each other in the middle cross-section of the bar. This occurs when $P = 2.34P_0$.

In the middle portion of the bar, where it is strained plastically on the tension as well as on the compression side, as long as $1.80P_0 < P < 2.34P_0$ the bending moment is:

$$M = \frac{ch^2s_0}{6} \left(2 - \frac{u'^4 - u''^4}{u' - u''} \right) = \frac{Px}{2}. \quad (50)$$

On the basis of the preceding formula the limits of the plastic areas for $P = 1.80P_0$ and for $P = 2.34P_0$ are represented to scale in Figs. 230 and 231. In these the plastic parts of the bar are represented by the cross-hatching.

It is clear that the above calculation insofar as it relates to the spread of the plastic regions under the larger loads will decrease in accuracy with the



FIGS. 230 and 231.—Limits of plastic regions in a freely supported bar of triangular cross-section bent by single load P at center. The boundaries of the plastic regions are indicated in true scale for two loads. Fig. 230 (above): Load $P = 1.80P_0$ just when lower side of bar starts to yield. Fig. 231 (below): $P = 2.34P_0$ when whole middle section yields. (P_0 is the load under which the bar just starts to yield at upper side.)

increasing load ($P = 2.34P_0$). At the higher loads the validity of the simple assumptions made relative to the shape of the stress-strain curve $s = f(\epsilon)$, (*viz.*, that the yield stresses are independent of the strains ϵ) on which the calculation is based, do not hold accurately. How these assumptions may be improved is indicated in the following chapter.

CHAPTER 25

PLASTIC BENDING CONSIDERING WORK HARDENING

The assumptions regarding the shape of a stress-strain curve, on which the treatment of Chap. 24 is based, do not take into account the increase in yield stresses or the strengthening of the material (work hardening) which occurs for most ductile metals with increasing strain. There is, however, no difficulty in taking this factor into account. How this can be done will be illustrated by the following example of the plastic bending of an iron bar with a rectangular cross-section.

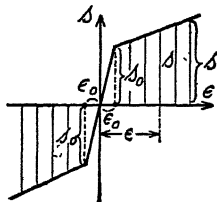


FIG. 232.—Idealized stress-strain curve for steel, taking into account work-hardening.

a. **Stress-strain Curve, According to Fig. 232.**—The calculation can be based on a stress-strain curve composed of three straight lines as shown in Fig. 232:

$$\begin{aligned} \text{for } -\epsilon_0 > \epsilon, & \quad s = -s_{00} + s''\epsilon, \\ \text{for } -\epsilon_0 < \epsilon < \epsilon_0, & \quad s = s'\epsilon, \\ \text{for } \epsilon_0 < \epsilon, & \quad s = s_{00} + s''\epsilon. \end{aligned}$$

If we introduce here instead of the constant s_{00} the yield stress for tension s_0 and consider that at the break of the curve $\epsilon = \epsilon_0$ the stress is:

$$s_0 = s'\epsilon_0 = s_{00} + s''\epsilon_0, \quad (51)$$

we then have:

$$s_{00} = s_0 \left(1 - \frac{s''}{s'} \right). \quad (52)$$

The stress-strain curve is thus determined by the following three constants depending on the material: the yield stress s_0 , which is the same for tension and compression, a constant s' for the elastic, and a constant s''

for the plastic strain (s' is equal to the modulus of elasticity of the material E , s'' is a measure of the increase in yield stresses under increasing strain, i.e., of the strengthening or cold-working effect).

The length of the bar is designated by l , the width of the rectangular cross-section by b , the height by h , and the loading of the bar by P .

On account of the symmetrical distribution of bending stresses, it is not necessary in this case to determine the position of the neutral axis. The stresses in the cross-section, distributed according to Fig. 233, give the following bending moment:

$$M = 2(P_{1\eta_1} + P_{2\eta_2} + P_{3\eta_3}). \quad (53)$$

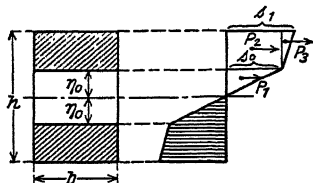


FIG. 233.—Distribution of bending stresses in cross-section.

In this P_1, P_2, P_3 represent the resultant values of force produced by those portions of the stress diagram (Fig. 233) which are bounded by the straight lines shown; and η_1, η_2, η_3 represent their moment arms relative to neutral axis (Fig. 233):¹

$$\left. \begin{aligned} P_1 &= \frac{s_0 b \eta_0}{2}, & \eta_1 &= \frac{2\eta_0}{3}, \\ P_2 &= s_0 b \left(\frac{h}{2} - \eta_0 \right), & \eta_2 &= \left(\frac{h}{2} + \eta_0 \right) \cdot 2 \\ P_3 &= \frac{s_0 b s''}{2 s' \eta_0} \left(\frac{h}{2} - \eta_0 \right)^2, & \eta_3 &= \frac{(h + \eta_0)}{3}. \end{aligned} \right\} \quad (54)$$

(The symbols relate to Figs. 232 and 233.) If we put:

$$\left. \begin{aligned} u &= \frac{2\eta_0}{h}, \\ v &= \frac{1}{2} \left[3 - u^2 + \frac{s''(1-u)^2(2+u)}{s'u} \right], \end{aligned} \right\} \quad (55)$$

the bending moment becomes:

$$M = \frac{Px}{2} = \frac{P_0 l v}{4}. \quad (56)$$

The bar begins to yield under a load:

$$P_0 = \frac{2bh^2 s_0}{3l}. \quad (57)$$

The above equation for M holds for $P > P_0$. The variables u and v are to be considered as functions of x . In the middle of the bar we have for $x = l/2$, $v = P/P_0$. If this value of v is designated by $v_0 = P/P_0$, the equation of the boundary curve of the plastic region is determined from the following relation:

$$x = \frac{lv}{2v_0} = \frac{l}{4v_0} \left[3 - u^2 + \frac{s''}{s'} \cdot \frac{(1-u)^2(2+u)}{u} \right]. \quad (58)$$

At a certain load P , where $P > P_0$, at those points of the cross-section, where $u = 1$ and $v = 1$, the yield point in the fibers farthest from the neutral axis is just reached. The abscissæ of these cross-sections may be obtained from (58) by substituting $u = 1$ and $v = 1$:

$$x = x_1 = \frac{l}{2v_0}. \quad (59)$$

In the plastically bent part of the bar $x_1 < x < l/2$, the maximum stress at the edge of the cross-section having the abscissa x is given by:

$$s_1 = \pm (s_0 + s''(\epsilon_1 - \epsilon_0)) = \pm s_0 \left[1 + \frac{s''}{s'} \cdot \frac{1-u}{u} \right]. \quad (60)$$

¹ P_3 is determined as follows: let s_1 equal the stress along the edge and ϵ_1 the corresponding strain for $\eta = \frac{h}{2}$. Then $P_3 = \frac{b(s_1 - s_0)}{2} \left(\frac{h}{2} - \eta_0 \right)$. Since $1/\rho = \epsilon_0/\eta_0 = 2\epsilon_1/h$, we have $\epsilon_1 = h\epsilon_0/2\eta_0 = (s_1 - s_0)/s''$, from which we obtain $s_1 - s_0 = \frac{s_0 s''}{s'} \left(\frac{h}{2\eta_0} - 1 \right)$. Introducing this in the above expression for P , we obtain the value given in Eq. (54).

The shape of the elastic line of the bent bar for that portion where the strains are purely elastic, is determined from the well-known equation:

$$\frac{d^2y}{dx^2} = \frac{M}{JE} = -\frac{Px}{2JE}, \quad y = -\frac{Px^2}{12JE} + c_1x + c_2, \quad (0 < x < x_1).$$

In the plastically bent part of the bar it is determined by the formula:

$$\frac{1}{\rho} = \frac{\epsilon}{\eta} = \frac{\epsilon_0}{\eta_0}$$

If the strain ϵ_0 in this formula be replaced by s_0/E and the ordinate η_0 of the boundary curve of the plastic region by $\eta_0 = hu/2$ and if the curvature $1/\rho$ is replaced by $-d^2y/dx^2$, we obtain for the plastically bent part ($x_1 < x < l/2$) the following differential equation of the elastic line:

$$\frac{d^2y}{dx^2} = -\frac{2s_0}{Eh} \cdot \frac{1}{u}. \quad (61)$$

As will be recognized from the formulæ and the expressions for the limiting curves of the plastic regions, the elastic region in the middle part of the bar, at sufficiently large loading P , shrinks up into a narrow strip.

In a bar which is plastically bent under heavy loading, it is possible to differentiate three different parts: an elastic part, having pure elastic tensions ($0 < x < x_1$), an elastic-plastic part ($x_1 < x < x_2$), and a completely plastic part ($x_2 < x < l/2$).

Under high loadings, producing severe yielding, in the transition part of the bar $x_1 < x < x_2$, u and v may usually be replaced by the simpler expressions:

$$v = \frac{3 - u^2}{2}, \quad u = \sqrt{3 - \frac{4Px}{P_0l}} \quad (62)$$

and in the plastic part these may be replaced by:

$$v = \frac{3}{2} + \frac{s''}{s'} \cdot \frac{1}{u}, \quad \frac{s''u}{s'} = \frac{2Px}{P_0l} - \frac{3}{2}. \quad (63)$$

The deflection of a bent bar at high loads may be calculated with sufficient accuracy in that portion where $0 < x < x_2$ from the differential equation:

$$y'' = -\frac{Px}{2JE}. \quad (64)$$

In the plastic part $x_2 < x < l/2$, it may be calculated from the equation:

$$y'' = -\frac{s_0}{s''h} \left(\frac{4Px}{P_0l} - 3 \right) \quad (65)$$

The limiting curves of the plastic regions in a severely bent bar may be observed experimentally in various ways. In bars of very soft iron the limits of the plastic regions may be indicated by suitable etching combined with previous thermal treatment of the test bar. For this purpose the etching method of A. Fry already referred to above or etching of the iron by heating to its recrystallization temperature is of value.¹

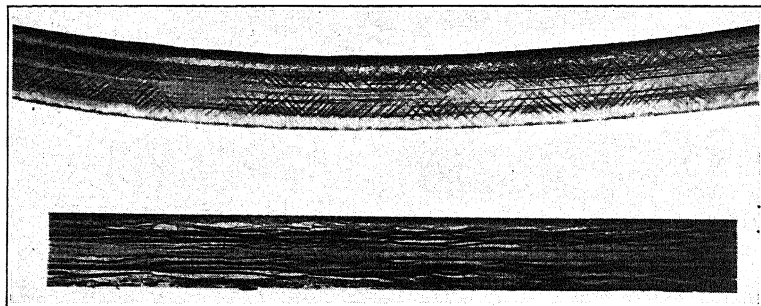
¹ FISCHER, FR. P., *Kruppsche Monatshefte*, vol. 4, p. 77, 1923.

A few photographs of the markings obtained using Fry's method in the longitudinal sections and cross-sections of plastically bent steel sheets are shown in Figs. 234 to 237. Figures 234 and 235 show two longitudinal sections in the plane of bending of a steel plate. Figure 236 shows a section perpendicular to



FIG. 234.—Etching of a section through an old boiler plate showing flow lines and cracks. (*According to B. Strauss and A. Fry.*)

the plane of bending. The position of the flow layers is indicated in the sketch of Fig. 237. As will be seen, the flow layers in a bent steel sheet practically coincide with the surfaces of maximum shear. In longitudinal cross-sections of a wrought iron bar bent



FIGS. 235 and 236.—Lüders' lines in sections perpendicular and parallel to axis of a steam boiler. The flow lines were produced by the bending of the boiler plate in the bending machine. (*According to B. Strauss and A. Fry.*)

beyond the plastic limit, the shape of boundary lines of the plastic region could be demonstrated using Fry's etching method. The boundaries of the dark surfaces in the etchings were practically identical with the shape calculated by the above methods for the case of a simply supported bar loaded in the middle.

Using the second method, the steel bar stressed above the yield point is heated for some time at 650° to 750°C . The annealing treatment at this temperature induces in the stressed steel a rearrangement of its microstructure, and, according to a well-known law, under recrystallization the largest crystal grains are formed at the limits of the plastic region, which then may be made visible by the usual etching process (for example by means of copper-ammonium-chloride).



FIG. 237.—Flow lines in a plate produced by bending.

b. Other Examples of Plastically Deformed Regions in Bent Bars.—In calculating the shape of the boundary curves of the plastic region it was assumed that the stress-strain curve of the material is represented by the broken line of Fig. 227.

1. *Simply Supported Bar with a Single Load in the Middle.*—If the material begins to flow under constant stress, the constant $s' = 0$ in the formula (55). From formulæ (56) and (55), the bending moment becomes:

$$M = \frac{Px}{2} = \frac{P_0 l (3 - u^2)}{8}, \quad (66)$$

from which the equation of the boundary of the plastic area follows:

$$u^2 = 3 - \frac{4Px}{P_0 l}. \quad (67)$$

The plastic area is, therefore, bounded by two parabolas, which shift along the bar as the load increases. The limiting position which these parabolas can take up is that position in which their vertices just touch in the middle of the bar. The force is then $P_{\max} = 3P_0/2$.

2. *Simply Supported Bar Loaded with a Uniformly Distributed Load.*—The length of the bar is l ; the rectangular cross-section has a width b and a height h , while the load per unit length of the bar is p . The bar begins to yield under a load p_0 :

$$p_0 = \frac{4bh^2s_0}{3l^2} \quad (68)$$

If $p > p_0$, there occur in the middle of the bar two plastic regions which are bounded by two branches of a hyperbola. The boundary line of the plastic zone has the equation:

$$\frac{\eta^2}{A^2} - \frac{x^2}{B^2} = 1 \quad (69)$$

In this the semi-axes are:

$$A = \frac{h}{2} \sqrt{3 - \frac{2p}{p_0}}, \quad B = \frac{l}{2} \sqrt{\frac{3p_0}{2p} - 1}; \quad (70)$$

at a load $p = 3p_0/2$, the hyperbolas coincide with their asymptotes (Fig. 238).

3. *Bar Having Built-in Ends with Uniformly Distributed Load.*—In this case the plastic regions are bounded by elliptical arcs.

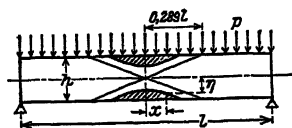


FIG. 238.—Plastic regions in a bar bent by uniformly distributed load p .

CHAPTER 26

BUCKLING AFTER THE YIELD POINT IS EXCEEDED

It was shown by von Kármán¹ that the theory of bending of bars may be extended to those cases in which bars axially loaded in compression are stressed beyond the yield point. If a bar be loaded in compression its equilibrium may, as is well known,

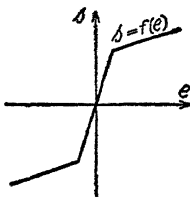


FIG. 239.—Idealized stress-strain curve for buckling after the yield point is exceeded.

become unstable if the slenderness ratio is sufficiently large. The bar then tends to buckle. Now, if the stresses which occur when the bar is straight and subjected to axial compression, reach the yield point, it is clear that during bending the compressive stresses on the convex side of the bar are decreased (by the tensile stresses set up by bending), while those on the concave side are increased. In this consideration

the treatment will be based on a stress-strain curve (Fig. 239), such as was assumed in Chap. 25. The bar has a rectangular cross-section of width b and height h , a length l , and is loaded axially by a compressive force P to an average stress s_k , which is higher than the yield stress s_0 of the material. It is desired to find the critical value of compressive stress s_k or the limiting force $P_k = bhs_k$, at which the equilibrium of the bar in its straight form becomes unstable, and buckling results.

In Fig. 240 the stress distribution in a bar is represented. Before bending, the stress distribution would follow the horizontal straight line $s = s_k$. After bending, the stress distribution is represented by the broken line A_1OA_2 . The equilibrium of the stresses requires that:

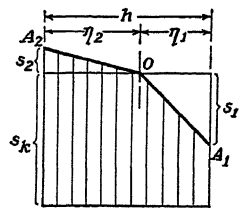


FIG. 240.—Bending stresses s in bar starting to buckle.

$$s_1 \eta_1 = s_2 \eta_2. \quad (1)$$

¹ Untersuchungen über Knickfestigkeit, *Mitt. u. Forschungsarb. d. V.D.I.*, Heft 81, Berlin, 1909.

Since the cross-section remains plane during bending, using the symbols of Eq. (2), page 161, and of Eq. (51), page 173, we have:

$$\epsilon_1 = \frac{s_1'}{s'} = \frac{\eta_1}{\rho}, \quad \epsilon_2 = \frac{s_2'}{s''} = \frac{\eta_2}{\rho}; \quad s_1 = \frac{s'\eta_1}{\rho}, \quad s_2 = \frac{s''\eta_2}{\rho}. \quad (2)$$

Moreover:

$$\eta_1 + \eta_2 = h \quad (3)$$

From these expressions it follows that:

$$s'\eta_1^2 = s''\eta_2^2$$

and

$$\eta_1 = \frac{h\sqrt{s''}}{\sqrt{s'} + \sqrt{s''}}, \quad \eta_2 = \frac{h\sqrt{s'}}{\sqrt{s'} + \sqrt{s''}}. \quad (4)$$

The bending moment is equal to:

$$M = \frac{b}{3}(s_1\eta_1^2 + s_2\eta_2^2), \quad (5)$$

or applying Eq. (4) we have:

$$M = \frac{bh^3}{12} \cdot \frac{1}{\rho} \cdot \frac{4s's''}{(\sqrt{s'} + \sqrt{s''})^2}. \quad (6)$$

Using the symbols:

$$J = \frac{bh^3}{12}, \quad E_0 = \frac{4s's''}{(\sqrt{s'} + \sqrt{s''})^2} \quad (7)$$

(J being the smallest moment of inertia of the cross-section about a gravity axis) we thus obtain the differential equation for the deflection of the bar:

$$\frac{1}{\rho} = -\frac{dy^2}{dx^2} = \frac{M}{JE_0} = \frac{Py}{JE_0} \quad (8)$$

From this it follows that:

$$y = A \sin \sqrt{\frac{P}{JE_0}}x + B \cos \sqrt{\frac{P}{JE_0}}x. \quad (9)$$

Using the boundary conditions:

$$x = \pm \frac{l}{2}, \quad y = 0, \quad P = n^2\pi^2 \frac{JE_0}{l^2}, \quad (n = 1, 2, \dots). \quad (10)$$

The smallest load at which the bar buckles is therefore:

$$P_k = \pi^2 \cdot \frac{JE_0}{l^2} \quad (11)$$

This formula is of the same type as Euler's formula for elastic buckling, namely:

$$P_k = \pi^2 \cdot \frac{JE}{l^2}.$$

It is seen that the value of modulus of elasticity E given by Euler's formula has simply to be replaced by the value E_0 , given by Eq. (7).

The formula (7) derived for rectangular cross-section may be immediately generalized for any arbitrary cross-section. From the condition of equilibrium $\int sdA = 0$, using:

$$s = \frac{s_1}{\eta_1}, \text{ or } s = \frac{s_2}{\eta_2},$$

the following equation results:

$$\frac{s_1}{\eta_1} \int_0^{\eta_1} \eta \, dA = \frac{s_2}{\eta_2} \int_0^{\eta_2} \eta \, dA.$$

Putting:

$$s_1 = \frac{s' \eta_1}{\rho}, \quad s_2 = \frac{s'' \eta_2}{\rho},$$

the former equation simplifies to:

$$s' S_1 = s'' S_2,$$

by means of which condition an axis in the cross-section is determined along which the stresses do not change during the first instant of buckling. Putting S_1, S_2 equal to the static moments and J_1, J_2 equal to the moments of inertia of the two halves of the cross-section relative to this axis, and $J = J_1 + J_2$ equal to the moment of inertia of the complete cross-section, the bending moment becomes:

$$M = \int s \eta \, d\eta = \frac{s_1 J_1}{\eta_1} + \frac{s_2 J_2}{\eta_2} = \frac{1}{\rho} (s' J_1 + s'' J_2) = \frac{1}{\rho} J E_0.$$

From this the value E_0 , from which the buckling load P_k may be calculated, becomes:

$$E_0 = \frac{s' J_1 + s'' J_2}{J_1 + J_2}. \quad (12)$$

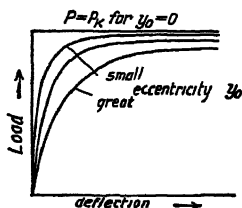


FIG. 241.—Elastic buckling. Load deflection curves for various eccentricities of load.

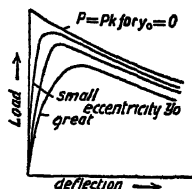


FIG. 242.—Plastic buckling. Load deflection curves for various eccentricities of load. (According to Kármán.)

A peculiarity of the buckling process, accompanying the exceeding of the yield point, which von Kármán has especially emphasized, is the decrease in the axial compressive force during bending. If one plots the maximum deflection of a bar during buckling as abscissæ and the compressive load P at which the bar bows out, as ordinates, for various values of the eccentricity of the axial load and for elastic buckling the series of curves shown in Fig. 241 is obtained. All curves have for their common asymptote the horizontal straight line which corresponds to Euler's critical load, $P_k = \pi^2 J E / l^2$.

With buckling, accompanied by average stresses exceeding the yield point, one obtains a series of similar curves shown in Fig. 242 with the difference that now with increasing eccentricities the axial maximum compressive loads which produce buckling decrease considerably.

If one plots the compressive stress at the instant of buckling against the so-called "slenderness ratio" l/i (where $i = \sqrt{J/A}$ equals the radius of gyration of the cross-section), there is obtained according to Kármán's tests a line such as is represented

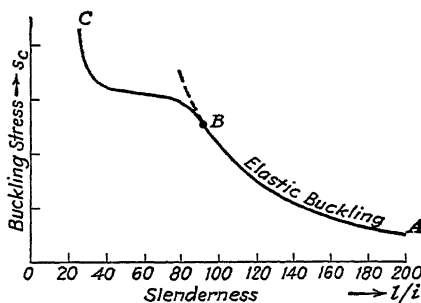


FIG. 243.—Buckling loads for various ratios of slenderness $l:i$.

by the heavy line in Fig. 243. The portion of the curve AB corresponds to elastic buckling as given by Euler's buckling formula:

$$P_k = \pi^2 \cdot \frac{JE}{l^2}.$$

The portion BC corresponds to buckling after the yield point is exceeded.¹

¹ Relative to the practical application of the results of the theory of buckling in bridge design and in proportioning structural compression members Cf. W. GEHLER, "Vorschlag einer Gebrauchsformel für Knickung," *Mitt. d. Normenausschusses d. deutschen Industrie*, vol. 2, nos. 11, 12, 15, November, 1923; in *Bauingenieur*, 1923. Relative to buckling of a bar of unelastic material such as concrete and reinforced concrete, cf. BACH and BAUMANN, "Elastizität und Festigkeit," 9th ed., Julius Springer, Berlin, 1924; and E. MÖRSCH, "Der Eisenbetonbau, seine Anwendung und Theorie," 5th ed., Stuttgart. Lately F. W. GECKELER in *Z. f. ang. Math. u. Mech.*, 1928, has calculated the buckling load for the case of unelastic buckling of a thin-walled cylinder, which is loaded in an axial direction. The buckling of such a cylinder is accompanied by symmetrical corrugations or waves.

Finally, an extension of the work of v. KÁRMÁN by H. M. WESTERGAARD and W. R. OSGOOD, *Strength of Steel-columns*, *A.P.M.* 50. 9., *A.I.M.E. Trans.*, p. 65, 1928, shall be mentioned here. These authors give the theory of steel columns which are stressed beyond the proportional limit and which are eccentrically loaded or initially curved.

CHAPTER 27

THE PLANE PROBLEM

This is the case where all stresses and strains depend only on two coordinates: x and y if rectangular, r, ϕ if polar coordinates are chosen. We distinguish two cases: *a. The plane problem of the first kind: plane strain:* In this case the principal strain ϵ_z , perpendicular to the xy plane, is either constant ($\epsilon_z = \text{const.}$) or equal to zero ($\epsilon_z = 0$). In such cases the body under stress must be assumed very long in the z direction. Many examples of engineering practice are comprised under this heading. An example is the stress distribution which results when rolling a sheet which is very wide in the direction perpendicular to the direction of rolling. Other examples are the stress distributions in a thick-walled tube, deformed plastically under internal pressure or in a long rotating drum. *(b) The plane problem of the second kind: plane stress:* In this case the principal stress perpendicular to the xy plane is zero: $s_z = 0$. This case occurs in a thin sheet which is loaded in its own plane. Examples of such cases

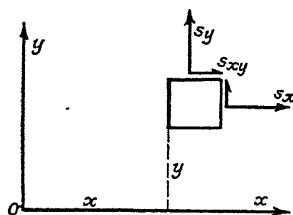


FIG. 244.—Stress components for plane problem.

are the stress distribution after the yield point has been reached in the neighborhood of the enlarged ends of a flat test bar (the “heads” of the bar) in tension, that in the neighborhood of a rivet hole in a tension member, or the stresses in a rotating disc.

a. Plane Strain. $\epsilon_z = 0$.—We designate the coordinates of a given point by x and y , both normal stresses and the shearing stress of the state of plane strain at the point (x, y) by s_x, s_y, s_{xy} respectively (Fig. 244), and the unit strains and the unit shearing strain by $\epsilon_x, \epsilon_y, \epsilon_{xy}$. Next we arrange to determine the normal stress under the assumption that the strain perpendicular to the xy plane $\epsilon_z = 0$ is zero.

A strain ϵ has in general an elastic part ϵ' and a plastic part ϵ'' . The elastic part ϵ_z' of the strain ϵ_z can be taken according to

Hooke's law equal to:

$$\epsilon_z' = \alpha[s_z - \nu(s_x + s_y)].$$

The plastic part ϵ_z'' according to Eq. (18) page 78 is equal to:

$$\epsilon_z'' = \beta[s_z - \frac{1}{2}(s_x + s_y)]$$

(In these equations, $\alpha = 1/E$, β is an undetermined factor, E the modulus of elasticity, and ν Poisson's ratio.) The sum of both strains must, according to our assumptions, vanish. Hence:

$$\epsilon_z' + \epsilon_z'' = \alpha[s_z - \nu(s_x + s_y)] + \beta[s_z - \frac{1}{2}(s_x + s_y)] = 0.$$

As the expressions within the brackets cannot be simultaneously equal to zero we must have:

$$s_z = \frac{\beta + 2\nu\alpha}{2(\alpha + \beta)} \cdot (s_x + s_y)$$

Considering the effect of s_z we can therefore differentiate three regions in the stressed body: In one part only elastic strains will exist, so that we have:

$$\beta = 0, s_z' = \nu(s_x + s_y).$$

In a second region the plastic strains are predominant so that β is large relative to α and we have:

$$s_z'' = \frac{1}{2}(s_x + s_y).$$

Between these two regions lies an elastic-plastic region in which the values of s_z take on values between s_z' and s_z'' .

The following statements referring to plane strain with one vanishing principal strain ($\epsilon_z = 0$) are limited to plastic regions where the permanent parts ϵ_x'' , ϵ_y'' of the strains ϵ_x and ϵ_y are predominant, so that the elastic strains ϵ_x' , ϵ_y' may be neglected. We may then put simply the principal stress

$$s_3 = s_z = \frac{1}{2}(s_x + s_y). \quad (1)$$

Using the formulæ for plane stress as derived on page 46, we see, that the principal stresses s_1 and s_2 are given by the Eq. (21), Chap. 8 or by

$$\left. \begin{aligned} s_1 &= \frac{s_x + s_y}{2} + s_m \\ s_2 &= \frac{s_x + s_y}{2} - s_m \end{aligned} \right\} \quad (2)$$

where s_m designates the principal shearing stress:

$$s_m^2 = \frac{(s_x - s_y)^2}{4} + s_{xy}^2. \quad (3)$$

In order to express the fact that we have an equilibrium of stresses in the plastic state, we have to introduce a condition of plasticity. Taking the general form of this condition (see Eq. (8) page 73).

$$(s_1 - s_2)^2 + (s_2 - s_3)^2 + (s_3 - s_1)^2 = 2s_0^2, \quad (4)$$

where the constant s_0 designates the yield stress in pure tension, we see that using Eq. (1) this expression simplifies considerably and becomes in terms of principal stresses:

$$(s_1 - s_2)^2 = \frac{4s_0^2}{3} = \text{const.} \quad (4a)$$

Hence the condition of plasticity is:

$$s_1 - s_2 = \pm \frac{2s_0}{\sqrt{3}} = \text{const.} \quad (5)$$

Writing for the constant $s_0/\sqrt{3} = k$ and using (2), (3) this last equation can also be expressed in terms of the stress components s_x, s_y, s_{xy} in rectangular coordinates:

$$(s_x - s_y)^2 + 4s_{xy}^2 = 4k^2 = \text{const.} \quad (6)$$

Under the assumption that plasticity occurs when the sum of the squares of the three principal stress differences Eq. (4) is a constant (this is identical with the condition of constant energy of distortion) we see that we obtain in the case of plane strain exactly the same condition of plasticity as would have been found using the maximum shear theory, with the single difference that according to the latter the constant k on the right side of Eq. (6) is equal to $s_0/2 = 0.500s_0$, while assuming condition (4) and (5) k is equal to $s_0/\sqrt{3} = 0.577s_0$.

Hence we see that the theory of plane plastic strain for the case $\epsilon_z = 0$ is mathematically exactly the same in both cases, either if we use as condition of plasticity the condition of constant energy of distortion [Eq. (4)] or that of constant maximum shearing stress ("theory of maximum shear"). The value of the constant has to be taken in the first case equal to $k = 0.577s_0$ and in the second case equal to $k = 0.500s_0$, where s_0 is the yield stress in pure tension.

b. Plane Stress.—In this case the third principal stress vanishes

$$s_3 = s_z = 0$$

Hence Eq. (4) becomes

$$(s_1 - s_2)^2 + s_1^2 + s_2^2 = 2s_0^2 \quad (7)$$

and the condition of plasticity now takes the form

$$\underline{s_1^2 - s_1 s_2 + s_2^2 = s_0^2.} \quad (8)$$

In rectangular coordinates s_1, s_2 this is the equation of an ellipse with the semi-axes $a = \sqrt{2} \cdot s_0$ and $b = \sqrt{\frac{2}{3}} \cdot s_0$ (see Fig. 245).¹ The principal stresses in a thin plate can therefore at no time become larger than $2s_0/\sqrt{3} = 1.155s_0$, which is the farthest

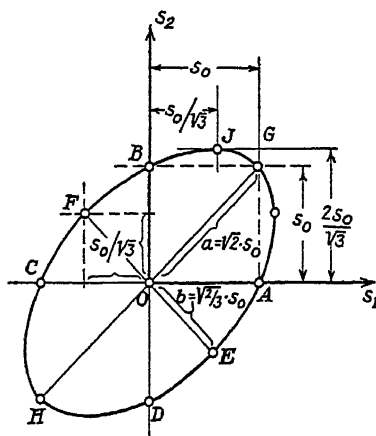


FIG. 245.—Ellipse of plasticity for plane stress: s_1, s_2 principal stresses; $s_3 = 0$, s_0 yield stress for pure tension.

distance of a point J of this ellipse from the coordinate axis OA (see Fig. 245).²

In terms of s_x, s_y, s_{xy} the condition of plasticity takes now the form:

$$\underline{s_x^2 - s_x s_y + s_y^2 + 3s_{xy}^2 = s_0^2.} \quad (9)$$

In the following chapters several applications of these cases will be discussed.

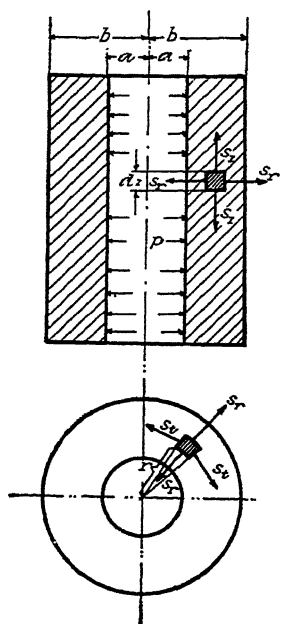
¹ This ellipse is the intersection of the surface of yielding $f(s_1, s_2, s_3) = 0$ (cf. Chap. 13, p. 72) with the plane $s_3 = 0$. If this surface is a circular cylinder with radius $s_0/\sqrt{3}$, we see at once that Eq. (8) must be that of an ellipse.

² In Fig. 245, the points A and B correspond to states of pure tension, C and D to pure compression, E and F to states of pure shear, G and H to states of stress with two equal principal stresses, etc.

CHAPTER 28

THE THICK-WALLED TUBE UNDER INTERNAL PRESSURE

One of the simplest cases of the equilibrium of the stresses in thick-walled tubes or rings, subjected to high internal pressures, is, that in which the stresses reach the limit of plasticity in the entire tube or ring. In the following the assumption will be made that the material has a well defined limit of plasticity and that it has not been strained much above a unit elongation of some few per cent. Under these circumstances it is permissible to treat the deformations of the tube as if the stresses would be independent of the deformations, *i.e.*, independent of the unit elongations in a radial or in a tangential direction. Later, more complicated cases will be discussed, in which the tube yields only partially, so that there is a plastic region in it, surrounded by a region stressed below the limit of plasticity. In the latter portion of the tube the equations must satisfy the conditions of stress and strain of a perfectly elastic body and expressed by Hooke's generalized law. Another possible application of the theory to materials with more general stress-strain relations, including the effect of cold work, will be indicated.



FIGS. 246 AND 247.—Tube under internal pressure.

In a thick-walled cylinder stressed symmetrically with respect to its axis and uniformly along the length, no shearing stresses will be transmitted along any co-axial cylindrical surface or any plane which is perpendicular to the axis. The shearing stress components acting on these surfaces must hence vanish, and with

these latter the directions of principal stress must coincide. In the tube there acts only (1) a normal stress s_r in a radial direction, (2) a tangential normal stress s_t in a circumferential direction, and (3) a normal stress s_z parallel to the axis of the cylinder (see Figs. 246 and 247). Since everything is symmetrical with respect to the axis of the tube, all three stress components s_r , s_t , s_z are principal stresses and depend only on one independent variable, the distance r of a point P in the tube from the axis O .

Under the assumptions made above, the deformation of the tube can be determined at once. All points P along a circle of radius $r = OP$ are displaced in the direction of the radius by the same amount. These small displacements will be designated by ρ (Fig. 248). Moreover, in the case of plane strain the crosssections of the cylinder remain plane, the unit extension of the tube parallel to its axis ϵ_z is therefore constant along the tube. During the plastic flow the material will be stretched and the amount of the unit elongation in the radial and the circumferential directions will be denoted by ϵ_r and ϵ_t . The radial and tangential unit elongations (strains) are

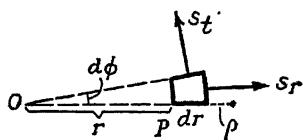


FIG. 248.—Radial and tangential stress in tube.

$$\epsilon_r = \frac{d\rho}{dr}, \quad \epsilon_t = \frac{\rho}{r}. \quad (10)$$

As the volume of any element is not changed by the plastic deformation the sum of the three unit extensions in the radial, tangential, and axial directions (ϵ_r , ϵ_t , ϵ_z) must vanish:

$$\epsilon_r + \epsilon_t + \epsilon_z = 0. \quad (11)$$

Remembering that ϵ_z must be constant and independent of r , the last condition determines completely the radial displacement ρ . Using the expressions for ϵ_r and ϵ_t given in Eq. (10), we have the following differential equation for the radial displacement ρ ,

$$\frac{d\rho}{dr} + \frac{\rho}{r} = -\epsilon_z = \text{const}, \quad (12)$$

from which

$$\rho = -\frac{\epsilon_z r}{2} + \frac{c}{r}. \quad (13)$$

In this c is an integration constant.

a. Tube under Internal Pressure Yielding without Change of Axial Length.—If the axial extension $\epsilon_z = 0$, we have seen that

one condition for the radial and tangential stress s_r and s_t is the condition of plasticity, Eq. (5) Chap. 27:

$$s_t - s_r = \pm \frac{2s_0}{\sqrt{3}} \quad (14)$$

A second equation for calculating the unknown stresses s_t , s_r is given by the condition of equilibrium of the forces acting on a small element of dimensions $r d\phi$ and dr . This condition is

$$\frac{d(rs_r)}{dr} - s_t = 0. \quad (15)$$

From this it follows that

$$r \frac{ds_r}{dr} = s_t - s_r. \quad (16)$$

Taking into account that the stress difference on the right side of this last equation according to (14) equals a constant, namely $\pm 2s_0/\sqrt{3}$, the last equation can be integrated, which gives the radial stress s_r ,

$$s_r = c_1 \pm \frac{2s_0}{\sqrt{3}} \ln r, \quad (17)$$

where \ln designates the natural logarithms, and c_1 an integration constant. In a tube with the inner radius a and the outer radius b the radial stress is

$$\begin{aligned} \text{for } r = a, \quad s_r &= -p, \\ \text{for } r = b, \quad s_r &= 0, \end{aligned}$$

if the tube is subjected to internal pressure p . In this case in Eq. (14) the upper sign must be taken and from the last condition it follows that

$$c_1 = -\frac{2s_0}{\sqrt{3}} \ln b. \quad (18)$$

Hence the radial and the tangential stress s_r and s_t in the tube are given by the formulæ

$$\begin{aligned} s_r &= -\frac{2s_0}{\sqrt{3}} \ln \frac{b}{r} \\ s_t &= \frac{2s_0}{\sqrt{3}} \left(1 - \ln \frac{b}{r} \right). \end{aligned} \quad (19)$$

The first equation determines the pressure p under which yielding in the tube is maintained. Since for $r = a$, $s_r = -p$, the pressure p will be equal to

$$p = \frac{2s_0}{\sqrt{3}} \ln \frac{b}{a}. \quad (20)$$

In this case the axial stress s_z is [see Eq. (1)] at every point of the tube equal to the average value of the radial and the tangential stresses:

$$s_z = \frac{s_r + s_t}{2} = \frac{2s_0}{\sqrt{3}} \left(\frac{1}{2} - \ln \frac{b}{r} \right) \quad (21) *$$

The stress distribution corresponding to this case in a thick-walled tube under internal pressure is given in Fig. 249, in which

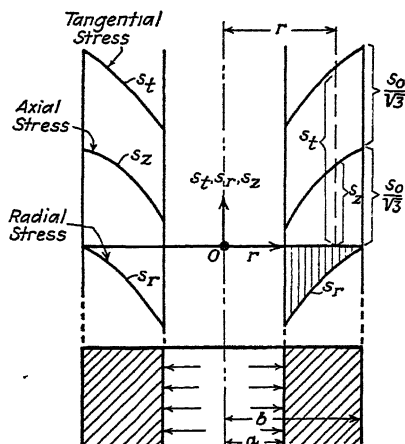


FIG. 249.—Distribution of stress in a thick-walled tube subjected to high internal pressure when entire tube yields plastically; s_0 yield stress for pure compression.

the three curves for the radial, tangential, and axial stress are shown. The three stress curves are represented by three equidistant logarithmic curves. The curves for the axial and the tangential stress s_z and s_t are obtained from the curve of the radial stress s_r by shifting the latter in the vertical direction by the amounts $s_0/\sqrt{3}$ and $2s_0/\sqrt{3}$, respectively.

b. Yielding in Thin Plate with Circular Hole or Flat Rings Radially Stressed.—A flat ring, with inner radius $r = a$ and

* We may note that if the axial extension is zero: $\epsilon_z = 0$, $\epsilon_r = -\epsilon_t$ and the radial displacement (the widening of the tube) is given by

$$\rho = \frac{c}{r}. \quad (22)$$

In this case the two smaller principal strain circles (see Mohr's circles of stress and strain, p. 43) have the same radius. According to the third law of plastic flow (see p. 75) the corresponding principal stress circles must also be equal. This is indeed the case because the axial stress s_z in the tube is at any point equal to the mean value of the two other principal stresses.

outer radius $r = b$, may be stressed by a pressure p uniformly distributed over the circumference having the radius a , and acting in the plane of the plate. The second circle $r = b$ will be assumed free. In a thin plate the principal stress which is directed normally to the plane of the plate can be taken equal to zero. Let s_z be this stress, so that $s_z = 0$. For the two unknown components of normal stress s_r and s_t we have now since $s_z = 0$ to take the condition (see Eq. (8), page 185) of plasticity in its second form:

$$s_t^2 - s_t s_r + s_r^2 = s_0^2 = \text{const}, \quad (23)$$

where s_0 is again the yield stress in pure tension. This equation together with the equilibrium condition Eq. (16):

$$r \frac{ds_r}{dr} = s_t - s_r \quad (24)$$

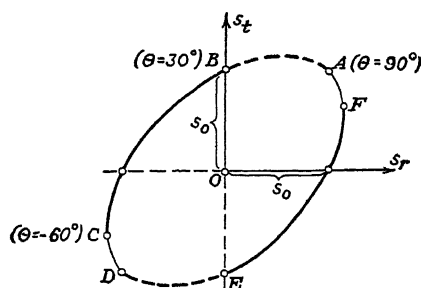


FIG. 250.—Ellipse of plasticity.

enables the determination of the unknown stress components s_r and s_t . We have already noted that Eq. (23) is the equation of an ellipse, if s_t and s_r are taken as rectangular coordinates of a point (see p. 185). The principal axes of this ellipse (Fig. 250) bisect the angle of the s_r and s_t axes and they were found equal to $A = \sqrt{2} \cdot s_0$ and $B = \sqrt{2/3} \cdot s_0$. This suggests the use, instead of s_r and s_t , of two new variables s and s' expressed by

$$\left. \begin{aligned} s &= \frac{s_t + s_r}{2} = s_0 \sin \theta, \\ s' &= \frac{s_t - s_r}{2} = \frac{s_0}{\sqrt{3}} \cos \theta. \end{aligned} \right\} \quad (25)$$

From this we see that

$$\left. \begin{aligned} s_r &= s - s' = \frac{2s_0}{\sqrt{3}} \sin \left(\theta - \frac{\pi}{6} \right) \\ s_t &= s + s' = \frac{2s_0}{\sqrt{3}} \sin \left(\theta + \frac{\pi}{6} \right) \end{aligned} \right\} \quad (26)$$

Eq. (23) when expressed in terms of s and s' takes the form

$$s^2 + 3s'^2 = s_0^2 \quad (27)$$

and is satisfied, if we introduce in it the second forms of s and s' depending on the new angular variable θ , while the equilibrium condition now takes the form

$$r \frac{d}{dr}(s - s') = 2s'. \quad (28)$$

Expressing s and s' by Eqs. (25) we get

$$r \frac{d}{dr} \sin \left(\theta - \frac{\pi}{6} \right) = \cos \theta. \quad (29)$$

This differential equation can easily be integrated by separation of the variables and the integral is

$$r^2 = \frac{c^2 e^{\sqrt{3} \theta}}{\cos \theta} \quad (30)$$

where c is an integration constant. To determine its value we have only to remember that the radial stress s_r , which in terms of θ was given by (26):

$$s_r = \frac{2s_0}{\sqrt{3}} \sin \left(\theta - \frac{\pi}{6} \right) \quad (31)$$

must vanish at the circumference $r = b$. Hence for $r = b$ θ must be chosen equal to $\theta = \theta_b = \pi/6$. To this value of θ corresponds in the ellipse, Fig. 250, the point B . If $\theta < \pi/6$, s_r will become negative and the radial stress will be a compression, on the contrary if $\theta > \pi/6$, s_r will become positive and the radial stress will be a tension. We see that evidently the former case must correspond to the case of a *ring with internal pressure* and the latter case to a *ring with external tension*.¹ Now taking $\theta_b = \pi/6$ for $r = b$, the constant c in (30) is determined by:

$$b^2 = \frac{2}{\sqrt{3}} c^2 e^{\frac{\pi\sqrt{3}}{6}} \quad (32)$$

and replacing its value in (30) we get finally:

$$r^2 = \frac{2}{\sqrt{3}} b^2 e^{\sqrt{3} \left(\theta - \frac{\pi}{6} \right)} \cdot \frac{1}{\cos \theta}. \quad (33)$$

¹ This has been shown in Fig. 250 by the full and the dotted arcs of the ellipse. The arc BC of the ellipse corresponds to the case of a ring with internal pressure and the arc AB to the case of a ring with external tension (infinite plate subjected to tension).

The radial and tangential stress are given by (26) or

$$s_r = \frac{2s_0}{\sqrt{3}} \sin \left(\theta - \frac{\pi}{6} \right) \quad (34)$$

$$s_t = \frac{2s_0}{\sqrt{3}} \sin \left(\theta + \frac{\pi}{6} \right).$$

Thus the complete solution for this case is worked out in terms of the parameter θ . To get the pressure p we have to compute

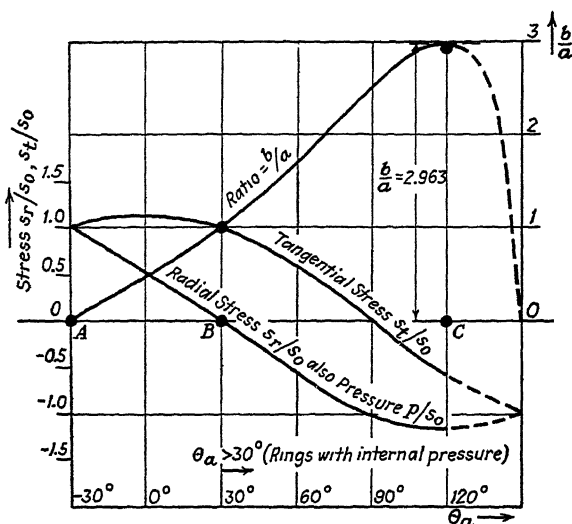


FIG. 251.—Radial and tangential stresses s_r and s_t at inner circle $r = a$ of flat rings subjected to high internal pressures p for various ratios b/a of outer to inner radius.

$\theta = \theta_a$ for $r = a$ from (33). For $r = a$ the radial stress $s_r = -p$ and hence the pressure p is given by

$$p = \frac{2s_0}{\sqrt{3}} \sin \left(\frac{\pi}{6} - \theta_a \right). \quad (35)$$

To each value of θ_a corresponds a value of the ratio b/a and a radial and tangential stress. Thus b/a , s_r , s_t are given as functions of the parameter θ_a . This has been shown in Fig. 251, where the ratio b/a and the radial and tangential stress at the inner circle $r = a$ are represented by the corresponding curve. To find the pressure p for a given ring we have to read the value of s_r (or p) below the value of the given ratio b/a of the outer to the inner radius.

The distribution of stress is also shown in Fig. 252, where the radial and the tangential stress s_r and s_t are plotted as functions of the radial distance r of a point of the ring from its center.

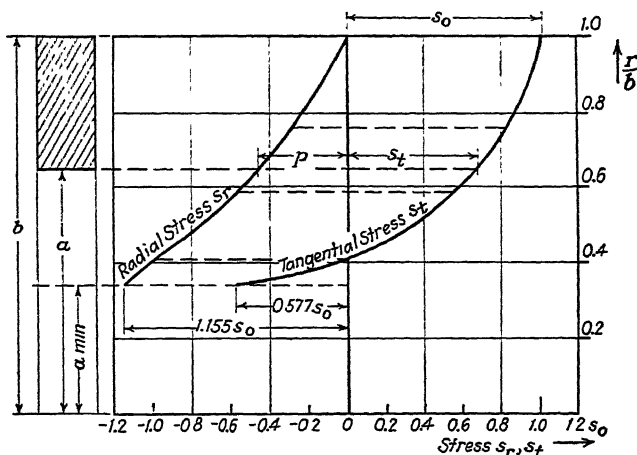


FIG. 252.—Distribution of radial and tangential stresses s_r and s_t in flat rings subjected to internal pressure p : r variable radius, a inner radius, b outer radius, s_0 yield stress in tension.

Figures 251 and 252 and the formulæ (34) show a remarkable fact. Comparing the shape of the stress curve in the two cases a ($\epsilon_2 = 0$) and b ($s_2 = 0$), which have been worked out above and which are shown in Figs. 249 and 252, respectively, we observe that in case a (thick-walled

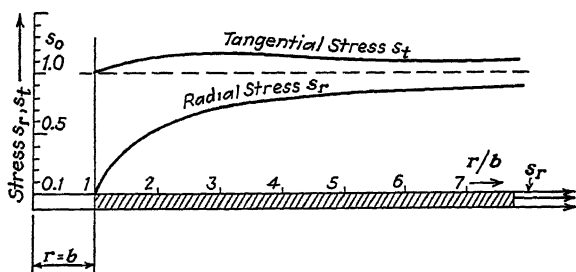


FIG. 253.—Distribution of stresses in plate having hole yielding under radial tension.

tube of infinite length and having no axial extension or contraction) the pressure p increases indefinitely with decreasing inner radius a . This is obvious. In the case of a flat ring, bounded by two concentric circles $r = b$ and $r = a$ and subjected to a uniform radial pressure p on the inner

circle $r = a$ (case b), however, the pressure p can never exceed a certain amount, i.e., $p_{\max} = 2s_0/\sqrt{3} = 1.155s_0$, where s_0 is the yield stress in tension. Moreover, equilibrium of the stresses in the plastic state in case b is only possible in flat rings under internal pressure with a ratio

$$1 < \frac{b}{a} < 2.963.$$

For $b/a > 2.963$ no completely plastic equilibrium corresponding to the equations is possible in a flat ring subjected to internal pressure. This follows from the fact that in a flat ring where $s_z = 0$ the stress components s_r and s_t must be the coordinates of the "ellipse of plasticity," Fig. 250, and, therefore, never can exceed the value $1.155s_0$.

It is perhaps noteworthy to draw another conclusion from the formulæ (34). They contain evidently also the case of plastic equilibrium of an infinite plate stressed uniformly in its plane in all directions and having a circular hole. This case results simply by choosing for θ the interval $30^\circ < \theta < +90^\circ$. The stress distribution is shown in Fig. 253.

c. Comparison of Both Cases with That of a Perfectly Elastic Tube.—This behavior of the plastic equilibrium of stresses in tubes or in flat rings stressed radially will now be compared with the well-known elastic distribution of stresses in such bodies, if stressed below the limit of plasticity. The distribution of the radial and tangential stress in a perfectly elastic material is in both cases (a and b) the same and given by

$$\begin{aligned} s_r &= \frac{pa^2}{b^2 - a^2} \left(1 - \frac{b^2}{r^2} \right), \\ s_t &= \frac{pa^2}{b^2 - a^2} \left(1 + \frac{b^2}{r^2} \right). \end{aligned} \quad (36)$$

Let the ratio of the inner to outer radius of the tube be chosen for example $a/b = 0.4$. For this case the stresses s_r , s_t in a perfectly elastic thick-walled tube are shown in Fig. 254, just when the limit of plasticity has been reached at the inner surface $r = a$ of the tube. At this moment the difference of the stresses s_t and s_r for $r = a$ must become equal $2s_0/\sqrt{3}$ and hence the pressure p_0 required for first yielding in a thick-walled tube is found from

$$(s_t - s_r)_{r=a} = \frac{2b^2 p_0}{b^2 - a^2}, \quad p_0 = \left(1 - \frac{a^2}{b^2} \right) \frac{s_0}{\sqrt{3}}. \quad (37)$$

If $a/b = 0.4$, $p_0 = 0.485s_0$.

In the next Fig. 255 is shown the plastic distribution of stress in a thick-walled cylinder, constrained not to expand or

contract in axial direction for case a ($\epsilon_z = 0$) for the same ratio $a/b = 0.4$. This requires a pressure

$$p = \frac{2s_0}{\sqrt{3}} \ln \frac{b}{a} \quad (38)$$

which is for $a/b = 0.4$:

$$p = 1.057s_0.$$

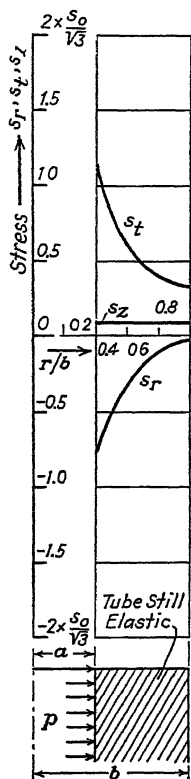


FIG. 254.

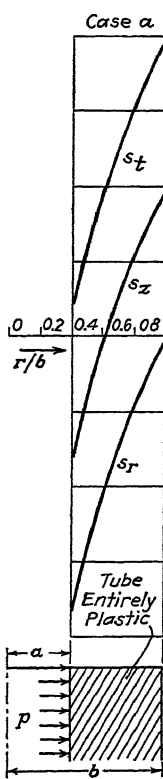


FIG. 255.

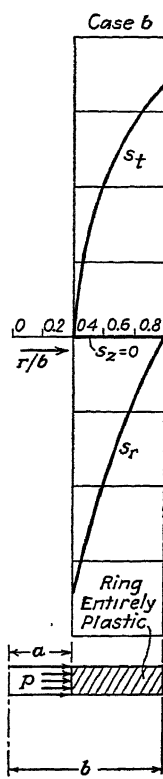


FIG. 256.

FIGS. 254, 255, and 256.—Distribution of stresses in thick-walled tubes and flat ring subjected to high internal pressure p . Radial, tangential and axial stresses s_r , s_t , s_z . Figure 254, when tube still elastic and first yielding starts. Figure 255, when tube is entirely in plastic state. Figure 256, stresses in a flat ring entirely in plastic state.

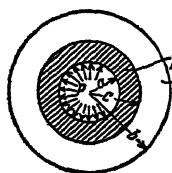
Finally in a flat ring with the same ratio b/a stressed radially, the pressure required to produce plastic flow in the entire ring is found approximately to be:

$$p = 1.00s_0. \quad (39)$$

The stress distribution in a flat ring is shown in Fig. 256.

Summing up the preceding we may conclude that while the distribution of radial and tangential stress in a perfectly elastic material is the same in either a long tube or a flat ring both having the same ratio b/a of the outer to the inner radius, this changes completely if plasticity is considered. The radial distribution of stress under plastic equilibrium in a thick-walled cylinder subjected to internal pressure is given (1) in the case a of a tube which does not stretch in an axial direction ($\epsilon_z = 0$) by the logarithmic functions Eqs. (19) and (2) in the case b of a flat ring ($s_z = 0$) by the trigonometric functions Eqs. (34).

d. **Partial Yielding in a Thick-walled Tube.**—If the pressure p in the tube is gradually increased from zero the tube will be stressed only elastically at first. We have seen before that in a tube which cannot expand in the axial direction ($\epsilon_z = 0$) the first yield will occur at a pressure



$$p_0 = \left(1 - \frac{a^2}{b^2}\right) \frac{s_0}{\sqrt{3}} \quad (40)$$

FIG. 257.—Partial yielding in thick-walled tube.

under which the limit of plasticity is reached at the inner surface $r = a$ of the tube. If $p > p_0$, considering a cross-section of the tube, a ring-shaped plastic region will begin to penetrate into the tube. In the outermost ring-shaped area of the cross-section, extending from an intermediate radius $r = c$ to $r = b$, an elastic state of stress will exist. If $\epsilon_z = 0$ the elastic stress distribution in this portion of the tube is given by the well-known formulæ:

$$\begin{aligned} s_r' &= c_1 + \frac{c_2}{r^2}, \\ s_t' &= c_1 - \frac{c_2}{r^2}, \quad (c \leq r \leq b), \\ s_z' &= \nu(s_r' + s_t') = 2\nu c_1, \end{aligned} \quad (41)$$

where c_1, c_2 are constants and ν is Poisson's ratio.¹

Within the ring area $a < r < c$ (Fig. 257) a plastically stressed portion will exist extending from $r = a$ to $r = c$. The stresses in the plastic ring have been calculated before and are given according to Section a page 188, Eqs. (14), (17) and (21):

$$\begin{aligned} s_r &= c_3 + s^* \ln r, \\ s_t &= c_3 + s^* (\ln r + 1), \quad (a \leq r \leq c) \\ s_z &= c_3 + s^* (\ln r + \frac{1}{2}), \end{aligned} \quad (42)$$

¹ See TIMOSHENKO, S., and J. M. LESSLETS, "Applied Elasticity," p. 249; TIMOSHENKO, "Strength of Materials," Part II, p. 528. Van Nostrand Co., New York.

where s^* stands now for

$$s^* = \frac{2s_0}{\sqrt{3}} \quad (43)$$

and s_0 is the yield stress in pure tension and c_3 a constant.

To find the three constants c_1 , c_2 , c_3 three conditions may be prescribed, *i.e.*, that:

$$r = b, \quad s_r' = 0; \quad r = c, \quad s_r = s_r', \quad s_t = s_t'. \quad (44)$$

By the first, the condition is expressed that the outer surface of the tube $r = b$ is free; the two others express the condition of continuity at the boundary of the plastic region $r = c$. It is easy to satisfy these three conditions. We take:

$$u = \frac{r}{b}, \quad \alpha = \frac{a}{b}, \quad \gamma = \frac{c}{b}. \quad (45)$$

Then the result of the computation can be expressed by the formulæ:

$$\text{in elastic portion } c < r < b \quad \begin{cases} s_r' = -\frac{s^*}{2} \cdot \gamma^2 \left(\frac{1}{u^2} - 1 \right) \\ s_t' = \frac{s^*}{2} \cdot \gamma^2 \left(\frac{1}{u^2} + 1 \right) \\ s_z' = s^* \cdot \nu \gamma^2 \end{cases} \quad (46)$$

$$\text{in plastic portion } a < r < c \quad \begin{cases} s_r = -p + s^* \ln \frac{u}{\alpha}, \\ s_t = -p + s^* \left(\ln \frac{u}{\alpha} + 1 \right), \\ s_z = -p + s^* \left(\ln \frac{u}{\alpha} + \frac{1}{2} \right), \end{cases} \quad (47)$$

$$\text{where } s^* = \frac{2s_0}{\sqrt{3}} \quad (48)$$

and the pressure p required to produce yielding in the tube to the radius $r = c$ is found by

$$p = \frac{s_0}{\sqrt{3}} \left(2 \ln \frac{\gamma}{\alpha} + 1 - \gamma^2 \right), \quad (49)$$

where s_0 is the yield stress in pure tension.

In Fig. 258 the stress distributions in a thick hollow cylinder under internal pressure are shown for the case $a/b = 0.4$ and for four different values of the pressure p . From this figure it can be seen how the stresses vary if the pressure increases and yielding gradually starts from the inner surface. The upper curves show the distribution of the tangential stresses s_t and the lower curves that of the radial stresses s_r for $c = 0.4, 0.6, 0.8$ and $1.0b$. The thin curves are the axial stresses s_z .

In a second Fig. 259 the pressures p required to produce progressive yielding in thick hollow cylinders are plotted for 10

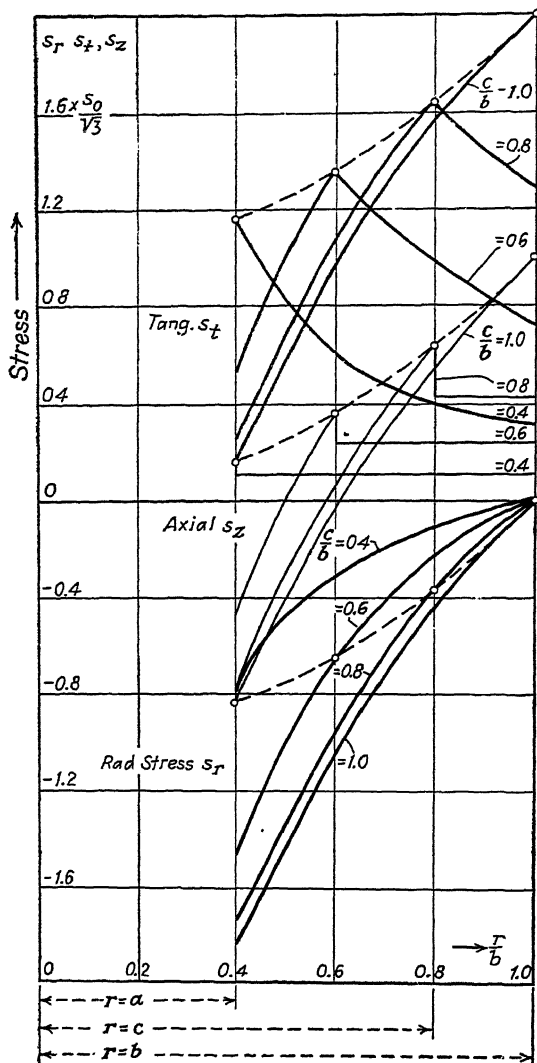


FIG. 258.—Partial yielding in thick-walled tube subjected to internal pressure p . Curves indicate distribution of radial, tangential and axial stresses s_r , s_t , s_z when $c:b = 1, 0.8, 0.6, 0.4$; a inner, b outer, r variable radius, c radius of outer boundary of plastic region.

different ratios of $\alpha = a/b = 0.1, 0.2, \dots 1$. The abscissæ in this figure (Fig. 259) are $\gamma = c/b$, the ordinates are the pressures

p . For example the curve belonging to $\alpha = 0.8$ shows how the pressure p in a tube of the ratio α of the inner to the outer radius

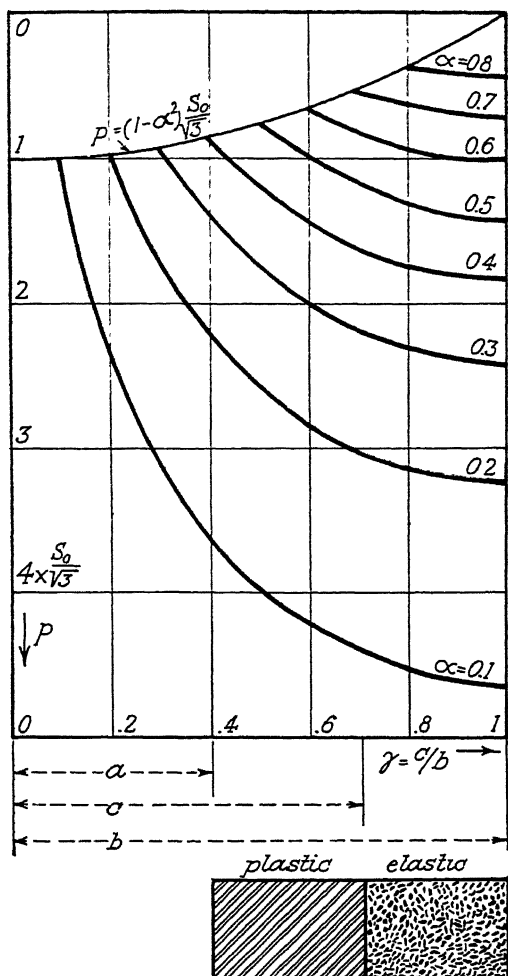


FIG. 259.—Partial yielding in tubes. Curves indicate how pressures p would increase in thick-walled tubes with outer radius c of plastic region. The pressure curves are plotted for 10 different ratios of $\alpha = a/b$ of inner to outer radius of tube.

$a/b = 0.8$ would increase with the increasing radius c of the cylindrical surface to which yielding has penetrated in the tube.

As a further example the case of a long cylindrical cavity in an infinite elastic body might be mentioned (Fig. 260), assum-

ing that in the hole of radius a a pressure p acts. If yielding has penetrated to the depth $r = c$ the stresses will be:

$$\text{in the plastic region } r < c. \quad \begin{cases} s_r = -\frac{s_0}{\sqrt{3}} \left(1 + 2 \ln \frac{c}{r} \right), \\ s_t = \frac{s_0}{\sqrt{3}} \left(1 - 2 \ln \frac{c}{r} \right), \\ s_z = -\frac{2s_0}{\sqrt{3}} \ln \frac{c}{r}; \end{cases} \quad (50)$$

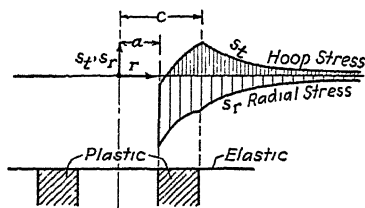


FIG. 260.—Yielding around a cylindrical cavity in infinite elastic body under internal pressure.

the pressure p will be equal to

$$p = \frac{s_0}{\sqrt{3}} \left(1 + 2 \ln \frac{c}{a} \right) \quad (51)$$

and in the outer, elastic region $c < r$

$$s_r = -s_t = -\frac{s_0}{\sqrt{3}} \cdot \frac{c^2}{r^2}, \quad s_z = 0. \quad (52)$$

In both regions the radial displacement is given by

$$\rho = \frac{(1 + \nu)s_0}{\sqrt{3}E} \cdot \frac{c^2}{r}. \quad (53)$$

CHAPTER 29

PLASTIC FLOW IN HOLLOW CYLINDER FOR ARBITRARY LAW OF DEFORMATION CONSIDERING WORK HARDENING

Until now all cases have been treated under the assumption that the yield stress was not dependent on the amount of plastic deformation. We have seen that this assumption was a good approximation of the facts observed on such ductile metals as mild steel which have (1) a well-marked yield point, and (2) begin to deform in the plastic region under a nearly constant stress.

It can be shown, that the case of plastic flow in a thick-walled tube under high internal pressure can also be treated under more general assumptions regarding the law of plastic deformation provided only that the tube does not expand or contract in the axial direction.

Assuming that the unit elongation parallel to the axis of the cylinder $\epsilon_z = 0$, we see that the two other unit extensions ϵ_r and ϵ_t must be equal and have opposite signs:

$$\epsilon_r = -\epsilon_t, \quad \text{since } \epsilon_r + \epsilon_t + \epsilon_z = 0. \quad (1)$$

A consequence of this is that the radial displacement ρ of a point at the distance r must be equal (see Eq. (13), page 187) to:

$$\rho = \frac{c}{r}, \quad (2)$$

where c is a constant,¹ and hence the tangential extension ϵ_t must be $\epsilon_t = \rho/r = c/r^2$. If $\epsilon_r = -\epsilon_t$, the rule of plastic flow requires that the axial normal stress shall become equal to the average value of the two other normal stresses:²

$$s_z = \frac{s_r + s_t}{2}. \quad (3)$$

¹ The constant c has evidently the value $\rho_a a$ if ρ_a designates the radial displacement at the radius $r = a$.

² Otherwise the figure of the three principal circles in Mohr's stress diagram would not be similar to the figure of the three principal circles of strain.

Under these circumstances the state of strain in every element of the tube is a pure shear. At a distance r from the axis of the tube this unit shear must be

$$\gamma = \epsilon_t - \epsilon_r = 2\epsilon_t = \frac{2c}{r^2}. \quad (4)$$

Evidently all the small elements of the tube are deformed in a similar manner as are the elements in a solid cylinder under the action of a twisting moment as described in Chap. 18. The only difference is that the shear in the tube under internal pressure has now a different direction from that in the cylinder under torsion. It is easy to see that the stresses in the tube can be determined if the stress-strain diagram of the material in pure shear is known. This latter could, for example, be determined by an ordinary torsion test with a bar of circular cross-section as shown in Chap. 18. Let the law of plastic deformation in pure shear be given by a function:

$$s_s = f(\gamma), \quad (5)$$

where s_s is the maximum shearing stress and γ the unit shear. For a hollow cylinder stressed by an internal pressure p , the maximum shearing stress is given by

$$s_s = \frac{s_t - s_r}{2} \quad (6)$$

and the unit shear γ given by

$$\gamma = \epsilon_t - \epsilon_r = \frac{2c}{r^2}. \quad (7)$$

These two expressions have then to be combined with the condition of equilibrium of the stresses, or

$$\frac{ds_r}{dr} = \frac{s_t - s_r}{r}. \quad (8)$$

Integrating this expression between the limits r and b and taking into consideration that the radial stress s_r must vanish for $r = b$, the radial stress is found to be

$$-s_r = \int_r^b \frac{s_t - s_r}{r} dr. \quad (9)$$

Replacing here the variable r by the variable γ using (6) and (7):

$$\frac{dr}{r} = -\frac{d\gamma}{2\gamma}, \quad s_t - s_r = 2s = 2f(\gamma), \quad (10)$$

the radial and the tangential stresses are found to be

$$s_r = - \int_{\gamma_b}^{\gamma} f \gamma \frac{d\gamma}{\gamma} \quad (11)$$

$$s_t = 2f(\gamma) - \int_{\gamma_b}^{\gamma} f' \gamma \frac{d\gamma}{\gamma}. \quad (12)$$

The lower limit in this integral γ_b designates the value of γ for $r = b$ or $\gamma_b = 2c/b^2$.

Since for $r = a$ the radial stress $s_r = -p$, from the last equation for s_r , the pressure p under which the whole tube will yield can be calculated. It is given by the integral:

$$p = \int_{\gamma_b}^{\gamma_a} f(\gamma) \frac{d\gamma}{\gamma}. \quad (13)$$

The limits of this integral are,

$$\gamma_a = \frac{b^2}{a^2} \gamma_b \text{ and } \gamma_b. \quad (14)$$

So far none of the above expressions contain any assumptions with regard to the special form of stress-strain diagram of a material in pure shear, and they can therefore be used for any material. We can also try to employ some analytical expression for this function and to calculate the corresponding stresses, if such a function can readily be established.¹

On the other hand, if the stress-strain diagram of a material in pure shear is known and has, for example, been observed by means of a torsion test, all the expressions given above can be calculated by graphical integration.

If a torsion diagram is not available, but a stress-strain diagram, taken by an ordinary tensile test, has been determined, we may also use the latter for the construction of a diagram in torsion.

a. Yielding of a Die-cast Aluminum Tube.—Such an example of an experimentally determined tensile stress-strain curve is shown in Fig. 261 for die-cast aluminum. Provided that we restrain all deformation to small amounts such as in the part of a tensile diagram given in Fig. 261, we may

¹ For example, if the stress-strain diagram in pure shear can be approximated by means of a power function

$$s_s = s_0 \left(\frac{\gamma}{\gamma_0} \right)^{\frac{m}{2}}, \quad (15)$$

the radial and tangential stresses will be given by the expressions:

$$s_r = - \frac{pb^m}{a^m - b^m} \left(\frac{a^m}{r^m} - 1 \right), \quad s_t = \frac{pb^m}{a^m - b^m} \left[(m-1) \frac{a^m}{r^m} + 1 \right]. \quad (16)$$

The exponent m must be taken $0 < m < 2$.

construct from the plastic tensile diagram of a material the diagram of pure shear as follows. If s is the tensile stress in a tensile diagram which corresponds to a unit elongation ϵ and s_s is the shearing stress in the diagram for pure shear which corresponds to a unit shear γ then

$$s = F(\epsilon) \quad (17)$$

is the tensile diagram and

$$s_s = f(\gamma) \quad (18)$$

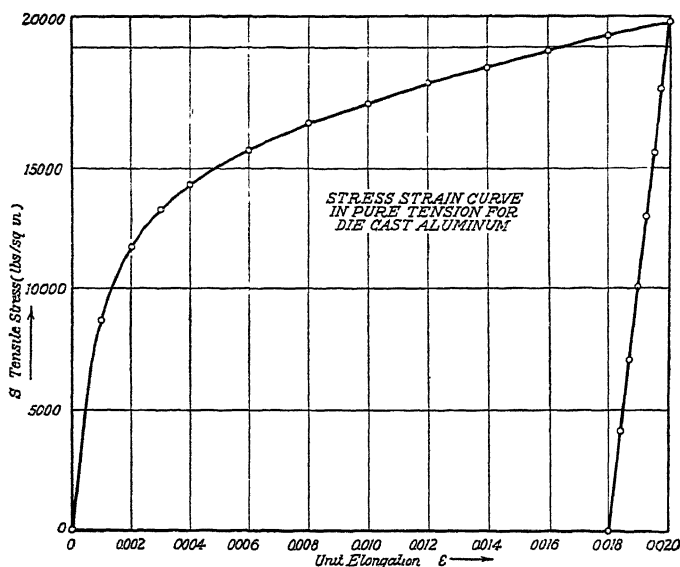


FIG. 261.—Tensile diagram for die-cast aluminum.

is the diagram in pure shear. To find the second diagram assuming that the shape of the curve $F(\epsilon)$ in the first is known, we have to multiply all abscissæ¹ ϵ by $\frac{3}{2}$ and to divide all ordinates² s by $\sqrt{3}$ taking thus:

$$\gamma = \frac{3\epsilon}{2} \quad \text{and} \quad s_s = \frac{s_t}{\sqrt{3}} \quad (19)$$

in the diagram for pure shear as the point corresponding to a point ϵ , s of the tensile stress-strain curve. This has been done in Fig. 262. Figure

¹ In the pure plastic deformation during a tensile test the specimen extends by ϵ_1 longitudinally and contracts by $\epsilon_2 = -\epsilon_1/2$ in the lateral direction, hence the maximum unit shear in pure plastic tension is given by

$$\gamma = \epsilon_1 - \epsilon_2 = \frac{3\epsilon_1}{2}.$$

² The yield stress in pure shear is = the yield stress in pure tension times $1/\sqrt{3}$. (Compare Chap. 13, p. 74.)

261 shows the original tensile diagram as experimentally observed. From this the diagram in pure shear was constructed (Fig. 262).¹ In Fig. 263 the distribution of stress in a die-cast aluminum tube, subjected to plastic flow under the action of an internal pressure p and having a ratio of inner to outer radius $a/b = 0.6$, is given as determined by the formulae from the

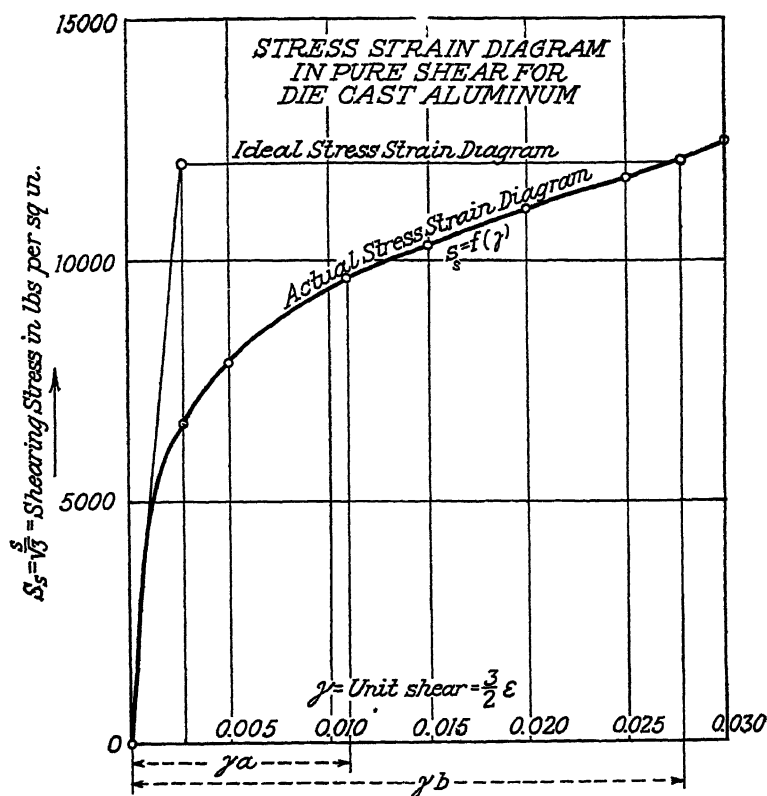


FIG. 262.—Diagram for pure shear for die-cast aluminum constructed from tensile diagram shown in Fig. 261.

diagram Fig. 262. The tube is shown with the stress distribution under an internal pressure of about

$$p = 10,600 \text{ lb./sq. in.}$$

In the same figure three other curves for the stresses s_r , s_t , s_z are shown in thinner lines. These curves represent an ideal stress distribution which would be obtained if the stress-strain characteristic of the material would

¹ The author is indebted to H. Friedman of Boston for having carried out the graphic integrations required for the determination of the stresses in the tube.

not follow the law used above, but would consist of an ideal diagram consisting of two straight lines (these lines are also drawn in the shear diagram, Fig. 262). It can be seen from the comparison of both sets of curves in Fig. 263 that the character of the curves of the stress distribution is not greatly changed by replacing the actual stress-strain curve as observed in test with

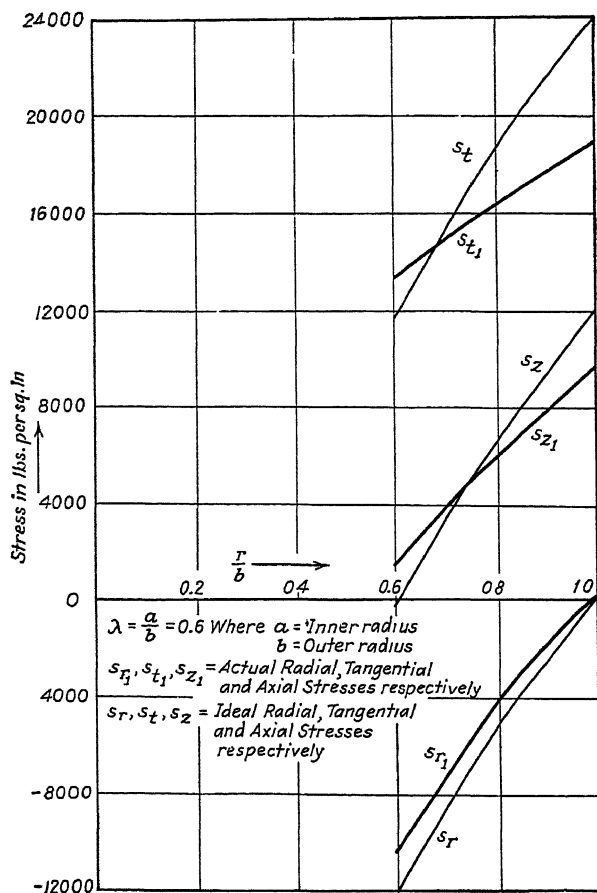


FIG. 263.—Distribution of radial, tangential and axial stresses in hollow tube of die-cast aluminum subjected to internal pressure under plastic equilibrium.

a ductile metal (such as die-cast aluminum which shows a work hardening effect) by an ideal stress-strain diagram consisting of two straight lines. The tangential stresses s_t in the outer portion of the tube are considerably smaller, if the material has a stress-strain curve as represented in Fig. 262

than the stresses derived from an ideal stress-strain curve with a well-defined yield stress such as shown with the two straight lines in the same figure.

b. Similarity of Three Stress Distributions under General Law of Plastic Deformation. 1. *Plastic Torsion of Bar with Circular Cross-section.*—Let

$$s = f(\gamma) \quad (20)$$

be the stress-strain diagram of the material in pure shear, θ be the angle of twist per unit of length, a the radius of the bar. Then the twisting moment producing a maximum unit shear γ_a at the extreme fiber is

$$M = \frac{2\pi}{\theta^2} \int_0^{\gamma_a} f(\gamma) \gamma^2 d\gamma \quad (21)$$

where the upper limit of the integral is $\gamma_a = \epsilon a$. (Cf. Chap. 18.)

2. *Pure Plastic Bending of Bar with Rectangular Cross-section.*—If the material has a stress-strain diagram in pure tension which is identical with that for compression:

$$s = F(\epsilon) \quad (22)$$

and ρ is the radius of curvature of the elastic line of the bar, then the bending moment M is found by

$$M = 2b\rho^2 \int_0^{\epsilon_a} F(\epsilon) \epsilon d\epsilon, \quad (23)$$

where b designates the width of the bar and ϵ_a the unit elongation in the extreme fiber. (Cf. Chap. 23.)

3. *Tube under Internal Pressure without Axial Expansion.*—If the material has the stress-strain diagram in pure shear

$$s = f(\gamma), \quad (24)$$

the pressure p in the tube is given by

$$p = \int_{\gamma_a}^{\gamma_b} f(\gamma) \frac{d\gamma}{\gamma}, \quad (25)$$

where γ_a and γ_b are the unit shears at the extreme fibers $r = a$ and $r = b$.

CHAPTER 30

DISTRIBUTION OF STRESS IN ROTATING CYLINDERS AND DISCS

The theory of the distribution of stress in rotating cylinders or in rapidly revolving discs after the yield point has been reached is very similar to that of the stress distribution in a thick-walled tube or flat rings treated in the preceding chapters. That such questions have practical importance is indicated by the fact that engineers have long found it necessary to specify a high degree of ductility in the materials used for machine elements such as the rapidly revolving discs or heavy spindles of steam turbines or the heavy cylindrical rotors of large turbo-generators, which are mainly stressed by the centrifugal forces. In overspeed tests of such highly stressed cylinders or discs the yield point of the material may be reached or passed in certain portions of the discs. As A. Stodola mentions,¹ attempts have been made to improve the stress distribution in rotating discs with a central hole by running them during manufacture at a speed such that the inner part of the disc is permanently stretched. This question has also been considered by H. Hencky, F. László, and others.² Therefore it will be perhaps useful to work out in what follows some of the simplest cases of plastic flow in rotating cylinders or discs.

a. Rotating Cylinder under Plane Strain.—In this case the unit elongation in the direction parallel to the axis of the cylinder $\epsilon_z = \text{constant}$ and the case which was worked out on page 187 applies. Hence the radial displacement ρ is given by

$$\rho = -\frac{\epsilon_z r^2}{2} + \frac{c_1}{r}. \quad (1)$$

Now in a *solid cylinder*, which case will be treated first, the constant c_1 must be chosen equal to zero: $c_1 = 0$. In a solid

¹ "Steam and Gas Turbines," Eng. ed., LOEWENSTEIN, L. C., vol. 2, p. 1080, McGraw-Hill Book Company, Inc., New York.

² See a paper by L. H. DONNELL and the author in *Trans. Amer. Soc. Mech. Eng.*, 1928, on Rotating Discs, where a bibliography on this subject can be found.

cylinder the radial displacement ρ and the tangential and radial strains ϵ_t and ϵ_r must be

$$\rho = -\frac{\epsilon_z r}{2}, \quad \epsilon_t = \frac{\rho}{r} = -\frac{\epsilon_z}{2} \quad (2), (3)$$

$$\epsilon_r = \frac{d\rho}{dr} = -\frac{\epsilon_z}{2}. \quad (4)$$

We see that in a solid rotating cylinder in the plastic state, the deformation in each element is practically the same. It consists evidently of a unit elongation $\epsilon_z = \text{const.}$ parallel to the axis of the cylinder which is a uniform contraction and negative, accompanied by a lateral elongation of half of this amount and equal in all directions perpendicular to the axis of rotation which will be therefore a uniform expansion in the radial direction.

According to the rule of plastic flow, we see at once that since $\epsilon_r = \epsilon_t$, also at every point the radial and tangential stresses must be equal:

$$s_r = s_t, \quad (5)$$

as otherwise the figure of Mohr's principal stress circles would not remain geometrically similar to that of the principal strain circles (see page 75). The condition of plasticity

$$(s_r - s_t)^2 + (s_t - s_z)^2 + (s_z - s_r)^2 = 2s_0^2 \quad (6)$$

becomes therefore simply

$$s_t - s_z = \pm s_0 = \text{const.}, \quad (7)$$

where s_0 is the yield stress in pure tension. In the condition of equilibrium an additional term must be introduced to take into account the action of the centrifugal forces. Let ω be the angular velocity of the cylinder, λ the specific weight of the material (weight in lb. per cubic inch) g the acceleration of gravity, and a the radius of the cylinder. Then

$$\frac{ds_r}{dr} = \frac{s_t - s_r}{r} - \frac{\lambda \omega^2}{g} \cdot r \quad (8)$$

According to Eq. (5), the first term on the right side of this equation is now zero and the equation of equilibrium takes the simple form

$$\frac{ds_r}{dr} = -\frac{\lambda \omega^2}{g} \cdot r, \quad (9)$$

whence by integration:

$$s_r = \frac{\lambda \omega^2}{2g} (a^2 - r^2) \quad (10)$$

using here the condition that for $r = a$, $s_r = 0$. The tangential stress s_t is according to Eq. (5) equal to s_r .

According to Eq. (7) two distinct cases may be obtained, depending on whether the upper or the lower sign is taken. Taking the upper sign, the axial stress is given by

$$s_z = s_t - s_0. \quad (11)$$

In a freely rotating cylinder, which can contract freely in an axial direction the resultant of the axial stresses s_z

$$2\pi \int_0^a s_z r dr = 0 \quad (12)$$

should become zero. From this condition the peripheral speed $u = a\omega$ is found under which the entire cylinder will yield:

$$u = a\omega = 2\sqrt{\frac{s_0 g}{\lambda}}. \quad (13)$$

Now the peripheral speed u_0 of a free ring of small cross-section rotating with a uniform angular velocity and stressed to a stress s_0 is given by the expression

$$u_0 = \sqrt{\frac{s_0 g}{\lambda}} \quad (14)$$

and this is the speed under which in a free ring the yield stress s_0 will just be reached. Hence

$$u = 2u_0. \quad (15)$$

The distribution of stress under which the whole rotating cylinder becomes plastic is finally given by the set of formulæ

$$\text{radial and tangential stress} \dots s_r = s_t = 2s_0 \left(1 - \frac{r^2}{a^2}\right) \quad (16)$$

$$\text{axial stress} \dots s_z = s_0 \left(1 - 2\frac{r^2}{a^2}\right). \quad (17)$$

The central part of the cylinder receives tensile and the region near the periphery compressive stresses in the axial direction, but the action of the former balances that of the latter, so that no resultant axial force is acting.

b. Comparison with Elastic Rotating Cylinder.—In free, solid cylinders of an elastic material of radius a rotating with an angular velocity ω or with a peripheral velocity $u' = a\omega$ the stresses are, according to the theory of elasticity, given by

$$\left. \begin{aligned} s_r &= \frac{(3-2\nu)s}{8(1-\nu)} \cdot \left(1 - \frac{r^2}{a^2}\right) \\ s_t &= \frac{s}{8(1-\nu)} \left[3 - 2\nu - (1+2\nu)\frac{r^2}{a^2}\right] \\ s_z &= \frac{\nu s}{4(1-\nu)} \cdot \left(1 - 2\frac{r^2}{a^2}\right) \end{aligned} \right\} \quad (18)$$

where ν is Poisson's ratio and s stands for the constant:

$$s = \frac{\lambda \omega^2 a^2}{g} = s_0 \frac{u'^2}{u_0^2} \quad (19)$$

For steel, for example, if $\nu = \frac{1}{3}$, the stresses at the center of the cylinder are:

$$r = 0, \quad s_r = s_t = 0.437s, \quad s_z = 0.125s \quad (20)$$

and at the periphery of the cylinder

$$r = a, \quad s_r = 0, \quad s_t = 0.125s, \quad s_z = -0.125s, \quad (21)$$

and first yield will occur at the center $r = 0$ of a steel cylinder when at this point

$$s_t - s_z = \frac{(3 - 4\nu)s}{8(1 - \nu)} = s_0, \quad s = 3.20s_0. \quad (22)$$

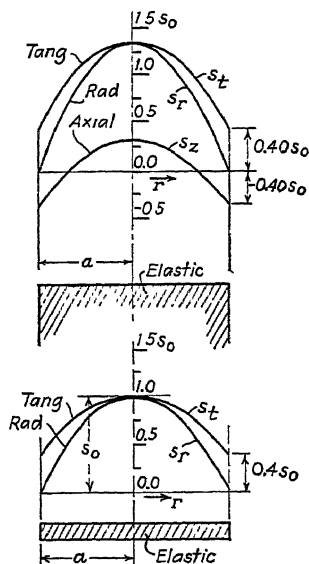
Hence a solid rotating steel cylinder of radius a will start to yield at the center if the peripheral velocity u' is equal to

$$u' = u_0 \sqrt{\frac{s}{s_0}} = 2u_0 \sqrt{\frac{2(1 - \nu)}{3 - 4\nu}} = 1.789u_0. \quad (23)$$

Above we found that the whole cylinder becomes plastic at a speed $u = 2u_0$. Comparing u with u' it is seen that from the moment at which the first yield occurs, an increase of speed of about 12 per cent will bring the entire cylinder into the plastic state. The plastic region, therefore, spreads comparatively rapidly with changing speed, and an increase of only 12 per cent suffices to obtain plastic deformation in the entire cylinder, provided its material follows the law of deformation which was assumed, i.e., that the material yields under a constant stress s_0 in pure tension.

The stress distributions in these two cases—for first yielding and for complete yielding—are shown in the Figs. 264 and 266.

We may mention, that the case of a hollow rotating plastic cylinder can also be worked out completely without difficulty, but the expressions for the stresses become slightly more complicated.



FIGS. 264 and 265.—Elastic equilibrium. Stresses in rotating cylinder and disc just when first yielding starts.

c. **Rotating Disc.**—In a rotating disc having a uniform thickness, which is a comparatively small fraction of its diameter, the approximate value of the stresses can very easily be found in the cases of both partial and complete yielding. As in this case one principal stress, namely s_z vanishes throughout the disc, the two other principal stresses in the plastic region must satisfy the condition Eq. (8), Chap. 27, and must also be the rectangular coordinates of an ellipse. Now in a disc stretched by centrifugal forces both stresses s_r and s_t will be tensile stresses and as the tangential stress always remains the larger, we may replace the arc of the ellipse expressing the condition of plasticity used before (see Eq. (23), page 190, and the arc of the ellipse in Fig. 250 between A and B) simply by a horizontal line. The condition of plasticity will therefore be expressed with sufficient approximation by

$$s_t = c = \text{const.} \quad (24)$$

As the value of the constant c we may take either the average value of the yield stress s_0 in pure tension (which is the ordinate of point B in Fig. 250, page 190) and of the maximum possible ordinate of the ellipse (which is $= 2s_0\sqrt{3} = 1.155s_0$) by taking

$$s_t = c = \left(\frac{1}{2} + \frac{1}{\sqrt{3}}\right)s_0 = 1.077s_0 \quad (25)$$

or we may use the theory of maximum shear, according to which s_t also should be chosen equal to the constant:

$$s_t = s_0 = \text{const.} \quad (26)$$

(We see that the above approximate value of the constant c differs by 8 per cent from the value obtained from using the theory of maximum shear.)

1. *Solid Disc.*—In the case of a partially plastic solid rotating disc of radius a we have an outer elastic portion and an inner plastic region.

As long as the stresses are below the yield point they are given by the expressions derived from the theory of elasticity, namely

$$\left. \begin{aligned} s_r &= \frac{(3 + \nu)s}{8} \left(1 - \frac{r^2}{a^2}\right), \\ s_t &= \frac{s}{8} \left[3 + \nu - (1 + 3\nu)\frac{r^2}{a^2}\right], \end{aligned} \right\} \quad (27)$$

$$s_z = 0, \quad (28)$$

where again ν denotes Poisson's ratio and s stands for the constant

$$s = \frac{\lambda \omega^2 r^2}{g} = s_0 \frac{u'^2}{u_0^2} \quad (29)$$

(u' peripheral speed of disc, u_0 speed of free rotating ring, which yields under stress s_c).

The disk yields first at its center $r = a$, at a peripheral speed u' found by equating s_t for $r = 0$ to s_0 .

This gives

$$s = \frac{8s_0}{3 + \nu} \text{ and } u' = u_0 \sqrt{\frac{s}{s_0}} = u_0 \sqrt{\frac{8}{3 + \nu}} = 1.56u_0. \quad (30)$$

If $u' > 1.56 u_0$ there will be an elastic portion extending from a radius $r = c$ to $r = a$ in which the stresses will be equal to:

$$\left. \begin{aligned} s_r' &= -\frac{(3 + \nu)s}{8} \cdot \frac{r^2}{a^2} + c_1 - \frac{c_2}{r^2} \\ s_t' &= -\frac{(3\nu + 1)s}{8} \cdot \frac{r^2}{a^2} + c_1 + \frac{c_2}{r^2} \end{aligned} \right\} \quad (31)$$

and a plastic portion extending from $r = 0$ to $r = c$, in which according to the theory of maximum shear

$$\left. \begin{aligned} s_r &= s_0 - \frac{sr^2}{3a^2} \\ s_t &= s_0 \end{aligned} \right\} \quad (32)$$

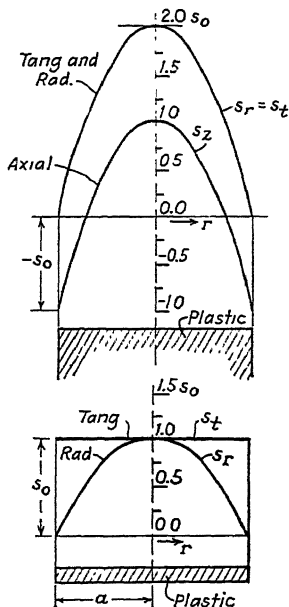
The three unknown constants s , c_1 , c_2 can be found from the conditions that for $r = a$, $s_r = 0$ and for $r = c$, $s_r = s_r'$, $s_t = s_t'$. Using the theory of maximum shear ($s_t = s_0 = \text{const.}$), the peripheral speed u can be computed explicitly at which the plastic portion will extend to a given radius $r = c$

$$u^2 = u_0^2 \cdot \frac{24a^4}{3(3 + \nu)a^4 - 2(1 + 3\nu)a^2c^2 + (1 + 3\nu)c^4} \quad (33)$$

From this if $c = a$ we see that the entire disc will yield if the peripheral speed will be equal to

$$u = \sqrt{3} \cdot u_0 = 1.73u_0. \quad (34)$$

Comparing this last value with $u' = 1.56u_0$ which was the speed for first yield, we see that an increase of about 11 per cent in the speed is sufficient to spread the plastic state through the whole



FIGS. 266 and 267.—Plastic equilibrium. Stresses in rotating cylinder and disc when entirely in plastic state.

disc. Figures 265 and 267 show the state of stress in the rotating disc at the moment of first yielding and for complete yielding.

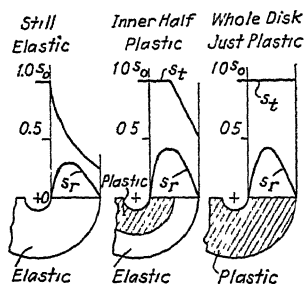
2. *Rotating Disc with Hole*.—In this case an additional term has to be introduced in the expression for the radial stress s_r , within the plastic region $a < r < c$:

$$s_r = s_0 - \frac{s_0^2}{3a^2} + \frac{c^3}{r} \quad (35)$$

Using again the theory of maximum shear the peripheral speed under which the disc will yield to a radius c is found

$$u^2 = u_0^2 \cdot \frac{12[2b^4c - ab^2(b^2 + c^2)]\frac{a^2}{b^2}}{3(3 + \nu)b^4c - (1 + 3\nu)(2b^2 - c^2)c^3 - 4a^3(b^2 + c^2)} \quad (36)$$

Here a and b designate the inner and outer radius of the disc



FIGS. 268, 269, and 270.—Rotating disc with hole. s_r radial, s_t tangential stress, s_0 yield stress for pure tension.

and u_0 the speed in a free ring of small cross-section for yielding. ($u_0^2 = s_0 g / \lambda$, s_0 is the yield stress in pure tension, g the gravity acceleration, λ the specific weight of the material of the disc, ν is Poisson's ratio.) According to the last formula the first yielding starts at the inner surface $r = a$ at a peripheral speed $u' = \omega b$ given by the value of u for $c = a$, which is

$$u'^2 = \frac{4u_0^2 \frac{a^2}{b^2}}{3 + \nu + (1 - \nu) \frac{a^2}{b^2}} \quad (37)$$

and the plastic region will spread completely to the outer surface at a peripheral speed u given by the value of u for $c = b$, which is

$$u^2 = \frac{3a^2 u_0^2}{a^2 + ab + b^2} \quad (38)$$

We may verify this last result by computing the value of u for the case that a tends to become equal to b . In this case the disc becomes a thin ring with small thickness in a radial direction. Formula (38) gives for $a/b = 1$,

$$u = u_0 \cdot \sqrt{\frac{3}{2}} = u_0 \quad (39)$$

in agreement with the speed u_0 for a free rotating ring of small cross-section and just at the yield point. Figure 269 shows an example of a stress distribution in a rotating disc with a hole and in a partially plastic state.¹

¹In the paper mentioned above (see footnote 2, p. 208) L. H. Donnell has worked out several cases numerically under the assumption used above and also by using the more general condition of plasticity.

CHAPTER 31

GENERAL PROBLEM OF PLASTIC FLOW WITH AXIAL SYMMETRY ABOUT AN AXIS

Under this heading are comprised all such cases of stationary plastic flow in cylindrical bodies in which the components of stress and of strain are dependent only on a single variable coordinate, namely the distance r of a point in the body from an axis. We have already treated several simple cases of this more general problem in the preceding chapters, such as the stress distribution in thick-walled tubes under high internal pressure or in rotating cylinders under certain assumptions. In more complicated cases, such as the plastic equilibrium of a hollow cylinder with thick walls subjected to internal pressure combined with an axial tension or compression or with twist, it is necessary to work out a more general theory. Especially will it be necessary also to include the stress-strain relations for plastic flow, as developed in Chap.

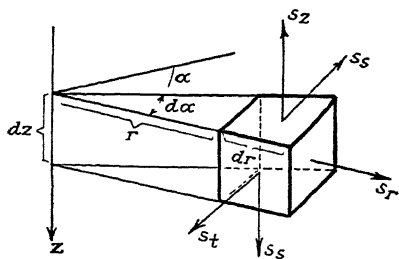


FIG. 271.—Stresses for axial symmetry about z axis.

14 and to introduce besides the three components of normal stress s_r , s_t , s_z , a shearing stress s_s . This latter acts in the planes perpendicular to the axis of the cylinder and in a direction tangent to the circles $r = \text{const.}$ (see Fig. 271).

We give here some results of the calculation¹ for two special cases.

a. Hollow Cylinder Subjected to Internal Pressure and Axial Load.—The pressure p required to produce plastic flow throughout an entire thick-walled tube which expands in the axial direction is given by

$$p = \frac{s_0}{\sqrt{3}} \ln \frac{u_b + \sqrt{1 + u_b^2}}{u_a + \sqrt{1 + u_a^2}} \quad (1)$$

¹ For the complete report see, On the Mechanics of the Plastic State of Metals, *Trans. Amer. Soc. Mech. Eng., Applied Mech. Division*, 1930.

Here s_0 is the yield stress in pure tension and u_a and u_b are constants given by the expressions

$$u_a = \frac{1}{\sqrt{3}} \left(1 + \frac{2\epsilon_a}{\epsilon_z} \right), \quad u_b = u_a \cdot \frac{a^2}{b^2}. \quad (2)$$

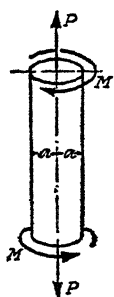


FIG. 272.—Combined torsion and tension.

ϵ_a is the value of the tangential unit elongation at the outer surface $r = a$ of the tube and ϵ_z is the axial elongation. The distribution of stress and the magnitude of the pressure p depend mainly on two parameters: the ratio of the outer to inner radius a/b and on the ratio ϵ_a/ϵ_z .

b. Combined Torsion and Axial Tension in Solid Cylindrical Bar.—In this case $s_r = s_t = 0$, the axial normal stress s_z and the shearing stress s_s are given by

$$s_z = s_0 \cos \alpha, \quad s_s = \frac{s_0}{\sqrt{3}} \sin \alpha, \quad (3)$$

where the variable parameter α is defined by

$$\tan \alpha = \frac{\theta r}{\sqrt{3} \cdot \epsilon_z}. \quad (4)$$

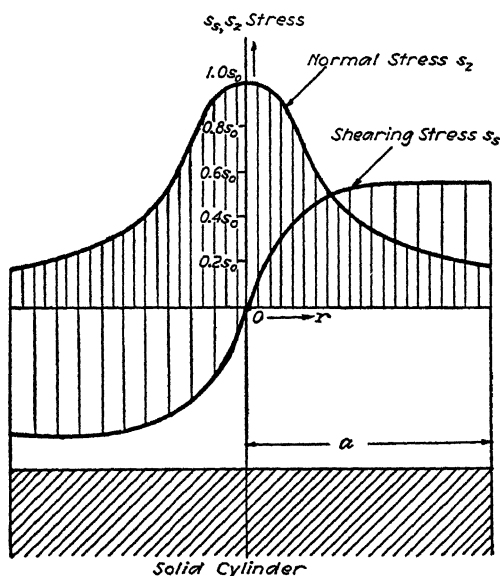


FIG. 273.—Plastic stress distribution under combined torsion and tension in solid cylinder.

θ is the angle of twist per unit of length, ϵ_z the axial unit elongation of the bar. θ and ϵ_z are considered as given. A distribution

of stress according to this formula is represented in Fig. 273 for a value of $\tan \alpha_a = 5.25$ (α_a is the value of α for $r = a$). As can be seen from this figure, the tensile stress becomes a maximum at the center of the cylinder. As at this point the shearing stress vanishes, the normal stress at the axis of the bar becomes exactly equal to the yield stress s_0 in pure tension. With increasing radius the shearing stress s_s must increase and consequently the normal stress s_z decreases.

CHAPTER 32

SYSTEMS OF SLIP LINES IN TWO-DIMENSIONAL PROBLEMS

The state of stress in the case of a two-dimensional flow of a plastic mass extending to infinity, as H. Hencky¹ first observed, may be determined independent of the deformation. For determining the three stress components s_x , s_y , s_{xy} , the two conditions of equilibrium:

$$\frac{\partial s_x}{\partial x} + \frac{\partial s_{xy}}{\partial y} = 0, \quad \frac{\partial s_y}{\partial y} + \frac{\partial s_{xy}}{\partial x} = 0, \quad (1)$$

and the condition of plasticity are available.

For the latter, according to Chap. 27, Eq. (6), the condition of constant energy of distortion may be assumed, thus:²

$$(s_x - s_y)^2 + 4s_{xy}^2 = 4k^2. \quad (2)$$

The constant k has the value $k = s_0/\sqrt{3}$ (s_0 being the yield point in tension). Using the maximum shear theory as the condition of plasticity the same equation holds, except that the constant $k = s_0/2$. The three stress components s_x , s_y , s_{xy} may be expressed according to Eq. (23), page 46, in terms of the principal stresses s_1 and s_2 as follows:

$$\left. \begin{aligned} s_x &= \frac{s_1 + s_2}{2} + \frac{s_1 - s_2}{2} \cos 2\alpha, \\ s_y &= \frac{s_1 + s_2}{2} - \frac{s_1 - s_2}{2} \cos 2\alpha, \\ s_{xy} &= \frac{s_1 - s_2}{2} \sin 2\alpha. \end{aligned} \right\} \quad (3)$$

¹ Über einige statisch bestimmte Fälle des Gleichgewichts in plastischen Körpern, *Z. f. ang. Math. u. Mech.*, vol. 3, p. 241, Berlin, 1923.

² According to St. Venant, who derived condition (2) from the maximum shear theory, Eqs. (1) and (2) may be solved with the help of a stress function F . Both conditions of equilibrium are satisfied by putting

$$s_x = \frac{\partial^2 F}{\partial y^2}, \quad s_y = \frac{\partial^2 F}{\partial x^2}, \quad s_{xy} = -\frac{\partial^2 F}{\partial x \partial y}.$$

The third condition (that of plasticity) gives, using these expressions, the following partial differential equation of the second order and second degree for determining the stress function F :

$$(F_{yy} - F_{xx})^2 + 4F_{xy}^2 = 4k^2.$$

Here α is the angle which the algebraically greater principal stress s_1 makes with the x axis. The maximum shearing stress is, according to Eq. (22), page 46:

$$s_{xy\max} = +\sqrt{\frac{(s_x - s_y)^2}{4} + s_{xy}^2} = \frac{s_1 - s_2}{2} \quad (4)$$

In a soft mass, in which the stresses are at the plastic limit, we must have according to Eqs. (2) and (4):

$$s_{xy\max} = \frac{s_1 - s_2}{2} = k = \text{const.}$$

Putting the mean value of the normal stresses equal to s , thus:

$$s = \frac{s_x + s_y}{2} = \frac{s_1 + s_2}{2}, \quad (5)$$

Eq. (3) may be written in a more compact form:

$$\left. \begin{aligned} s_x &= s + k \cos 2\alpha, \\ s_y &= s - k \cos 2\alpha, \\ s_{xy} &= k \sin 2\alpha. \end{aligned} \right\} \quad (6)$$

At an arbitrary point P having the coordinates x and y , there are two cross-sections in which the shearing stress takes on its maximum or minimum value $\pm k$. We will in the future call the directions of these cross-sections the *directions of principal shear*. Both these directions are inclined at 45° to the principal stress s_1 .

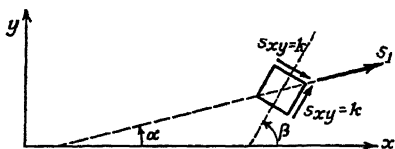


FIG. 274.—Directions of principal shear.

Introducing, instead of α , an angle β in Eq. (6) thus:

$$\beta = \alpha + 45^\circ, \quad (7)$$

β being the angle of the "first" principal shearing-stress direction with the x axis (Fig. 274) (the other being $\alpha - 45^\circ$) formulæ (6) become:

$$\left. \begin{aligned} s_x &= s + k \sin 2\beta, \\ s_y &= s - k \sin 2\beta, \\ s_{xy} &= -k \cos 2\beta. \end{aligned} \right\} \quad (8)$$

If the two directions of the principal shearing stresses are indicated at each point (x, y) of the plane, two series of curves may be constructed, whose tangents at each point of the x, y plane coincide with the directions of the principal shearing stresses at these points (Fig. 275).

These sets of curves cross each other everywhere at right angles and are called the *slip lines of the plane distribution of stress*.

We may easily derive the differential equation of these slip lines. If $y = f(x)$ is the equation of a slip line whose tangent at the point (x, y) makes the angle β with the x axis, we have, for the differential equation of the first family of slip lines:

$$\frac{dy}{dx} = \tan \beta. \quad (9)$$

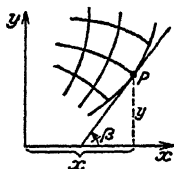


FIG. 275.—Slip lines.

For the second family of slip lines, we have:

$$\frac{dy}{dx} = \tan \left(\frac{\pi}{2} + \beta \right) = -\cot \beta \quad (10)$$

The angle β occurring on the right side of these equations may be calculated for a given state of plane stress from Eq. (20), page 45, thus:

$$\tan 2\beta = \frac{s_y - s_x}{2s_{xy}}. \quad (11)$$

In this β is to be treated as a given function of x and y .

CHAPTER 33

PLASTIC MASS PRESSED BETWEEN TWO ROUGH PARALLEL PLATES

From the three fundamental equations of the two-dimensional stress problem, a few solutions may be easily obtained by immediate integrations. These equations are (Eqs. (1) and (2), Chap. 32):

$$\frac{\partial s_x}{\partial x} + \frac{\partial s_{xy}}{\partial y} = 0, \quad \frac{\partial s_y}{\partial y} + \frac{\partial s_{xy}}{\partial x} = 0, \quad (s_x - s_y)^2 + 4s_{xy}^2 = 4k^2.$$

If the first two equations are differentiated with respect to y and x , respectively, the difference gives:

$$\frac{\partial^2}{\partial x \partial y}(s_x - s_y) = \frac{\partial^2 s_{xy}}{\partial x^2} - \frac{\partial^2 s_{xy}}{\partial y^2}.$$

Substituting in this the value of $s_x - s_y$ obtained from the third equation, which is:

$$s_x - s_y = \pm 2\sqrt{k^2 - s_{xy}^2}$$

we obtain for the shearing stress s_{xy} the following partial differential equation:

$$\pm 2 \frac{\partial^2 \sqrt{k^2 - s_{xy}^2}}{\partial x \partial y} = \frac{\partial^2 s_{xy}}{\partial x^2} - \frac{\partial^2 s_{xy}}{\partial y^2}. \quad (12)$$

A solution of this equation may be obtained if we assume $s_{xy} = f(y)$. The equation then gives:

$$\frac{\partial^2 s_{xy}}{\partial y^2} = 0, \quad s_{xy} = c_1 + c_2 y. \quad (13)$$

The shearing stress s_{xy} cannot become greater than k . If c_1 be chosen equal to 0, there are two straight lines $y = \pm a$, along which the shearing stress s_{xy} reaches the maximum absolute value possible (k). The sign of the constant c_2 is to be chosen according to whether $s_{xy} = +k$, or $s_{xy} = -k$, for $y = a$. If we assume that for $y = a$, $s_{xy} = -k$, we must then take $s_{xy} = -ky/a$. Both straight lines $y = \pm a$ form natural limits for the plastic mass. The analytic functions representing the stress distribution cannot logically be extended beyond these limits and the solution has a physical meaning only inside the parallel strip $-a \leq y \leq +a$.

Both stresses s_x and s_y may be calculated from the conditions of equilibrium (1) thus:

$$\left. \begin{aligned} \frac{\partial s_x}{\partial x} &= -\frac{\partial s_{xy}}{\partial y} = +\frac{k}{a}, & s_x &= +\frac{kx}{a} + f_1(y), \\ \frac{\partial s_y}{\partial y} &= -\frac{\partial s_{xy}}{\partial x} = 0, & s_y &= f_2(x). \end{aligned} \right\} \quad (14)$$

Both arbitrary functions $f_1(y)$, $f_2(x)$ must be so determined that the condition of plasticity will be identically satisfied, thus:

$$\begin{aligned} s_x - s_y &= \pm 2\sqrt{k^2 - s_{xy}^2} \\ + \frac{kx}{a} + f_1(y) - f_2(x) &= \pm 2k\sqrt{1 - \left(\frac{y}{a}\right)^2}. \end{aligned}$$

From this we have:

$$f_1(y) = c \pm 2k\sqrt{1 - \left(\frac{y}{a}\right)^2}; \quad f_2(x) = c + \frac{kx}{a}.$$

From this the stresses may be determined thus:

$$\left. \begin{aligned} s_x &= c + \frac{kx}{a} \pm 2k\sqrt{1 - \frac{y^2}{a^2}}, \\ s_y &= c + \frac{kx}{a}, \\ s_{xy} &= -\frac{ky}{a}. \end{aligned} \right\} \quad (15)$$

As these equations show, under the above assumptions,¹ two different solutions are obtained, according to whether in the expression for s_x the positive or the negative sign is taken. From the equations, a very noteworthy peculiarity of these solutions may be discerned, namely that at both limits $y = \pm a$, both solutions give exactly the same stresses:

$$s_{xy} = \mp k, \quad s_y = c + \frac{kx}{a}.$$

We now determine the equations of the slip lines under both stress conditions. The proper sign to use in the right-hand member of the equation for s_x in (15) may be determined as follows, use being made of variable β and formula (8). According to the latter we have:

$$s_{xy} = -k \cos 2\beta, \quad s_x - s_y = 2k \sin 2\beta \quad (16)$$

Moreover, according to (15)

$$s_{xy} = -\frac{ky}{a} \quad \text{and} \quad s_x - s_y = \pm 2k\sqrt{1 - \frac{y^2}{a^2}}. \quad (17)$$

Therefore $\cos 2\beta = y/a$ and the sign of the radical must be chosen positive or negative, according to whether the variable β is taken between $0 < \beta \leq \pi/2$ or between $\pi/2 < \beta < \pi$.

¹ These solutions and the statement relative to the slip lines were first given by L. Prandtl, see *Z. f. ang. Math. u. Mech.*, vol. 6, 1923.

The equations of the slip lines are determined from the differential equation in the simplest way by using the variable β as a parameter.

Since,

$$y = a \cos 2\beta,$$

it follows that:

$$\frac{dy}{dx} = -2a \sin 2\beta \cdot \frac{\partial \beta}{\partial x}.$$

The differential equation of the first family of slip lines is, according to (9):

$$\frac{dy}{dx} = \tan \beta = -2a \sin 2\beta \cdot \frac{\partial \beta}{\partial x}.$$

That of the second family is according to (10):

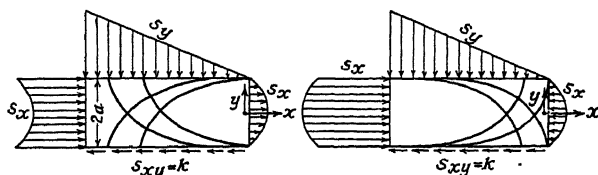
$$\frac{dy}{dx} = -\cot \beta = -2a \sin 2\beta \cdot \frac{\partial \beta}{\partial x}$$

From these the following equations for the slip lines are determined

$$\text{first family } \begin{cases} x = -a[2\beta + \sin 2\beta] + \text{const} \\ y = a \cos 2\beta \end{cases} \quad (18)$$

$$\text{second family } \begin{cases} x = a[2\beta - \sin 2\beta] + \text{const} \\ y = a \cos 2\beta. \end{cases} \quad (19)$$

If the quantity 2β be replaced by a parameter t (time) it will be recognized that these are equations of a family of cycloids, a being the radius of the



State I.

State II.

Figs. 276 and 277.—Slip lines and distribution of stress in a plastic mass pressed between two rough parallel plates. Fig. 276 showing passive, and Fig. 277 active plastic state.

rolling circle and t the angle through which it has rolled. The slip lines are represented by the two systems of cycloids (Fig. 276) which cross one another at right angles. Each straight line $y = \pm a$, along which the shearing stress s_{xy} reaches its maximum value k , and which we recognize as a natural limit of the plastic region, is at the same time an envelope of one series of slip lines. If the angle β lies between 0 and $\pi/2$ the first solution results in a position of the slip lines according to Fig. 276, while if $\pi/2 < \beta < \pi$ the second solution gives the position of the slip lines according to Fig. 277.

Under conditions of the kind represented in Figs. 276 and 277, a soft, pasty, plastic mass is squeezed between two wide parallel plates of hard material, provided the material may flow only towards one side. To produce the stress distribution I the solid

plates must be brought together. Under distribution II, however, the horizontal compressive stresses are the driving forces; under their action the horizontal plates are forced apart. Since the limiting conditions relative to stress along the horizontal compression plates $y = \pm a$ are the same for both stress distributions, one may also—to differentiate both stress distributions from one another—say, that on the compression plate in the state of stress I a passive compression acts, while in the state of stress II an active one acts.

Relative to the behavior of a plastic mass in the neighborhood of a rigid rough surface we may, therefore, differentiate between two states: State I may be called the passive plastic and II the active

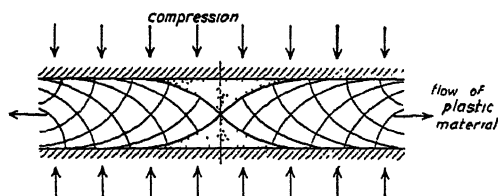


FIG. 278.—Slip lines in cross-section of a plastic mass pressed between rough parallel plates. Symmetrical case of flow.

plastic state.¹ The active and the passive flow may be visually represented by the corresponding systems of slip lines. One may think of the state of stress I (which corresponds to a positive sign of the radical or the region where the variable β is between 0 and $\pi/2$) as represented by its slip lines in a plane I, while the state of stress II (corresponding to the negative sign and $\pi/2 < \beta < \pi$) is represented in a second plane II. These two branches or regions of the solution may be thought of as coinciding along the “branch lines” $y = \pm a$ to a single function. Plane I contains the slip lines of the passive and plane II those of the active flow. The envelopes of the slip lines are two “branch lines” of the solution along which two states of stress, distinct in physical space, bound each other. We may finally say: Solution Eq. (15) repre-

¹ This method of designation corresponds to the active and passive earth pressure in the theory of earth pressure. In this respect there is a near analogy between the compressive action of a soft plastic mass on a rough, rigid plate and the pressure of loose earth on a firm wall (supporting wall). Cf. the author's report on Plasticity in “Handbuch der Physik,” vol. 6, Julius Springer, Berlin, 1928.

sents the plane flow of a perfectly plastic mass, *which has two parallel lines as "branch lines."*

The relations near the free edges of a plastic mass compressed between two rigid plates cannot be determined by the above equilibrium conditions. In the net of slip lines, in the neighborhood of the free boundaries of the mass, new regions must be considered in which the stress condition cannot be expressed by formula (15). It is difficult to predict how a continuation of the slip lines would appear, as long as the other mechanical properties of the mass (its ultimate strength in pure shear and tension) are not considered since these determine the form of the slip lines at the edges and free surfaces. On the basis of observations on distortion and slip, one would expect that

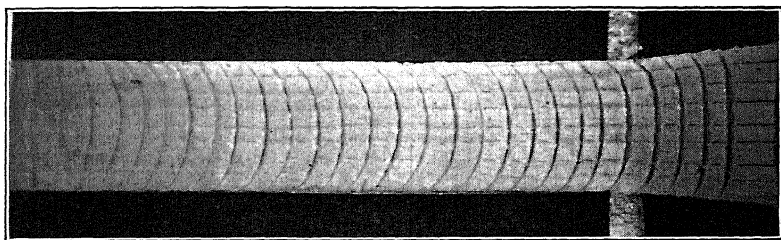


FIG. 279.—Cross-section of a plastic mass after compression between two rough parallel plates. (According to W. Riedel.)

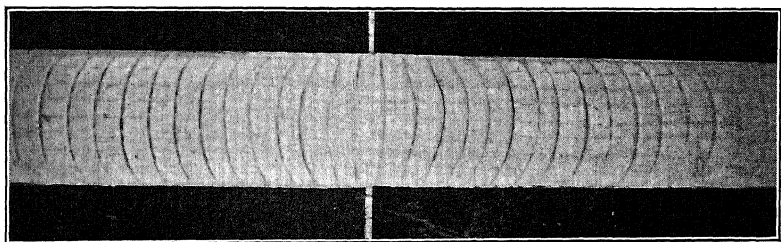


FIG. 280.—Cross-section of a plastic mass after compression showing the distorted form of an originally rectangular network of straight lines. Observe the elliptical shape of markings in greater distance from white center line of symmetry.

the slip lines in the neighborhood of a free surface would tend to converge toward an edge in the form of rays (cf. the photograph of the slip lines in a plane compression test, Fig. 117, page 116). In this connection Prandtl has proposed possible forms for the continuation of the slip lines.¹ If the plastic flow may be considered as two-dimensional, but the plastic mass is permitted to flow away in both directions between compression plates, there arises in the middle of the layer (in the axis of the test piece) an area (Fig. 278) in which the shearing stresses (the friction) along the compression plates do not reach their maximum possible value. It is only necessary to

¹ *Loc. cit.*

consider that in the axis of the test piece the friction of the plates must be zero on the basis of symmetry conditions. Hence, in this middle part of the mass, the limits of plasticity will not be reached. This region is shown dotted in Fig. 278.

It should finally be noted that formula (15) offers the possibility of accurately determining the displacements of the material in the plastic layers. A system of components of displacements u and v compatible with the system of slip lines of Eqs. (18) and (19) can be found. The displacement component u parallel to the compression plates is given by the ordinates of half of an ellipse, with respect to the variable y .

By squeezing out a highly plastic mass (wet clay or plastic plaster) compressed between two parallel rigid plates W. Riedel has obtained deformations which support the conclusions arrived at above. In Fig. 279 the distorted form of an originally rectangular network of straight lines can

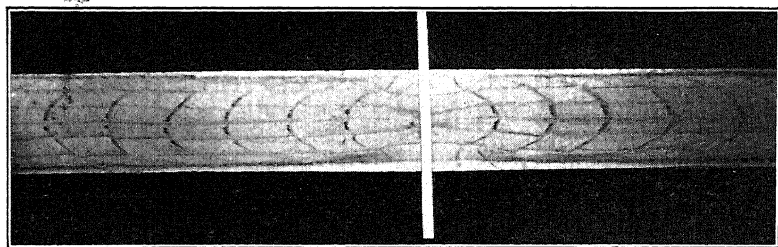


FIG. 281.—Distortion of network after severe compression. Observe points of inflection in markings near white center line. (According to W. Riedel.)

be recognized. The horizontal lines remained parallel, but the vertical lines were transformed into curves very similar to halves of ellipses as predicted by the theory. In Figs. 280 and 281 the central portion of a plastic mass can be seen, flowing symmetrically to both sides. This latter case of deformation corresponds to Fig. 278 of the slip lines and one can clearly see from Figs. 280 and 281 that the ellipses are completely disturbed at the center of the mass according to what must be expected from Fig. 278.

Since one would suspect that the properties of the mathematical solution given above for a plastic mass compressed between two parallel plates may be generalized to include other stress conditions, it appears worth while to investigate other cases of plane stress on the basis of these properties. This will be done in the next chapter.

CHAPTER 34

OTHER CASES OF PLANE PLASTIC FLOW

If, instead of right-angled coordinates x and y , we use the polar coordinates r and ϕ , the three equations of the plane plastic flow assume such a form as may easily be obtained, if one considers the equilibrium of the forces acting on a small element represented in Fig. 282. Designating by s_r the radial normal stress, by s_t the tangential normal stress, and s_{rt} the shearing stress, the equations of equilibrium take the form:

$$\frac{\partial}{\partial r}(rs_r) - s_t + \frac{\partial s_{rt}}{\partial \phi} = 0, \quad (1)$$

$$\frac{\partial s_t}{\partial \phi} + \frac{\partial}{\partial r}(rs_{rt}) + s_{rt} = 0. \quad (2)$$

To this we add as the third equation, the condition of yielding:

$$(s_r - s_t)^2 + 4s_{rt}^2 = 4k^2. \quad (3)$$

Eliminating s_r and s_t , the differential equation for the shearing stress s_{rt} takes the form:

$$\pm 2 \frac{\partial^2}{\partial r \partial \phi} (r \sqrt{k^2 - s_{rt}^2}) = r^2 \frac{\partial^2 s_{rt}}{\partial r^2} + 3r \frac{\partial s_{rt}}{\partial r} - \frac{\partial^2 s_{rt}}{\partial \phi^2} \quad (4)$$

a. Radial Yielding.—If s_r and s_t depend only on r and are principal stresses (s_{rt} being 0) we have:

$$\frac{d}{dr}(rs_r) - s_t = 0. \quad (5)$$

$$s_r - s_t = \pm 2k. \quad (6)$$

The solution is:

$$s_r = \pm 2k \ln \frac{a}{r}, \quad s_t = \mp 2k \left(1 - \ln \frac{a}{r}\right), \quad (7)$$

where a is an arbitrary length. These formulæ have been given already on page 188. *The slip lines are two orthogonal systems of logarithmic spirals.* These spirals are commonly observed in wrought-iron plates or in the cross-sections of thick-walled tubes, in which the material has been stressed above the yield point, the stress distribution being symmetrical with respect to the axis.

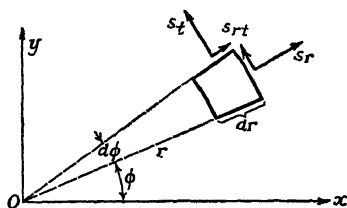


FIG. 282.—Stress components in polar coordinates r, ϕ .

W. Krüger,¹ has observed such flow figures in the shape of logarithmic spirals at one end of a thick-walled tube, which had been

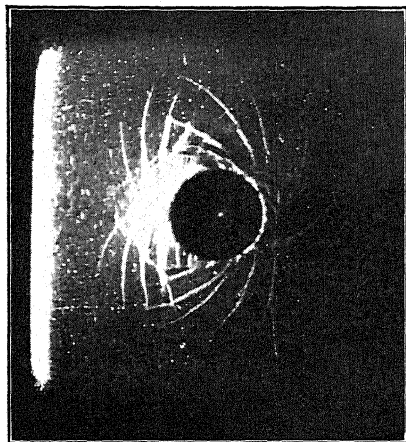


FIG. 283.—Slip lines on surface of a steel block produced by forcing a cylindrical punch into it.

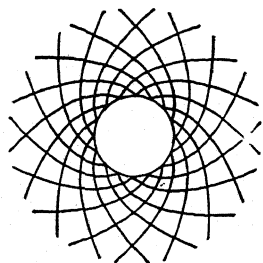


FIG. 284.—Family of slip lines consisting of system of orthogonal logarithmic spirals.

subjected to high internal pressure. Figure 283 shows similar markings or flow figures on the polished surface of an iron piece obtained by forcing a cylindrical punch into the test piece. From these markings we may conclude that the forcing of a punch of cylindrical cross-section into a plastic metal, such as wrought iron, tends to cause, at least in the thin surface layer, a plastic flow of radial symmetry having the radii and the circles as the directions of principal stress.² These slip lines have no envelope.

¹ *Mitt. ü. Forschungsarb., V.D.I.*, vol. 87, 1910.

² Slip lines in the form of logarithmic spirals may be frequently observed in the heads of steam boilers subjected to plastic bending under an axially symmetrical stress field (cf. the paper by KÖRBER and SIEBEL in *Mitt. d. K.-W.-Inst. f. Eisenforschung*). These slip lines are also frequently visible around punched rivet holes. In the well-known Brinell hardness tests, the metal is obviously stressed in a similar way in a ring-shaped area of the surface layer. Similar flow figures may be often observed around the Brinell indentations while testing iron for hardness.

b. Circles as Envelopes of Slip Lines.—We assume that the shearing stress s_{rt} is only a function of r not of ϕ . If it is denoted simply by s , then Eq. (4) takes the simpler form:

$$r \frac{d^2 s}{dr^2} + 3 \frac{ds}{dr} = 0. \quad (8)$$

The solution of this equation is:

$$s = \frac{c_1}{r^2} + c_2. \quad (9)$$

To obtain the solution the boundary conditions:

$$r = a, \quad s = -k$$

and

$$r = b, \quad s = +k$$

are used. Thus, a ring-shaped plastic area is obtained, bounded by the two concentric circles of radii a and b . These circles are the envelopes of the slip lines. The Equations (1) and (2) may be integrated completely to determine the stresses and the equations of the slip lines.¹

c. Vortical Flow in a Plastic Mass.—We content ourselves in this case with the statement of the formula for the case that the integration constant in Eq. (9) $c_2 = 0$. We may then put:

$$s_{rt} = -k \frac{a^2}{r^2} \quad (r \geq a). \quad (10)$$

Furthermore, we introduce an angle β , at which the first series of slip lines cross the radius vector. We then have, corresponding to Eq. (8), page 219:

$$\left. \begin{aligned} s_r - s_t &= 2k \sin 2\beta \\ s_{rt} &= -k \cos 2\beta = -k \frac{a^2}{r^2} \end{aligned} \right\}, \quad (11)$$

also

$$\cos 2\beta = \frac{a^2}{r^2} \quad (12)$$

The condition of equilibrium is:

$$r \frac{ds_r}{dr} = s_t - s_r = -2k \sqrt{1 - \frac{a^4}{r^4}}, \quad (13)$$

from which

$$s_r = -2k \int \frac{dr}{r} \sqrt{1 - \frac{a^4}{r^4}} + c. \quad (14)$$

¹ Cf. "Handbuch der Physik," vol. 6, art. on Plasticity, Julius Springer, Berlin, 1928. The slip lines are epi- and hypo-cycloids.

After introducing the variable β as given by Eq. (11), the integration may be easily carried out, and the stresses s_r , s_t , s_{rt} determined as functions of the parameter β :

$$\left. \begin{aligned} s_r &= -k \left[\ln \tan \left(\beta + \frac{\pi}{4} \right) - \sin 2\beta \right] \\ s_t &= -k \left[\ln \tan \left(\beta + \frac{\pi}{4} \right) + \sin 2\beta \right] \\ s_{rt} &= -k \cos 2\beta. \end{aligned} \right\} \quad (15)$$

Moreover, the equations of the slip lines may be determined thus.

The equations for the first and second family of slip lines are given in parametric form:

$$\left. \begin{aligned} \phi &= \arctan v - \arctan v + c_1, & \phi &= -\arctan v - \arctan v + c_2 \\ r^2 &= a^2 \cdot \frac{1+v^2}{2v}, & r^2 &= a^2 \cdot \frac{1+v^2}{2v}. \end{aligned} \right\} \quad (16)$$

At a large distance r from the center the slip lines approximate logarithmic spirals making an angle of 45° with the radial direction.

A type of vortical flow compatible with this system of stress and slip lines is given by the following displacements:

$$u' = c \frac{a}{r}, \quad v' = c \frac{r}{a} \left(1 - \sqrt{1 - \frac{a^4}{r^4}} \right). \quad (17)$$

In this u' is the radial and v' the tangential displacement along the circle $r = \text{constant}$. At the inner circle of the plastic area, the mass flows at an angle of 45° across the circle $r = a$; its vortical motion, however, quickly dies down at a large distance from the center of the circle.

d. Radial Distribution of Stress in a Wedge-shaped Plastic Space.—If the shearing stress s_{rt} depends only on the angle ϕ , the differential Eq. (4) may be immediately integrated once with respect to ϕ , thus giving

$$\frac{ds_{rt}}{d\phi} = \mp 2\sqrt{k^2 - s_{rt}^2} + 2ck. \quad (18)$$

In this the constant of integration is designated by $2ck$. For $c = 0$, we obtain:

$$s_{rt} = \mp k \sin (c_1 + 2\phi). \quad (19)$$

The corresponding stresses given by this particular solution constitute a homogeneous tension or compression.

The integral curves (19) have, however, as may be seen, two envelopes, namely the straight lines $s_{rt} = \pm k$. These are two singular solutions of the differential Eq. (18), no constant of integration appearing. If $s_{rt} = \pm k$, according to the condition of plasticity s_r must equal s_t . The two equations of equilibrium then give:

$$s_r = s_t = \mp 2k\phi + \text{const.} \quad (20)$$

The stress distribution represented by the following equation:

$$s_r = s_t = \mp 2k\phi + \text{const.}, \quad s_{rt} = \pm k \quad (21)$$

has for its slip lines the lines $\phi = \text{const.}$ passing through the origin and the concentric circles $r = \text{const.}$ while the trajectories of principal stress are logarithmic spirals.

This state of stress has a practical meaning, since it may give the relations, which must exist in the sectors of severely distorted regions under compressive loading. If a stiff plate is pressed on a plastic mass, observations show that on account of the friction, ray-shaped areas extend from the edges. In these the material has suffered extraordinarily large shearing displacements, as indicated by the sketch of Fig. 285. (At this point reference may be made to the photographs of compressed test specimens on page 116.) The points corresponding to the projections of the edges bounding the compression surfaces of a test specimen of soft material, compressed between hard plates, are singular points of the stress distribution. Wedge-shaped regions extend from these straight edges into the inside of the specimen; the plastic strains in these regions increase the nearer the point considered is to the edge. The enormous strains, which must arise here, make it obvious why the sliding fractures in compression tests usually start along these regions (pyramids and cones produced by fracture of brittle materials in compression tests).

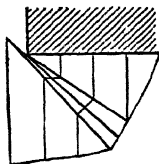


FIG. 285.—The ray-shaped region with extraordinarily large shearing displacements radiating from the edge of a compression plate.

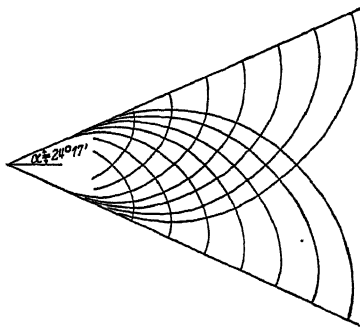


FIG. 286.—Slip lines having two inclined straight lines as their envelope.

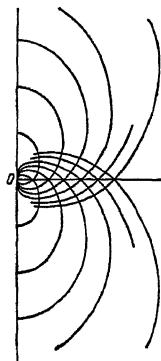


FIG. 287.—Case where angle α of Fig. 286 is $\alpha = \pi/2$.

It is noteworthy that the radial stress distribution of a plastic mass arises from a stress function of the form $F = kr^2\phi$, which corresponds in the plane problem also to a possible condition of equilibrium of a perfectly elastic material.¹

¹ Regarding applications of the radial stress distribution given by Eq. (23) for determination of the breaking conditions in a compressed test specimen of brittle material, cf. *Z. f. Phys.*, p. 106, 1924.

If, however, in Eq. (18) $c \neq 0$, there results, as a more detailed investigation shows,¹ a stress distribution in the form of a wedge-shaped area with two straight lines as envelopes of the slip lines. Also this distribution of stress may be completely determined. Two examples of the net of the slip lines are shown in Figs. 286 and 287.

A particular case is that of the equilibrium of a plastic mass compressed between two rigid and rough plates, whose planes are inclined at a small angle to each other:

$$\begin{aligned} s_r &= k \left[\frac{1}{\alpha} \ln \frac{a}{r} + 2\sqrt{1 - \frac{\phi^2}{\alpha^2}} \right], \\ s_t &= \frac{k}{\alpha} \ln \frac{a}{r}, \\ s_{rt} &= \frac{k\phi}{\alpha}. \end{aligned} \quad (22)$$

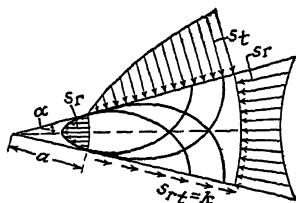


FIG. 288.—System of slip lines and distribution of stress in a plastic mass pressed between two inclined rigid plates.

The compressive stress varies along the plates as the logarithm of the distance r from the point of the wedge. In this α is equal to half the angle of opening of the wedge (Fig. 288). The slip lines are given by the following equations:

$$\begin{aligned} \ln \frac{r}{c_1} &= \sqrt{\alpha^2 - \phi^2} + \alpha \arcsin \frac{\phi}{\alpha}, \\ \ln \frac{r}{c_2} &= \sqrt{\alpha^2 - \phi^2} - \alpha \arcsin \frac{\phi}{\alpha}. \end{aligned} \quad (23)$$

The above expressions, if the angle α is made infinitely small, reduce to those given in formula (15), which applies to the case of a mass compressed between two parallel plates.

¹ *Z. f. Phys.*, p. 106, 1924.

CHAPTER 35

HARDNESS

Difficulties have been encountered in attempting to find a more exact definition of the property of materials of construction which is expressed by the words: hard or hardness—used as the contrary of soft. Several attempts have been made to treat hardness as an original mechanical property of materials in addition to such properties as designated by the terms: elasticity, ductility, or strength. A closer examination of these numerous attempts will show that unfortunately the term hardness is often used in different senses by engineers, metallurgists, and mineralogists while the same term may refer to very different properties.¹

The second and perhaps more serious difficulty in finding a general definition and a quantitative testing method of measuring hardness was encountered in the fact that practically in most, or perhaps all, of the methods proposed for the measurement of hardness the distributions of stress, actually applied, are not of a simple nature. It was, therefore, not possible to predict these stress distributions more accurately. The distribution of stress in the vicinity of an indentation is, furthermore, affected by many factors, among which elasticity, plasticity, after-flow, and strength must first be mentioned.

The metallurgist, for example, in producing alloys of metals may wish to harden one soft metal by alloying with it another metal or substance in small quantities. The effect he wishes to bring about is usually to raise the value of the stresses, at which permanent and plastic deformations begin to

¹ This fact was clearly brought out in a paper by L. B. Tuckerman, *Hardness and Hardness Testing*, *Mech. Eng.*, vol. 47, January, 1925 in which he states that "hardness in common parlance represents a hazily conceived conglomeration or aggregate of properties of a material more or less related to each other. These properties include such varied things as resistance to abrasion, resistance to scratching, resistance to cutting, ability to cut other materials, resistance to plastic deformation, high modulus of elasticity, high yield point, high strength . . ." He also says that "the immediate usefulness of hardness tests in determining uniformity of materials should not be allowed to obscure the real need for a fundamental investigation of hardness."

occur and possibly at the same time to increase the strength of the alloy. The mechanical property, which the metallurgist wishes to improve and which he expresses by "hardness" is here apparently the limit of plasticity or that of rupture, which we have seen, at lower temperatures, mainly depend on the three principal stresses or on other conditions.

Mineralogists, on the other hand, use "scratching" for the determination of hardness. They have established a certain scale of standard minerals, each scratching the next standing in the row below and define hardness by the destruction of the surface of a mineral. Martens, using a sharp diamond under a determined load, and measuring the width of the scratch under a microscope, has improved this method somewhat. Here some resistance against tearing apart is involved but this is not obtained by a simply determined homogeneous state of stress such as pure tension, pure shear, etc., but rather by an unknown and probably fairly complicated distribution of stress produced by a normal and a tangential load which forces a rigid cone into the material.

In the *Brinell hardness test* a hardened steel ball under a given load (for materials such as steel a 10-mm. ball under a load of 3,000 kg.) is forced into a ductile metal and the average pressure in the surface of contact is measured. In this test, therefore, a certain average stress involving plastic equilibrium is measured under a load concentrated on a small spherical area.¹ In case of *P. Ludwik's cone hardness test* instead of a ball a cone having an apex angle of 90° is used. While the Brinell hardness number depends on the arbitrary load which was used to force the steel ball into the metal (3,000 kg. for hard, 500 kg. for soft materials) the stress derived by dividing the load by the projection of the area of contact in Ludwik's cone hardness test is independent of the load. Hence, the cone hardness number is independent of the load.

In the *Shore scleroscope hardness test* the height of rebound of a falling steel ball is measured. This is certainly much affected by the elastic properties as well as the plastic properties of the material to be investigated. In the *Rockwell hardness test* the depth of the indentation made by a steel ball is automatically recorded. In the *Herbert pendulum hardness test* the damping of the vibrations of a pendulum, supported by a steel ball resting on the indentation in the material tested, is measured.

To define elasticity and measure it as a mechanical property of matter, it is advantageous and necessary to first test the materials under simple homogeneous states of stress, such as pure tension, pure compression, or pure shear, in order to show how stress depends on strain in these special cases and then also in more general cases (establishment of Hooke's generalized law). On the other hand, the elastic states of stress produced by loads concentrated on comparatively small areas may in certain cases (as, for example, in the case of axial symmetry) be analyzed, but in general

¹ A very thorough treatment of hardness-testing methods and laws governing the relation between force and diameter of indentation for the Brinell hardness test, is contained in the work of EUGEN MEYER in *Mitt. u. Forschungsarb.*, nos. 65, 66, 1909. With respect to the various methods of measuring hardness cf. SACHS, "Grundbegriffe der mechanischen Technologie der Metalle," 1925, as well as other textbooks on material testing.

such cases of concentration of pressure are not simple and consequently less suitable for defining elasticity. Something analogous may be said, if under severe pressures a permanent indentation is produced in a material and this yields partially under a concentrated load. Hence "Hardness," if tested by such a method, cannot be considered as simple a mechanical property as elasticity or plasticity.

In the following a few observations relative to the plastic deformations near the regions of contact of materials deformed by indentations in various ways will be given. For the purpose of making plainly visible the slight distortions of the surface near the indentation, these surfaces were well polished before the indentation was made. The distorted surfaces were photographed by means of the "Schlieren"-method described above, page 91.

PENETRATION OF CYLINDRICAL PUNCHES

A steel punch with hardened ends was forced into test pieces of cast zinc, soft and hard copper, and soft iron. As will be seen from the following photographs the various metals behave very differently when an indentation is made by a punch.

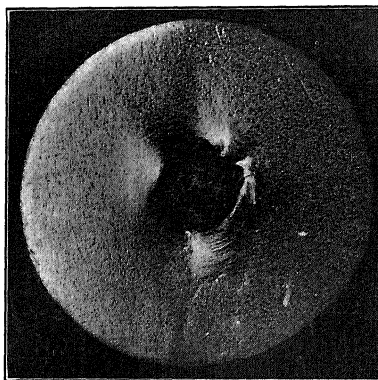


FIG. 289.

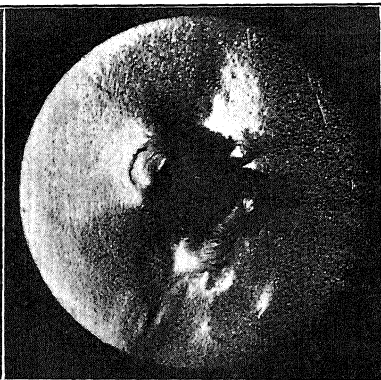


FIG. 290.

ZINC

Figure 289.—The test piece after loading to 3,140 kg./cm.²: On account of the formation of cracks the distortion of the surface is not axially symmetrical. The grooves and markings produced by the lathe tool are in evidence, although the surface has been finely polished. An explanation of the reappearance

of these grooves is that the zinc has been work-hardened along these grooves by the lathe tool. Under the new plastic deformation caused by the compression of the punch, the work-hardened portions are less deformed than the soft portions and project through the smooth surface making the grooves again visible.

Figure 290.—The same test piece after compressive loading to 4,700 kg./cm.²: The surface has become badly distorted, since the cast zinc, on account of its small tensile strength, could not withstand the tensile stresses set up in the tangential direction so that fine radial cracks developed at certain points.

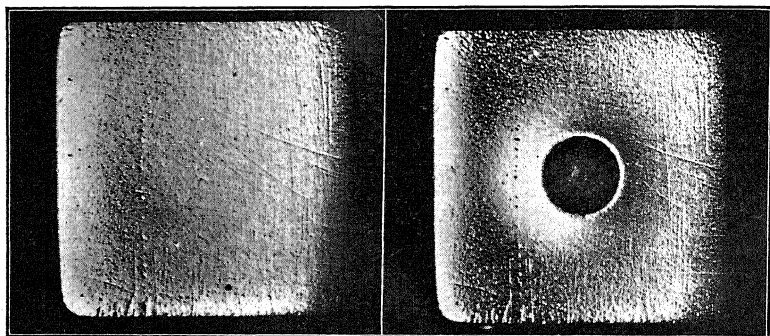


FIG. 291.

FIG. 292.

COPPER

Figure 291.—The unstressed surface of one side of a cubical copper test specimen.

Figure 292.—Indentation of a cylindrical punch under a mean compressive stress $s = 6,300$ kg./cm.²; the bulging or enlargement around the indentation may be noted. In the bulging ring-shaped area, the microscope showed a system of slip lines packed closely together in the crystal grains.

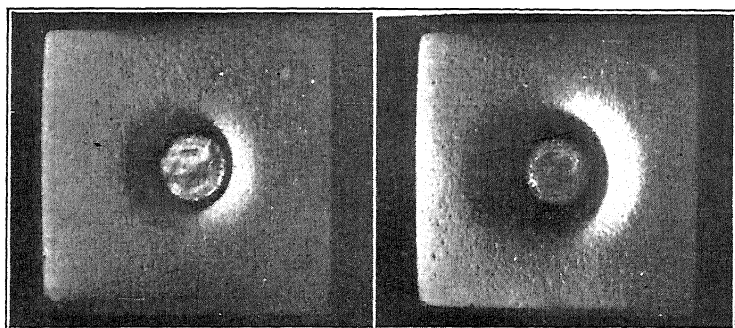


FIG. 293.

FIG. 294.

Figures 293 and 294.—Indentations of a cylindrical punch in *soft* copper at $s = 1,570$ kg./cm.² and $s = 2,800$ kg./cm.² respectively. Note the funnel-shaped indentation in the soft copper contrary to the bulging in case of the hard copper.

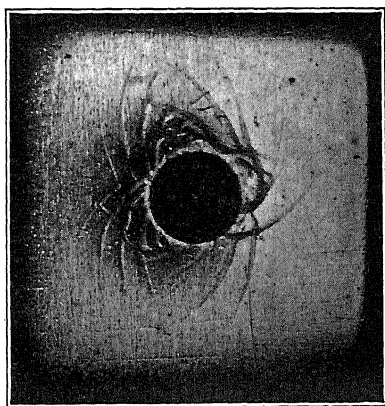


FIG. 295.

MILD STEEL

In the neighborhood of the impression, systems of slip lines having the form of logarithmic spirals may often be seen. In the surface layers, the directions of the principal stresses are in the radial and tangential directions, the directions of slip making angles of approximately 45° to those of the principal stresses; therefore the slip lines have the shape of logarithmic spirals (Fig. 295).

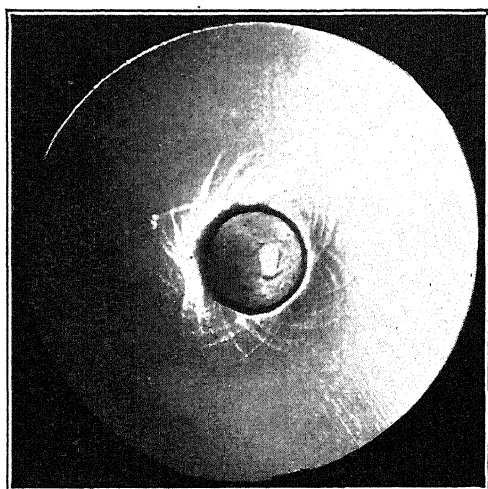


FIG. 296.

Figure 296.—This shows the beginning of the appearance of the spiral-shaped slip lines in the neighborhood of the indentation of a cylindrical punch.

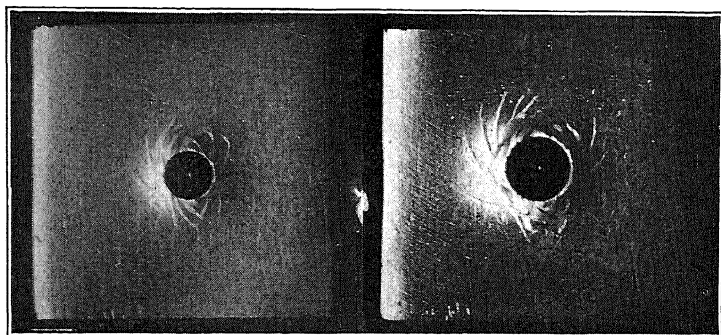


FIG. 297.

FIG. 298.

Figures 297 and 298.—Indentations of hard balls in steel.

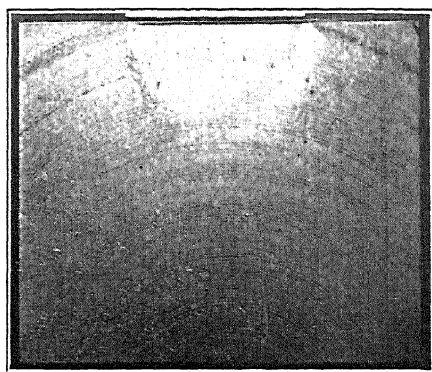


FIG. 299.

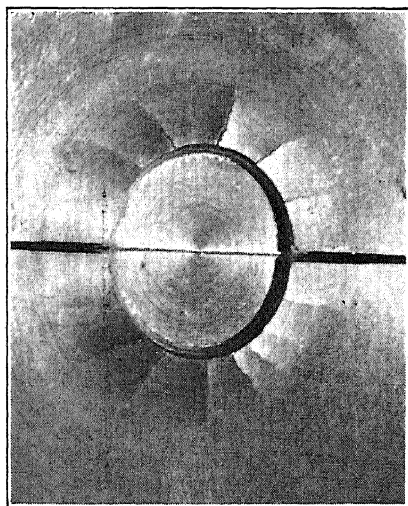


FIG. 300.

PARAFFIN

Figure 299.—This shows one half of a paraffin cylinder split along a plane through its axis. A compression test had been made with a cylindrical punch. A semicircular area of plastic deformation produced by the compression surfaces of the punch is seen. The other view of the test specimen showing the radial crack's radiating from the indentation can be seen in Fig. 300.

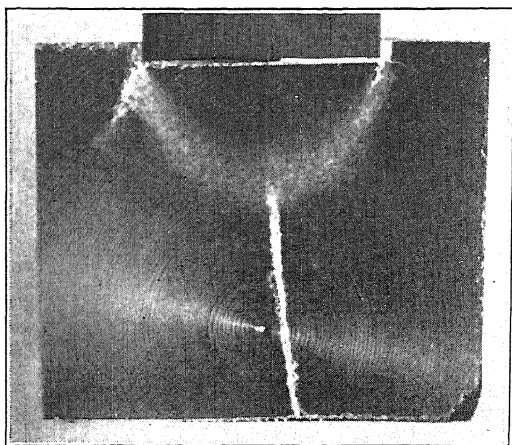


FIG. 301.

Figure 301.—Longitudinal section of a test specimen of paraffin, compressed rapidly by a cylindrical punch. The distorted region appears in the longitudinal section as a bright crescent-shaped figure.

CHAPTER 36

THE PROBLEM OF CONTACT OF ELASTIC BODIES

a. General Remarks.—If two bodies with convex surfaces are brought in contact and pressed against each other by two forces in the direction of the common normal, the surfaces become somewhat flattened near the point of contact and, as a result, stresses of considerable value are set up. H. Hertz¹ developed a mechanical theory of the contact of elastic bodies. If we imagine the convex surfaces in the neighborhood of the point of contact between two elastic bodies replaced by two flat ellipsoids, the distances between opposite points of the surfaces at the instant of mathematical or point contact is a homogeneous quadratic function of the coordinates x and y of these points (taken with respect to a right-angled coordinate system in the plane of contact). Hertz determined the shape of the surface of contact and the distribution of stresses in this surface and its neighborhood. According to him the boundary curve of the area of contact was found to be an ellipse while the pressure in the compressed surfaces was found to vary as the ordinates of an ellipsoid. This means, that if the pressure in the area of contact is plotted as a function of the coordinates x and y , the surface thus found is half an ellipsoid. On the basis of his calculation, Hertz proposed to define, as the measure of the hardness of the material, the value of compressive stress at the elastic limit in the middle of the area of contact of two equal balls compressed together. On account of the difficulty of determining the elastic limit, and on account of the cracks arising at the edges of the compressed areas in case brittle materials are tested when two balls are pressed together, as well as, in the case of ductile materials, on account of the almost unavoidable plastic compression, this method proposed by Hertz was not found practical for determining hardness and has therefore never been used.

b. Contact of Two Perfectly Elastic Spheres.—According to the Hertz theory for elastic contact, the area of contact of two spheres having radii

¹ HERTZ, H., "Gesammelte Werke," vol. 1.

r_1 and r_2 and being made of the same material, when pressed together is bounded by a circle of radius a , where

$$a = \sqrt[3]{\frac{3(1-\nu^2)Pr_1r_2}{2E(r_1+r_2)}} = 1.109\sqrt[3]{\frac{Pr_1r_2}{E(r_1+r_2)}} \quad (1)$$

and the maximum pressure acting in the center of the circle of contact is

$$p_{\max} = 0.388 \cdot \sqrt[3]{PE^2\left(\frac{r_1+r_2}{r_1r_2}\right)^2}. \quad (2)$$

Here P denotes the force under which the spheres are pressed together, E Young's modulus of elasticity, and ν Poisson's ratio. The latter is taken $\nu = 0.3$.

If a sphere of radius r is pressed on the plane surface of an elastic body of the same material the circle of contact has the radius

$$a = 1.109\sqrt[3]{\frac{Pr}{E}} \quad (3)$$

and the pressure p_{\max} is

$$p_{\max} = 0.388\sqrt[3]{\frac{PE^2}{r^2}}. \quad (4)$$

c. Contact of Two Perfectly Elastic Cylinders.—If *two cylinders with parallel axes* and radii r_1 and r_2 are pressed together by a pressure p (taken per unit of length) in the direction of the generatrices of the cylinders, the area of contact has a width $2a$, where

$$a = 1.522\sqrt{\frac{pr_1r_2}{E(r_1+r_2)}}. \quad (5)$$

The normal stress s in the area of contact is

$$s = \frac{2p}{\pi a^2}\sqrt{a^2 - x^2} \quad (6)$$

(x is here the distance of a point in the area of contact from its center line), hence the greatest pressure is given by

$$s_{\max} = \frac{2p}{\pi a}. \quad (7)$$

A cylinder of radius r , pressed on the plane surface of a body of the same material, will be in contact with the plane along a strip having a width $2a$, where a is given by

$$a = 1.522\sqrt{\frac{pr}{E}}, \quad (8)$$

p being the pressure per unit of length.

CHAPTER 37

PHOTO-ELASTIC CONTACT TESTS AND OBSERVATION OF SLIP LINES UNDER PLASTIC IMPRESSIONS

a. **Shearing-stress Lines (Isochromatics) and Shearing-stress Trajectories (Slip Lines).**—In the following a number of cases of elastic contact problems will be briefly discussed, in which the stresses depend only on two coordinates. In these cases analytical expressions for the stresses which have been established by mathematicians are available. The intention is, however, to compare the results of these calculations with certain results obtained from photo-elastic tests and also with observations of slip lines of similar cases in plastic bodies.

If a transparent specimen in the form of a thin sheet is stressed in its plane and linearly polarized light is sent through the stressed specimen by means of a nicol prism, interference phenomena or colored fringes can be produced and observed on a screen by the use of a second nicol. The credit for having developed the photo-elastic method for technical investigations belongs principally to Prof. E. G. Coker of London, to whom reference will frequently be made in the following.¹ What is essential here is that all points of a transparent stressed test piece, which are submitted to the same difference of principal stress, produce the same optical effect on the screen, on which the illuminated test piece is projected. Hence, on the screen certain colored lines will appear in regular repetition and a constant stress difference will correspond to each color. On an ordinary photographic copy of the colored picture black and white lines will appear, the black and the white lines corresponding to certain colors of the colored bands or certain given differences of principal stress and these differences may be determined by suitable calibrating methods.

¹ In this connection special reference is made to the Thomas Hawksley lecture of PROFESSOR COKER on Elasticity and Plasticity, *Proc. Inst. Mech. Eng.*, p. 897, London, November, 1926, in which he calls attention to several problems of plasticity and refers to possible applications of photo-elastic methods to treat such questions.

In a thin sheet, stressed by forces in its plane, the normal stress which is perpendicular to the plane of the sheet is zero and this direction is a principal stress direction. We call isochromatic lines the lines connecting points having the same color and corresponding to curves along which the difference of the two other principal stresses s_1 and s_2 is a constant:

$$s_1 - s_2 = \text{const.} \quad (9)$$

These curves are also lines of constant principal shearing stress, because one of the three principal shearing stresses is equal to one-half of the above difference. The isochromatic lines may also be called *shearing-stress lines*.

From the *isochromatics* or *lines of constant principal shearing stress* we must sharply distinguish the trajectories of principal shearing stress called hereafter *shearing-stress trajectories*. These latter have as their tangents the directions along which the principal shearing stresses act. They intersect the trajectories of principal normal stress at an angle of 45° . The trajectories of principal shearing stress are two orthogonal systems of curves and they coincide approximately with the lines of slip along which the Lüders' lines appear in a mild-steel test piece when the limit of plasticity is reached.

Several interesting two-dimensional cases having important practical applications may be mentioned here. An infinite body extending indefinitely on the side $y > 0$ of the x, z plane will be assumed.

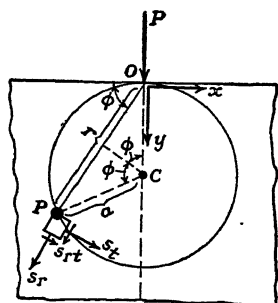


FIG. 302.—Single force P (distributed along z axis) stress s_r , a tangential normal stress s_t , and a acting on a plane surface of a shearing stress s_{rt} . The stress distribution found by Michell,

$$s_r = -\frac{2P \sin \phi}{\pi r}, \quad s_t = 0, \quad s_{rt} = 0, \quad (10)$$

consists only of radially distributed stresses, as the tangential normal and the shearing stress vanish at every point of the stressed body. The radial stresses increase indefinitely with decreasing distances r from the origin and have a resultant force P at the origin, acting in a direction perpendicular to the plane $y = 0$ and parallel to the positive direction y . The force P is,

¹ *Proc. London Math. Soc.*, vol. 32, p. 35, 1900.

hence, the resultant of the radial stresses s_r acting along any half circle having a radius $r = \text{const.}$ and taken per unit of length in the third direction, parallel to z .

The isochromatics or lines of constant maximum shearing stress are here the curves along which

$$s_r - s_t = \text{const or } \frac{\sin \phi}{r} = \text{const.} \quad (11)$$

In a circle of radius a (Fig. 302) having its center C on the y axis at distance $OC = a$, the length of the chord OP is r , and hence

$$\frac{r}{2} = a \sin \phi \quad \text{or} \quad \frac{\sin \phi}{r} = \frac{1}{2a} = \text{const.} \quad (12)$$

The isochromatics are therefore the circles containing the point O of application of the force P and being tangent to the x axis (Fig. 303). This is confirmed by the black and white strips of a photo-elastic test shown in Fig. 304, made on a celluloid piece on which a single force was applied.¹

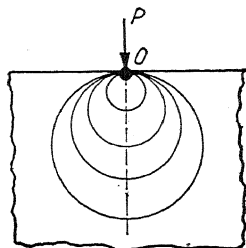


FIG. 303.—The isochromatics are the circles passing through O and tangent to plane surface.

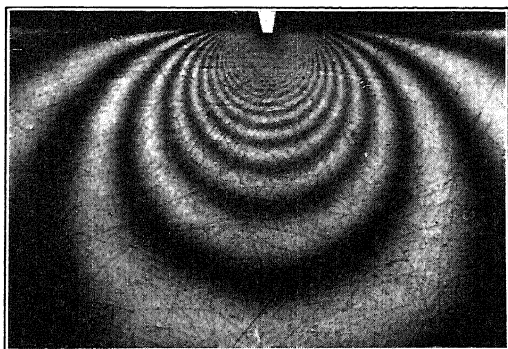


FIG. 304.—Single force on straight edge. Photo-elastic test showing circles as isochromatics.

2. *Uniform Pressure along Half Plane.*²—In an elastic body a system of plane stress can be given in polar coordinates by r, ϕ by means of a stress function F as follows:

$$s_r = \frac{F_r}{r} + \frac{F_{\phi\phi}}{r^2}, \quad s_t = F_{rr}, \quad s_{rt} = -\frac{\partial}{\partial r} \left(\frac{F_{\phi}}{r} \right), \quad (13)$$

¹ Among PROF. E. G. COKER'S numerous photo-elastic tests, most of which are published in *Engineering*, London, (a short résumé of his tests can be found in the *Proc. 1st. Internat. Congress for Applied Mechanics*, Delft, 1924) this case has also been tested. The photographs, published above, are taken from the Doctor's thesis of G. MESMER, "Vergleichende Spannungsoptische Untersuchungen und Fließ-Versuche unter konzentriertem Druck," *Z. f. tech. Mech. u. Thermodyn.*, vol. I, nos. 2 and 3, V.D.I., Berlin, 1930.

² Cf.: "Die elastischen Platten," Julius Springer, Berlin, 1925.

where the subscripts on the right side designate derivatives, the stress function F being a solution of the biharmonic equation:

$$\Delta \Delta F = 0. \quad (14)$$

Taking for F

$$F = \frac{pr^2}{2\pi} \left(\frac{\sin 2\phi}{2} - \phi \right), \quad (15)$$

we get the following distribution of stress

$$\left. \begin{aligned} s_r &= -\frac{p}{\pi} \left(\phi + \frac{\sin 2\phi}{2} \right), \\ s_t &= -\frac{p}{\pi} \left(\phi - \frac{\sin 2\phi}{2} \right), \\ s_{rt} &= \frac{p}{2\pi} (1 - \cos 2\phi), \end{aligned} \right\} \quad (16)$$

from which it may be seen, that on the side of the plane $y = 0$, $\phi = 0$ no stresses act, while for $\phi = \pi$ the stresses reduce to a uniform pressure $s_t = -p$

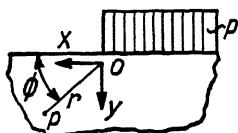


FIG. 305.—Uniform pressure p along half plane.

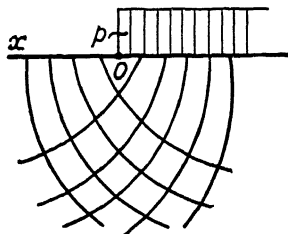


FIG. 306.—For uniform pressure p acting along a half plane the trajectories of principal stress are confocal parabolas.

(see Fig. 305). The left side of the plane $y = 0$ (Fig. 305) is free of stress, the right side is subjected to a constant pressure p .

If α is the angle of one of the directions of principal stress with the radial lines $\phi = \text{const.}$, then

$$\tan 2\alpha = \frac{2s_{rt}}{s_r - s_t}, \quad (17)$$

using Eq. (16), this reduces to

$$\tan 2\alpha = \frac{1 - \cos 2\phi}{-\sin 2\phi} = -\tan \phi, \quad (18)$$

whence either

$$\alpha = -\frac{\phi}{2} \quad \text{or} \quad \alpha = \frac{\pi}{2} - \frac{\phi}{2}. \quad (19)$$

This is characteristic of a parabola. The lines of principal stress form a system of orthogonal parabolas having the origin O as their common focus (see Fig. 306). The isochromatics or shearing-stress lines are a pencil of rays passing through the origin O , which is a singular point of the stress distribution.

3. *Uniform Pressure along a Parallel Strip.*—The superposition of two distributions of stress, as mentioned under 2, together with a uniform tension leads to the case shown in Fig. 307. The plane $y = 0$ is subjected to the action of uniform pressure $p = \text{constant}$, directed perpendicularly to the plane along a strip having a width $2a$. The stress function is

$$F = -\frac{p}{2\pi}(r_1^2\phi_1 - r_2^2\phi_2) \quad (20)$$

and the stresses are given in rectangular coordinates by

$$\left. \begin{aligned} s_x &= -\frac{p}{2\pi} \left[2(\phi_1 - \phi_2) + \sin 2\phi_1 - \sin 2\phi_2 \right], \\ s_y &= -\frac{p}{2\pi} \left[2(\phi_1 - \phi_2) - \sin 2\phi_1 + \sin 2\phi_2 \right], \\ s_{xy} &= \frac{p}{2\pi} \left[\cos 2\phi_1 - \cos 2\phi_2 \right]. \end{aligned} \right\} \quad (21)$$

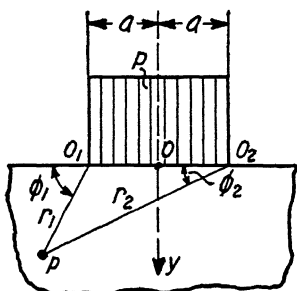


FIG. 307.—Uniform pressure $p = \text{const.}$ acting along a parallel strip on plane surface of a body.

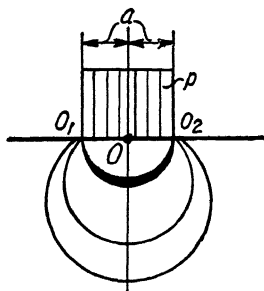


FIG. 308.—For constant pressure p acting along strip the isochromatic lines are circles passing through O_1 and O_2 .

From the formula for the maximum shearing stress at an arbitrary point

$$s_{s_{\max}}^2 = \frac{(s_x - s_y)^2}{4} + s_{xy}^2 \quad (22)$$

and using the former set of expressions for the stresses, we find

$$s_{s_{\max}} = \frac{p}{\pi} \sin (\phi_1 - \phi_2). \quad (23)$$

Hence the isochromatics are here circles, which pass through the points O_1 and O_2 (Fig. 307 or 308). The greatest value of

$$s_{s_{\max}} = \frac{p}{\pi} \quad (24)$$

is attained if $\phi_1 - \phi_2 = \pi/2$, that is on the semicircle having the width $2a$ as diameter and O as center (this circle in Fig. 308 is marked with heavy lines). On this circle the material will yield first under a pressure found by taking $s_{s_{\max}} = s_0/\sqrt{3}$

$$p = \frac{\pi}{\sqrt{3}} s_0 = 1.81 s_0, \quad (25)$$

where s_0 is the yield stress in pure tension. The trajectories of principal normal stress are a system of confocal ellipses and hyperbolas (Fig. 309)

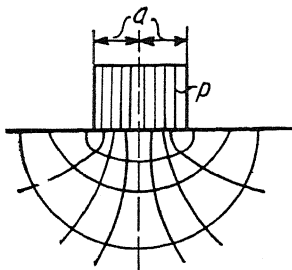


FIG. 309.—For constant pressure p along a strip the trajectories of principal stress are confocal ellipses and hyperbolas.

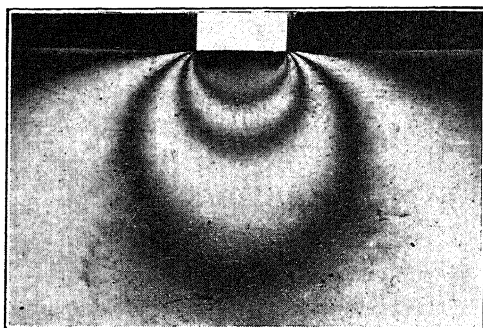


FIG. 310.—Photo-elastic test with celluloid punch producing nearly constant contact pressure. The isochromatics are circles passing through the corners of the punch.

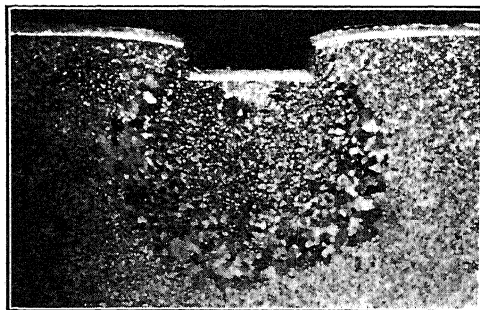


FIG. 311.—Steel. Recrystallized grain structure in zone of deformation under punch.

G. Mesmer was able to produce the isochromatics for this case by using certain precautions in preparing a special stamp of celluloid with two

carefully rounded corners, which was pressed against the test piece. The isochromatic lines, thus obtained experimentally, (see Fig. 310) were found to be very nearly circles passing through the corners of the punch as predicted by the theory.

It is perhaps of interest to mention here that by means of other well-known changes in structure due to local plastic deformations combined with a subsequent heat treatment similar observations may be demonstrated on metal pieces. This can be done by reheating a test specimen which has been previously deformed plastically until the grains recrystallize. Two such tests are shown in Figs. 311 and 312. These figures reveal the astonishing

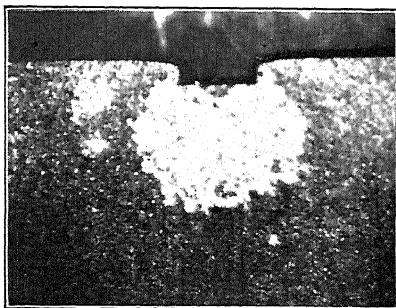


FIG. 312.—An etching of mild steel showing in white circle recrystallized zone under indentation of a punch.

fact, that the boundary of the recrystallized zone under an indentation and the lines connecting recrystallized grains of the same magnitude have a shape quite similar to the isochromatic lines of the photo-elastic tests. The degree of exactness of this correspondence has not, however, been demonstrated as yet.

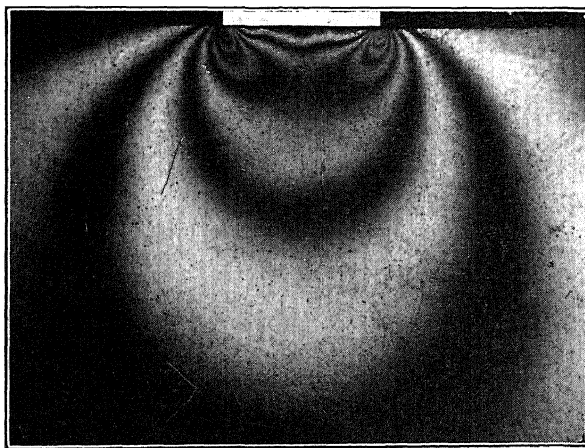


FIG. 313.—Photo-elastic test. Isochromatic curves under the pressure zone of a rigid punch with sharp corners indicating sharp concentration of stress at corners of punch.

4. *Rigid Punch*.—Using a fairly rigid metal punch having a perfectly straight edge on a piece of celluloid a distribution of isochromatic lines is obtained as shown in Fig. 313. This indi-

cates clearly that in this case (1) the isochromatics are not circles, and (2) that the stresses increase considerably towards the two corners of the punch. According to the elastic theory the pressure in the surface of contact must become theoretically infinite at

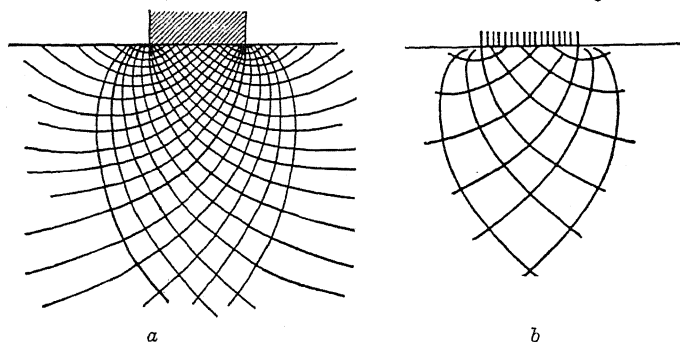


FIG. 314.—*a*. Slip lines for concentrated constant pressure acting along edge determined by G. Mesmer. *b*. Slip lines for same case as observed by photoelastic test in celluloid plate.

the corners of the punch. Figure 313 shows a great concentration of the stress by the repetition of the fringes at the corners. Hence, immediately after the slightest application of a load under a perfectly rigid plane punch, yielding must start at the sharp edges of the punch. Consequently, a radiating system of slip or flow lines frequently can be observed in soft-steel pieces under the action of concentrated loads and starting



FIG. 315.

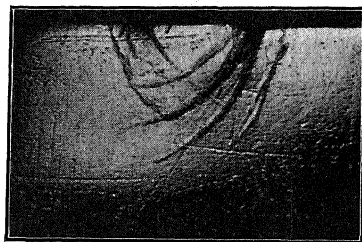


FIG. 316.

FIGS. 315 and 316.—Slip lines produced by punch in steel.

from the sharp edges of the punch. In more brittle material fracture would start from these edges. General observations of this kind will be quoted in the following.

5. *Slip Lines*.—It is of interest to compare the shape of the trajectories of principal shearing stress in a perfectly elastic

material with the shape of the slip lines as observed in similar cases of punching in mild steel. The former lines can be determined mathematically from the stress field as obtained analytically or by a photo-elastic test, while the latter may be produced by a test on steel under concentrated pressure and be observed directly by suitable etching. Figures 314 to 318 show such a comparison. In Fig. 314*b* the trajectories of principal shearing stress can be seen as obtained by a photo-elastic test and in Fig. 314*a* as computed by the formulæ 21. In the etchings, Figs. 317 to 324 the slip lines, which appear as



FIG. 317.—Slip lines and plastic region under pressure zone of a rigid punch in mild steel (Etching.)

dark lines or strips, can be compared. These figures and others observed by Mesmer (compare also Fig. 330) indicate that as a first approximation the *Lüders'* lines have a shape similar to the shearing-stress trajectories in the most highly stressed portion under a concentrated load for an elastically deformed material under the same system of applied stress. How nearly exact this is, however, has not yet been thoroughly investigated.

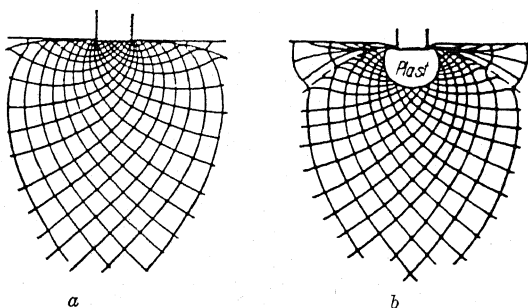


FIG. 318.—Slip lines determined by photoelastic tests under rigid punch. *a.* Under comparatively small local pressure. *b.* Under high local pressure. (According to G. Mesmer.)

c. Two Concentrated Loads. Plastic Flow in the Rolling Process.—If a thin sheet of metal is rolled between two rigid cylinders, plastic flow is produced by two concentrated loads acting in two parallel straight strips on the surface of the rolled

sheet. To study the distribution of stress which is produced under this kind of severe compression, so much used in the process of rolling, test specimens of mild steel of the shape shown in Fig. 320 were severely stressed locally in compression by two hard steel punches. The manner of yielding depends largely on the

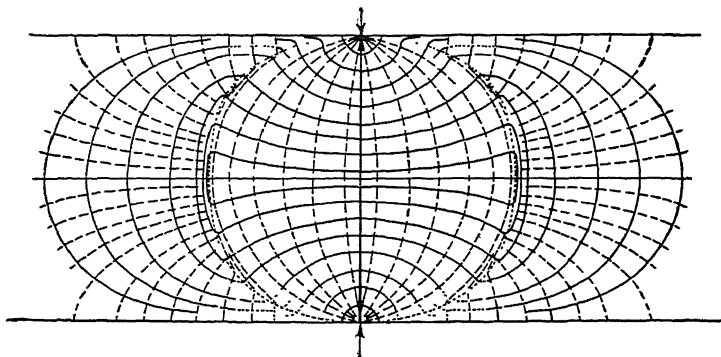


FIG. 319.—The trajectories of principal stress produced by two equal concentrated forces P in a strip of a perfectly elastic material. The forces P act in the perpendicular direction to the free edges of the strip. (According to G. Mesmer.)

ratio of the width c of the pressure surface to the thickness of the specimen measured in the direction parallel (and also perpendicular) to the direction of the compressive forces.

If the length l of the punch is several times (at least five times) the width c of the punch (Fig. 320), assuming a uniform application of the load and close parallelism of the compression surfaces, there results in the middle part of the test piece plane plastic strain. (The stresses depend only on two coordinates.) If, however, the length l is not very different from the width b , a three-dimensional strain distribution results. If l is small compared with c , the material flows away toward the free sides of the specimen and the plastic flow is entirely different from that for the case of "plane strain."

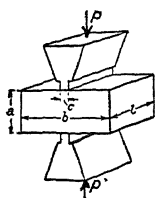


FIG. 320.—Arrangement to apply two concentrated loads.

On the other hand, if the height a of the test specimen is comparable with the width c of the punch, the stresses produced by each of the two opposite punches influence those produced by the other. If, on the contrary, a is much larger than c , the stress distribution in the neighborhood of the punch is about the same as if the second punch were not present and the first acted on an infinitely large test piece.

A few photographs of the regular markings observed on the sides of such test pieces of mild steel and of etchings of slip lines in the plastically deformed portions in cross-sections are shown in Figs. 321–323. Such observations may help in analyzing the distribution of stress encountered in the process of rolling of steel blocks or sheets.

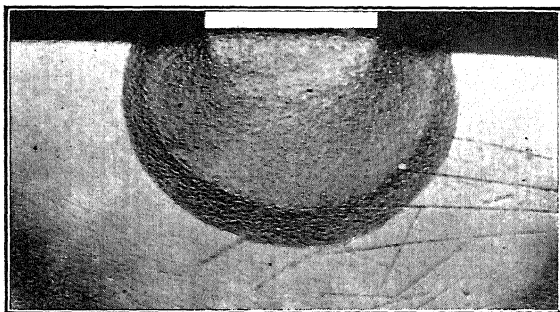


FIG. 321.—Bulging of surface of a thin sheet of steel under concentrated pressure along narrow edge.

The influence of the dimension l , measured parallel to the edge of the punch and perpendicular to the plane of the photographs, is shown in Figs. 321, 322, and 323. Both Figs. 321 and 322 represent essentially about the same case, namely, the action of a concentrated load distributed over a rectangular area of contact. If the load is applied along the narrow edge

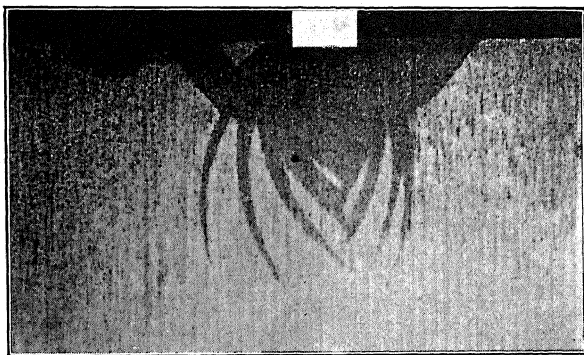


FIG. 322.—Slip lines in pressure zone of a long rigid punch in mild steel. (Etching.)

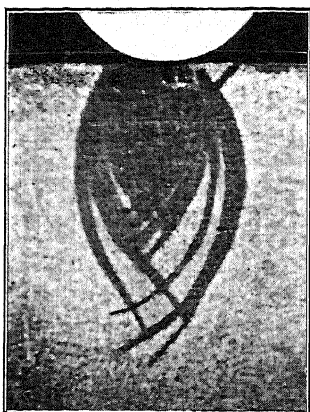
of a thin sheet, below the area of contact, both flat sides of the sheet will bulge out. The test specimen in Fig. 321 had a thickness $l = 1.1$ mm., a height $a = 37$ mm., and a width $b = 45$ mm.; the width of the punch was $c = 9$ mm. On both sides of the test piece slight bulges appeared, such as the one shown in Fig. 321, which were bounded by curves similar to

ellipses. The material tends in this case to flow away toward the free sides of the flat specimen. In the other case, where the length l was large compared with the width c of the punch, slip lines appear like those shown in the

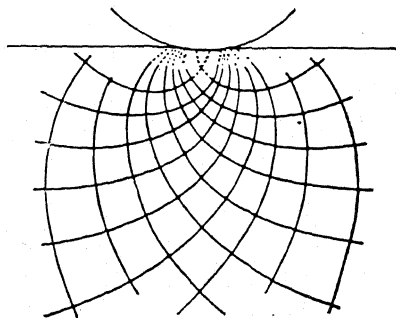


FIG. 323.—Pressure zone in steel produced by concentrated load. (Etching.)

photograph of an etched cross-section (Fig. 322) of the test piece. Now, a wedge-shaped plastic portion of the specimen is driven by the punch into the elastically reacting neighborhood and numerous slip lines appear. Another similar example can be seen in the photograph, Fig. 323 of a Fry etching.



a



b

FIG. 324.—*a*. Slip lines in steel piece obtained by impression of a hard cylinder. (Etching.) *b*. Slip lines under contact area of a rigid cylinder with a celluloid sheet obtained by photo-elastic test. (According to G. Mesmer.)

The impression of a long, solid, rigid cylinder on a soft-steel piece is shown in section by the etching of Fig. 324*a*. In the next Fig. 324*b* are shown the shearing-stress trajectories for the same case, as they were constructed from

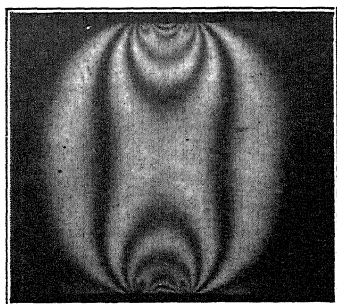


FIG. 325.

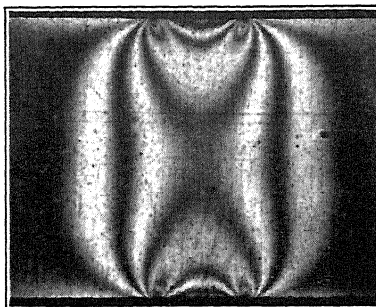


FIG. 326.

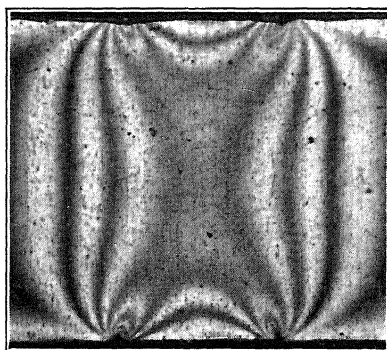


FIG. 327.

FIGS. 325, 326, and 327.—Photo-elastic tests. Isochromatic lines in pressure zones of a thin sheet of celluloid compressed between two rigid punches. Ratio of height of specimen to width of punch $a:c = 3, 2, 1$.

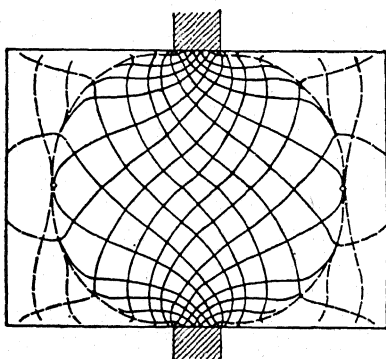


FIG. 328.

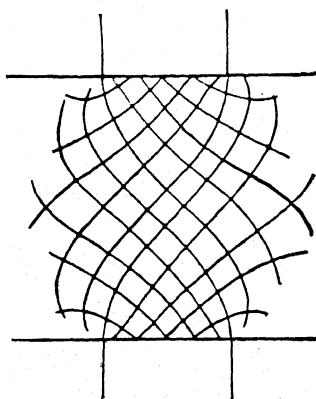


FIG. 329.

FIGS. 328 and 329.—Slip lines obtained by photo-elastic test in sheet compressed between two punches. Fig. 328 for $a:c = 3$; Fig. 329 for $a:c = 2$.

a photo-elastic test by G. Mesmer with a celluloid test piece stressed purely elastically. The slip lines in the steel specimen apparently have a resemblance to the net of the trajectories as obtained from the photo-elastic test.

The large influence of the ratio a/c on the stress distribution is clearly shown by comparing the three photographs of isochromatic lines in Figs.

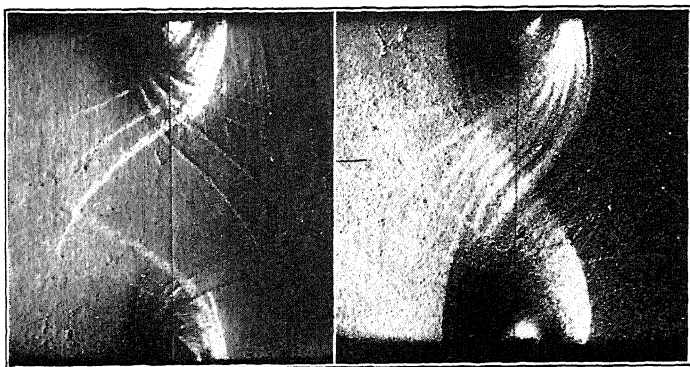


FIG. 330.

FIG. 331.

Figs. 330 and 331.—Slip lines in steel piece compressed between two rigid punches. Ratio $a:c = 3$.

325, 326, and 327, which were obtained for a ratio of the height a of the specimen to the width c of the punch equal $a/c = 3, 2$, and 1 . The corresponding trajectories of shearing stress are shown in Figs. 328 and 329 for $a/c = 3$ and 2 , and the lines of slip for the case $a/c = 3$ in Figs. 330 and 331.

A very interesting set of slip lines was obtained by H. Meyer and F. Nehl in a cold-rolled steel sheet, which can be seen in Fig. 333. These lines

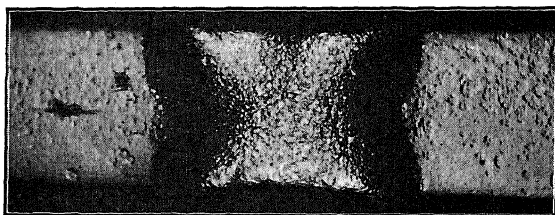


Fig. 332.—Bulging of narrow side of a steel piece under severe local pressure. Ratio $a:c = 1$.

were gradually formed during the rolling of the sheet. When the rigid rolls travel along the surfaces of the sheet, they produce in the area of greatest compression a set of slip lines not greatly dissimilar to those in Figs. 330 to 331, and gradually, during the rolling, these lines proceed forward, relative to the rolled sheet, in a continuous manner.

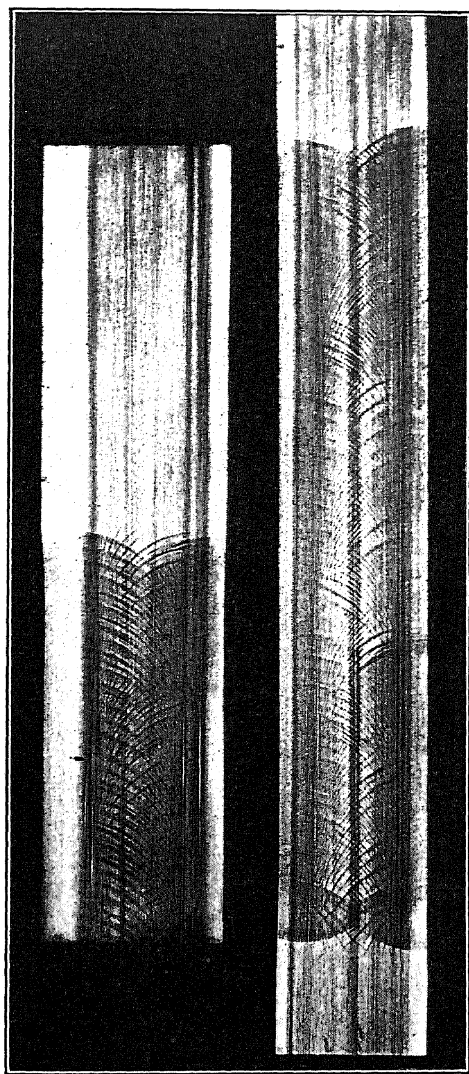
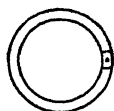


FIG. 333.—Slip lines in longitudinal section of a cold-rolled steel sheet. (Etching.) (According to H. Meyer and F. Nohl, *Stahl und Eisen*, 1925.)

CHAPTER 38

INHERENT AND RESIDUAL STRESSES

By inherent stresses¹ we will understand a system of internal stresses, which may exist in a body when no external loads or moments act on the surface of the body. The entire surface of the body can be free of stress, which means, that on each element of the surface the corresponding components of the normal and of the shearing stress vanish. But it should be noticed, that this is not a necessary condition for the existence of a system of inherent stresses in a body. All that is necessary is that the *resultant* forces and *resultant* moments produced by these stresses, acting along the surface, shall vanish within limited parts of this latter.



Inherent stresses can be produced or may be present in a perfectly elastic material. Such stresses will be produced, for example, if a ring of elastic material (for example, spring steel) be slotted radially (Fig. 334), after which the ends are elastically bent until they are brought together and then welded. If all traces of welding be effaced, an observer who had no knowledge of the previous treatment of the ring will not suspect that the ring is stressed and if he suspects it, he will not be able to decide definitely whether or not the ring is stressed until he applies special methods. In elastic materials, inherent stresses may result especially from non-uniform heating; in such cases we speak of "thermal stresses." These will result, for instance, in the case of a tube or pipe cooled on the outside and carrying a hot fluid.

¹ German engineers refer to such stresses, which may be present in a body free of external loads or moments as "Eigenspannungen," analogous to mathematicians, who use the word "Eigenfunktionen" if they wish to express the fact that a set of functions belongs to a differential or integral equation under given boundary conditions. It seems that there is no adequate term for both expressions commonly used in English. The word "inherent stress" for "Eigenspannung" was proposed by B. F. Langer of the Research Laboratories of the Westinghouse Electric and Manufacturing Company. The word "residual stress" expressing the German "Nachspannung" has been used by mechanical engineers for a long time.

If, in a stressed material, only one portion is permanently strained, and then the external forces are removed, the material in the neighborhood of the permanently strained region will, in general, be subjected to inherent stresses. Stresses of this kind, remaining after partial plastic flow, may be called *residual stresses*.

If, for example, a hardened steel ball is pressed into a piece of soft iron or ductile metal, the material in the neighborhood of the permanent indentation, after removal of the load, cannot remain unstressed. In the region which has been permanently deformed by the ball, besides the normal stresses, acting parallel to the load, considerable compressive stresses also must have acted in the lateral direction. The latter will cause stresses in the elastic neighborhood of the indentation and a part of these will continue to exist after the compressive load has ceased to act. The plastically distorted part behaves, under the compression of the ball, like a hard wedge driven into a tree trunk. The inherent or residual stresses present after severe plastic deformation are familiar to steel men and engineers on account of their deleterious action on pressed, forged, or rolled bars, especially after a treatment under decreasing temperatures or after the bars or sheets have undergone severe cold work. Fractures are caused frequently by the action of residual stresses, if the forged or rolled pieces are not annealed before they are further deformed. Methods of estimating these residual stresses may have several practical applications.

The theory of residual stresses can be based on assumptions analogous to those on which is founded the theory of plastic deformations, which are the causes of the existence of these stresses. As in the case of the fundamental assumptions with regard to the mechanical conditions of plastic flow, for residual stresses several cases may be distinguished, according to the magnitude of the deformations after the removal of the load or to the character of the stress-strain relation for loading and unloading. In the following, two cases will be discussed.¹

¹ For methods relative to the calculation of residual stresses, there may be mentioned papers by E. HEYN, MARTENS-HEYN, "Materialkunde," 2d ed., p. 280, 1912; *Festschrift Kaiser-Wilhelm Gesellsch.*, p. 121, 1921; and *Stahl und Eisen*, 1917, G. MASING, several papers publ. by the Siemenskonzern, Berlin, 1923-1926, CH. DUGUET, *loc. cit.*, A. U. L. FÖPPL, "Drang u. Zwang," vol. 2, p. 297, Munich, 1920, and others.

In a rigid aggregation of crystal grains, a number of grains may undergo permanent shearing deformation, while the neighboring ones may be deformed only elastically. From this it follows that internal stresses are also of importance in considering the phenomena of small relative displacements occurring in the microstructure of a plastically deformed metal. The permanent displacements, which one may recognize in photomicrographs of the structure of plastically deformed metals as translations, etc., in certain crystal grains, must be accompanied by an elastic stress in the neighborhood. We have recognized two different types of slip surfaces which accompany plastic deformation of metals, namely, the coarse flow figures (Lüders' lines) and the small gliding surfaces inside the crystal grains themselves. In an analogous way, *two kinds of inherent stresses may be distinguished* according to whether the elements, in which they occur, are comparable in size to that of the stressed material body or whether these elements are of the order of size of the crystal grains. Although so far no quantitative statements relative to the internal stresses in the microstructure of materials may be made,¹ the magnitude and distribution of the inherent or residual stresses in large portions of stressed metal pieces after severe plastic deformation may be quantitatively estimated, as shown in the following.

a. First Method of Calculating Residual Stresses Assuming a Linear Stress-strain Relation for Unloading.—In metals having a definite yield point, the residual stresses after unloading may, as a first approximation, be obtained by assuming that after plastic deformation and subsequent removal of the load the metal behaves like a perfectly elastic material. To show what is meant by the preceding statement, let us consider in Fig. 335 an idealized stress-strain diagram for mild steel. If a bar of soft iron, previously stressed somewhat above the yield point in tension, be unloaded, a diagram *OABC* (Fig. 335) will result. If the bar is loaded again in tension, it will be found, as long as the stress remains below a certain value smaller than the original yield stress, that it behaves not only as an elastic body, but that the modulus of elasticity will be found of practically the same value as that observed before permanent strain. It is, therefore,

¹ The significance of the elasticity of the metals, in connection with their plastic deformations with consideration of the phenomena occurring in the crystal grains and the question of residual stresses has been recognized by E. HERN particularly in his papers quoted above. His "hidden elastic" stresses relate mainly to residual stresses in the crystal grains in contrast to his "Reckspannungen." On residual stresses in brass compare also C. MASING (*Veröffentlichungen aus dem Siemenskonzern*, Berlin, vol. 3, no. 1, 1923; no. 2, 1924; vol. 5, nos. 1 and 2, 1925; *Z. f. Metallkunde*, p. 257, 1924; also *Proc. 1st and 2d Internat. Cong. for Applied Mechanics*, Delft and Zürich; and Beckinsale.

permissible to replace the line BC corresponding to the removal of the stress in a tensile test by a straight line having the same inclination to the base line as "Hooke's straight line" OA for the first loading (Fig. 335).

In other words, it is possible to obtain in some degree a corresponding picture of the residual stresses in soft iron after plastic deformation if from the stresses

$$s_x^*, s_y^*, \dots \quad (1)$$

acting during the plastic flow certain ideal stresses

$$s_x', s_y', \dots \quad (2)$$

are subtracted. The latter are assumed to act as if the body would be a perfectly elastic body and they are so chosen, that when combined with the preceding system of stress the required values of the resultant forces and moments acting on the body will result. For complete unloading for example, these external resultant forces and moments must vanish. The corresponding resulting system of stress

$$s_x = s_x^* - s_x', s_y = s_y^* - s_y', \dots \quad (3)$$

is the system of residual stresses.

Hence, this simplest theory of residual stress assumes that, during the process of unloading, Hooke's law for stress and strain holds. Some examples to which the preceding shall be applied, are the following:

1. *Residual Stresses in Twisted Bar.*—As an example let us determine the residual stresses which will result if a steel bar with circular cross-section is twisted above the yield point in torsion, and subsequently the torque is released. Neglect-

ing at first the cold-work or work-hardening effect on the material during yielding, an ideal stress-strain curve in pure shear similar to that shown in Fig. 335 for tension can be assumed. This means that the original distribution of stress in the twisted bar (which acts during the yielding of the bar and which was denoted above by the asterisk) will consist of shearing stresses s^* , dependent on the variable radius r such as represented by the broken line OAB in Figs. 336, 337 and 338. Let us represent the values of shearing stress s , of the unit shear γ at a distance r

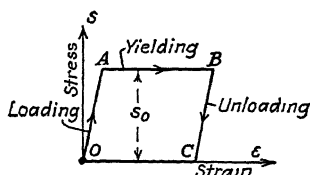


FIG. 335.—Idealized stress-strain diagram for loading and for unloading.

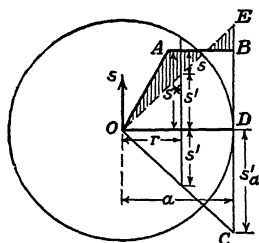


FIG. 336.—Torsion. The shaded ordinates are the residual stresses s in a permanently twisted round bar. Broken line OAB represents initial distribution of shearing stresses s^* .

from the axis of the bar and of the angular twist θ at the instant that yielding is interrupted by s^* , γ^* , θ^* . If the bar be unloaded, it untwists through some angle θ' . The unit shear along a circle of radius r then decreases an amount $\gamma' = r\theta'$ from its original value $\gamma^* = r\theta^*$, so that its value becomes

$$\gamma = \gamma^* - \gamma' = r(\theta^* - \theta'). \quad (4)$$

Since Hooke's law holds for unloading, the shearing stress having the initial value s^* decreases by an amount proportional to γ' , namely by $s' = G\gamma'$ where G designates the modulus of rigidity. Therefore, to obtain the resultant stress s after a certain reduction of the applied torque it is necessary to subtract from the original plastic distribution of stress represented

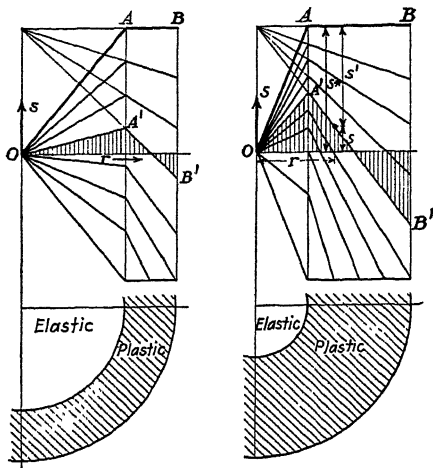


FIG. 337.

FIG. 338.

Figs. 337 and 338.—Torsion. The thin broken lines represent the shearing stresses in a round bar stressed above the yield stress and during the subsequent unloading of the bar. The line OAB gives the initial distribution of stress; the line $OA'B'$ indicates the residual stresses after removal of the external torque.

by the broken line OAB in Figs. 336 to 338 a linear distribution of stress s' , indicated by the straight line OE chosen so that $DE = DC$. In both Figs. 337 and 338, which represent two different degrees of plastic flow (in the second figure plasticity has penetrated to a greater depth than in the first), the distributions of stress during the removal of the torque are shown by sets of broken lines. As may be seen, the shearing stresses farthest from the center decrease the most during unloading. To determine now those lines which correspond to a complete removal of the external torque, the line OE in Fig. 336 must be so chosen, to set up shearing stresses having the same twisting moment $M' = M^*$ as the stresses s^* . From the theory of elastic torsion or by integrating the stresses s' over the section it is known that the moment of the stresses s' must be

$$M' = \frac{\pi a^3 s_a'}{2}. \quad (5)$$

This equation determines the shearing stress s_0' at the outer fiber $r = a$, if the moment M' be equated to the moment M^* at which plastic flow was stopped. The residual stresses after unloading are shown in Figs. 336, 337 and 338 by shaded ordinates.

The preceding methods may also be applied to those cases in which the stresses during yielding are not independent of deformation, but may increase with deformation according to some given law such as was the case in Chap. 18 for calculating the shearing stresses in a plastically twisted round bar, under a general law of deformation. If, for example, plastic flow in a twisted bar with circular cross-section is interrupted at a stress distribution as represented by the curve 1 in Fig. 339, the distribution of the residual stresses after unloading is given by the curve 3, which was obtained by subtracting from the ordinates of the curve 1 those of the straight line 2-2. The slope of the latter is to be so chosen that the "ideal" moment M' of the shear stresses s' is equal to the given moment M^* of the stresses represented by curve 1.

2. *Residual Stresses in Hollow Cylinders Stressed by Internal Pressure and in Rotating Cylinders Stressed beyond the Yield Point.*—In a similar manner the residual stresses in a thick-walled tube or in a rotating cylinder may be obtained. If, for example, the stress-strain curve of the material can be expressed by a power function

$$s = s_0 \left(\frac{\gamma}{\gamma_0} \right)^m, \quad (6)$$

where s is the shearing stress producing a unit shear γ (s_0 , γ_0 are two arbitrarily chosen corresponding values of stress and unit shear in the diagram for pure shear) and the exponent m must be taken $0 < m < 2$; then using the methods given in Chap. 29 the radial and tangential stresses s_r^* and s_t^* in a thick-walled cylinder may be computed for the moment when the plastic flow is interrupted by the following equations:¹

$$\left. \begin{aligned} s_r^* &= -\frac{pb^m}{a^m - b^m} \left(\frac{a^m}{r^m} - 1 \right) \\ s_t^* &= \frac{pb^m}{a^m - b^m} \left((m-1) \frac{a^m}{r^m} + 1 \right) \end{aligned} \right\} \quad (7)$$

Here a and b are the outer and inner radii of the tube, and p is the internal pressure. It is assumed that the tube does not change its dimensions in the axial direction.

Assuming that during the subsequent decreasing of the pressure p a linear stress-strain law would hold, the second stress system (denoted by

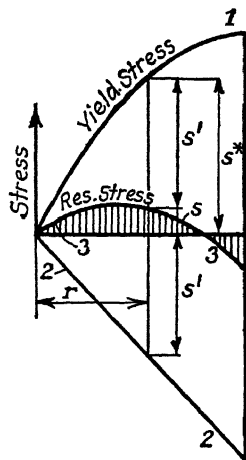


FIG. 339.—Initial yield stresses s^* and residual stresses s in round bar after permanent twist. (General law of deformation for loading.)

¹ *Trans. A.S.M.E., Applied Mech.*, 1930.

the primes) would be given by exactly the same formulæ as the one just referred to taking $m = 2$

$$\begin{aligned}s_r' &= -\frac{pb^2}{a^2 - b^2} \cdot \left(\frac{a^2}{r^2} - 1\right), \\ s_t' &= \frac{pb^2}{a^2 - b^2} \cdot \left(\frac{a^2}{r^2} + 1\right).\end{aligned}\quad (8)$$

Hence, the residual stresses acting in the tube after the internal pressure p has been removed will be given by the stress differences

$$s_r = s_r^* - s_r', \quad s_t = s_t^* - s_t'. \quad (9)$$

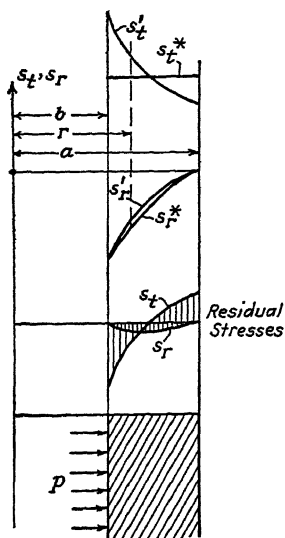


FIG. 340.—Residual stresses in a thick-walled cylinder which has been permanently deformed by high internal pressure p ; s_r^* , s_t^* are the stresses just when plastic flow was interrupted.

It should be remembered, however, that these expressions will only hold when at no place within the tube is the limit of plasticity reached a second time during the removal of the pressure. An example is shown in Fig. 340 taking $m = 1$ for the stress-strain curve.

A further example from practical engineering may be mentioned here. The high-speed rotating discs of steam turbines are stressed by centrifugal force. In order to prevent unforeseen destruction of these discs by hidden flaws, they are tested at a speed considerably above normal. Thus they are made to deform plastically in certain parts and this plastic stress distribution may be determined. The question then arises as to what residual stresses may be expected in these overstressed discs. Recently, it has been proposed to over-speed these discs with the idea of obtaining a better stress distribution under ordinary running conditions. By producing plastic deformation near the center of the discs the residual stresses present are such as to reduce considerably the stresses due to centrifugal force in these most highly stressed parts when the rotor is operating at normal speed.¹

b. Experimental Demonstration of Residual Stresses.—The residual stresses existing in severely cold-rolled or drawn bars of ductile metals can be demonstrated by suitable methods. The late E. Heyn has worked out such a method.² From a brass bar containing 58 per cent copper, 41 per cent zinc, and 1 per cent lead, which was cold drawn from a diameter of 28 mm. to 25 mm.

¹ Cf. STODOLA, A., "Steam and Gas Turbines," Engl. transl., p. 1080; also F. LÁSZLÓ, Geschleuderte Umdrehungskörper im Gebiet bleibender Deformation, *Z. f. ang. Math. u. Mech.*, No. 5, p. 281, 1929.

² "Metall und Erz," p. 411, Halle, 1918.

two test pieces were cut and the length very carefully measured. Then a certain portion of the cylindrical surface was machined

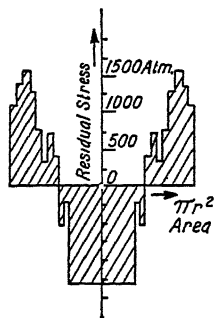


FIG. 341

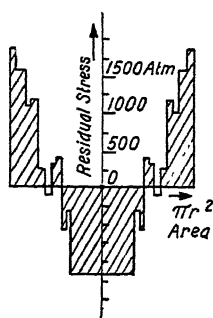


FIG. 342.

FIGS. 341 and 342.—Residual stresses in cold-drawn brass bars. The ordinates are the axial normal stresses in the circular cross-section. (According to E. Heyn.)

down in a lathe, the length again measured, and this procedure subsequently repeated several times. From the changes of length thus observed Heyn could show that the cold-drawn cylinder contained considerable stresses in the axial direction. He found the distribution of residual axial stress, which is reproduced in Figs. 341 and 342. The first shows the residual stresses five days, the second two years after drawing. Using the theory worked out above we may compute the residual stresses from the observed changes in length as follows. Let $s = f(r)$ be the unknown distribution of these stresses acting in the axial direction in a circular cross-section of a bar whose outer radius is a . As there is no resultant force acting over any cross-section, equilibrium demands that

$$\int_0^a s r dr = 0. \quad (10)$$

This means that the integral of the stress curve plotted with the variable (r^2) must have equal positive and negative areas when (r^2) varies from 0 to a^2 . If now an outer portion of the bar is machined down and the outer radius a of the bar is brought down to r the shaded areas in Fig. 343 under the stress curve are

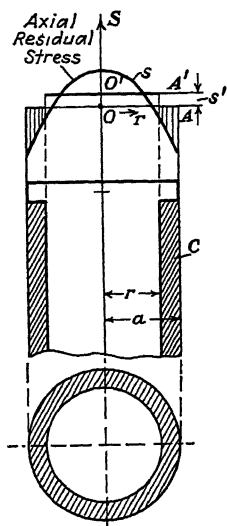


FIG. 343.—Heyn's method to measure axial residual stresses in cold-drawn round bars.

annihilated. Hence, equilibrium requires a shifting of the zero line which was originally OA by an amount s' to the position $O'A'$ given by

$$\pi r^2 s' = 2\pi \int_r^a s dr \quad (11)$$

Solving this equation for s by taking the derivative gives

$$s = -\frac{1}{2r} \frac{d(r^2 s')}{dr}. \quad (12)$$

The shifting of the zero line by s' is observed by the changes of the unit extensions $\epsilon' = s'/E$ of the bar (E = Young's modulus). Thus the residual stresses s are found.

If for example the observed change in length after subsequent machining may be expressed by a power function

$$s' = c \left(-1 + \frac{r^n}{a^n} \right), \quad (13)$$

the residual axial stresses will be given by the equation

$$s = c \left(1 - \frac{n+2}{2} \cdot \frac{r^n}{a^n} \right), \quad (14)$$

containing the same power r^n . If in the inner portion of the bar tensile (residual) stresses are acting by removal of an outer layer the compressive stresses will be annihilated; hence the tensile stresses at the center must also be diminished and the bar will contract during the subsequent reductions of its diameter. If, on the contrary, the outer portion is under tension, the bar will expand longitudinally. The latter case was observed by Heyn in the cold-drawn brass bars; the former case in quenched steel bars (quenched from 600°C. in water at 25°C.). Cold-drawn bars have compressive residual stresses in their central portion while quenched bars have tensile residual stresses in this portion.

c. Second Method of Finding Residual Stresses Assuming a General Law of Deformation for Unloading.—Tests with subsequent change of sign in stress, for example, tests where the specimen is subjected first to tensile and later to compressive stress, or torsion tests where the bar is twisted first in one direction and then in the opposite direction above the plastic limit, show that the stress-strain curve for the reversal of stress may differ considerably in its shape from that of the first stress-strain curve for direct loading. As an example, the shape of a stress-strain diagram in pure shear containing also the portion of the curve for reversed twisting is shown in Fig. 344 for mild steel. The shape of such curves for twisting in a reversed sense seems also to depend on the amount of cold work to which the material has been subjected in the previous plastic deformation. The

curves for unloading after different amounts of cold work may differ from each other as shown in Fig. 346 for pure shear. The first section PQ (Fig. 344) of the curve for the unloading, however, seems to differ but little from a straight line.

Using these observations, known also as the "Bauschinger effect," it is possible to improve the first method of calculation as

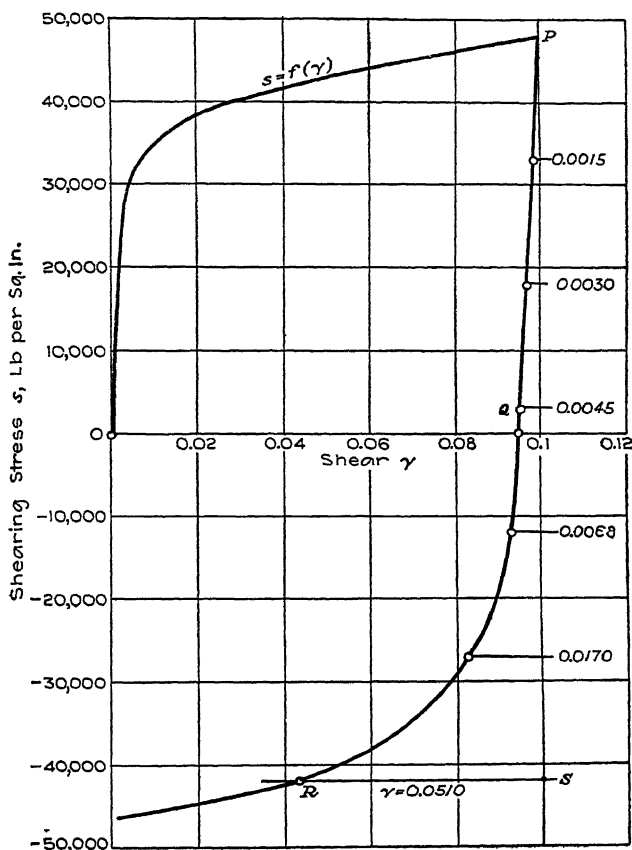


FIG. 344.—The stress-strain diagram in pure shear for direct and for reversed loading. Abscissae: unit shear γ ; ordinates: shearing stress s . (Curve PQR for unloading and loading in reversed sense.)

mentioned above under section a) and to construct the curve of residual stresses by using a curved stress-strain diagram not only for loading but also for unloading as obtained from tests, such as the line PQR in Fig. 344.¹

¹ Relative to such tests see W. BADER, Dissertation, University of Göttingen, 1927.

We may first assume that the same curve PQR can be used for example to obtain the residual stresses in a twisted bar of circular cross-section having

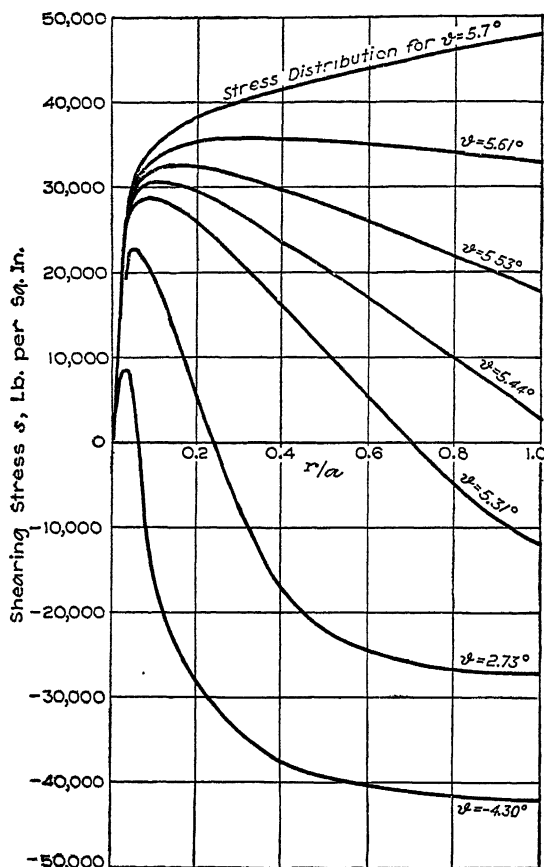


FIG. 345.—Distributions of shearing stress s in a round bar under torsion during unloading and subsequent twisting in reversed sense for various angles of twist ψ per unit of length. Abscissae: r/a ; r radius of point in which stress indicated, a outer radius of bar ($a = 1$ in.). Ordinates: shearing stress s . (Stress curves $s = f(r/a)$ were obtained using stress-strain diagrams shown in Fig. 344.)

a diagram of pure shear as given in Fig. 344 at all distances r from the center of the bar.¹ The result of this analysis is contained in Fig. 345 which shows the residual stresses in a cylindrical bar of 2-in. diameter for the

¹ A more general assumption would be to consider corresponding to each grade of cold work an individual curve $s' = f(\gamma')$ for unloading as shown in Fig. 346 and to apply the same method as used above for computation of the residual stresses in Fig. 345.

angles of twist indicated in the figure. The sharp corners of the previous curves (Figs. 337 and 338) have now disappeared.¹

By cold drawing the mechanical properties of a wire are not changed uniformly. A cold-drawn steel wire is, as has been shown by Lea and Batey,² for example harder in the central than in the peripheral parts. The distri-

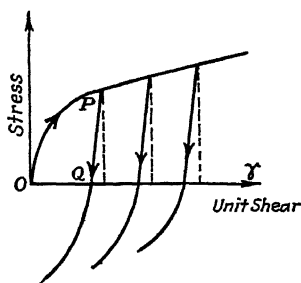


FIG. 346.

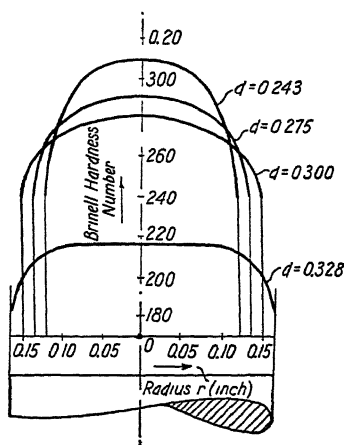


FIG. 347.

FIG. 346.—Stress-strain curves in pure shear for direct loading, for unloading and loading in reversed sense corresponding to different grades of cold work.

FIG. 347.—Change of Brinell hardness with subsequent cold drawing of wire; d diameter of wire. (According to Lea and Batey.)

bution of the Brinell hardness number over the cross-section of cold-drawn wires after subsequent drawing and cold work is shown in Fig. 347 for the wire diameters $d = 0.328, 0.300, 0.275$, and 0.243 in. Since obviously larger amounts of cold work correspond to larger Brinell hardness numbers (measured, perhaps, by the principal stress difference necessary for yielding) we understand why in cold-drawn wires comparatively great residual stresses must remain. To remove these stresses it is necessary to anneal the wire.

¹ For examples of distributions of residual stresses, see *Trans. A. S. M. E. Mech. Div.*, 1930.

² *Proc. Inst. Mech. Eng.*, no. 4, p. 865, London, 1928.

CHAPTER 39

ELASTICITY AND PLASTICITY AT ELEVATED TEMPERATURES. CREEP OF METALS

a. Isotropic Elasticity.—We have seen, that of the polycrystalline materials mild steel, if subjected to a homogeneous state of stress at normal temperatures shows a fairly well-defined limit of plasticity or yield point with increasing stress. Tests have led to the result, that the limit of plasticity of mild steel under sufficiently low temperatures might be considered in first approximation to depend on a certain stress condition. Designating by s_1 , s_2 , and s_3 the principal stresses and by s_0 the yield stress in pure tension, if

$$(s_1 - s_2)^2 + (s_2 - s_3)^2 + (s_3 - s_1)^2 < 2s_0^2, \quad (1)$$

the strains produced remain purely elastic and the six components of stress can be expressed as linear functions of the six components of strain (Hooke's generalized law of elastic deformation). The isotropic elastic materials including the polycrystalline metals have two elastic constants, *i.e.*, Young's modulus of elasticity E and Poisson's ratio ν . The other elastic constants or moduli depend on these two, for example the modulus of rigidity is $G = E/2(1 + \nu)$ and the bulk modulus (modulus of compressibility) is $K = E/3(1 - 2\nu)$. If the sum of the square of the three principal stress differences (formula 1) is just equal to $2s_0^2$, non-reversible or permanent strains will gradually develop, in addition to the elastic strains.

b. Perfect Plasticity.—Now an idealized state of equilibrium in the plastic state or "*a perfectly plastic*" mass may be considered by assuming that, while plastic flow occurs, the stresses do not change and remain independent of deformation as well as of velocity of deformation. We have seen that for a few per cent unit extension, compression or unit shear, plastic flow at ordinary temperature in ductile metals—such as soft steel—may be considered as approaching these idealized conditions, if large velocities of deformation, such as may be produced by impact in connection with plastic deformation, are excluded.

The rules regarding stress and strain (Chap. 14) were given for the equilibrium of a perfectly plastic mass. Perfect plasticity depends only on one physical constant, *i.e.*, the yield stress s_0 in pure tension. The great simplicity, which was attained by using these assumptions, justifies their introduction even in such cases where departure of the idealized conditions is apparent.

To express briefly the difference which exists between the cases of perfect elasticity and of perfect plasticity, we may also say, that in the first case there is a single-valued correspondence between the state of strain and the state of stress. To six given components of stress correspond six definite components of strain and the six equations expressing these relations are linear (Hooke's law).¹

In the second case, however, of a slow stationary plastic flow, only five equations are available to express the stress-strain relations (Chap. 14), leaving one of the components of strain undetermined. In consequence, if the six components of stress are given, one of the strain components can always be chosen arbitrarily, while the values of the five other components of strain then follow from the five stress-strain relations.²

c. Work Hardening.—We have seen that besides the idealized facts, expressed under section b, several further experimental circumstances must be taken into account if larger deformations

¹ In the case of perfect elasticity besides the six stress-strain relations, three more equations determine the state of equilibrium and three further equations of compatibility are available, thus making in all 12 equations which are sufficient to determine the 12 unknown stress and strain components.

² As was pointed out in one of the preceding chapters (see Chap. 14, page 78, Eq. [18]), one may also write down the stress-strain relations for a perfectly plastic mass exactly in the same form as for an elastic mass. There are then six equations, in which instead of Young's modulus an undetermined "modulus of plasticity" is used and Poisson's ratio is taken equal to $\nu = \frac{1}{2}$. Thus, in the case of a perfectly plastic mass 13 unknown quantities have to be determined *i.e.*, the 12 stress and strain components and also the modulus of plasticity, which itself must be considered dependent on x, y, z . For the 13 unknowns now are available: six stress-strain relations, three conditions which express the state of equilibrium, three equations of compatibility and, finally, the condition of plasticity (Eq. [1] with the sign of equality), making all together 13 equations. But as the modulus of plasticity is now one of the unknown functions of x, y, z , its values may be chosen in some way arbitrarily on the boundary of the plastic mass, thus constituting an infinite set of different states of strain, all of which will be compatible with the computed state of stress.

are to be treated. First among these is the fact that all the ductile metals, including mild steel, at sufficiently low temperatures show the effect of work hardening or cold work. If subjected to a tensile test for example, the ductile metals show a gradual increase of stress to maintain plastic flow with deformation. Besides this property, a second fact has to be mentioned, namely, that for several polycrystalline metals such as soft, annealed copper, aluminum, etc., under comparatively small strains the limit of plasticity loses its significance and a definite yield point may not be observed (because the plastic or permanent parts of the deformations practically begin to develop at the lowest stresses). This has already been pointed out (Chap. 5).

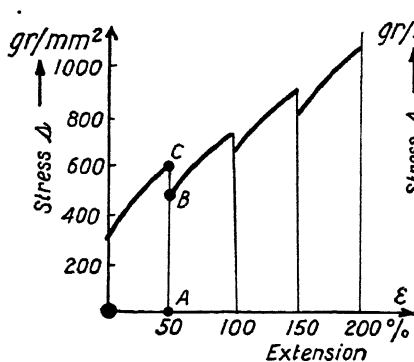


FIG. 348.

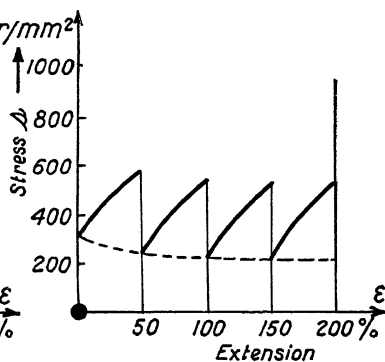


FIG. 349.

FIGS. 348 and 349.—Recovery of zinc single crystals tested in tension. (According to E. Schmid and O. Haase.) Figure 348, wire stretched at intervals of 30 to 40 sec.; Fig. 349, at intervals of 24 hr.

It seems, however, that a yield point appears again if the plastic deformation is interrupted (point A, in Fig. 11 page 24) by unloading, and the specimen is again loaded. It has not yet been possible to establish the generalized stress-strain relations for plastic flow involving the phenomenon of work hardening, but it was possible to work out the theory for several cases under simple states of stress such as torsion or bending, or for the radial flow in thick-walled tubes.

d. Recovery.—The opposite of the effect of work hardening may be termed recovery, an effect which may be observed after a metal test piece has been subjected to severe cold work. On zinc single crystals, stretched at room temperature, O. Haase and E. Schmid¹ have shown that if the tensile test is suddenly

¹ *Z. f. Phys.*, vol. 33, nos. 5 and 6, p. 413, 1925.

interrupted, the crystal unloaded and loaded again, the stress-strain curve appears shifted downward. Figures. 348 and 349 exhibit this in the case of two tests, in which the zinc crystal was stretched several times by 50 per cent each time, at intervals of 30 to 40 sec. between subsequent unloadings in Fig. 348, and of 24 hrs. between two consecutive tests in Fig. 349. As can be seen from these figures, yielding of the crystal after a period of rest starts at a lower stress AB than the last stress AC , to which the crystal was stretched in the previous test. The recovery of the zinc crystal after 24 hrs. is very considerable; it has almost completely lost the strength, due to previous work hardening. It is very probable also that polycrystalline metals will show the effect of recovery, especially if the phenomenon of recrystallization is also taken into consideration, which fact may be of importance in long time-tests.

e. **The Influence of the Velocity of Deformation.**—A second experimental fact must now be mentioned which has not yet been considered.

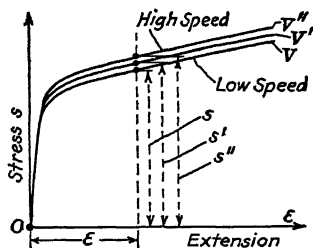


FIG. 350.—Stress-strain diagrams taken under various speeds $v = d\epsilon/dt$.

If plastic flow is treated under the assumptions stated under section b, one component of strain remains undetermined. Under the assumptions stated under section c, however, the state of strain is fully determined by the six components of stress. Now, accurate tests at slightly elevated temperature have shown that the shape of the stress-strain curves as obtained for example under pure tension, pure compression,

or pure shear appears also to be affected by the speed of deformation. For example, if a tensile stress-strain diagram of steel or of copper is taken under a constant rate of elongation per unit of time, the height of the stress-strain curve is slightly affected by the velocity of the deformation. The higher the speed $v = d\epsilon/dt$ and the quicker the test bar is extended, the greater the yield stresses observed corresponding to equal unit extensions ϵ . This is indicated in the diagram, Fig. 350. P. Ludwik,¹ Cassebaum,² and

¹ "Elemente der technologischen Mechanik," Berlin, 1908; see also later papers of P. LUDWIK.

² Dissertation, University of Göttingen.

Bailey¹ have independently arrived at the conclusion that as a first approximation (with the exception of the region of very small velocities, where $v = 0$ and the formula is not valid) a logarithmic law

$$s = s_1 + s_0 \ln \frac{v}{v_0} \quad (2)$$

seems to express this fact. The yield stresses s, s', s'', \dots corresponding to a given extension ϵ , but to different rates of flow v, v', v'', \dots will increase as the terms of an arithmetic progression, if the rates of flow v, v', v'', \dots required to produce these yield stresses, were chosen as the terms of a geometric progression.

It appears from this that under higher rates of extension the yield stress increases much less rapidly with velocity of deformation than under low rates of elongation. We may mention that a similar effect of speed on the stress-strain curves has also been observed on metallic single crystals by E. Schmid.

f. The Stress-strain-velocity Diagram.—From the preceding it follows that a more complete picture of the laws of plastic flow will be obtained by plotting yield stress s not only as a function of a single variable $s = f(\epsilon)$, namely, of strain or unit elongation ϵ , as was assumed previously, but also by comparing yield stresses corresponding to different rates of flow $v = d\epsilon/dt$. This can be done by considering the yield stress s as a function of two independent variables: of unit elongation ϵ and of rate of flow $v = d\epsilon/dt$

$$s = F(\epsilon, v). \quad (3)$$

Such a function of two variables can always be represented graphically by a curved surface, plotted as a surface above ϵ and v as rectangular coordinates. In this way a diagram is obtained as represented in Fig. 351. It is obvious that the vertical profiles of this surface $s = F(\epsilon, v)$ obtained by cutting it by a set of parallel planes $\epsilon = \text{const.}$ must give curves of a character as expressed by the logarithmic function Eq. (2).

On the other hand, the intersections of the surface $s = F(\epsilon, v)$ with the planes $v = \text{const.}$ must determine the shape of the

¹R. W. BAILEY, Creep of Steel under Simple and Compound Stresses, *Trans. Tokyo Sectional Meeting of World Power Conference, Tokyo*, vol. III, p. 1089, 1929. This paper contains very valuable information on the effect of the rate of plastic flow on the yield stress and on creep tests under combined stress.

"stress-strain diagram" at the various speeds or rates of flow v . It will be shown below that on these surfaces further important curves can be considered.

g. Homologous Temperatures.—It is furthermore evident, that such a surface as $s = F(\epsilon, v)$ will correspond only to a given temperature t . With varying temperature we must expect that the shape of the surface $s = F(\epsilon, v)$ will change considerably. For the full understanding of the behavior of solid matter under stress it is now of importance to describe more exactly the changes of shape of the surface $s = F(\epsilon, v)$ which occur if the temperatures are gradually increased.

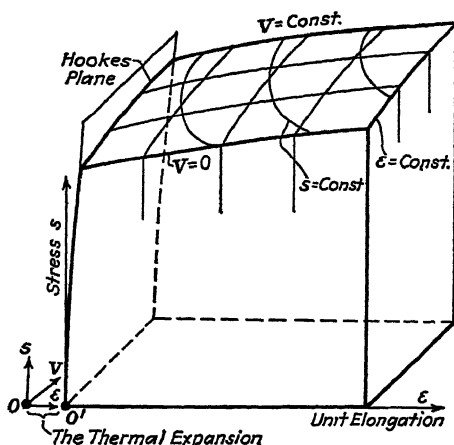


FIG. 351.—The stress-strain-velocity diagram for a metal having a well-defined plastic limit. (At comparatively low temperature.)

Before we do this, it will be good to introduce a new quantity for measuring temperatures first proposed by P. Ludwik¹ which appears to be useful if the behavior of several metals having different melting temperatures is to be compared. Let t and t' be the temperatures in degrees centigrade of the two metals to be compared; T and T' the corresponding absolute temperatures ($T = t + 273^\circ$) and T_m and T_m' the absolute melting temperatures. Then T and T' will be called homologous temperatures, if the ratios for the two metals

$$\theta = \frac{T}{T_m} \text{ and } \theta' = \frac{T'}{T_m'} \quad (4)$$

¹ Valuable information on molecular homology and related questions are given in LUDWIK's papers, *Z. d. V.D.I.*, vol. 59, p. 657, 1915, and in *Stahl und Eisen*, vol. 35, No. II, p. 1183, 1915.

are the same. The utility of using θ instead of T as the variable expressing the temperature is based on the fact that at the melting temperature the mechanical properties of the metals (and of the crystalline substances in general) undergo sudden changes, and on the fundamental observation that some of the important mechanical properties of the metals such as elasticity, yield stress, strength, show remarkably similar variations with temperature if plotted as functions of θ . Take for example lead and iron. The melting temperature of lead is $t_m = 327^\circ\text{C}$, and hence the absolute melting temperature of lead is $T_m = 600^\circ$; that of iron $T_m' = 1510 + 273 = 1783^\circ$. A test with lead at room temperature $t = 20^\circ\text{C}$. corresponds to a test with iron made at $T' = \frac{T_m'}{T_m} T = \frac{1,783}{600} \cdot 293 = 870^\circ$ or $t' = 597^\circ\text{C}$. Hence

the homologous temperature t' under which iron will behave similarly to lead, stressed at room temperature, is $t' = 597^\circ\text{C}$. Lead at room temperature behaves like iron at red heat.

The effects of a rising temperature on the mechanical and metallurgical properties of the metals are manifold. It is important to know, that, with rising temperature, not only the general shape of the surface $s = F(\epsilon, v)$ will change considerably but also the shape of those steeper parts of these surfaces bordering along the two axes $\epsilon = 0$ or $v = 0$, where either the deformation ϵ or the rate of elongation v have small values. Furthermore, certain discontinuities of the surface must be expected corresponding to isomorphous changes in the crystalline structure, when metals exhibit such changes.

Special attention must be paid to the more exact determination of the shape of the surface $s = F(\epsilon, v)$ along the ϵ and the v axes.

The surface $s = F(\epsilon, v)$ of a metal for example, exhibiting a well-defined yield stress at low temperatures and having hence a sharply limited elastic portion in the stress-strain diagram, will in the bordering region of the ϵ, v plane, where ϵ is small, i.e., along the v axis—consist in a steeply inclined plane (Fig. 351). This plane must intersect the ϵ, v plane in a line parallel to the v axis at a distance given by the thermal expansion of the metal at this temperature. The slope of this plane is determined by the value of the modulus of elasticity E at the temperature considered.

On the other hand, we must expect that the surface $s = F(\epsilon, v)$ of a metal at a moderately elevated temperature *tends to approach the ϵ axis and perhaps will pass through the ϵ axis*. (This case is shown in Fig. 352.) In other words, this would mean that the behavior of a metal at a sufficiently high temperature and for comparatively small stresses can perhaps be characterized by saying that stress at a given elongation ϵ is proportional to the rate of flow v . It seems probable that at sufficiently high temperature, the surface $s = F(\epsilon, v)$ approaches the v axis or passes through it. Plastic flow at such temperature and for *low stresses* could thus be considered as viscous

made by Koch and Dieterle,¹ in which the modulus of elasticity E , the modulus of rigidity G , and the coefficient of linear expansion α are plotted against the ratio $\Theta = T/T_m$ of the absolute temperature T to the absolute melting temperature T_m of aluminum. Only the full part of the curves is based on tests, the dotted parts are proposed extrapolations not based on tests. Both moduli E and G decrease with the rising temperature. Apparently Young's modulus E decreases little less rapidly

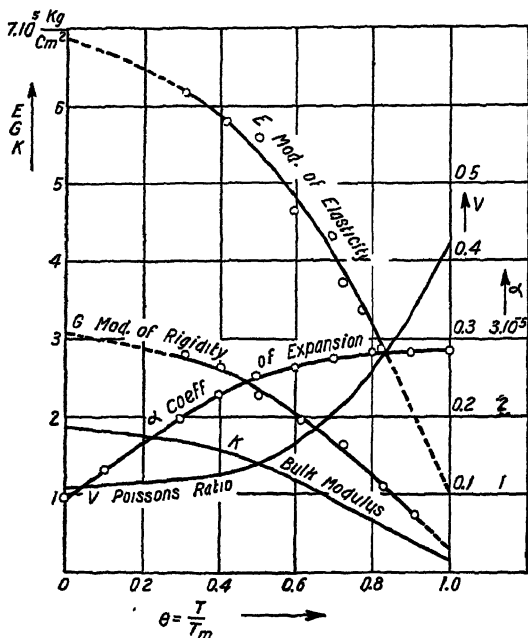


FIG. 353.—Variation of the elastic properties of aluminum with temperature. (According to Koch and Dieterle.)

than the modulus of rigidity G . The decrease in the value of E and G from the absolute zero to the melting temperature may be estimated equal to approximately 86 per cent and 90 per cent, respectively.

From E and G the curves for Poisson's ratio ν and the bulk modulus $K = \frac{E}{3(1-2\nu)}$ were computed, the former showing

¹ The variation of the modulus of elasticity E with temperature has been determined by KOCH and DIETERLE, *Annal. d. Phys.*, vol. 68, p. 441, 1922; and that of the rigidity modulus by KOCH and DANNECKER, *Annal. d. Phys.*, vol. 41, p. 197, 1915.

a tendency to increase with temperature, while the latter has a similar shape to the E or G curve. The values of ν are much affected by the uncertainties in the values of E or G , and therefore it is probable that the ν curve will change considerably when more tests are available. Finally, in Fig. 353, the coefficient of expansion as computed from

$$\alpha = \frac{1}{l_0} \cdot \frac{\partial l}{\partial t} \quad (5)$$

is plotted against the temperature. Here l_0 is the length of a bar at a standard temperature t_0 , and l the length at the temperature t .

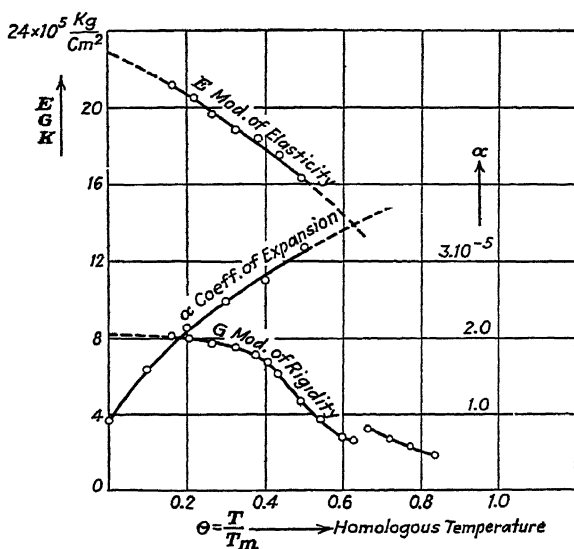


FIG. 354.—Variation of the elastic properties of iron with temperature.

A second diagram (Fig. 354) contains test results for steel. Here a discontinuity in the curve of G can be seen, which corresponds to the change from α to γ iron.

The elastic properties of *tungsten* (besides strength and other physical properties) were carefully investigated by W. E. FORSYTHE and A. G. WORTHING¹ in a wide range of temperatures up to about 2000°C. The modulus of rigidity of tungsten was found to vary as follows:

At absolute temperature T : 300° 700° 1100° 1500° 1900°.
 Modulus of rigidity $G(kg/cm^2)$: 21.6 21.2 20.6 12.3 4.3 $\times 10^5$.

¹ The Properties of Tungsten and the Characteristics of Tungsten Lamps, *The Astrophysical Journal*, Chicago, vol. LXI, pp. 146-185, 1925.

For the modulus of elasticity E values from about 3.5 to 4.2 millions kg/cm^2 at room temperature have been found. Tungsten seems to have the highest modulus of elasticity of all substances recorded. From room temperature (300° abs.) to 1300°K. a slow decrease amounting to about 10 per cent was found.

The variation of the coefficient of thermal expansion from room temperature to about 2300°K. was found to be represented well by a function:

$$\alpha = \frac{l - l_0}{l_0} = [4.40t + 4.5 \times 10^{-5}t^2 + 2.2 \times 10^{-7}t^3] \cdot 10^{-6}$$

where $t = T - 300$ is the increase of temperature above room temperature ($= 300^\circ \text{K.}$) and l and l_0 refer respectively to the lengths at t and $t = 0$. The coefficient of expansion was found at

$T = 300^\circ$	1300°	2300°K.
$\alpha = 4.44$	5.19	7.26×10^{-6} per degree.

The elastic properties of tungsten vary greatly with the size and the grain structure of the wire.

i. The Effect of Temperature on Plasticity and on the Shape of the Stress-strain Diagram Is Twofold.—With rising temperature the yield stress decreases rapidly in general. Of the metals only steel shows an exceptional behavior, inasmuch as ultimate strength of medium carbon steel increases first with temperature up to the "blue heat" range at 200 to 250°C. At temperatures approaching the melting temperature the yield stress of the polycrystalline metals in general is but a small fraction of its value at low temperatures. Furthermore, generally speaking, the stress-strain diagrams at elevated temperatures show a more curved transition line at the lower elongations than is the case at comparatively low temperatures. From this it may be seen that it must be comparatively difficult to determine the slope of Hooke's straight line at elevated temperature or the values of E or G , because the plastic part of the elongation is in most cases comparable with the elastic part, and can be separated only if precautions are taken and the speed of deformation is increased (vibrations).

The second important effect of a rising temperature is that work hardening gradually disappears. This was clearly shown by the tests of M. Polányi and E. Schmid¹ which were carried out with single metal crystals at the temperatures of liquid air and liquid hydrogen and by comparing the shape of similar stress-strain curves of single crystals as obtained at room tempera-

¹ *Naturwissenschaften*, vol. 17, p. 301, 1929.

ture. Figure 355 shows the curves for a zinc single crystal obtained in a tensile test at the absolute temperatures $T = 20^\circ$, 83° , and 300° . It must be remembered that if the true component of the shearing stress, acting in the planes of slip in a single crystal, is plotted against the true amounts of slip, the curves obtained will be somewhat different from those indicated in Fig. 355.

As a measure of what is called "work hardening" can be considered the slope $df/d\epsilon$ of the stress-strain curve $s=f(\epsilon)$, if true stress s is plotted against true strain ϵ . The derivative $df/d\epsilon$ at a given strain ϵ , increases rapidly with decreasing temperature.

An important conclusion of the tests mentioned above is that the metals (in the form of single crystals) at the lowest possible temperatures have clearly shown the phenomenon of slip and that a single-metal crystal close to the absolute zero of the temperature scale, at which the inter-atomic vibrations due to the thermal agitation of the atoms disappear, has a definite yield stress and a limit of plasticity. This shows that a main part of the mechanism

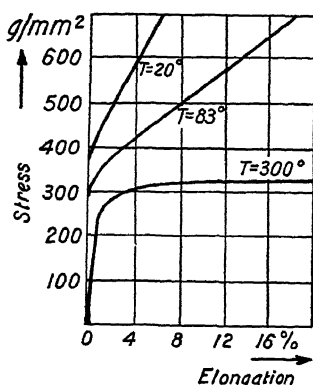


FIG. 355.—Stress-strain diagrams of zinc single crystals at various temperatures. (According to M. Polányi and E. Schmid.)

of plasticity of a crystal and of the polycrystalline metals is due to slip. On the other hand, tests made with polycrystalline metals at elevated temperatures indicate the same effect, i.e., that work hardening disappears at temperatures near the beginning of recrystallization and approaching the melting point.

Also, from the careful investigations of E. Schmid and his collaborators the variation of the limiting shear stress with temperature under which single cadmium-, zinc-, and Bi-crystals begin to yield is known.¹

The single-metal crystals were tested in a wide range of temperature between 20°abs. (the temperature of liquid hydrogen) and the melting point of the metal. Contrary to previous assumptions of A. Joffe,² who thought that the elastic limit (limit of plasticity) of rock salt, aluminum, and Mg single crystals drops down to the value zero at the melting point, the result of the tests of Schmid was that the shearing stress causing first yield at low

¹ Cf. BOAS, W., and E. SCHMID, *Z. f. Phys.*, p. 575, 1929.

² *Proc. Internat. Cong. of Applied Mechanics*, p. 64, September, 1924.

temperatures decreases at first about linearly with the increasing temperature (for the same initial orientation of the planes of slip relatively to the axis of tension), but becomes nearly independent of temperature when the melting point is approached. Thus metal crystals have a small but finite limit of plasticity at temperatures approaching the melting point.

M. Polányi and E. Schmid¹ distinguish three types of plasticity:

1. Plasticity of single crystals at low temperatures—The limiting shearing stress is independent of the rate of flow, the shape of the stress-strain diagram of the crystal (for similar initial orientation of the planes of slip) does not depend on temperature or rate of flow.

2. Plasticity of amorphous matter—The yield stress depends on the speed of deformation; this plasticity is dependent on temperature and ceases at the absolute zero of the temperature scale.

3. Ordinary plasticity of crystals—Shows the effect of the lowering of the yield stress with temperature, which is explained as a simultaneous recovery of the crystal from the previous work hardening.

j. Viscosity.—One of the most remarkable mechanical properties of liquids is their viscosity or their internal resistance to movement exhibited between thin parallel layers in the tangential direction. The simplest expression of this property is that the resisting force per unit of area or the shearing stress s acting between two moving layers is proportional to the rate of change of the velocity of the liquid in a direction y perpendicular to the force s or

$$s = \eta \frac{\partial u}{\partial y}, \quad (6)$$

where y designates the distance of a particle of the liquid from the plane of the shear and u the velocity of the particle. η is called the coefficient of viscosity.²

Regarding the mechanism which is thought to explain the viscosity of liquids, we may briefly note that viscosity is ordinarily considered as a transfer of momentum in the fluid from one layer to a neighboring layer. The atoms or molecules of a fluid in motion will move in a layer with a certain average velocity, but some molecules or groups of molecules may temporarily have small components of velocity in the perpendicular direction to the main flow. If such a group of molecules gets

¹ *Naturwissenschaften*, vol. 17, p. 301, 1929.

² The term "viscosity" is sometimes given a broader meaning by writers, especially if the phenomena of creep or of plasticity at elevated temperatures are considered. In the text above, the word viscosity is always used in the restricted sense of expressing the fact that shearing stress is directly proportional to rate of flow.

in the neighboring layer having the smaller velocity, it will tend to increase the velocity of this latter; and, on the contrary, if it gets in the layer having the larger velocity it will tend to retard its movement. By these infinitesimal impulses, due to the laws of the momentum, tangential forces parallel to the main flow must be exerted by one layer on the next. These forces will tend to accelerate the motion of the slower and to retard the motion of the faster layers thus producing shear stress, a characteristic of viscous flow.

As the polycrystalline substances in the solid state of aggregation gradually lose their resistance to permanent deformation if the temperature approaches the melting point, and on the other hand all substances in the liquid state show an increase of viscosity with decreasing temperature—it seems not unreasonable to assume that viscosity—or, expressed more generally, the changes in position of atoms or groups of atoms because of the thermal agitation—as a general property of all liquids or of solid matter in its amorphous state of aggregation, may be present, to at least some extent, just after solidification of a liquid into a polycrystalline solid. It will therefore be logical to list the viscosity and the changes in position of atoms due to thermal agitation as a property of imperfect polycrystalline solid materials at temperatures near the melting point which also depends on the temperature.

k. Change of the Viscosity of Liquids with Temperature.—One of the most remarkable properties of liquids is the decrease of their viscosity with temperature. Recently S. E. Sheppard¹ and E. N. da C. Andrade² independently have proposed a formula expressing the law of variation of the coefficient of viscosity of liquids η with temperature

$$\eta = Ae^{b/T}, \quad (7)$$

which was derived from certain assumptions regarding a physical mechanism of fluid motion and was found to agree very well with observations. A and b are constants, T is the absolute temperature. The following table shows the agreement for one example (butyl alcohol).

¹ *Journal of Rheology*, No. 2, vol. 1, p. 208, January, 1930.

² *Nature*, p. 309, March 1, 1930; and p. 580, April 12, 1930.

Temperature, °C.	Calculated	Observed
0	0.0523	0.0519
20	0.0293	0.0295
40	0.0177	0.0178
60	0.01135	0.01139
80	0.00765	0.00766
100	0.00538	0.00539

For water and similar liquids the formula has to be modified.¹

The viscosity of undercooled liquids was investigated by G. Tammann.² He found that the viscosity of an undercooled liquid increases at first slowly with undercooling, but, with further decrease of the temperature, viscosity increases very rapidly, until the liquid becomes a vitreous solid or an amorphous glass. An investigation of the law of change of viscosity with temperature for liquids may therefore throw some light on the behavior of vitreous or amorphous solid substances such as glass. As was already stated above, these substances do not show a definite melting point, they soften if heated, or solidify if cooled, quite gradually within a greater range of temperatures. It is probable that the plasticity of the amorphous, non-crystalline masses will have a close relation to the viscosity of liquids. As such amorphous masses are supposed to exist also in polycrystalline substances (where they are supposed to be present in thin layers or within the grain boundaries) one kind of plasticity, especially that which depends on temperature, may tend to approach the laws of viscous liquid flow, if the temperature is high enough.³

¹ In connection with this subject attention shall be called to a number of recent valuable contributions to the knowledge concerning the nature of the liquid state of matter contained in papers published in the *Journal of Rheology*, among which should be mentioned especially those by S. E. SHEPPARD and R. C. HOUCK, *The Fluidity of Liquids*, vol. 1, No. 4, pp. 349-371, 1930, and by M. RAINER, *The General Law of Flow of Matter*, vol. 1, No. 1, pp. 11-20, 1930. SHEPPARD and HOUCK point to the increasing evidence based upon numerous recent tests confirming the formula Eq. 7 and thus the conception of a regional orientation of the molecules in a liquid. The molecules of a liquid are, according to these latter authors and to the x-ray investigations of G. W. STEWART and others, regarded as distributed in both a freely moving and a regionally oriented manner. With respect to the viscosity of liquids Cf. also: EUGENE C. BINGHAM, "Fluidity and Plasticity," McGraw-Hill Book Co., Inc., New York.

² "Aggregatzustände, etc.," p. 244, Leopold Voss, Leipzig, 1922.

³ For certain commercial kinds of glass the change of viscosity with temperature has been very carefully investigated. WASHBURN and SHELTON, *Univ. of Illinois Bull.* 140, Eng. Exp. Sta., 1924, have, for example, found that the coefficient of viscosity of glass decreases as the temperature is

1. **Creep.**—If a metal bar subjected to tension or some other simple mode of stress is heated up and the temperature kept constant while the load acts continuously, the bar will stretch continuously at sufficiently high stresses. A study of the mechanical behavior of the ductile metals with a high melting point at temperatures at which the work-hardening effect begins to decrease and recrystallization may participate, is of practical importance on account of the tendency to use such working temperatures and stresses in boilers, steam-turbine discs and casings, in the cylinders of internal combustion engines, and in certain apparatus used by chemical industries.

The so-called “long-time” tests, which were carried out with the purpose of studying plastic flow of metals at elevated temperatures, have contributed much to the knowledge of the laws of plastic flow in general.¹ These questions may be studied by means of the stress-strain-velocity diagram and it may be stated, that plasticity at high temperatures with special reference to the phenomenon known as “creep” and described in recent investi-

raised from the temperature of softening up to 1,500°, in the ratio of 10⁹ to 1. LE CHATELIER, *Ann. de phys.*, vol. 3, p. 5, 1925, proposed a double logarithmic formula to express this enormous change of η with the temperature: $\log \log \eta = at + b$.

Sometimes the opinion is expressed that glass tubes, if stored at room temperature and freely supported at their ends, would bend permanently under their own weight. LORD RAYLEIGH, *Nature*, p. 311, March 1, 1930, found that a glass rod 4.9 mm. in diameter and about 1 m. long, supported freely at its ends and loaded by 300 g. at the middle which produced an elastic deflection of about 2.8 cm., did not show an appreciable permanent increase in its deflection after a period of seven years. Apparently the viscosity coefficient η of glass at room temperature is so large that it would require a much longer time to produce measurable effects at this low temperature and comparatively low stress. C. D. SPENCER, Cleveland, *Nature*, p. 707, May 10, 1930, found, however, that a glass tube of 110 cm. length, 1 cm. diameter and 1 mm. in wall thickness on supports 1 m. apart and loaded by 885 g. at the center (a load which was little less than the force necessary to break the tube in bending) showed a *permanent* deflection of 9 mm. after the lapse of six years of loading.

¹ The author is much indebted to Mr. P. G. McVetty of the Research Laboratories of the Westinghouse Electric and Manufacturing Company for much valuable information in the field of high-temperature work and long-time tests, which he received during discussions. The author must express his sincere thanks for the willingness of Mr. McVetty to discuss these questions with him.

gations¹ will perhaps be understood more fully and treated in a more general way if the function

$$s = F(\epsilon, v) \quad (8)$$

was known for the metals and alloys of higher melting points.

The shape of the surface F can be studied by obtaining from tests certain curves situated on it. One method frequently used

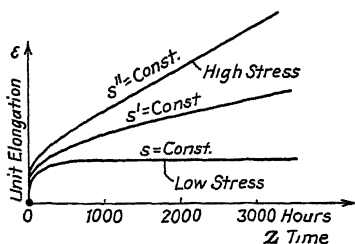


FIG. 356.—Extension tests of long duration.

is to observe the extension of bars under a constant load with time. By observing how the unit elongation $\epsilon = \Delta l/l_0$, taken for some gage length l_0 increases with time z curves like those in Fig. 356 may be obtained, giving ϵ as a function of time

$$\epsilon = \varphi(z). \quad (9)$$

If ϵ does not exceed certain small values (of some few per cent) a test carried out under a constant load P can be considered also to be a test carried out under a constant stress s . If, however, ϵ changes very considerably, the true stress s computed with respect to the actual area of cross-section A and found by

$$s = \frac{P}{A} \quad (10)$$

will increase with ϵ . We have seen that the true stress (see Chap. 15) is equal to

$$s = (1 + \epsilon)s_0 \quad (11)$$

where

$$s_0 = \frac{P}{A_0} \quad (12)$$

is the stress as computed by dividing the load by the original cross-section A_0 .

¹ A very complete bibliography on the question of the creep of metals is contained in F. K. NORTON'S, "The Creep of Steel at High Temperatures," p. 80, McGraw-Hill Book Company, Inc., New York, 1929; 88 pp. Papers to which reference is made above are mainly those of R. W. BAILEY, COURNOT and SASAGAWA, FRENCH, LEE, LYNCH, MOCHEL and McVETTY, POMP and DAHMEN, and the monograph mentioned above.

Research on creep up to 1924 is reported in: The Effect of Temperature upon the Properties of Metals, a symposium; meeting held at Cleveland, 1924, *Trans. Amer. Soc. Mech. Eng.*, vol. 46, 1924.

By means of the last equations the true stress can be found if the tests are not carried out under $s = \text{const.}$ but only under constant load. From the time-elongation diagram of a long-time test the rate of flow

$$v = \frac{d\epsilon}{dz} \quad (13)$$

is found as the derivative of the curves $\epsilon = \varphi(z)$ with respect to the time z . Thus corresponding values of the three variables: stress s , elongation ϵ and rate of flow v may be obtained and the surface $s = F(\epsilon, v)$ be constructed if points in sufficient number are determined.

A complete picture showing the elastic-plastic behavior of a metal will be obtained, if the surfaces $s = F(\epsilon, v)$, each corresponding to a given temperature T are plotted above ϵ and v as independent variables and for a set of temperatures T extending from low temperatures up to or above the region of softening and recrystallization. Two such surfaces were plotted in the schematic Figs. 351 and 352.

Considerable discussion has centered around two questions: Do the metals at any sufficiently high temperature always show a creep limit or not and how may the tests which now require a long time be shortened in duration?

A limit of creep means that at a given temperature a certain stress s_c exists, below which the metal can be stressed for an indefinite time without observable creep or without showing a gradual further increase in elongation. In the time-extension diagram Fig. 356 this would mean, that if the stresses s (which are kept constant for each curve) do not exceed the creep limit s_c , all ϵ curves approach horizontal branches and have horizontal asymptotes.

As, on the other hand, the data obtained from creep tests clearly indicate, that for sufficiently high temperatures and high stresses the curves $\epsilon = \varphi(z)$ definitely rise with time z , a further consequence of the existence of a creep limit would be that the asymptotes of these curves would be

$$\begin{aligned} &\text{horizontal if } s < s_c \\ &\text{and inclined if } s > s_c^1 \end{aligned}$$

¹ Cournot and Sasagawa, *Revue de métallurgie*, p. 753, 1925, believe they have found by tests that a creep limit exists, but the data, on which they base their conclusions, seem to the writer not sufficiently conclusive.

From a physical standpoint it is hard to conceive why the character of certain curves such as $\epsilon = \varphi(z)$ should suddenly change if no new reason¹ is apparent which would cause such a change, as is the case, for example, on the *other* bordering part of the surface $s = F(\epsilon, v)$ for small values of ϵ . If ϵ is small, such a reason exists indeed in the phenomenon of yielding, due to slip in the crystal grains.

The important question as to whether there is a break in the surface $s = F(\epsilon, v)$ at sufficiently high temperatures in the region of small values of the variable v (in the parts of the plane ϵ, v bordering along the ϵ axis) similar to that existing along the other, the v axis, at lower temperatures and for small ϵ (thus exhibiting there what is called "a well-defined" yield stress), will have to be cleared up in the future by determining more accurately the shape of the surfaces $s = F(\epsilon, v)$ at higher temperatures and at the low rates of flow v .

If viscous flow and changes in position of the atoms due to thermal agitation are also an essential part of the plasticity of matter in the polycrystalline state of aggregation at elevated temperatures, *i.e.*, if stress s as a first approximation can be considered as proportional to rate of flow v , at least at low values of s as compared with the stresses s necessary to maintain plastic flow at greater speeds—and tests seem to indicate that such a thing is true in the case of the amorphous solid substances—a creep limit will not exist, because of the fact, that at sufficiently high temperatures the smallest stress will cause flow and a small but finite velocity of deformation, thus causing also increasing deformations. The fact, that the coefficient of viscosity η which is expressed by the ratio s/v , is itself a pronounced function of temperature T and changes extraordinarily rapidly with T , then may explain some of the fundamental observations regarding the questions of creep.

¹ Softening of a work-hardened metal after long exposure to a relatively low temperature might cause a bending up of the curve $\epsilon = \varphi(z)$ after a *longer* period of time, as was remarked by P. G. McVetty. This relief of the work hardening might be caused by the simultaneous action of strain and recrystallization.

PART II

SOME APPLICATIONS OF THE MECHANICS OF THE PLASTIC STATE OF MATTER TO GEOLOGY AND GEOPHYSICS

CHAPTER 40

FINITE HOMOGENEOUS STRAIN

If we wish to obtain a more exact estimate of the plastic deformations and of the distortions occurring in the earth's strata, we will have to analyze the deformation of the solid layers of rock by applying methods similar to those used by engineers and physicists to analyze stress and strain. These methods, as developed in Chaps. 7, 8, and 9, may therefore be used in order to describe quantitatively the geological displacements observed in the rock layers of the earth. For the convenience of geologists who may be less acquainted with the analysis of stress and strain, a few essentials of this subject, given in previous chapters, will be briefly recapitulated here.

If we wish to determine quantitatively the amounts of distortion in some parts of the earth crust, we should begin with the initial position of the rock layers at an earlier time and compare this original position with that after deformation. The fulfillment of this self-evident condition is scarcely ever possible. In so far as the geological processes of deformation concern sedimentary rock layers, we may try to choose a system of rectangular coordinates x, y, z with an origin O as the reference system, relative to which the distortions of the rock layers are to be determined. For one such recommended system of reference a horizontal position for the x, z plane might be chosen, with the origin fixed to some point in the earth crust in a region where relative distortions can be considered as negligible. How far it is possible to satisfy this condition, cannot be further discussed here.

Another possibility is to disregard, for the moment, the general motions in the earth's strata relative to a fixed surface of the earth globe, and only analyze the relative motion of a part of the earth's crust with respect to a neighboring part. A third possibility, which has long been used in geology, is to study the distortions of the boundaries of the rock layers, as they exist at the present time, especially in vertical sections

taken through mountains. In this procedure, it is tacitly assumed that the boundaries of the layers were originally more or less parallel and in a horizontal position. (An exception are "non-conformities" as the traces of former eroded surfaces of the earth crust, crossing the horizontal layers, buried under the strata deposited later.)

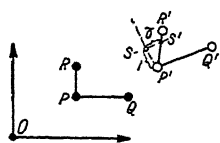


FIG. 357.

If, in a cross-section of the rock layers before deformation has occurred, a straight line be thought of as drawn between two neighboring points P and Q (Fig. 357), we may consider the change in the distance PQ caused by the deformation. Because of the distortion the line PQ changes over to the line $P'Q'$. We call the ratio

$$\epsilon = \frac{P'Q' - PQ}{PQ}$$

the unit strain of the rock in the direction $P'Q'$. If, in addition we consider two directions PQ and PR , initially perpendicular to each other, we will in general find that these directions after deformation, $P'Q'$, $P'R'$, will not be perpendicular to each other but will form a certain angle $Q'P'R'$ with each other. If, in the plane of the angle $P'Q'R'$, a line is drawn perpendicular to one of the directions $P'Q'$ or $P'R'$ in the distorted end positions, an appropriate measure of the angular distortion may be taken as the distance $\gamma = SS'$, through which a point S at a distance 1 from P (1 cm. or 1 in.) has been displaced parallel to $P'Q'$ to the point S' . We call γ the unit shear at the point P parallel to one of the directions $P'Q'$ or $P'R'$.

An exact analysis shows that, in general, the distortion in a material in the neighborhood of an arbitrary point P may be described by means of nine quantities. There are three mutually perpendicular directions PA , PB , PC , which have the property that after distortion they still remain perpendicular to each other. After distortion these lines arrive at three positions, $P'A'$, $P'B'$, $P'C'$, which are also mutually perpendicular. We call these latter the *directions of principal strain* of the material. For these three directions there is no change of angle and therefore the unit-shearing deformation is zero. Moreover, for these three directions, the unit strains become analytic maxima and minima, and because of this, the strains parallel to these three directions ($P'A'$, $P'B'$, $P'C'$) are called the *principal strains*

ϵ_1 , ϵ_2 , ϵ_3 .

Since the designation of three fixed directions in space requires three quantities (angles), the complete designation of the state of strain in the neighborhood of a point P requires nine quantities, as follows: Three quantities are necessary to define the initial position of the three straight lines PA, PB, PC ; three additional quantities are necessary to define the new directions $P'A', P'B', P'C'$, which the initial three straight lines assume after the deformation; and by means of $\epsilon_1, \epsilon_2, \epsilon_3$ three quantities are given which determine the amount by which the material is strained parallel to these three latter directions. The state of pure strain of rocks is therefore determined by six quantities only (the three principal directions $P'A', P'B', P'C'$ in the strained position of the material and the three principal strains $\epsilon_1, \epsilon_2, \epsilon_3$), if one considers the rotation of the principal axes from the undistorted position to the distorted position as an effect of secondary interest.

We can therefore say that the general state of strain in an element of a stressed body consists of a pure extension of the elements of the body in three definite mutually perpendicular directions and of a rotation of the entire element as is possible in a rigid body. A noteworthy particular case is the state of strain where the rotation vanishes: then the three principal directions PA, PB, PC , which after deformation become principal strain directions, remain parallel. (An example of distortion without rotation is given in Fig. 375 below.) Contradictions and uncertainties in the description of mountain folding and distortions in the rock strata can be avoided if these simple laws and a few of the following particular rules are considered.

If in the interior of the material in the initial position 1, we think of a small sphere with an extremely small radius r circumscribed around a point P , in the final position this sphere will deform in a very simple manner; it becomes an ellipsoid with the major semi-axes $(1 + \epsilon_1)r, (1 + \epsilon_2)r, (1 + \epsilon_3)r$. Each parallel bundle of straight lines is deformed in such a way that it again becomes a bundle of straight and parallel lines. We call this state of strain a *homogeneous strain* and can say that in general the state of strain in the vicinity of a point is essentially homogeneous.

Two states of strain are important in geological movements, and these will be mentioned here.

a. Distortion without Change of Volume.—In the solid rocks made up of sediments which have been deposited for an extremely long time and which have become thoroughly settled down, and in solid igneous rocks, it may be assumed that during subsequent displacements or distortions of the rocks, the volume does not change. Then we have for the three principal strains the following additional condition:

$$(1 + \epsilon_1)(1 + \epsilon_2)(1 + \epsilon_3) = 1. \quad (1)$$

This equation expresses the fact mathematically that the volume remains constant. If, for example, two of the principal strains, ϵ_1 and ϵ_2 , are given, the third principal strain ϵ_3 is already determined and can be calculated from this equation.

b. A Second Important Particular Case Is Plane Strain.—In the case of many geological movements, as for example are observed in the formation of mountain ranges in parallel chains, all movements inside of a limited portion of the earth's crust occur substantially in parallel planes. These parallel planes do not change their distance from each other during the distortion (they are perpendicular to the crests or the valleys of the mountain ranges). In these cases, the unit strain perpendicular to these planes or in a direction parallel to the mountain ranges is equal to zero. Assuming that ϵ_3 is the strain in this direction, we have $\epsilon_3 = 0$ and hence from Eq. (1):

$$(1 + \epsilon_1)(1 + \epsilon_2) = 1, \text{ from which } \epsilon_2 = -\frac{\epsilon_1}{1 + \epsilon_1}. \quad (2)$$

Therefore one principal strain is always positive and the other always negative. If because of a lateral thrust, the rocks at great depth below a mountain chain have been compressed; it follows from the foregoing that in a direction perpendicular to the thrust they *must* have extended. Relative to plane strain with constant volume a few additional statements will be given here.

c. Simple Shear.—In this case we again assume that $\epsilon_3 = 0$, the deformation consisting of a simple shear as shown in the opposite Figs. 358 and 359. The distortion of the body consists essentially of a movement of all straight lines parallel to the direction OX in a direction parallel to these lines. The value of this movement u parallel to the x axis increases in proportion to the coordinate y so that

$$u = \gamma y \quad (3)$$

The components v and w of the displacement parallel to the coordinate axes y and z will be taken equal to zero. The coordinates x, y of an arbitrary point P (Fig. 358), after the deformation have changed into the coordinates x', y' of a point P' (Fig. 359) which are evidently

$$\left. \begin{aligned} x' &= x + \gamma y \\ y' &= y. \end{aligned} \right\} \quad (4)$$

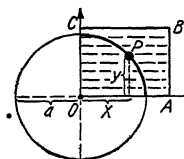


FIG. 358.

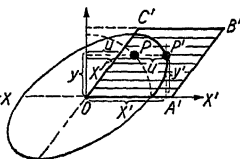


FIG. 359.

FIG. 358 and 359.—Simple shear. Initial (left) and distorted (right) position of body.

In order to determine in what manner a circle will be distorted by this type of deformation, we consider various points P which are all upon a given circle in the initial position (see Fig. 358), and investigate the curve into which this circle is distorted if the body is subjected to simple shear parallel to the x direction. If the points $P(x, y)$ lie upon a circle with radius a and having a center O we have

$$x^2 + y^2 = a^2 \quad (5)$$

If we replace x and y by their values from Eq. (4):

$$\left. \begin{aligned} x &= x' - \gamma y' \\ y &= y' \end{aligned} \right\} \quad (6)$$

we obtain

$$(x' - \gamma y')^2 + y'^2 = a^2 \quad (7)$$

or

$$x'^2 - 2\gamma x'y' + (1 + \gamma^2)y'^2 = a^2 \quad (8)$$

i.e., this is an equation of an ellipse in the variables x', y' .

d. Determination of the Principal Axes for Simple Shear.—In order to determine the two mutually perpendicular directions OA and OB in the undistorted initial position of the body, which after distortion will become the axes of principal strain OA' and OB' (Figs. 360 and 361), the expression for a radius $AP' = r'$ of the ellipse will be used. This is

$$r'^2 = x'^2 + y'^2 \quad (9)$$

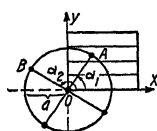


FIG. 360.

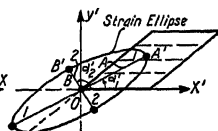


FIG. 361.

FIG. 360 and 361.—Strain ellipse for finite shear. Position of principal strain axes in unstrained (left) and strained (right) state of body. (A, B , semiaxes of strain ellipse.)

or using Eq. (6)

$$r'^2 = (x + \gamma y)^2 + y^2 = x^2 + 2\gamma xy + (1 + \gamma^2)y^2 \quad (10)$$

For the principal axis r' must be a maximum or minimum, i.e.,

$$r' dr' = [x + \gamma y] dx + [\gamma x + (1 + \gamma^2)y] dy = 0. \quad (11)$$

We have the additional condition

$$r^2 = x^2 + y^2 \quad \text{or} \quad x dx + y dy = 0. \quad (12)$$

The simultaneous use of Eqs. (11) and (12) gives

$$\frac{dy}{dx} = -\frac{x}{y} = -\frac{x + \gamma y}{\gamma x + (1 + \gamma^2)y}. \quad (13)$$

According to the latter proportion we must have

$$\begin{aligned} x + \gamma y &= \lambda x \\ \gamma x + (1 + \gamma^2)y &= \lambda y. \end{aligned} \quad (14)$$

Using the ratio $y/x = \tan \alpha$ in these equations we obtain the following expressions:

$$\frac{y}{x} = \frac{\lambda - 1}{\gamma} \quad \text{and} \quad \frac{y}{x} = \frac{-\gamma}{1 + \gamma^2 - \lambda}. \quad (15)$$

Since both expressions must be equal, we obtain for λ

$$\begin{aligned} \frac{\lambda - 1}{\gamma} &= \frac{-\gamma}{1 + \gamma^2 - \lambda} \\ \lambda^2 - (2 + \gamma^2)\lambda + 1 &= 0. \end{aligned} \quad (16)$$

This quadratic equation for λ has the following roots

$$\begin{aligned} \lambda_1 &= 1 + \frac{\gamma}{2}(\gamma + \sqrt{4 + \gamma^2}) \\ \lambda_2 &= 1 + \frac{\gamma}{2}(\gamma - \sqrt{4 + \gamma^2}). \end{aligned} \quad (17)$$

Using these we obtain the angles α_1 and α_2 for the two directions OA and OB

$$\begin{aligned} \tan \alpha_1 &= \frac{\lambda_1 - 1}{\gamma} = \frac{\gamma + \sqrt{4 + \gamma^2}}{2} \\ \tan \alpha_2 &= \frac{\lambda_2 - 1}{\gamma} = \frac{\gamma - \sqrt{4 + \gamma^2}}{2}, \end{aligned} \quad (18)$$

from which we recognize that OA is perpendicular to OB (since the relation holds $\tan \alpha_1 \cdot \tan \alpha_2 = -1$).

After multiplication of Eq. (14) by x or y and subsequent addition we obtain finally the semi-axes A and B of the ellipse from

$$\begin{aligned} \lambda_1 x_1^2 &= x_1^2 + \gamma x_1 y_1 \\ \lambda_1 y_1^2 &= \gamma x_1 y_1 + (1 + \gamma^2) y_1^2 \\ \hline \lambda_1 (x_1^2 + y_1^2) &= x_1^2 + 2\gamma x_1 y_1 + (1 + \gamma^2) y_1^2 \end{aligned}$$

or

$$\lambda_1 a^2 = A^2$$

from which the semi-axis of the ellipse

$$A = a \sqrt{\lambda_1}$$

and in a similar way the semi-axis

$$B = a \sqrt{\lambda_2} \quad (19a)$$

is found.

Examples:

1. Simple finite shear through an angle $\beta = 45^\circ$. We have $\gamma = \tan 45^\circ = 1$ and

$$\begin{aligned}\lambda_1 &= 1 + \frac{1}{2} \cdot (1 + \sqrt{5}) = 2.62 \\ \lambda_2 &= 1 + \frac{1}{2} \cdot (1 - \sqrt{5}) = 0.382,\end{aligned}$$

giving $A = 1.62a$, $B = 0.618a$. A circle of radius a is thus distorted into an ellipse with these semi-axes. In the direction OA the material stretches about 62 per cent, while at the same time in the direction OB perpendicular to OA the material must contract about 38 per cent. At the same time the directions OA and OB rotate to the positions OA' and OB' so that using the angles α_1 and α_2 (given by Eq. [18]) the angles α_1' and α_2' are determined by:

$$\begin{aligned}\tan \alpha_1' &= \frac{y_1'}{x_1'} = \frac{y_1}{x_1 + \gamma y_1} = \frac{y_1}{\lambda_1 x_1} = \frac{\tan \alpha_1}{\lambda_1} \\ \tan \alpha_2' &= \frac{\tan \alpha_2}{\lambda_2}\end{aligned}$$

2. Finite shear of value $\gamma = 4$. We have $\tan \beta = \gamma = 4$, $\beta = 76^\circ$, i.e., the verticals in the body are displaced obliquely through an angle of 76° . Since

$$\begin{aligned}\lambda_1 &= 1 + 2(4 + \sqrt{20}) = 17.944 \\ \lambda_2 &= 1 + 2(4 - \sqrt{20}) = 0.0558,\end{aligned}$$

the semi-axes of the strain ellipse are

$$\begin{aligned}A &= \sqrt{\lambda_1} \cdot a = 4.24a \\ B &= \sqrt{\lambda_2} \cdot a = 0.236a.\end{aligned}$$

This means that the material is stretched in the direction of maximum strain by an amount more than four times its original length and at the same time in the perpendicular direction the material is shortened to less than one-fourth its original length. The principal directions OA and OB of the undistorted material form angles α_1 and α_2 with the x axis such that

$$\begin{aligned}\tan \alpha_1 &= \frac{\lambda_1 - 1}{\gamma} = \frac{16.944}{4} = 4.236, \quad \alpha_1 = 77^\circ, \\ \tan \alpha_2 &= \frac{\lambda_2 - 1}{\gamma} = -\frac{0.9442}{4} = -0.2361, \quad \alpha_2 = 167^\circ.\end{aligned}$$

From these we obtain after the shearing displacement

$$\begin{aligned}\tan \alpha_1' &= \frac{\tan \alpha_1}{\lambda_1} = \frac{4.236}{17.944} = 0.2361, \quad \alpha_1' = 13^\circ, \\ \tan \alpha_2' &= \frac{\tan \alpha_2}{\lambda_2} = -\frac{0.2361}{0.0558} = -4.236, \quad \alpha_2' = 103^\circ.\end{aligned}$$

The cross OA , OB rotates at the same time through an angle of 64° in a clock-wise direction.

The Strain Ellipse.—Recapitulating briefly the preceding, we see that for simple shear a circle of radius a is distorted into an ellipse (the "strain ellipse") with semi-axes A and B

$$A = a \cdot \sqrt{\lambda_1}, \quad B = a \cdot \sqrt{\lambda_2}, \quad (20)$$

in which the values of λ_1 and λ_2 are determined by

$$\begin{aligned} \lambda_1 &= 1 + \frac{\gamma}{2}(\gamma + \sqrt{4 + \gamma^2}) \\ \lambda_2 &= 1 + \frac{\gamma}{2}(\gamma - \sqrt{4 + \gamma^2}). \end{aligned} \quad (21)$$

Using these equations, the two principal strains ϵ_1 and ϵ_2 , in a rock where the verticals are all displaced obliquely through an angle β or in which there is a unit shear of value $\gamma = \tan \beta$ may be calculated from

$$\begin{aligned} \epsilon_1 &= \frac{A}{a} - 1 = \sqrt{\lambda_1} - 1 \\ \epsilon_2 &= \frac{B}{a} - 1 = \sqrt{\lambda_2} - 1. \end{aligned} \quad (22)$$

Obviously, since the volume is assumed constant, we have

$$(1 + \epsilon_1)(1 + \epsilon_2) = \sqrt{\lambda_1 \lambda_2} = 1. \quad (23)$$

These formulæ serve to make it possible to estimate quantitatively the actual strains occurring during relative slippage or shear of rock layers in nature. The angles α_1 , α_2 for the principal directions, are given before the distortion (Fig. 360) by

$$\tan \alpha_1 = \frac{\lambda_1 - 1}{\gamma}, \quad \tan \alpha_2 = \frac{\lambda_2 - 1}{\gamma} \quad (24)$$

and after the displacement (Fig. 361) by

$$\tan \alpha_1' = \frac{\lambda_1 - 1}{\gamma \lambda_1}, \quad \tan \alpha_2' = \frac{\lambda_2 - 1}{\gamma \lambda_2} \quad (25)$$

A simple finite shear is therefore connected with a finite rotation through an angle

$$\alpha_1 - \alpha_1'. \quad (26)$$

There are two series of parallel straight lines which in the case of simple shear have the property that their length remains unchanged. One series is obviously parallel to the x axis. The lengths parallel to the x axis remain in each intermediate

position unchanged. There is yet a second series of parallel lines which retain their original length, namely, the series of straight lines $y = -\frac{2x}{\gamma} + \text{const.}$ These become after the displacement the straight lines $y = \frac{2x}{\gamma} + \text{const.}$ In the case

of this second system, however, the straight lines do not retain their initial length in all intermediate positions during the process of deformation. It will be recognized that a simple shear or the above-considered homogeneous plane strain may be described as follows:

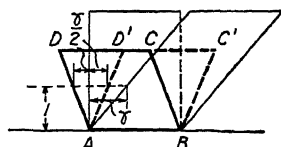


FIG. 362.—Simple shear.

There exists in the stressed body a rhombus $ABCD$ (Fig. 362), which becomes after the distortion a congruent rhombus $ABC'D'$. The angles of the rhombus are interchanged so that the obtuse angle before distortion becomes the acute angle and *vice versa*.

e. Simple Shear in Rock Layers.—Traces of homogeneous strains such as described above, which indicate that the rock layers have undergone severe permanent deformations in the plastic state, are sometimes disclosed by fossils. An example observed by A. Heim can be seen in Fig. 362a. The remains of the fossil fish clearly indicate that the rock was deformed by plastic flow in the direction of the arrow.

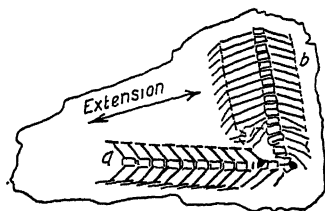


FIG. 362a.—Fossil fish remains deformed together with rock in which they were imbedded. The two pieces a and b of the broken spine of a fossil fish belonged to the same skeleton of *Lepidopus*. Being buried at a different angle to the main direction of the plastic extension (marked with arrows) they appear distorted by different amounts. Tertiary rocks; Alps. (According to Albert Heim, *Geologie der Schweiz*, part 3, p. 88, 1920, Tauchnitz, Leipzig.)

The observed displacements of the rock layers which occur in nature, often have as their fundamental characteristic a simple shear such as has been described above. Geologists call a sudden discontinuity in the rock layers, as shown in Fig. 363, a *fault*. In other cases, the distortion is in the form of a flat wave

or undulation in the position of the rock layers, with crests (anticlines) and troughs (synclines) (Fig. 364). In the case of large distortions, geologists speak of "folds," vaults of folding, or arching, etc. The axis of the fold appears to be considerably

inclined to the vertical, and in the case of large inclinations there result the so-called "recumbent" folds (Fig. 365). Relative to these, geologists have long ago observed that the *thickness of the layers* (measured perpendicular to the boundary of the layers) is often quite variable; for example, in the "middle limb" of the fold (Fig. 365) the thickness is much smaller, while in the "vault or trough," it is much larger than in the "upper" or "lower

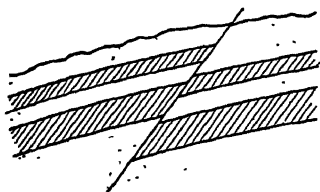


FIG. 363.—Fault.

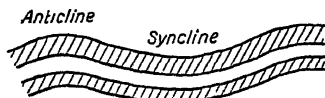


FIG. 364.

limbs," where the distortion is small. As W. Schmidt has recently pointed out, similar deformation phenomena which at first glance are hard to understand *may be very simply explained* if the observed distortions in the rocks are considered, not as a "bending" or "arching action," but as a *consequence of simple shears of variable value parallel to some given direction, more or less inclined to the undisturbed position of the strata*. A more exact

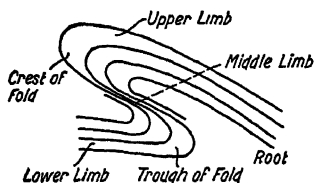


FIG. 365.—Recumbent fold.
(According to A. Heim, *Geologie der Schweiz*, part 3, p. 8.)

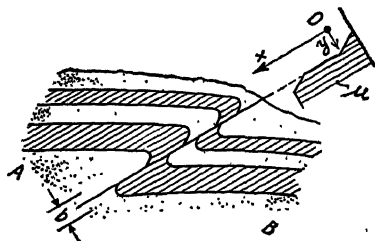


FIG. 366.—Fault.

observation of the profile of a fault surface shows that the boundary layers are often distorted somewhat as shown in Fig. 366. Obviously, the fault is not confined to a single plane as is theoretically assumed. The rock is distorted in a layer of thickness b and the value of the probable relative displacement of a part A with respect to a part B of the mountain follows a curve somewhat as shown in the upper right part in Fig. 366 by the displacements u . In this layer the rock structure is sometimes greatly changed

and in certain particles or grains of the rock definite traces of large distortions may be found.¹

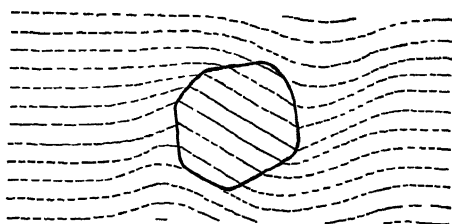


FIG. 367.—Rotation of laminar markings in rock around and within garnet inclusion. (According to W. Schmidt.)

If the amount of the displacement u is measured in the direction in which the two large masses are displaced relative to each other, we have in general $u = f(y)$, i.e., u is a function of the coordinate y perpendicular to the direction of displacement. Since the unit shear γ is defined as the value of the dis-

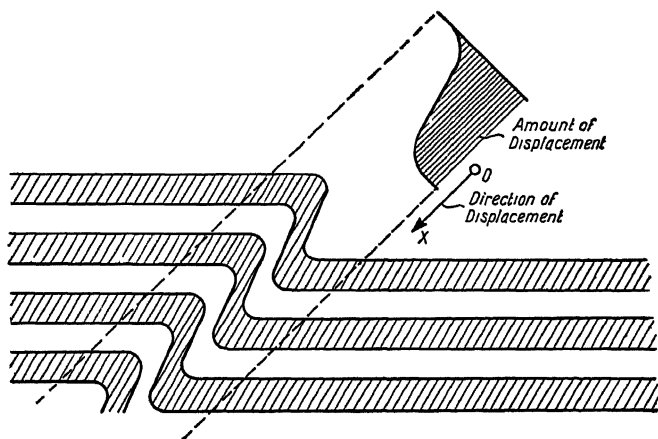


FIG. 368.—Simple shearing displacements in a strip crossing strata at an angle.

placement per unit of length (in the perpendicular direction) in such a case, the unit shear

$$\gamma = \frac{\partial u}{\partial y} = \frac{df}{dy}$$

¹ An instructive example is given by W. Schmidt: In certain rock layers in the eastern Alps, the garnets in the severely distorted rock show a rotation of the previous stratification (Fig. 367); this phenomenon is literally as if rigid balls or rolls had been rolled along the fault surface, surrounded by the plastic rock.

is given by differentiating the displacement curve u in Fig. 366 or 368 with respect to y . Not the displacement component u but rather the unit shear γ is the precise measure of the degree of specific deformation of the rock.

In Figs. 368 to 370 additional examples of simple shear are given. In Fig. 369 is given an example of a group of strata distorted in two mutually

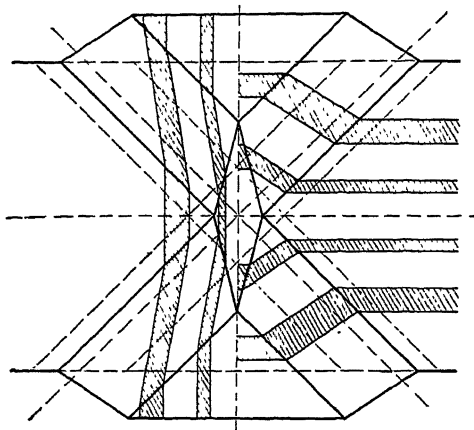


FIG. 369.—Sketch showing result of two simultaneous shearing displacements of equal amount in two perpendicular strips.

perpendicular directions by the same amount of unit shear $\gamma = \text{const.}$ In this it was assumed that the two slip layers were formed *at the same time*. Figure 370 shows a case in which the assumption was made that the slip layer I was first formed, and the slip layer II later. As seen from Fig. 370 it is noticeable that a portion of one layer is almost completely enclosed by

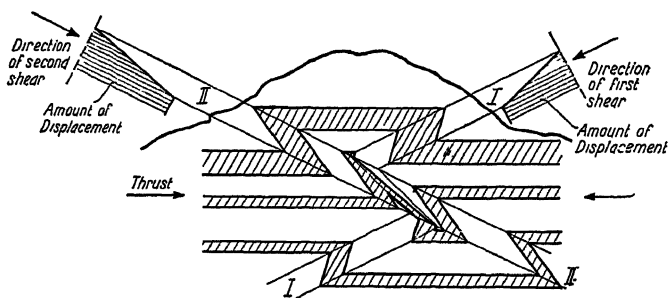


FIG. 370.—Sketch showing distortion of horizontal strata as result of two consecutive shearing displacements acting in two different directions I and II.

the distorted portion of the other. Similar distortions which seem so mysterious at first glance may, however, be simply and easily explained. It is noticeable that in the so-called "Deckentheorie" of the Alps a great use was made of similar explanations. The phenomena observed in the Swiss Alps, in which the older rock layers were found enclosed on all sides

by younger layers and the younger rock was often found above as well as below the older, may be explained by one or several approximately horizontal overthrusts.¹

The developing of an *overthrust* may be seen from Figs. 371 to 373. The plane of the main fault is marked *cc*. Evidence has been given by geologists that sliding movements of several miles along such planes must have occurred in some of the mountainous regions of Europe (Swiss Alps) and America (Rocky Mountains). Whole mountains have been described lying above strata which are younger than those in the mountains them-

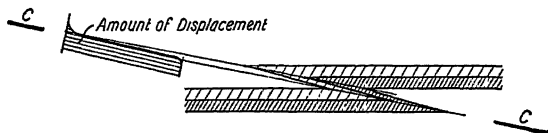


FIG. 371.

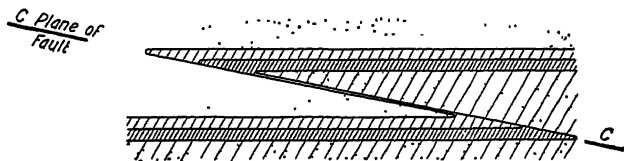


FIG. 372.

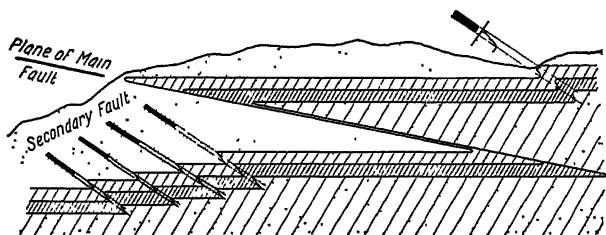


FIG. 373.

FIGS. 371, 372, and 373.—Three progressive stages in the formation of a fault.

selves. The strata deposited in more recent geological periods appear today buried deep below the older strata, as a result of the overthrusts.

Figure 374 shows a second example of the result of a distortion consisting of two subsequent simple shears in two layers crossing horizontal beds. The amounts of the displacements are here assumed to change gradually as indicated by the two curves with the shaded ordinates. Again certain parts of the originally horizontal layers appear almost completely enclosed by other layers.

If the lower halves of the schematic figures, as shown in Fig. 370 or 374, are not observed in nature and distortions such as indicated in the lower

¹ Cf. HEIM, A., "Geologie der Schweiz," 3d Hauptteil, Tauchnitz, Leipzig, 1919.

layers can not be detected, it may be possible that the lower layers are many times more plastic than the upper. If, for example, a brittle series of layers lies upon a definitely plastic layer, there will result from a displacement process, as shown schematically in Fig. 374, only the upper half.

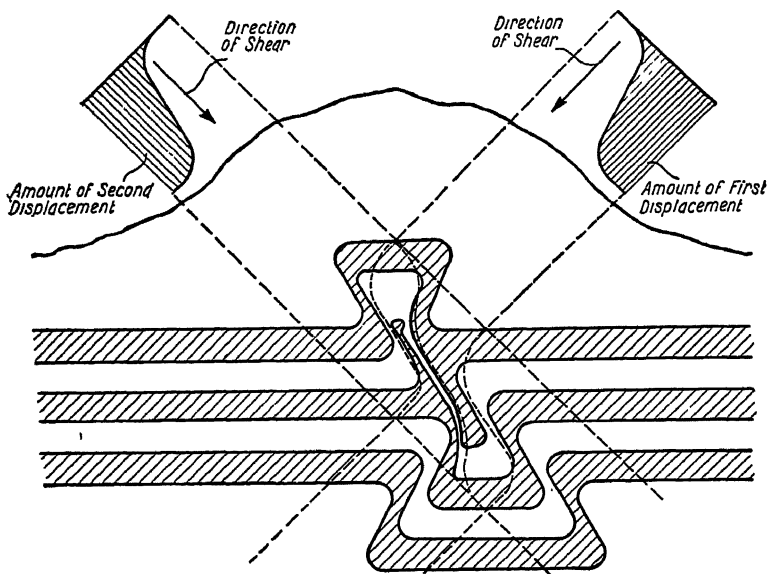


FIG. 374.—The distortions of a set of parallel lines (layers) as a result of two consecutive shearing displacements acting in two intersecting directions.

f. Pure Shear.—In addition to these considerations relative to simple shear, a second type of plane strain, namely, that of *pure shear* will be here mentioned for comparison. This is represented by Fig. 375. The material is stretched in one direction (which is here chosen as the horizontal or x direction) by an amount ϵ_1 and compressed by an amount ϵ_2 in a perpendicular direction.

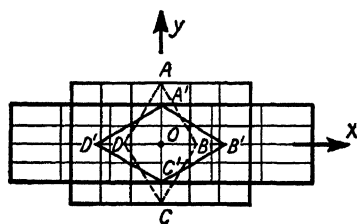


FIG. 375.—Pure shear.

Also

$$(1 + \epsilon_1)(1 + \epsilon_2) = 1$$

and the third strain $\epsilon_3 = 0$. The components of displacement u and v parallel to the x and y axes are now given by

$$u = cx,$$

$$v = -\frac{c}{1+c} \cdot y$$

($c > 0$ means an extension, $0 > c > -1$ means a compression). The principal strains ϵ_1 and ϵ_2 are

$$\epsilon_1 = \frac{u}{x} = c, \quad \epsilon_2 = -\frac{\epsilon_1}{1 + \epsilon_1} = -\frac{c}{1 + c}.$$

There is obviously a rhombus $ABCD$ in the material which changes after the distortion into a congruent rhombus $A'B'C'D'$, in which case again, as has been shown for simple shear, the acute and the obtuse angles are interchanged. It will thus be recognized that "simple" and "pure" shear are fundamentally one and the same kind of strain process. The difference is merely in the rotation. In the case of pure shear there is no rotation of the body, while in the case of simple shear a definite rotation occurs, i.e., a rotation through the angle $\alpha - \alpha'$ computed before.

g. The Phenomenon of Slip in Rocks. Surfaces of Slip.—As shown in Chap. 16 in the case of an infinitesimal homogeneous plane plastic deformation, there result two families of slip surfaces. These are in general

surfaces along which the disturbances are propagated inside a plastic mass. They are perpendicular to the plane of the largest and smallest principal stresses. Denoting by s_1, s_2, s_3 the three principal stresses, if $s_1 > s_2$, while s_3 is the mean principal stress, they form equal angles ϕ with the direction of s_1 , these angles being always $> 45^\circ$

(or at most equal to 45°) (Fig. 376). In the case of an infinitesimal plastic deformation, the position of both systems of slip surfaces does not change appreciably relative to the stressed body. This is not true, however, if the strains and shears are of finite value. We shall only consider the case here where the angle ϕ of the slip surfaces is 45° and both families of slip surface remain mutually perpendicular.

1. *Finite Simple Shear.*—If one studies the formation of the infinitesimal slip surfaces, while a plastic mass is subjected to a simple shear of finite value, it will be immediately recognized that one family of slip surfaces (namely, those parallel to the x axis) remains continuously in the same position relative to the body during deformation. The slip lines of the second family,

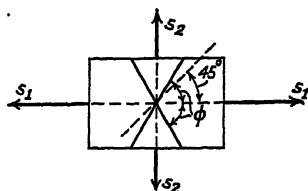


FIG. 376.—Orientation of planes of slip in a plastic mass with reference to principal stress directions marked with s_1 and s_2 .

however, formed earlier, rotate with respect to their previous positions. It is clear that this type of deformation will, in the case of large shearing deformations, completely change the initially isotropic structure of the rock. Parallel to the x direction, the material becomes much more densely interspersed with slip surfaces, perpendicular to which *long* slip surfaces cannot however form, since they will always be obstructed in their propagation by the slip layers previously formed and crossing them. There then results the laminated structure, well known to geologists and mineralogists in many rocks. We can express these facts as follows: During a finite simple shearing displacement of large value, one system of slip surfaces remains continuously parallel to its original position (the plane of the laminations), while the other system must continually rotate with respect to the stressed body. The material thus becomes gradually loosened in texture by the slip surfaces which remain continuously parallel to themselves; therefore from the initially isotropic material there results a rock with parallel cleavage planes (shale).

2. *Pure Shear*.—In the case of *pure shear*, however, conditions, are different; in this case the rotation is zero, *i.e.*, the direction of the maximum strain does not change. Both systems of slip lines, which occur at infinitesimal strains, at all times form angles of 45° to the directions of principal strains, and both directions in which these slip lines begin to form, rotate relative to the stressed body through the same angle. Those straight lines, which at the beginning of the deformation were at 45° to the x direction, become more and more inclined to the x axis as the deformation progresses. The new lines along which infinitesimal slip surfaces form during the progressive stages of the deformation differ from those formed earlier, so that the cohesion of the plastic mass is probably not weakened so much in this case as in the other considered under section 1.

h. *Plastic Deformation with Volumetric Extension*.—In the case of the hard rocks (granite, basalt, the hard sediments, etc.) it is possible in most cases when considering the geological deformation of the upper layers of the earth's crust, to neglect changes in volume. However, in the case of the loose—sandy or earthy—layers, or in the younger sediments, the volume does change. The water contained in the pores, where the layer is subjected to pressure, flows to regions of smaller pressure. Thereby the volumetric content of the layer is changed. The settling, drying and swelling processes in loam or clay layers, or mud are a consequence of the volume

changes due to absorption or ejection of the water contained in the pores. Since the laws of the plasticity of these soft masses have been thoroughly elucidated by K. v. Terzaghi in his "Erdbaumechanik," reference shall be made to this work and to "Ingenieurgeologie" written by K. A. Redlich, K. v. Terzaghi, and R. Kaempe,¹ in which among further subjects the technical applications of geology are treated.

¹ Published by Julius Springer, Wien, 1929. 708 pp , 417 figs.

CHAPTER 41

THE PRESSURE IN THE EARTH'S INTERIOR

a. **The Elastic Compressibility of the Rocks.**—With increase in depth toward the earth's interior, the temperature and pressure increase continuously. There arises the question of what changes in volume of the rocks occur at great depths because of increased pressure and high temperature. Under hydrostatic pressure and at constant temperature, most of the hard rocks are compressed mainly elastically. (An exception is afforded by materials having a porous structure such as wood, cork, deposited sand, etc., or materials such as damp earth or tufa, which under gradually increasing hydrostatic pressure show a considerable permanent change in volume.) At pressures of 10,000 to 20,000 atm., which have already been applied in the laboratory by test, the decrease in volume due to the elastic compressibility of solid materials such as the hard rocks and metals is only a relatively small fraction of the initial volume. The small change in the volume of the rocks produced by pressure, together with certain anomalies which may be observed in the behavior of certain volcanic rocks, plays possibly an important part in the mechanism of volcanic action.

The linear law expressing the small change of volume from v_0 to v at relatively small changes of the temperatures t and of the pressures p , namely

$$v = v_0(1 + \beta p)$$

$$v = v_0(1 + \alpha t)$$

may not be assumed to hold true at great depth in the earth. The tests of P. W. Bridgman already mentioned in Chap. 2 have shown that the linear law does not hold with increasing pressure for liquids and solid metals if pressures of several thousand atmospheres are applied. In other words, α and β are themselves dependent on p or t .

The compressibility of minerals and rocks has been thoroughly investigated in the Geophysical Laboratory at Washington, D. C., by L. H. Adams and E. D. Williamson¹ at pressures

¹ The Compressibility of Minerals and Rocks at High Pressures, *Jour. Franklin Inst.*, vol. 195, p. 475, 1923; see also L. H. ADAMS and R. E. GIBSON, *Proc. Nat. Acad. Sci.*, vol. 15, p. 713, 1929; and other papers of L. H. Adams.

ranging from 0 to 12,000 megabars.¹ The specimens in shape of cylindrical rods were immersed in kerosene and tested under high hydrostatic pressures in a thick-walled vanadium-steel cylinder. The volume change of the specimens could be obtained by subtracting from the total change as indicated by the movement of a piston, the decrease of the volume of the liquid applied, and the volume change of the vessel. The compressibility β was here defined as

$$\beta = -\frac{1}{v_0} \frac{dv}{dp}$$

the diminution in volume for an increment of one megabar pressure divided by the volume v_0 at a standard pressure and temperature. Thus a compressibility of 1×10^{-6} means a volume change of one-millionth for one megabar increase in pressure.

The compressibility β , the modulus of rigidity G , and the bulk modulus K in megabars per square centimeter are given in the following table as found by Adams and Williamson for some igneous rocks.

Rocks	Pressure p (megabars)	Compressibility $\beta \times 10^6$	Modulus of rigidity G	Bulk modulus K	Density ρ
Granite.....	{ 2,000 10,000	2.12 1.88	260,000 290,000	470,000 530,000	2.61 2.66
Gabbro.....	{ 2,000 10,000	1.49 1.20	360,000 450,000	670,000 830,000	3.05 3.08
Dunite.....	{ 2,000 10,000	0.93	590,000	1,800,000	3.38 3.41

In general the compressibility β decreases with the density of the rock and is for the more acid rocks little less than that of plate glass ($\beta = 2.2 \cdot 10^{-6}$). The compressibility β decreases the most for the first 2,000 megabars and for the acid rocks (granite) more than for the basic rocks; gabbros and peridotites show for pressures from 2,000 to 12,000 megabars approximately a constant compressibility.

Although it appears from these tests, that the compressibility of the heavier basic rocks does not change much with increasing pressure, it would be premature to extrapolate the β curves to the pressures acting at great depths of several thousand kilometers in the earth.

¹ The megabar is independent of the force of gravity. One megabar = 1.0197 kg./cm.² = 0.987 atm. at Washington, D. C.

Under these conditions, no choice is left but to make certain plausible assumptions as to the distribution of density in the interior of the earth, as suggested by geophysical considerations and from these to compute the pressures. These considerations give pressures at the earth's center of the order of a few million atmospheres and a density which must be substantially larger than that of copper or steel under normal pressure. In spite of the increasing temperature with depth, causing a definite expansion of the rocks, the mean density definitely increases with depth.

b. The Change in Gravitational Acceleration and Pressure with Depth.—As a first approximation, we may neglect the flattening of the earth and also the centrifugal forces due to the earth's rotation in estimating the pressure p at great depths. The ellipticity e of the meridian, *i.e.*, the relative difference of the radii a and b at the equator and at the poles, respectively,

$$e = \frac{a - b}{a}$$

has a value of only about $e = \frac{1}{297}$. The centrifugal force at the equator decreases the gravitational acceleration by only about 0.3 per cent. It can therefore be assumed that the density ρ and the gravitational acceleration g are functions only of the distance x from the center of the earth (and independent of the polar angle). The force F , with which an element of mass m is attracted to a second element of mass m_1 at a distance r from m is given by

$$F = f \cdot \frac{mm_1}{r^2} \quad (1)$$

where f is the constant of gravitation.

The potential of the mass m at a distance r or the work which is produced by a mass equal to unity when it approaches the mass m from an infinite distance to the distance r is equal to

$$\phi = \frac{f m 1}{r}. \quad (2)$$

Since the potential ϕ of a homogeneous spherical mass m at an arbitrary external point P at a distance r from the center of a sphere is the same as if the total mass $4\pi \int \rho x^2 dx$ of the sphere were concentrated at its middle point, therefore the gravitational potential ϕ_1 of a point P at the surface $x = r$ of a sphere with variable density $\rho = f(x)$ is equal to

$$\phi_1 = \frac{4f\pi}{r} \int_0^r \rho x^2 dx. \quad (3)$$

On the other hand, the potential inside a spherical shell of radius x and of thickness dx is constant and equal to the potential at its surface, namely,

$$d\phi_2 = \frac{f dm}{x} = \frac{4\pi f \rho x^2 dx}{x} = 4\pi f \rho x dx. \quad (4)$$

Therefore, the potential ϕ at an inner point P of a sphere of radius a with variable density $\rho = f(x)$, the point P being at a distance $r < a$ from the center of the sphere is

$$\phi = \phi_1 + \phi_2 = 4\pi f \left[\frac{1}{r} \int_0^r \rho x^2 dx + \int_r^a \rho x dx \right]. \quad (5)$$

The gravitational acceleration at the same point r is given by

$$g = -\frac{\partial \phi}{\partial r} \quad (6)$$

or

$$g = -4\pi f \left[-\frac{1}{r^2} \int_0^r \rho x^2 dx + \rho r - \rho r \right] = \frac{4\pi f}{r^2} \int_0^r \rho x^2 dx. \quad (7)$$

For $r = a$, this gives the gravitational acceleration g_a on the surface $r = a$ of the sphere equal to

$$g_a = \frac{4\pi f}{a^2} \int_0^a \rho x^2 dx \quad (8)$$

If this formula be applied to the earth, g_a is the mean gravitational acceleration as observed on the surface of a spherical and stationary (not rotating) earth, a being the mean radius of the earth.

Since the mass M of the earth is

$$M = 4\pi \int_0^a \rho x^2 dx = \frac{4\pi a^3}{3} \rho_m, \quad (9)$$

where ρ_m is the mean density of the earth, the gravitational constant f can be determined from the following expression

$$f = \frac{a^2 g_a}{M} = \frac{3g_a}{4\pi a \rho_m}. \quad (10)$$

The equilibrium of a small element of mass inside the gravitating sphere is given by the equation

$$\frac{dp}{dr} = -g \rho. \quad (11)$$

This latter equation combined with Eq. (7) suffices for the calculation of the pressure p at a distance r from the earth's center.

1. *The Homogeneous Sphere.*—The density in this case is $\rho = \rho_m = \text{const.}$ Since the gravitational acceleration g for such a sphere, according to Eqs. (7) and (8)

$$g = g_a \frac{r}{a} \quad (12)$$

is proportional to r , we obtain from Eq. (11) for the pressure p the condition

$$\frac{dp}{dr} = -\frac{g_a \rho_m}{a} \cdot r$$

from which

$$p = c - \frac{g_a \rho_m r^2}{2a}. \quad (13)$$

Since for $r = a$, $p = 0$, we have

$$p = \frac{g_a \rho_m a}{2} \left(1 - \frac{r^2}{a^2} \right). \quad (14)$$

The pressure p in this case, therefore, increases with the depth according to a parabolic law and at the center of the earth ($r = 0$, $p = p_0$) is equal to

$$p_0 = \frac{g_a \rho_m a}{2} = \frac{\gamma_a a}{2}, \quad (15)$$

where γ_a is the weight per element of volume of the material, composing the homogeneous sphere as measured on the surface $r = a$ of the sphere. We therefore have the pressure

$$p = p_0 \left(1 - \frac{r^2}{a^2} \right). \quad (16)$$

At the center of a sphere of constant density whose radius is equal to the mean radius $a = 6,367$ km. of the earth, and whose density is equal to the mean density $\rho_m = 5.5$ of the earth, a pressure of

$$p_0 = \frac{\gamma_a a}{2} = \frac{0.0055 \times 6.367 \times 10^8}{2} = 1,750,000 \text{ atm.}$$

must exist. (1 atm. being approximately 1 kg/cm.² or = 14.2 lb. per in.²). In a homogeneous ball of the density of water, p_0 must be equal to 318,350 atm.

2. *Parabolic Distribution of Density.*—It is known that the mean density of the rocks composing the outer earth's crust is 2.7 to 3, while the mean density of the earth is equal to $\rho_m = 5.50$. This indicates that the density ρ must increase greatly with depth. We now assume a parabolic distribution of density ρ , according to the function

$$\rho = \rho_0 - (\rho_0 - \rho_a) \frac{x^2}{a^2}. \quad (17)$$

In this expression ρ_a is the density at the surface $r = a$ of the sphere and ρ_0 the density at the center. Under these assumptions, the mean density ρ_m is given by

$$\rho_m = \frac{2\rho_0 + 3\rho_a}{5}. \quad (18)$$

Assuming the density of the rocks at the earth's surface ρ_a equal to 3 and the mean density of the earth ρ_m equal to 5.50 we obtain a density at the center of the earth ρ_0 equal to 9.25. The distribution of the pressure p and the gravitational attraction g for a sphere of the dimensions of the earth is now found by integration from Eqs. (7) and (11), from which we obtain an expression for the pressure p at the center $r = 0$ of the earth, assuming a parabolic distribution of density, which is

$$p = \frac{2\rho_0(\rho_0 + \rho_a) + \rho_a^2}{5\rho_m^2} p_0 = 1.56p_0 = 2,730,000 \text{ atm.}$$

In this, p_0 is the pressure at the center of a homogeneous sphere of density ρ_m having the same outer radius $a = 6,367$ km. as the earth. The variation of the density ρ , of the gravity acceleration g and of the pressure p with depth is shown in Fig. 377.

3. *The Metal Core and Silicate Shell.*—The analysis of seismographical observations of the effects of distant earthquakes

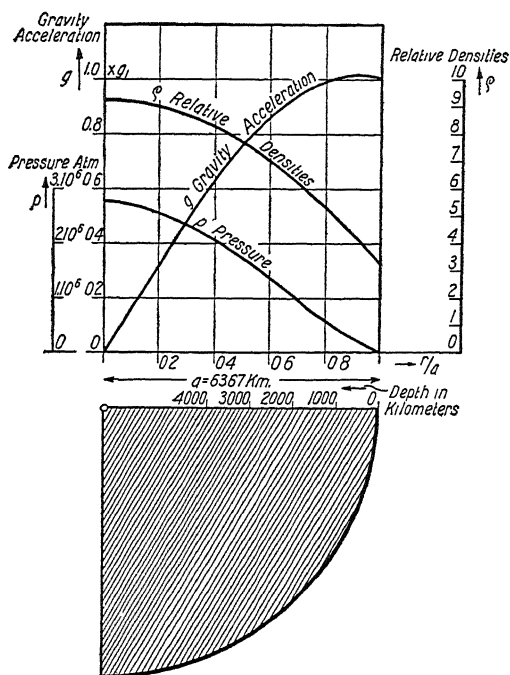


FIG. 377.—Variation of density ρ , of gravity acceleration g and of pressure p in interior of earth, assuming parabolic distribution of density ρ .

appears to indicate that at a great depth there is a *discontinuity* in the distribution of density of the earth's material. For the present, we neglect entirely additional discontinuities of density in the upper earth layers, which occur for example from sedimentation and differences in density of the ocean floor relative to the mean density of the continental shell, as indicated by recent seismographical observations and also by Wegener's theory of continental displacements. We may then assume, according to Wiechert's hypothesis, an outer silicate shell of small density which surrounds a much heavier core of perhaps nickel and iron (the principal constituents of a certain class of meteorites) (Fig. 378). The position of the surface of dis-

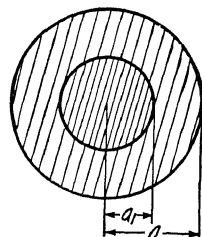


FIG. 378.—Metal core and silicate shell.

continuity has been estimated by Gutenberg, on the basis of earthquake observations, to have a radius of about $0.545a$.

If we assume with Wiechert and H. Jeffreys¹ that the hypothetical density distribution besides fulfilling the above condition, *i.e.*, that the mean density ρ_m is 5.50, should also be such as to satisfy a second condition, namely, that the moment of inertia of the earth's sphere is equal to the correct value as determined astronomically, it is then possible to determine at least the mean densities ρ_1 and ρ_2 in the silicate shell and in the metallic core. The moment of inertia of a homogeneous ball of density ρ is

$$I_0 = \frac{8\pi\rho a^5}{15} = \frac{2}{5}Ma^2 = 0.4Ma^2. \quad (19)$$

On the basis of the period of precession of the earth's polar axis (precession of the equinoctial points) which occurs because of the gravitational attraction of the sun on the swelled portion (elliptical enlargement) of the flattened earth around its equator, it must be concluded that the actual moment of inertia of the earth with respect to the polar axis is²

$$I = 0.334Ma^2. \quad (20)$$

Assuming for simplicity that the metallic core extends to half the earth's radius, so that the separation of core and shell is at a distance $r = a_1 = a/2$, and designating by $\alpha = a_1/a$, we have on the basis of density considerations

$$\rho_0\alpha^3 + (1 - \alpha^3)\rho_1 = \rho_m \quad (21)$$

and furthermore from the condition Eq. (20) with respect to the moment of inertia of the earth, we have:

$$\rho_0\alpha^5 + (1 - \alpha^5)\rho_1 = 0.334 \cdot \frac{5}{2} \cdot \rho_m \quad (22)$$

Taking $\alpha = \frac{1}{2}$, $\rho_m = 5.50$, we obtain for the mean density of the metallic core $\rho_0 = 14.0$ and for the mean density of the rock shell $\rho_1 = 4.28$. There results at the center of the earth a pressure equal to

$$p = \frac{\rho_0^2 + 2\rho_1^2 + \rho_0\rho_1}{4\rho_m^2}p_0 = 2.42p_0 = 4,230,000 \text{ atm.} \quad (23)$$

Since the density of the rocks at the surface is only 3, the density ρ_1 in the outer shell must increase with depth. This increase in density of the rock shell and the large value of the mean density of the core may partly also be traced to the elastic compression of the rocks due to the weight of the superimposed layers.

¹ "The Earth, Its Origin, History and Physical Constitution," The Macmillan Company, 2d edition, New York, 1924.

² Cf. JEFFREYS, H., "The Earth," p. 210.

CHAPTER 42

MOUNTAIN BUILDING

Geologists are familiar with the severe dislocations of the originally horizontal sedimentary layers in the mountainous regions of the earth. In the high mountains of the earth, for example in the Alps, Andes, or Himalayas, the originally horizontal position of the earth strata appears to be severely distorted, the form of the layers extraordinarily tangled, and their thickness quite variable. Numerous faults occur, along which the continuity of the layers is broken. Geologists speak of severely "folded" rock and compare the distorted boundary lines of the layers, as they appear in sections of mines or as shown by the observation of mountains, with the folding of a tablecloth which has been pushed together. Although the term "folding" is applied today in more or less a figurative sense, in geology, it may be perhaps useful to analyze a few of the most frequently observed types of deformation from the standpoint of mechanics. The folds of a crumpled sheet of paper or of a tablecloth pushed together on a smooth table surface, or the skin of a dried apple—examples which have been frequently used by the old school of geologists for the visualizing of the distortion processes occurring in the rock layers—must, however, be considered as a very incomplete type of description of these elementary processes. In a crumpled cloth, portions of the folds hang free in the air and those portions of the cloth resting on the table surface carry the weight of the suspended portions by means of the flexural elasticity of the cloth. On the other hand, the earth layers which have been pushed together horizontally in mountains, have been subjected to a completely different type of deformation than was the case in a folded cloth. The latter, therefore, cannot be taken as a mechanical model of the deformation of the earth layers since the plasticity of the freely suspended parts—if such would have existed for a time—would be sufficient to flatten out these parts in a short time. Freely suspended layers, which are able to retain their position by arch pressure, such as the blocks in a

stone-arch bridge, or large plates of rock which hang suspended over a hollow space because of the flexural elasticity of the rock, do not exist in nature in large dimensions. Isolated arches of rock, as are formed by the action of wind, ocean waves, or erosion (familiar examples are the Rainbow Bridge in Utah, the natural bridges in Virginia, or along the coast of Scotland) are usually formed of sedimentary layers as are also the arches of natural caves. These occur very seldom and are wonders of nature, but their dimensions are usually small in comparison with the wave lengths of the distorted layers in synclines and anticlines, which were considered above.

Rock layers in a freely suspended position cannot exist because of two reasons. First, all rocks possess a very small tensile strength. In a free horizontal plate of rock, held by means of its flexural rigidity, tensile stresses must exist; hence the layers would break immediately where tensile stresses occur. The second reason is to be found in the *plasticity of the rocks*. In the upper layers of rock, having a loose structure, equilibrium conditions exist as in loose sandy soil. The principal stresses, s_1 , s_2 , s_3 , are not equal and their absolute mean value increases with the depth. Moreover, in the compact upper rock strata (granite, sedimentary rocks, limestone, etc.) we have in general $s_1 \neq s_2 \neq s_3$. Since, however, with increasing depth the temperature increases, the static yield point and the viscosity coefficient must rapidly decrease as the depth increases. In an ideal earth crust (in which the elastic and strength properties of the material change only with depth and do not change in the horizontal direction) beginning with a certain depth, the differences which are likely to exist in the values of the three principal stresses will tend to become equal with time. The differences in the values of the three principal stresses must therefore, at a given point (with exception of the upper earth layers) gradually equalize throughout long geological periods, beginning with a certain depth. In other words, as the depth is increased the state of stress tends more and more to approach that of hydrostatic pressure $s_1 = s_2 = s_3$.

The differences in the values of s_1 , s_2 , s_3 , which may exist at a certain depth, will cause either a plastic strain, *i.e.*, a movement; or if no movement is possible, these stresses will tend to equalize with time. The regions of active mountain building on the earth at the present time are the places in the earth's crust in

which at present the principal stress differences are the greatest. The forces which produce these stress differences are those forces at work in mountain building.

The reasons why these principal stress differences occurred at certain regions of the earth's crust during earlier geological epochs, or the reasons why at the present they exist along certain strips of the continental shell cannot be considered here. It should only be noted that quite small differences in certain physical properties of the rock shell might perhaps account for the conditions prevailing. For example, if the viscosity coefficient along certain strips of the continents would have a smaller value than in other parts, or if the temperature gradient at certain regions would be different from that in others, because of the variability in the compactness of the sedimentary layers or on account of nearby volcanic regions, this would perhaps suffice to explain some causes for mountain building forces. It is known for example that the high mountain chains on the earth, as the Alps or the Himalayas, are formed from the lightest and loosest sedimentary layers.

On the basis of Wegener's theory of the origin of the oceans and continents¹ and the investigations by Born, Joly, and Jeffreys on the isostasy² of the large masses of the continents, as well as on the basis of earthquake research, it is apparent that the continents behave more or less as rigid plates floating on a semi-liquid substratum, similar to the way in which an iceberg floats on water. The above facts indicate also that the large continents have in the course of geological time been displaced relative to each other by large amounts. As a consequence of these long-time displacements and also as a result of local disturbances in the static equilibrium existing inside the continental shells, stresses are still at work to produce new distortions. The compressive stresses inside the continents produced by the weight of the floating rock masses may under the influence of various factors (variations in the cohesion or structure of the various sedimentary layers produced by previous geological processes, differences in the viscosity coefficient, action of plastic layers

¹ WEGENER, A., "Die Entstehung der Kontinente und Ozeane," 4th ed., Vieweg, Braunschweig, 1929.

² Cf. JEFFREYS, H., "The Earth"; A. BORN, "Isostasie und Schweremesung," Julius Springer, Berlin, 1923; J. JOLY, "Surface History of the Earth," Oxford, 1925.

between rigid layers, transgression of inland seas, with the accompanying deposition of less rigid sediments on strips of other more rigid sediments, and other factors) be changed so that a sufficiently large difference has gradually formed between the pressures in the vertical and horizontal directions to cause plastic distortion. Today we see in these continental strips the mountain-building forces at work—forces which have lifted the sedimentary layers several kilometers directly upward from their initial position. As a consequence in the midst of the high, folded mountain ranges, such as the Swiss Alps, along the central ridges of crystalline rock, because of erosion, the underlying granite layers are laid bare, or possibly were gradually pressed out from the depths as denudation progressed, like a plastic mass through enormous fissures.¹

¹ Cf. HEIM, A., "Geologie der Schweiz."

CHAPTER 43

PLASTIC LAYER BETWEEN BRITTLE LAYERS. THE ORIGIN OF THE ROCK-SALT DOMES

Cases where a layer of a very plastic material is pressed between two rigid parallel layers and as a consequence of the lateral pressure flows out to the sides or ascends through vertical fissures can be observed in nature on a large scale. Landslides on the mountain slopes in the neighborhood of lake shores arise because of the high plasticity of a clay layer enclosed between rigid layers. The yielding of a *single* layer can often be taken as the cause of many kinds of geological processes. The high degree of plasticity in a given layer can be due to various causes, for example, the presence of water or oil (clay layers, loam, "Schwimmsand") in strata. It may occur in the case of a slowly cooling volcanic rock while enclosed between brittle sedimentary layers, this volcanic rock itself behaving plastically relative to the neighboring rock because of its higher temperature. A further important example found in nature is shown by the rock-salt stocks or domes occurring in the North German plains and in the Mexican Gulf regions.

In the Magdeburg-Halberstadt basin, rock salt is quarried from the *salt stocks* ("Salzhorsten"). E. Seidl,¹ basing his opinion on his elaborate field investigations, attributed the formation of the rock-salt stocks to the circumstance that rock salt acts as a very plastic material under relatively small pressure differences. The salt stocks in the North German plains are accumulations of rock salt characterized by a limited horizontal extent of one to two miles and reaching from below the earth surface to great depths at times. They are today considered as apparently thickened parts of an originally thin rock-salt layer extending over large areas. In America in the Gulf Coast

¹ SEIDL, ERICH, "Die Permische Salzlagerstätte im Graf Moltke Schacht," Berlin, 1914, and "Schuerfen, Belegen und Schachtabteufen auf deutschen Salzhorsten," Berlin, 1921, publ. by the Preussische Geologische Landesanstalt.

territories, where oil is produced, similar accumulations of rock salt of sometimes remarkably regular lens-shaped form have been described and called rock-salt domes.¹

Initially the rock salt lies in a layer of approximately constant thickness between rigid strata, just as it was precipitated from the ocean by the slow drying of restricted portions of the sea during the Perm period and covered subsequently by other sedimentary rocks (Fig. 379). Rock salt has a specific gravity of 2.15 to 2.17. The specific gravity of the overlying beds may depend on their composition and may also increase with increasing depth below the earth surface. As the average density of more compact rocks is about 2.4 to 2.6, it seems not unreasonable to assume that the overlying rigid strata in general are denser than rock

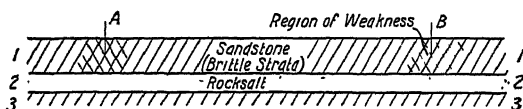


FIG. 379.

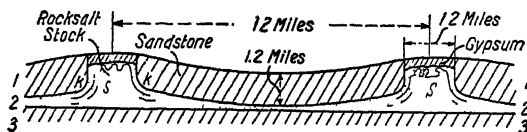


FIG. 380.

Figs. 379 and 380.—Stages of formation of rock-salt domes of German type, (According to E. Seidl.). 1. Brittle strata (*Bunt-Sandstein*). 2. Highly plastic rock-salt layer. 3. Underlying solid strata. S, rock-salt dome or stock.

salt. It will be sufficient to assume that the upper strata, lying above the rock-salt layer (layer 1 in Fig. 379), at certain points (denoted by the double cross-hatching at A or at B in Fig. 379) have a slightly smaller density than at other points. Below these regions the pressure in the rock-salt layer, due to the weight of the overlying strata, will be slightly smaller than in the surrounding points of this layer. Hence there will exist a small pressure difference in all radial directions meeting below the points such as A or B as centers. As rock salt is a highly plastic material, comparatively small differences of pressure will be

¹ Very valuable information regarding the salt-core structures of the United States and of Germany are contained in "The Geology of Petroleum and Natural Gas," by E. R. LILLEY, publ. by D. van Nostrand Company, New York, 1928; cf. p. 376, to which special reference is made.

sufficient to produce movement and plastic flow within the rock-salt layer. Due to the high degree of plasticity of the material in this layer, the salt will tend to flow radially inward towards the centers of lowest pressure designated by *A* or *B*, and will gradually accumulate there more and more, at the same time also bending and lifting up the overlying layer of the crust. Evidently this tendency for accumulation of the lighter sub-crustal material will last only until the slightly disturbed isostatic¹ equilibrium around the centers of flow has again been restored. That will be exactly the case if by the gain of the thickness of the rock-salt layer so much new material has accumulated below the points *A* and *B* that its weight will compensate the former lack of weight of the overlying stratum at *A* or *B*. Taking now also into consideration the effect of erosion on the bulged-up surfaces of the earth above the "regions of weakness" *A* or *B* of the upper strata, attention is called to a new fact apparently not yet noticed, namely, that erosion of the uplifted parts of the surface gives a new impetus to the accumulation of the lighter and highly plastic salt below the regions of weakness. Because of the loss of weight, due to erosion of the uplifted parts of the overlying beds and the constant replacement of the heavier rock masses by the lighter salt, the depression within the rock-salt layer will be maintained, radial flow will continue, and the salt will gradually accumulate in lens-shaped regions. Among other things supporting this explanation should be mentioned the fact that field investigations of the North American salt domes show that the horizontal as well as the vertical cross-sections of these salt cores have a remarkably regular shape. In the vertical profiles of the German salt stocks the sedimentary layers appear bent up, but in remarkable concordance. The contact surface of the salt with the surrounding layers is often very steep and sometimes nearly vertical. The salt appears as squeezed out from deep below the surface of the earth through vents of nearly circular or oval cross-section, thus forming the salt domes. Remarkable is the fact that in many vertical cross-sections of salt domes of North American or North German origin the "corners" of the upper strata (*kk* in Fig. 380) are round, just as if the following salt had rounded them. In large pieces, especially of certain German rock salts, the evidences of the plastic deformations can be observed directly, as seen in

¹ See next chapter.

Fig. 381, reproduced from the book of E. Seidl. It may be mentioned that, on the other hand, certain evidences of strain and severe plastic flow, which should be found in the deeper regions of the rock-salt stocks, where they gradually pass into the normal and thin salt layer—if the explanation given above is right—have possibly been blotted out by recrystallization. The presence of water in the upper layers is possibly a further cause of disturbances and of dislocation in the rocks, by virtue

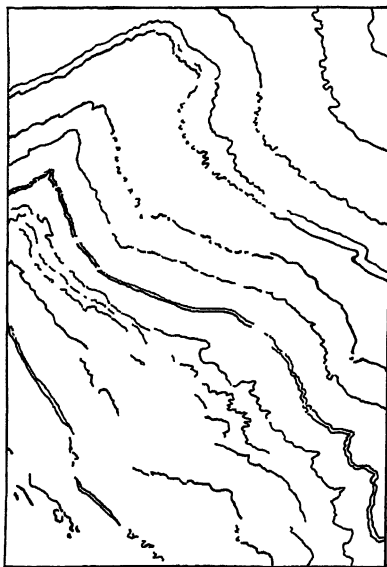


FIG. 381.—Typical older rock-salt of anhydrite region from saddle of Stassfurt (Germany). This sample shows the result of a number of consecutive shears in a complicated distortion of the originally parallel stratification lines. (According to E. Seidl: "*Die Permische Salzlagerstätte im Graf Moltke Schacht*," Berlin, 1914, Verlag Geologische Landesanstalt.) One-sixteenth of natural size.

of the leaching effect, which has not been considered here at all. Certain faults exhibiting clearly a sinking of the cap rocks, overlying the domes (see Fig. 121, page 385 of Lilley's book, mentioned above), may perhaps have been caused by the leaching of salt. The light gypsum layer frequently encountered at the top of rock salt domes has been formed by the leaching action of water.

As has been pointed out by Lilley, certain phenomena, as for example the regular orientation of the long axes of the domes with oval horizontal cross-section in North Germany (and the

clear relation of these latter to the directions of the folding movements in the neighboring old mountain ranges), indicate that mountain folding and orogenic forces might have had a further part in the formation of the rock-salt domes. Owing to the mountain-building forces large blocks of the rigid overlying strata may have been displaced as large rigid plates with respect to each other and to the lower beds. The presence of such a plastic material as rock salt in a thin layer, embedded between more or less rigid and brittle strata, accounts for the possibility of many other relative movements between the blocks. The rock salt must act as a lubricant, such as a layer of soap or paraffin between wood or metal plates, and it is certain that it must have greatly facilitated the relative movement between blocks of the overlying strata. Where breaks were formed between the blocks of sandstone, the rock salt was pressed out from below and has gathered together as stock, all these slow movements requiring long periods of time for their completion.

CHAPTER 44

THE WEIGHT OF THE CONTINENTS—ISOSTASY

Various observations, especially those relative to the velocity of earthquake waves, indicate that the ocean floor is composed of rocks somewhat denser than those composing the continents. Assuming the specific weight (weight per unit volume) of the rocks composing the ocean floor equal to $\gamma_2 = 3 \text{ tons}/m^3$ and assuming, as does A. Wegener,¹ that beneath the continental shell the same rocks are found as those below the oceans, so that the lighter continental rocks, having a mean specific weight of $\gamma = 2.7 \text{ tons}/m^3$, rest on a foundation with a specific weight

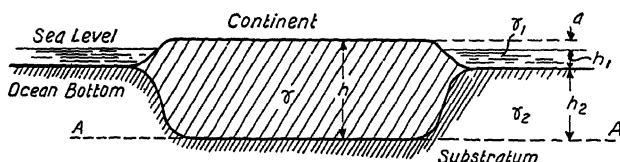


FIG. 382.—Isostatic equilibrium of floating continental slab.

$\gamma_2 = 3.0 \text{ tons}/m^3$, we obtain from the principles of hydrostatics relative to the equality of the pressure along the lower boundary surfaces *AA* (Fig. 382) of the continents the following equation:

$$h\gamma = h_1\gamma_1 + h_2\gamma_2$$

Here is h the thickness of the continental plate, h_1 the mean depth of the ocean (taken to be about 4.8 km.), and h_2 the thickness of the ocean floor above the plane *AA* (Fig. 382); γ_1 is the specific weight of water ($\gamma_1 = 1 \text{ ton}/m^3$). Since the mean height

$$a = h - (h_1 + h_2)$$

of the continents over the ocean surface is known and may be taken equal to about

$$a = 0.7 \text{ km.}$$

¹ Cf. WEGENER, A., *loc. cit.*, 4th ed., p. 34, 1929.

we may calculate the mean thickness h of the continents for the case of isostatic equilibrium

$$h = h_1 \cdot \frac{\gamma_2 - \gamma_1}{\gamma_2 - \gamma} + a \frac{\gamma_2}{\gamma_2 - \gamma}.$$

The first term on the right side of this equation

$$h_0 = h_1 \frac{\gamma_2 - \gamma_1}{\gamma_2 - \gamma} = 4.8 \times \frac{3 - 1}{3 - 2.7} = 32 \text{ km.}$$

gives apparently the thickness of a continent whose surface is flush with the ocean surface. Since, $\gamma_2/(\gamma_2 - \gamma) = 10$ we have

$$h = h_0 + 10a = 32 + 10a$$

in kilometers. From this formula, one of the facts emphasized by the fundamentals of the theory of isostasy is seen, namely that the thickness h of the continental shell below the high mountain ranges (in case their weight is found to be "compensated") obviously must be greatly increased and on the other hand, where depressions or rift valleys¹ are found in the continents, the thickness is smaller. A few values of the thickness h are contained in the table below.

THE EQUILIBRIUM OF TABLELANDS OF VARIOUS MEAN HEIGHTS

Tablelands				Rift valleys		
Mean height over the ocean surface, km.	Mean thickness of continent, km.	Amount of compression in horizontal direction		Amount of depression in meters	Mean thickness of continent, km.	Amount of elongation in horizontal direction, per cent
		b=km.	per cent			
$a = 0.0$	32	0	0	39	0.0
0.7	39	0	100	38	2.6
1.0	42	0.3	7.1	200	37	5.3
2.0	52	1.3	25.0	300	36	8.3
3.0	62	2.3	37.0	400	35	11.3
4.0	72	3.3	46.0	500	34	14.7
5.0	82	4.3	52.5	600	33	18.2
6.0	92	5.3	57.5	700	32	21.9

¹ Here the term rift valley (Germ. *Graben*) means strips or regions in the continents, where the layers have sunk in. (Rhine Valley; Red Sea, African "Graben.")

Below a high mountain chain of mean height $a = 3$ km. over the ocean surface, the continent must therefore be 62 km. thick or $62 - 39 = 23$ km. thicker than at those portions where the height of the continent over the ocean surface is equal to the mean height of all the continents or $a = 0.7$ km.

In another column of the table is given the percentage values by which the continent must have been compressed in a horizontal direction (in the case of depressions, it gives the amount of extension), in order to obtain the increase (or decrease) in mass required by the principle of isostasy. In this computation, it was assumed that the compression (or stretch) only occurred in *one* direction—namely, the direction perpendicular to the ridge of a chain of mountains. If l is the length along which a continental mass is thickened by compression (Fig. 383), h its thick-

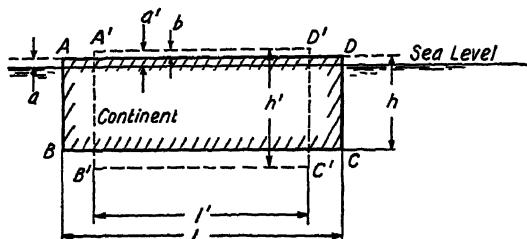


FIG. 383.—Elevation b produced by horizontal compression of continental slab.

ness, and l' , h' the corresponding values after the compression, and if $b = a' - a$ is the value of the "elevation," we must have

$$hl = h'l'.$$

The relative compression of the continental mass under a high mountain is

$$\epsilon = \frac{l - l'}{l} = 1 - \frac{h}{h'}.$$

Taking $a = 0.7$ km., $h = 39$ km., $h' = 39 + 10b$ this gives a compression

$$\epsilon = 1 - \frac{39}{h'} = \frac{b}{3.9 + b}.$$

The corresponding values are given in the third column of the table. In an analogous way, the relative horizontal stretch in the continental mass under a depression which has sunk in by an amount $b = a - a'$ (Fig. 384) is,

$$\frac{l' - l}{l} = \frac{h}{h'} - 1 = \frac{b}{3.9 - b}.$$

For example, to produce isostatic elevation of a strip of land (a mountain chain) above a continent by an amount $b = 2.3$ km., this strip must be compressed 37 per cent in a horizontal direction and concurrently a rift valley of 500 m. depth results (*i.e.*, the layers on the earth's surface must sink about 500 m. along a valley or strip) if the continent is stretched below the valley in a horizontal direction perpendicular to it by about 14.7 per cent. The figures relative to the isostatic elevation or depression may have to be corrected when the compensating effects of erosion or of new deposits of gravel and sedimentary layers on the amount of rising or sinking are considered.

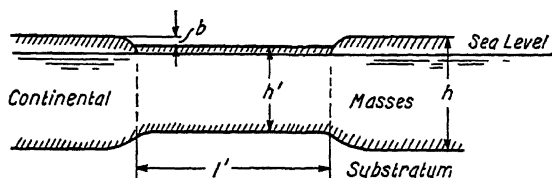


FIG. 384.—Depression b produced by horizontal elongation of floating continental slab.

As J. Geszti¹ has briefly pointed out, a consideration of smoothing of the folds of a chain of mountains by neglecting the changes of the vertical dimensions during horizontal displacements of the earth's crust, gives a very incomplete picture of the formation process of a chain of mountains.

The above remarks may perhaps be summarized by saying that the theory of isostasy has allowed conclusions to be made not only on the thickness of the rigid earth crust but also has allowed a valuable estimate of the amount of compression (or stretch) of the earth's crust in a horizontal direction, required to produce rising of a mountain chain (or sinking of a rift valley) of the observed mean height (or depth).

¹ GESZTI, J., "Zusammenschub der Erdrinde," *Gerland's Beiträge zur Geophysik*, vol. 21, Heft 1, 1929.

CHAPTER 45

TRACES OF MOTION IN THE STRUCTURE OF ROCKS

In rocks which have solidified from a molten condition occasionally a regular arrangement of the constituents of the macro- or micro-structure is found. In the following a few remarkable facts, such as the ordered position of certain constituents of igneous, volcanic rocks, or of the regular arrangement of the joints in such rocks, will be mentioned. This will be done, since these and similar observations provide a means for geologists to analyze more exactly and quantitatively the flow movements, the stresses or the plastic deformations in volcanic rocks after solidification.

a. The Streaks and Joints in Granite.—On the basis of the comprehensive investigations by H. Cloos¹ on large granite blocks ("Plutons"), known in the Riesengebirge in Germany, or in the Yosemite Valley and the Sierra Nevada in California, and on other granite stocks, formed by cooling from a molten condition and resulting in a cohesive mass, it has been observed that certain impurities arranged in thin layers may be noticed (Fig. 385). These layers tend to deceive one into thinking that a kind of stratification exists in the granite. In the homogeneous mass

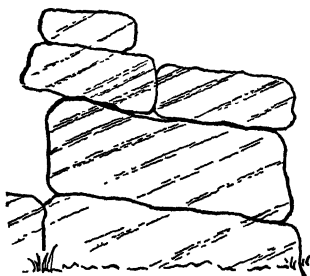


FIG. 385.—"Schlieren" in granite. (According to H. Cloos.)

of these granite blocks, there is discernible in the so-called "Schlieren" another color in the rock. These "Schlieren" or streaks were formed by non-uniformities already existing in the granite when it was yet in the fluid condition. Obviously,

¹ CLOOS, H., "Einfuehrung in die tektonische Behandlung magmatischer Erscheinungen: Granit Tektonik"; first part: Das Riesengebirge in Schlesien, 1925. Bau und Bewegung der Gebirge in Nord Amerika, Skandinavien, und Mitteleuropa, "Fortschritte der Geologie," vol. 7, No. 21, publ. by Gebr. Bornträger, Berlin.

the streaks in the latter were drawn out and moved in a manner similar to the layers of dirt on the surface of a puddle. As Cloos has shown, the thin streaks form large flat arches concave downwards, which cling to and rest on the edges (the "Contact") of the granitic mass, where the latter joins the sedimentary layers (Fig. 386), while inside the granitic mass at some distance from the edges, these arches run for miles approximately horizontal.

In the commemorative volume, in honor of the centenary of James Dwight Dana, "Problems of American Geology," published by his former pupils¹ similar observations in the study of large granitic masses of the "Canadian Shield" are described by F. D. Adams and A. P. Coleman. In three instructive

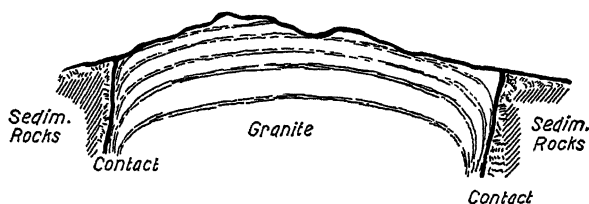


FIG. 386.—Arches formed by "Schlieren" streaks in a granitic mass. Vertical section showing also regions of contact of granitic mass with tertiary rock. (According to H. Cloos.)

pictures, there are shown three different stages in the mixing and the movements of these masses. It is also shown how the amphibolitic inclusions have been drawn out by the plastic deformation of the granitic masses. In Plate IV (first stage) these inclusions are contorted and very irregular, in Plate Va they have been drawn out in parallel layers, while in Plate Vb, the movement has developed a well-marked banding in the rock, the amphibolitic inclusions being shown as dark parallel bands. There is scarcely a doubt that the streaks in the granite² indicate traces of foreign impurities which were suspended in horizontal layers in the originally fluid mass. In the slowly cooling mass, the boundary zones in contact with the rigid neighboring rock cooled faster, while the friction produced by the swelling up of the mass retarded its vertical velocity. After the granitic mass became entirely rigid, the upper solid, but still mainly

¹ The Yale University Press, New Haven, 1915.

² Granite—"Schlieren" in Germany or in California, or respectively the amphibolitic inclusions in the Canadian Shield.

plastic crust was further arched, whereupon especially along the "Contact" numerous fan-shaped cracks appeared (Fig. 387). In these cracks (called "aplitic veins" if they again filled up with fluid magma, otherwise "Fiederspalten" and "marginal thrusts"), there will likewise be recognized a grandiose system which not only will be found in large stretches of granite but will also occur in the boundary rocks in countless small fan-shaped fault surfaces. The origin of these cracks and fissures will be considered in the next section. It will, however, be noted that besides the above-mentioned surfaces of cleavage, in the Silesian granites, as also in other granitic rocks additional systems of joints may be observed which tend to deceive one

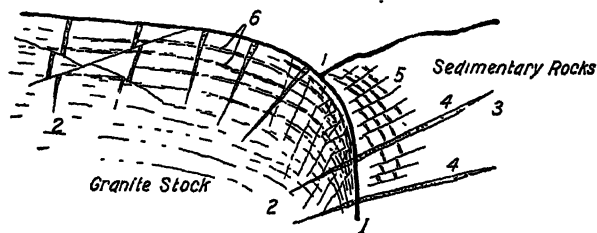


FIG. 387.—The vertical section through the region of contact of a granitic stock (left) with sedimentary rocks (right). (According to H. Cloos.) 1. Surface of contact. 2. Granite stock. 3. Sediments in greatly disturbed order. 4. Aplitic veins. 5. Marginal surfaces of slip. 6. Streaks or "Schlieren" in granite.

into thinking there exists a sort of stratification or bedding as in a sedimentary rock. The origin of these joints may be attributed to later deformation phenomena of these large, slowly cooling mountain masses. These joints have, however, no observable relation to the position of the streak surfaces and "Fiederspalten."

b. Tension Cracks—Shearing Surfaces.—By means of a model test with plastic clay, W. Riedel has carried out instructive observations, which may correspond to similar observations of geological movements—also of movements as the consequence of earthquakes—wherefore they will be mentioned here. If we place over two horizontal, rigid plates *A* and *B* (Fig. 388), a layer of damp loam or clay *C* the surface being covered with a thin film of water, and test the plates by displacing them horizontally with respect to each other and parallel to their edges *SS*, there result in a strip of a certain width *b* on the loam surface two distinct systems of parallel cracks (Fig. 388). The first consists of "tension cracks." Since the stresses in the wedge-shaped zone of fracture, pointing downward, are substantially of the type of pure shear, the shearing stresses must act parallel and perpendicular to the

direction of the straight line SS . At 45° to the direction SS , parallel to s_1 , tensile stresses and perpendicular to s_1 , compressive stresses must act. Since the loam, wetted artificially on its surface, may carry no tensile stresses (by covering the surface with water, the capillary attraction in the pores of the loam particles is nullified), it tears perpendicular to the principal stress s_1 along the lines 11 (Fig. 389). Besides the "tension cracks" 11, there is formed yet a second system of stepped *shearing cracks* parallel to the lines 33 (inclined about 12° to the direction of shear SS) as shown in Fig. 389. It should be noted that if the surface of the loam is not wetted, only the "shear cracks" will occur, the tensile strength of the unwetted clay or loam being apparently greater than its shearing strength.

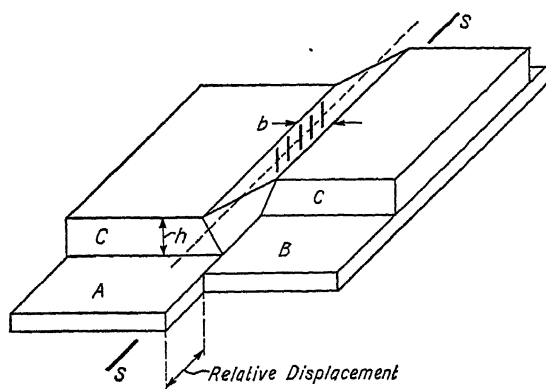


FIG. 388.

FIGS. 388 and 389.—System of cracks produced on surface of a plastic clay resting on two rigid plates A and B which have been displaced tangentially relative to each other. (According to W. Riedel.)

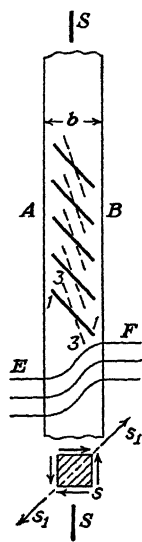


FIG. 389.

c. Ordered Arrangement of the Rock Inclusions. 1. *The Trachytic Cone of the "Drachenfels."*—An example of the ordered arrangement of certain rock inclusions in a volcanic cone is described by H. and E. Closs.¹ The "Drachenfels" along the Rhine at Bonn is a tertiary volcanic cone of "trachyte." From this rock, containing many greenish-yellow inclusions, were taken the blocks of the wonderful Cologne Cathedral. Trachyte contains long lamellar feldspar crystals (dimensions about 2 by 3 by $\frac{1}{2}$ in. thick) the so-called "Sanidine tables," which first crystallized out of the molten mass during cooling. These are distributed approximately uniformly and in large portions throughout the entire rock. A closer consideration

¹ Die Quellkuppe des Drachenfels am Rhein, *Z. f. Vulkanologie*, vol. 11, p. 33, 1927.

of this rock shows that the planes of the Sanidine tables are not placed in random directions, without order, but rather are arranged in certain definite directions. H. and E. Cloos, at many points in the trachytic mass, have determined the

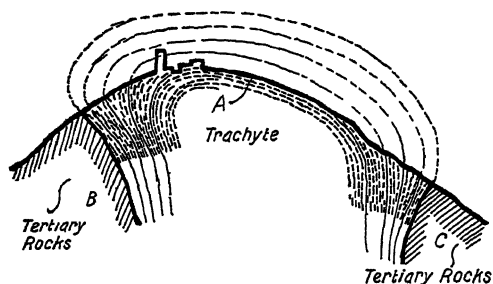


FIG. 390.—Ideal section through the "Drachenfels" on the Rhine (According to field observations gathered by H. Cloos.) The curves connect the most preferred directions along which the plate-shaped Sanidine inclusions were oriented in the trachyte.

orientation of these definite planes, relative to the mountain cone. Considering a profile of the cone, and thinking of the directions of the Sanidine plates as they appear intersecting the profile and forming continuous curves, there results a picture

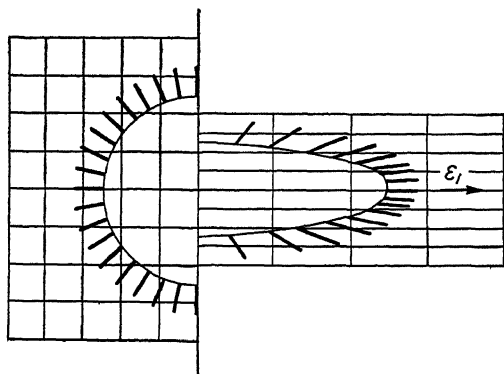


FIG. 391.—Sketch showing how preferred orientation of oblong inclusions in a rock is caused as result of plastic deformation. Left, before, right, after deformation.

as shown schematically in the sketch of Fig. 390. While these Sanidine plates near the highest point of the mountain (at A) are approximately horizontal, near the "contact" (at B and C) they are almost in a vertical position or parallel to the boundary surface between the trachyte and the tertiary rock.

An explanation of the placing of the Sanidine plates along definite directions is contained in the sketch of Fig. 391. If one thinks of n small plates distributed initially uniformly along the circumference of a circle, their planes extending radially so that they form a fan-shaped figure, in a given small angle $d\alpha$, there will be $\frac{n}{2\pi} d\alpha$ small plates. In case of homogeneous plane strain, this circle along which the plates are distributed becomes an ellipse. If ϵ_1 and ϵ_2 are the principal strains (the third principal strain ϵ_3 being taken zero)

$$\epsilon_2 = -\frac{\epsilon_1}{1 + \epsilon_1}.$$

In the vertex of the ellipse (at the end of the long axis) an element of the arc has obviously shortened relative to the corresponding arc of the circle by the ratio $1 + \epsilon_2$ to 1 or $= \frac{1}{1 + \epsilon_1}$. There occur, therefore, in an angle

$d\alpha$ along the vertex of the ellipse after deformation $\frac{n}{2\pi}(1 + \epsilon_1)d\alpha$ small plates. The ratio k of the number of plates orientated parallel to the direction of maximum stretch ($\epsilon_1 =$ maximum principal strain) to the number of plates orientated parallel to the direction of maximum compression (direction of the principal strain ϵ_2) is obviously

$$k = (1 + \epsilon_1) : \frac{1}{1 + \epsilon_1} = (1 + \epsilon_1)^2.$$

In a plastic mass, stretched in a given direction by 50 per cent, 100 per cent, 200 per cent, 300 per cent, the values of the ratio k are

$$k = 2.25, 4, 9, 16, \text{ respectively.}$$

(For example, in a rock stretched 100 per cent, four times as many flat inclusions will be found with their longitudinal directions parallel to that of maximum stretch as will be found with their directions parallel to that of maximum compression, under the assumption that all inclusions were initially radially distributed at random in the undistorted position, as assumed in Fig. 391.) We therefore see that the most frequently occurring direction of the longitudinal axes of elongated inclusions in a rock is the direction of the *maximum principal strain*.

2. *The Bulging-out of a Molten Volcanic Mass.*—Some model tests for making clear the mechanics of some flow processes of volcanic rocks are described by W. Riedel.¹ A volcanic mass cooling from the molten condition, which is pressed upward through a volcanic vent with an approximately circular cross-section or a long fissure between rigid sedimentary layers is

¹ "Das Aufquellen geologischer Schmelzmassen als plastischer Formänderungsvorgang," Neues Jahrbuch der Mineralogie, p. 151, Beilageband 67, abt. B, 1929.

deformed in a manner similar to that of a plastic mass pressed out through a rigid tube or between rigid plates. In Riedel's tests, a plastic mass was, by means of a piston, pressed out of a split wooden cylinder through an orifice. To make the deformation visible, a network which had been previously scratched in a longitudinal section of the mass, was photographed after deformation. A few pictures are shown in Figs. 392 and 393. It is seen from both figures that the portions of the mass in the corners of the cylindrical section do not take part in the motion.

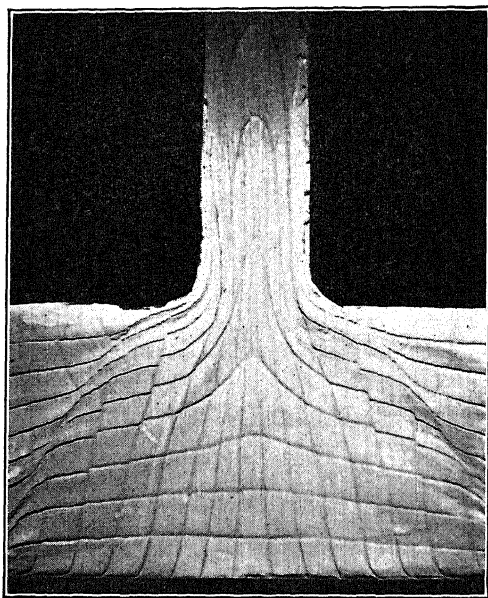


FIG. 392.—Distortion of an originally perpendicular net of straight lines caused by the flow of a plastic mass through an orifice. (*According to W. Riedel.*)

The figures also show how the friction along the inner surfaces of the tube hinders the uniform flow of the material outward. From the deformation of the net, the position of the principal strain directions in the condition shown in Fig. 393 could be determined. They are indicated in Fig. 395. The general contour of the lines of principal strain directions in the narrow tube show considerable resemblance to the contour of the lines along which the plate-shaped Sanidine inclusions in the lower parts of the trachyte cone of the "Drachenfels" are arranged (*cf.* Fig. 390). It will be seen from these few figures, how the

friction acting along the inner surfaces of a volcanic vent, which opposes the rising movement of a slowly cooling mass, deeply affects the whole upward flow thereof.

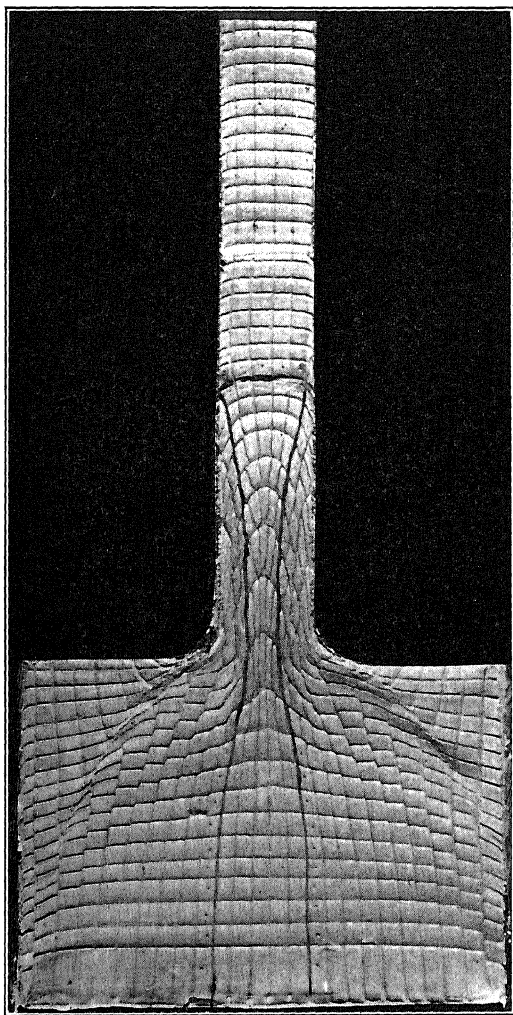


FIG. 393.—Model test with a plastic mass simulating the slow rising of a semi-fluid rock mass in a volcanic neck. (According to W. Riedel.)

It should be noted that a study of similar flow phenomena in the case of hot metals refers to technical processes such as pressing of cylindrical bars or tubes through dies or orifices.

3. *Oriented Structure of Rocks Developed in the Solid State.*—In the preceding section, an example of an ordered arrangement of certain inclusions in an igneous rock was discussed. Using the method of expression of Sanders and Schmidt,¹ we may call phenomena similar to those treated under section a and to the streaks or “Schlieren” in granite as “active orientation” of the

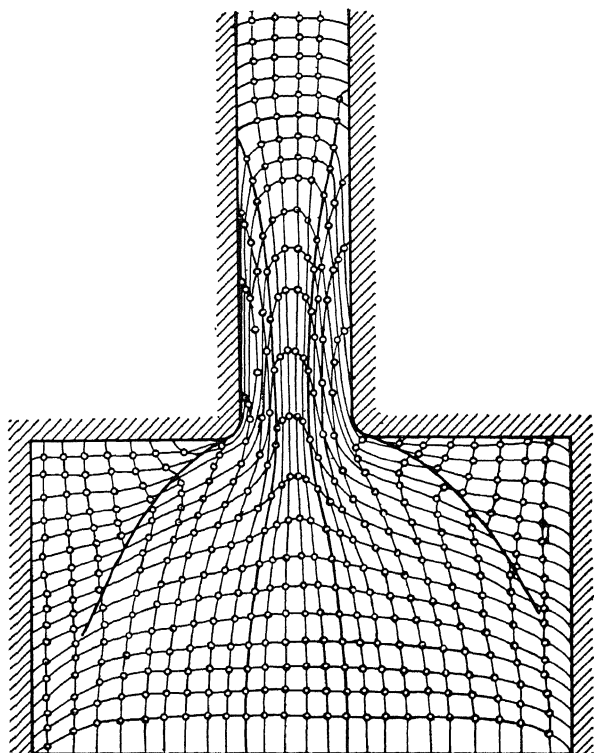


FIG. 394.—Network of lines used for determining principal strain directions in slowly moving plastic mass.

constituents of a rock structure. These phenomena owe their occurrence to the processes taking place when the rock was formed. On the other hand, for example, the so-called “fluidal structure” in a ductile metal does not depend on any such cause.

¹ SANDERS and SCHMIDT, W., “Gefügesymmetrie und Tektonik,” *Jahrbuch der geologischen Bundesanstalt*, Wien, p. 407, 1926. Also “Gesteinsumformung,” *Denkschrift des Naturhistorischen Museums*, Wien, vol. 3; *Geolog. Palæont.*, ser. 3, p. 64, 1925.

If the crystal grains in a solid mass have an oblong shape (Fig. 397), this type of structure may also be the consequence of a severe plastic deformation, to which the mass was subjected at low temperatures while it was in the solid state.¹ To this kind of "passively oriented structures" Schmidt ascribes the remarkable parallel arrangement of the axes of the quartz crystals in

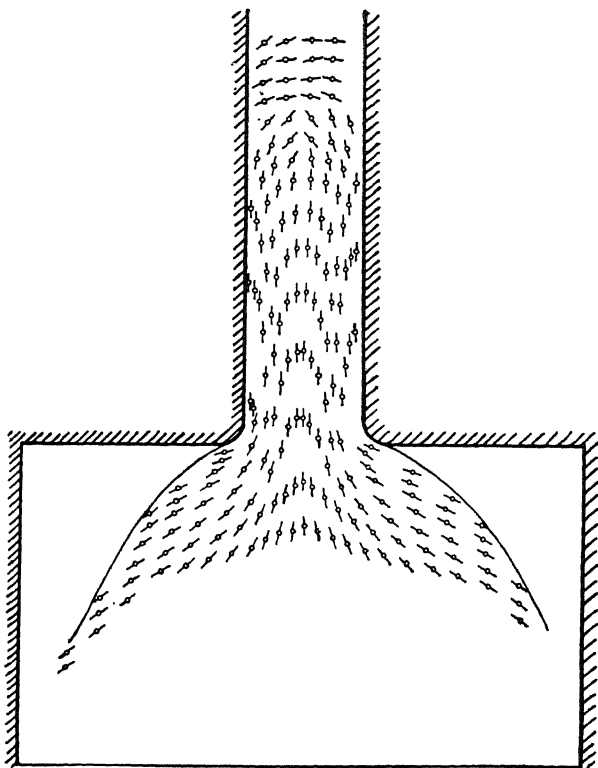


FIG. 395.—The orientation of the maximum principal strain directions in a plastic mass pressed through a channel visualizing the upward movement of a cooling volcanic mass through the neck of a volcano. (According to W. Riedel.)

some Alpine rocks. He found that the axes of the small quartz crystal grains in the rocks of the Alps in a region of many square kilometers extent all showed a common direction with respect

¹ It should be noted that in the mineralogy, phenomena occurring in the microstructure of the rocks are known which are entirely similar to those described in metals. More especially in many rocks, for example, marble, traces of "fluidal structure," of crystal "twinning" by plastic compression, and, in other rocks, of recrystallization structures have been observed.

to the points of the compass. Similar phenomena, namely, the arrangement of crystal axes in definite directions in specimens of metals as a consequence of severe plastic deformations, are well known. In a severely cold-rolled copper sheet, the space lattices of the crystal grains tend to arrange themselves more and more in a definite direction, relative to the direction of rolling and to the direction of the pressure of the rolls on the sheet.

The initial random orientation of the crystal axes in the grains in certain portions of a metal may be gradually changed by plastic deformation, if this latter is very severe. Inversely, W. Schmidt, from the initial orientation of certain crystal grains, for example the quartzes in the Alps, was able to draw conclusions as to the principal directions of strain of the rocks of an Alpine mountain. Moreover, on the basis of his measure-

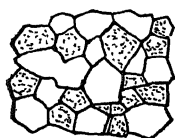


FIG. 396.—
Granular structure.

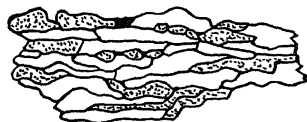


FIG. 397.—Fluidal structure.

ments, he could also determine the direction of the maximum plastic shearing displacements in the rocks.

While in case of oriented species treated under section c1. one constituent of the rock behaves approximately similar to a fluid, in the cases discussed in section c3. all deformations occur in the solid state. As W. Schmidt has especially emphasized, there are, however, further possible intermediate stages of rock formation in the solid state, in which in particular chemical processes, thermal conversions, and the growth of crystals by recrystallization may play an important rôle.

A remarkable example was mentioned by Schmidt. The parallel traces of the planes of scaling of the garnets (inclusions) existing in the shales which compose the principal substance of certain severely deformed Alpine rocks, appear to be turned or rotated with respect to the traces of the planes of scaling of the shale itself (Fig. 367). Such cases mean that here the entire rock was first deformed parallel to the plane of scaling. Later the garnets originated because of recrystallization. The garnets, being made of substantially more rigid material than the substance in which they were produced and imbedded, during the additional long-time plastic defor-

mation of the total mass could only roll as rigid inclusions. The rigid garnets then were rolled in the mountain masses deformed by severe plastic deformation, similar to the manner in which the balls of a ball-bearing roll between the races of the bearing.

BIBLIOGRAPHY

For Chapters 40 to 45

- BORN, A.: "Isostasie und Schweremessung, ihre Bedeutung für geologische Vorgänge," 159 pp., Julius Springer, Berlin, 1923.
- CLOOS, HANS: "Tektonische Behandlung magmatischer Erscheinungen," I. Das Riesengebirge, 194 pp., Gebr. Bornträger, Berlin, 1925.
- : Bau und Bewegung der Gebirge in Nord Amerika, Skandinavien und Mitteleuropa, "Fortschritte der Geologie," vol. VII, Heft 21, Gebr. Bornträger, Berlin, 1928.
- DALY, REGINALD ALDWORTH: "Igneous Rocks and Their Origin," 527 pp., McGraw-Hill Book Company, Inc., New York, 1914.
- : "Our Mobile Earth," 326 pp., Charles Scribner's Sons, New York-London, 1926.
- GEIKIE, JAMES: "Mountains, Their Origin, Growth and Decay," 302 pp., Oliver & Boyd, Edinburgh, 1913.
- HEIM, ALBERT: "Geologie der Schweiz," Tauchnitz, Leipzig, 1920.
- JEFFREYS, H.: "The Earth, Its Origin, History and Physical Constitution," 2d ed., The Macmillan Company, New York, 1924.
- JOLY, JOHN: "The Surface-History of the Earth," 192 pp., Clarendon Press, Oxford, 1925.
- KEMP, I. F.: "Handbook of Rocks," 5th ed., 300 pp., D. Van Nostrand Company, New York, 1929.
- T. LEE, WILLIS: "Stories in Stone," 219 pp., D. Van Nostrand Company, New York, 1925.
- "Problems of American Geology," a series of lectures; commemorative volume to the Centenary of T. D. Dana, 478 pp., Yale University Press, New Haven, 1915.
- QUIRKE, T. T.: "Elements of Geology," 405 pp., Henry Holt & Company, New York, 1925.
- REDLICH, A., K. v. TERZAGHI, AND R. KAMPE: "Ingenieurgeologie," 708 pp., Julius Springer, Wien, 1929.
- SANDER, B.: "Gefügekunde der Gesteine," 352 pp., Julius Springer, Wien, 1930.
- SCOTT, WILLIAM B.: "An Introduction to Geology," 788 pp., The Macmillan Company, New York, 1922.
- TUTTON, A. E. F.: "The Natural History of Ice and Snow," 302 pp., Kegan Paul, French, Triebner & Co., Ltd., London, 1927.
- WEGENER, ALFRED: "Entstehung der Kontinente und Ozeane," 4th ed., 230 pp., Vieweg, Braunschweig, 1929.
- Bulletin of the National Research Council*, No. 77, Volcanology, No. 78, the figure of the earth, National Academy of Sciences, Washington, D. C., 1931. (Cf. especially chapters on isostasy by W. BOWIE and H. F. REID and on physical geology by C. L. DUTTON.)

AUTHOR INDEX

A

Adams, L. H., 12, 308, 309
 Anthes, 138
 Archer, R., 19

B

Bach, C., 27, 85, 95, 96, 160
 Bader, W., 26, 144, 267
 Bailey, R. W., 274
 Barba, 95
 Bardenheuer, 28
 Batey, 270
 Baud, R., 100
 Baumann, R., 27, 95, 96, 160
 Bauschinger, 26, 267
 Becker, R., 33
 Beltrami, 59
 Berliner, 28
 Bingham, E. C., 19
 Boecker, R., 63, 64
 Bollnow, 14
 Boltzmann, 29
 Born, A., 317, 339
 Born, M., 14
 Bowie, W., 339
 Bragg, W. H., 14
 Bragg, W. L., 14
 Brandtzaeg, A., 63
 Bridgman, P. W., 8, 9, 10, 11, 12
 Brinel, 234, 269
 Brown, R. L., 63

C

Cassebaum, 22, 273
 Cloos, H., 328, 332, 339
 Coker, E. G., 143, 159, 243, 245
 Czochralski, 15, 19, 147

D

Dahmen, 22
 Daly, R. A., 339

Donnell, L. H., 208
 Duguet, C., 126, 259

E

Eichinger, A., 63
 Elam, C. J., 30
 Enger, 138
 Ewald, P. P., 14
 Ewing, 28

F

Fischer, F. P., 175
 Foepppl, A., 63, 64, 259
 Foepppl, L., 259
 Friedman, H., 138, 205
 Fry, A., 91, 93, 176

G

Geckeler, F. W., 181
 Gehler, W., 181
 Geikie, J., 339
 Geszti, J., 327
 Gibson, R. E., 308
 Glocker, R., 14
 Goerens, P., 19, 20
 Griffith, A. A., 13, 16, 69, 138
 Guest, J., 63
 Guillet, L., 19
 Guertler, 19

H

Haigh, 71
 Hall, I. W., 19
 Harbard, F. W., 19
 Hartmann, L., 61, 86
 Hausser, K. W., 15
 Heim, A., 229, 300, 318, 339
 Hencky, H., 70, 72, 74, 208, 218

Herbert, 126, 167, 234
 Hertz, H., 241
 Heyn, E., 86, 259, 260, 264, 265
 Hooke, 72, 160, 261
 Howe, H. M., 18
 Hoyt, S. L., 18
 Huber, M. I., 72
 Huebers, 121
 Hueckel, E., 16

J

Jeffreys, H., 314, 339
 Jeffries, Zay, 19
 Jevons, J. D., 86, 159
 Joly, J., 317, 339

K

Karman, T. v., 33, 57, 60, 64, 178,
 181
 Kemp, I. F., 339
 Keulegan, G. H., 29
 Kiesskalt, 10
 Kirsch, B., 100
 Koerber, F., 8, 19, 28, 84, 95, 228
 Koester, W., 93
 Krueger, W., 228

L

Langer, B. F., 258
 Laszlo, F., 208, 264
 Lea, 270
 Leblond, 97
 Lee, W., 339
 Lehmann, O., 16
 Lessells, J. M., 28, 196
 Lihotzky, 91
 Lilley, E. R., 320, 322
 Lode, W., 57, 63, 66, 74, 76
 Loewenstein, L. C., 208
 Love, A. E. H., 130
 Lueders, 76, 93, 99, 106, 176, 251
 Ludwik, P., 22, 63, 81, 83, 92, 95,
 234, 273, 275

M

Martens, 86, 95, 234, 260
 Masing, G., 26, 260, 261

Maxwell, C., 29
 Mesmer, G., 248, 251, 252
 Meyer, Eugen, 234
 Meyer, H., 122, 257
 Michell, 245
 Mieses, R. v., 70, 72, 73
 Mohr, O., 43, 44, 59, 61, 62, 76, 86
 Moser, M., 96
 Müller, A., 14

N

Nehl, F., 257
 Niggli, 33

O

Oberhoffer, P., 19, 147
 Osgood, W. R., 181

P

Poisson, 79, 271
 Polanyi, M., 30
 Pomp, 22, 124
 Portevin, A., 19
 Poulter, T. C., 13
 Prandtl, L., 29, 34, 91, 110, 116, 126,
 131, 222
 Price, G., 339
 Putnam, W. J., 63, 68

Q

Quirke, T., 339

R

Redlich, K. A., 307, 339
 Rejtö, A., 19, 82
 Richart, F. E., 63
 Riedel, W., 225, 333
 Rinne, 110
 Roberts-Austen, 18
 Rockwell, 234
 Rohland, W., 28
 Ros, M., 63, 68, 74
 Rudeloff, M., 95

S

Sachs, G., 19, 234
Sander, B., 336, 339
Sauveur, A., 18
Scheu, 92, 95
Schiebold, E., 147
Schilling, F., 136
Schleicher, F., 74
Schmid, E., 30, 35, 272
Schmid, W., 301, 336, 338
Scholl, 90
Scholz, P., 15
Scott, W. B., 339
Seely, F. B., 63, 68
Seidl, E., 147, 319, 322
Seigle, M. J., 150
Shore, 234
Smekal, A., 33, 35
Stodola, A., 208, 264
Strauss, B., 176

T

Tammann, G., 8, 14, 16, 19
Taylor, G. I., 30, 138
Tetmayer, 95

Therzaghi, K., 307
Timoshenko, S., 28, 99, 196
Toeppler, 91
Trefftz, E., 152
Tuckerman, L. B., 233
Turner, T. H., 86, 159
Tutton, A., 339

W

Wahl, A. M., 100
Warburg, E., 28
Weber, W., 29
Wegener, A., 313, 317, 324, 339
Welter, Z., 22
Wever, F., 8
Westergaard, H. M., 71, 181
Wiechert, 313, 314
Wyckoff, R., 14

Y

Young, 270

Z

Zwicky, F., 35

SUBJECT INDEX

A

- Action of liquids under pressure, 56
- Active plastic state, 223, 224
- Afterflow, 26
- Alps, 317, 337, 338
- Amorphous solids, 15, 20
- Angle of slip, 90, 145, 305
- Anhydrite region in rocksalt layers, 322
- Apparatus for torsional stress distribution, 138, 153
- Arrangement, of inclusions in rocks, 331
 - inordered of atoms, 14
 - ordered of atoms, 14

B

- Bending, of bars, 160
 - moment, 162
 - pure, 164
 - plastic, 168
 - with work hardening, 173
- Block structure, 148
- Branch lines, 224
- Brass, cold drawn, 264
- Brittleness, explained, 58
 - state of, 58
- Buckling load, 179
- Buckling, plastic, 178
- Bulging-out of volcanic mass, 333
- Bulk-modulus, 271

C

- Cementite, 92
- Circles as envelopes of slip lines, 229
 - as isochromatic lines, 245, 247
- Cohesion, in general, 84
 - of liquids, 13
- Cold-drawn brass, 264

- Cold-drawn wires, 269
- Combined stress, 66, 216
- Components of strain, 51
 - of displacements, 48
 - of stress, 40
- Compressibility of glasses, 12
 - of liquids, 12
 - of metals, 10
 - of rocks, 308, 309
- Compression tests with marble, 110, 120
 - with paraffin, 97
 - with prisms, 117
 - with rings, 115
 - with sandstone, 109
 - with specimen having holes, 97, 99, 104, 105
 - with steel, 104, 105, 108, 121
 - with various metals, 124
- Concentration of loads, 251, 252
- Condition of plasticity, 55, 72, 184, 185
 - of yielding, 55, 72, 184, 185
- Cone hardness, 234
- Cone of rupture, 114
- Constriction, effects of, 94
- Contact, of cylinders, 242
 - of elastic spheres, 241
 - pressures, 242
 - problems, 241
 - stresses, 247
 - tests with celluloid models, 245, 248, 249, 255
 - tests with steel, 253, 254, 256, 257
 - of volcanic masses, 330
- Continental drift, 317
- Continental slabs, 326
- Convex bodies under pressure, 242
- Copper, under combined stress, 66
 - compression test, 99, 106
 - hardness test, 236
 - tensile test, 83

Creep of metals, 280, 285
 Crumbling, 56
 Cycloids as sliplines, 223

D

Decken-theory (theory of nappes) of Alps, 302
 Density within earth globe, 312
 Destruction of structure, 56, 113
 Die-cast aluminum, tests with, 203, 206
 Displacement, components of, 51
 Distribution of stress in bending, 173
 in flat plate with hole, 189
 around holes, 100, 107
 in rotating disc and cylinders, 208, 212
 in thick-walled tubes, 186, 194, 198
 in torsion, 129
 Drop of load, 94
 Ductility, defined, 58

E

Earth pressure, 224
 Effect of holes, 100, 151, 153, 156
 Effect of temperature on elasticity, 277
 Elastic after-effect, 29
 Elastic-contact problems, 241, 242, 247
 Elastic deformation, 23
 Elastic distribution of stresses
 around holes, 100
 in rotating cylinders, 210
 in twisted bars, 130
 in tubes, 195
 Elastic hysteresis, 27
 Elastic plate with hole, 100
 Elastic region, 170
 Elastic strain energy, 71
 Elastic-stress function, 130
 Elastic theory of torsion, 130
 Elasticity at elevated temperatures 277
 Ellipse of plasticity, 185, 190

Elongation, defined, 48, 80
 Energy of deformation, 59
 of distortion, 72
 Etching figures on crystals, 15
 Extension, defined, 48, 80

F

Fault, 299
 Fissures (geologically), 330, 333
 Flow figures, 60, 91, 104, 108, 176
 Flow layers, 104, 145, 146, 155
 radial, 187
 stationary, 75, 270
 Fluidal structures in bending, 176
 in rocks, 336
 in torsion, 146, 147, 157
 Fold, 299
 recumbent, 300
 Fracture, 57, 58

G

Garnets, 301, 338
 Graben, 325
 Grain structure, 20
 Grain-boundary substance, strength of, 92
 Granite, inclusions in, 328
 stocks, 328
 Granular structure in rocks, 338
 Gravity acceleration in great depths, 311
 Grooves, effect of, 151, 156

H

Hardness, Brinel's test, 234
 definitions of, 233, 234
 Herbert's test, 234
 Ludwik's test, 234
 Martens' test, 234
 Rockwell's test, 234
 Shore's test, 234
 tests with punch, 228
 Homogeneous strain, 49
 Homologous temperatures, 275

I

Ice, varieties, 8
 Impact, 57
 Imperfections, effect on strength, 35

Impression of ball, 238
 of long cylinder, 254
 of rigid punch, 249
 Impurities, effect on strength, 20
 Inclusions in rocks, 331
 Indentation, study of shapes of, 235
 of hard balls, 238
 Isochromatic lines, 243
 around hole, 101
 for constant contact pressure, 248
 for rigid prismatic punch, 249
 for single concentrated force, 245
 Isostasy, 317, 324
 Isostatic equilibrium, 321, 324
 Isostatic elevation, 327

L

Limit of plasticity, 23
 Limiting states of stress, 55
 Limiting surface of yielding, 55, 70,
 72
 Limiting surface of rupture, 57
 Lines, Lüders', 87
 Lines of stress in twisted bars, 135
 Liquid crystals, 16
 Liquids, arrangement of atoms, 16
 compressibility of, 12
 Local stress effects, 247
 Logarithmical spirals, 228, 237, 238
 Longitudinal extension, 50

M

Marble, tests with, 65
 Marginal thrust, 330
 Mechanism of plastic flow, 30
 Membrane analogy for torsion, 130,
 152
 Metal core of earth, 313
 Mosaic crystals, 37
 Mountains, formation of, 315

N

Nitrogen, effect on flow figures, 93
 Notches, effect on flow figures, 96

O

Ordered arrangement of atoms, 14
 Overspreading of discs or cylinders,
 208

P

Paraffin compression tests, 111
 hardness tests, 239
 Parallel strip deformed, 247
 Partial yielding in tubes, 196
 Passive plastic state, 223, 224
 Peak in stress-strain curve, 93
 Pendulum hardness test, 234
 Penetration of punches, 235, 250
 Perfect elasticity, 23, 270
 Perfect plasticity, 270, 271
 Photo-elastic tests, 243
 with bar having hole, 102
 Photo-elastic contact tests, 245, 248,
 249, 255
 Plane problem, 114, 182, 227
 strain, 182
 stress, 184
 Plastic regions in bending, 177
 in torsion, 140, 154
 Plasticity, condition of, 55, 72
 at elevated temperature, 271
 perfect, defined, 270, 271
 states of, defined, 5
 of rocks, 316
 Plate with hole, yielding of, 189
 Polarized light methods, 243
 Polycrystalline materials, 18, 63
 Polymorphism, 8
 Pressure, behavior of matter under
 high, 7
 effect on index of refraction, 13
 on melting point, 8
 on rigidity, 12
 on viscosity, 9
 in great depths, 310
 Principal axes of strain, 295, 333
 Principal shear, 219
 Principal stresses, 41

Q

Quartz, 337

R

Radial distribution of stress, 230, 244
 Radial yielding, 227
 Recovery, 272

Recrystallized zones, 248, 249
 Regions of weakness, 321
 Regular markings on surface, 38
 Residual stresses, 259, 260, 266
 in cylinders, 265
 first theory of, 260
 second theory of, 266
 Rigid punch, impression of, 249, 250
 Rolling process, 254, 255
 Rolling tests, 254, 255, 257
 Rotating cylinders, 208
 Rotating discs, 264
 Rules of plastic flow, 75
 Rupture, surface of, 57, 68

S

Salt stock, 319
 Sand-heap analogy, 132, 141
 Sandstone, tests with, 64
 Sanidine plates, 331
 Schlieren in granite, 328
 Schlieren method, 91
 Scleroscope hardness, 234
 Shear, finite, 305
 maximum, 60
 pure, 50, 304, 306
 stress, 40, 126
 unit, 48, 54
 Shearing-stress lines, 243
 Shearing-stress trajectories, 244
 Silicate shell of earth, 313
 Similarity, mechanical, 84, 207
 Single crystals, 15, 272
 Single load, 245
 Slenderness, ratio of, 181
 Slip, 62, 88
 theory of, 218, 243, 305
 Slip bands, in crystals, 15, 30, 31, 33
 Slip lines, 38
 on marble, 110
 on paraffin, 111, 112
 on prisms, 118
 in torsion specimens, 145
 produced by contact pressures,
 250, 255, 257
 Slip planes, 90
 Spreading of plastic regions, in
 bending, 169
 in torsion, 140, 154

Soap-film analogy, 131
 Stationary plastic flow, 75
 Steel, under combined stress, 66
 hardness of, 206
 micrographs of, 87, 88
 tests with, 82, 85, 104, 108, 145
 Strain, circles of Mohr, 53
 components of, 51
 definition of, 48
 energy, 71
 ellipse, 52, 298
 figures, 60, 61, 86, 91
 finite, 291
 homogeneous, 53
 infinitesimal, 53
 maximum, 59
 principal, 292

Streaks in granite, 328
 Stress, circles of Mohr, 43, 76
 concentration, 100, 151
 components, 40
 definition of, 39
 function for elastic torsion, 130
 around hole, 101
 lines, 152
 maximum, 59
 for plane stress, 245
 for plastic torsion, 132, 134
 residual, 258

Stress-strain curves, 65, 80
 relations, 78
 for pure shear, 126, 268
 Structure, changes of, 38, 145, 147
 fibrous, 149
 Structure, sensitive properties of, 36
 Surface, limiting of yielding, 55
 limiting of rupture, 57
 of maximum slope, 133, 136
 of slip, 62, 88, 305

T

Tablelands, 325
 Temperature, effect of, on creep, 285
 on elasticity, 277
 on plasticity, 280
 on recovery, 273
 on shape of stress-strain dia-
 gram, 96

Temperature, effect of, on strength,
20

on work hardening, 272

on viscosity, 283

Tension cracks, 330

Tensile diagrams, 24, 80, 96

with bars with constricted portion,
94

with bar with hole, 100, 103

with bars with grooves, 98, 99

under elevated temperatures, 96

tests, 82, 83

Theories of strength, 59, 70

Thermal agitation, effects of, 34

Time effect, 21

Torsion, of cylinders, 126

problem of plastic, 129

tests, 144

theory of, 128

Trajectories of principal stress, 219,
248, 252

of principal shearing stress, 244

Triple point, 8

Twins, formation of, 30, 33

Twist, angle of, 126

Twisting movement, 127

U

Unit elongation, 48

shear, 48

V

Velocity, effect of, on stress-strain
diagram, 273

Viscosity, change with pressure, 9

defined, 4, 282

with temperature, 283

Vitreous state of solids, 15

Volcanic cones, 332

Volumetric extension, 50, 54

Vortical flow, 229

W

Wedge as plastic region, 230

Work hardening, 173, 201, 271

Y

Yield point, 24

Yield stress, 24

upper, 85, 94

lower, 85, 94

Yielding around cylindrical cavity,
200

of plate with hole, 189

of tube, 186

Z

Zinc, hardness tests, 235

single crystals, 272

structure of cast, 149

torsion tests, 148

W

2489